CELL FATE IN THE DEVELOPING MOUSE NEOCORTEX

by
TERESA ELIZABETH LEVERS

Thesis submitted for the degree of Doctor of Philosophy at the University of Edinburgh.

October 1999

DISCLAIMER

Myself (Teresa Levers) performed all of the experiments presented in this thesis unless otherwise clearly stated. Chapter 2 was done in collaboration with Dr Julia Edgar and Chapter 4 with Dr Steven Tait. No part of this work has been, or is being submitted for any other degree of qualification.

Signed Date 28.2.2000

ACKNOWLEDGEMENTS

There are a great many people who were of importance in the production of this thesis. Firstly, I would like to thank my supervisor Dr David Price for allowing me to study in his lab and for his encouragement over the last three years of this PhD. I also wish to thank my second supervisor Professor Peter Brophy for his guidance and assistance over the last three years.

Thanks are also due to the many members of both laboratories (past and present) many of whom became good friends. These include Gillian McGowan, Anne Aitkenhead, Julia Edgar, Natasha Warren, Leila Vali, Pundit Asavaritikrai, David Mcloughlin, Jon Butt, Tom Pratt, Guillermo Estivill-Torrus, Ian Simpson, Katie Gillies, Grace Grant, Steven Tait and Marie-Christine Birling.

Many people provided me with technical assistance during my PhD. These include Katy Gillies, Grace Grant and Vivian Allison for histological assistance and Linda Sharp for her expertise and assistance on the confocal. An extra thank-you to both Grace and Vivian who put in many hours of overtime to help recuperate data that was lost in the fire. Their help was invaluable. I would like to thank Tom Pratt and Katie Gillies for their hard work in keeping the lab running smoothly, and also to Katy for keeping me in order.

I would like to extend a special thank you to Gillian McGowan, Julia Edgar, Natasha Warren, Anne Aitkenhead and Stuart Baker for their friendship over the last three-years.

Thanks also to Dr Randall McKinnon and the members of his lab who all went out of their way to offer advice and friendship during my visit to his lab.

I would also like to thank Steven Tait, Rebecca Hardy and Andy Shering for their advice and expertise on the many different procedures involved in this thesis.

A special thanks to my dad who has provided encouragement and support and a nice new computer.

Finally, I wish to extend my thanks and love to Andy Shering

TABLE OF CONTENTS

LIST OF FIGURES **Page no.**

CHAPTER 1. General introduction

CHAPTER 2. Transition from neurogenesis to gliogenesis in the developing mouse neocortex

CHAPTER 5. Expression pattern of a novel RNA Binding protein.

ABBREVIATIONS

BDNF	Brain derived neurotrophic factor
BrdU	5-bromo-2-deoxyuridine
CDNA	Coding DNA
CM	Conditioned medium
CNPase	2',3'-cyclic nucleotide 3'-phosphohydrolase
CNS	Central nervous system
CNTF	Cilliary neurotrophic factor
CP	Cortical Plate
Ctx	Cortex
DAB	3,3' -diamonobenzidine
ddH_2O	Double distilled water
DMEM	Dulbeccos's Modified Eagle's Medium
DNA	Deoxyribonucleic acid
dNTP	Deoxy nucleotide triphosphate
E	Embryonic day
EDTA	Ethylenediaminetetraacetic acid
FCS	Foetal calf serum
FGF2	Fibroblast growth factor 2
GE	Ganglionic eminence
GFAP	Glial fibrilliary acidic protein
GDNF	Glial derived neurotrophic factor
ISH	In situ hybridisation
IZ	Intermediate zone
LIF	Leukaemia inhibitory factor
LGE	Lateral ganglionic eminence
MAP2	Microtubule associated protein 2
mg	milligram
µg	microgram
µl	micro litre
MGE	Medial ganglionic eminence
mRNA	Messenger ribonucleic acid
MZ	Marginal zone
O-2A	Oligodendrocyte-type 2 astrocyte
ORF	Open reading frame
P	Postnatal day
PBS	Phosphate buffered saline
PCR	Polymerase chain reaction
PDGF	Platelet derived growth factor
PVE	Primary ventricular epithelium
PZ	Proliferative zone
RT	Room temperature
SC	Sub cutaneous
SP	Subplate
SPP	Secondary proliferative population
SVZ	Subventricular zone
Th	Thalamus

TBS	Tris buffered saline
VZ	Ventricular zone
WM	White matter

ABSTRACT

The cerebral cortex (neocortex) is a laminated structure consisting of six layers. Each layer is specific in terms of its functional properties, the composition of cell types and the sets of connections they make. The two main cell types that populate the neocortex are neurones and glia. Interestingly, all the neurones and glia of the cerebral cortex arise from two layers of proliferating cells, the ventricular zone (VZ) which directly lines the cerebral ventricles and the adjacent subventricular zone (SVZ). Within these proliferative zones there are two distinct populations of cells, the pseudostratified ventricular epithelium (PVE) and the secondary proliferative population (SPP). Cells of the PVE give rise primarily to neurones and radial glial cells, whereas cells of the SPP give rise primarily to glial cells.

During neocortical development the timing of proliferation, migration and differentiation of neurogenesis is well understood. Gliogenesis (with the exception of radial glia) is known to take place after neurogenesis and continue into the postnatal period. However, the exact timings of proliferation, migration and differentiation of glial cells remains largely unknown.

To further investigate the timings of gliogenesis in the mouse neocortex, 5-bromo-2-deoxyuridine (BrdU) was used to label proliferating cells *in vivo* around the time that neurogenesis was ending. The proliferative and migratory behaviour of these cells was followed as they populated the cortical wall. Furthermore, immunocytochemical markers of neurones and glia were used to examine the fates of these cells. The exact time point at which neurogenesis finished and gliogenesis begins within the mouse neocortex was established.

Secondly, a study of the mechanisms involved in neuronal and glial cell fate decisions was investigated. For example, how does a progenitor cell know to become a neurone or a glial cell? A tissue culture technique was devised to study the possible roles of environmental factors versus cell autonomous mechanisms in cell fate decisions. The effects of intrinsic versus extrinsic factors were examined further using a heterochronic *in vivo* transplant technique. Results from the above two

approaches suggest that the environment does play a role in cell fate decisions within the mouse neocortex.

Finally, a subtractive cDNA library was screened to isolate and identify rare and novel genes, which are likely to be associated with neuronal/glial cell fate decisions. A novel RNA binding protein was isolated and its expression pattern was characterised in the developing mouse brain.

CHAPTER 1: GENERAL INTRODUCTION

The complex and diverse functions of the mature nervous system depend upon precise interconnections formed by many millions of neural cells. Due to this immense complexity and diversity we are still a long way from elucidating the exact processes by which the mature pattern of neuronal connections are established. It is incredible that the central nervous system, like the other organs and structures of the human body, arises from an apparently homogenous population of cells. The mechanics of how this homogenous population of cells develops into the complex structure of the mature CNS is a subject of extensive research, controversy and speculation.

1.1 Overview of the Cerebral Cortex

The cerebral cortex (neocortex) is a 6 layered structure, and is characterised by its immensely folded nature in higher mammals. It is an extremely complicated and highly interconnected neural structure, containing more than half the neurones of the whole brain (figure 1.1). The cortex is responsible for processing sensory and motor information, and is also responsible for many more complex cognitive functions such as learning, speech, language and spatial awareness.

The cortex is divided up into discrete areas, according to anatomy as well as function. In humans, surface convolutions known as *sulci* (grooves) and *gyri* (elevated regions) are used as landmarks to divide the cortex up into four specific lobes. These lobes are named after the overlying cranial bones: frontal, parietal, temporal and occipital (Kandel et al., 1991). Each of these lobes acts a specific functional unit. For example, the occipital cortex is responsible for the processing of visual information, the parietal cortex integrates sensory perceptions with movement, and the frontal lobes are involved in producing speech.

There is also a specific radial organisation within the cortex. The cortex is divided into six layers, numbered sequentially from the surface next to the pia (layer 1) to the white

Figure 1.1

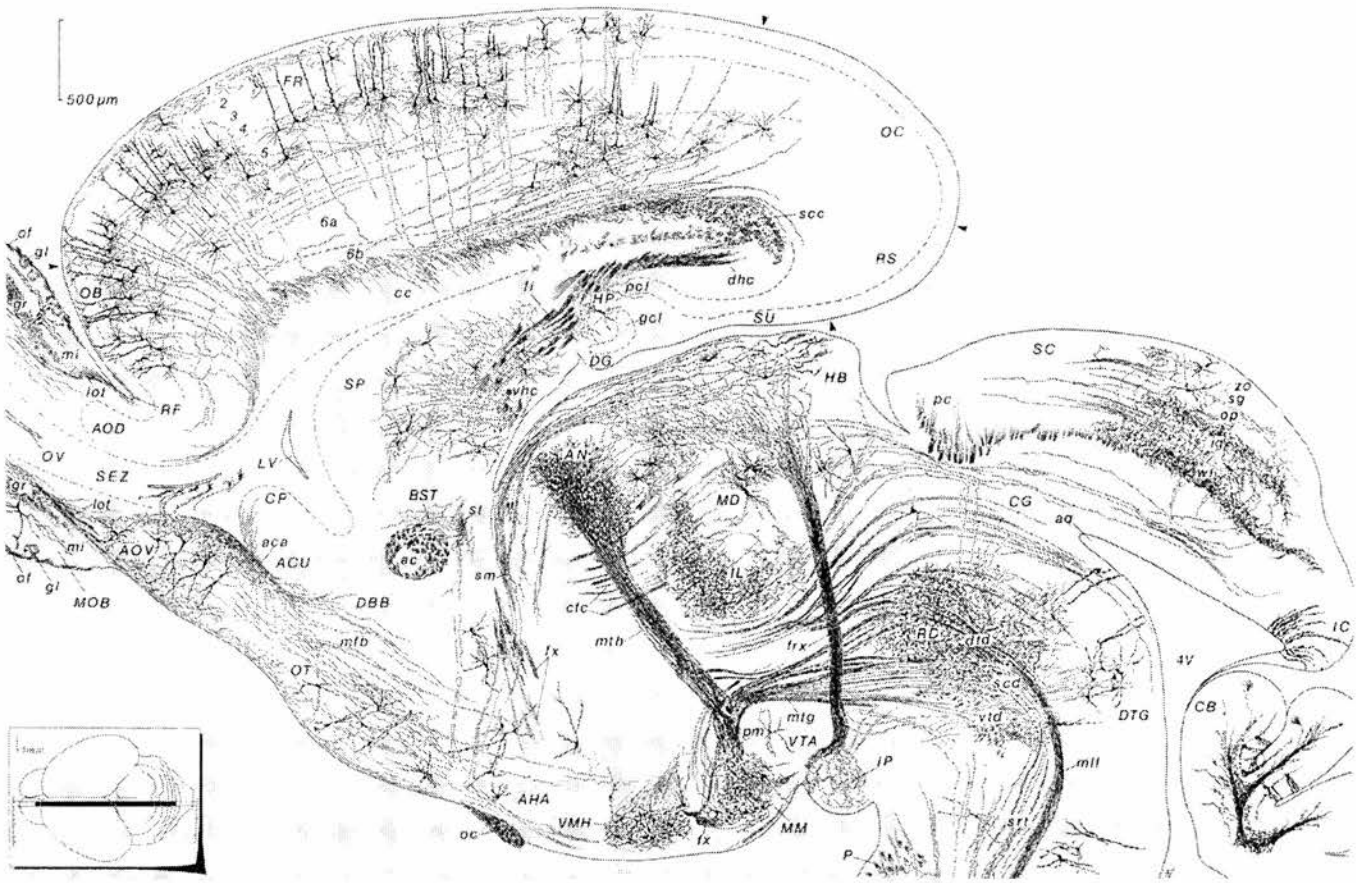

Figure 1.1

Camera lucida drawing of a P2 parasagittal mouse brain section stained using the golgi technique. Note the stereotypical laminar distribution of neuronal cell bodies and the complex and intricate lacework of axon collaterals within the cortex. Diagram taken from Golgi atlas of the mouse brain, Valverde. (http://www.cajal.csic.es/valverde/)

matter underlying the cortex (layer 6). Each of the layers differs from the others in its functional properties, the types of neurones found therein, and the sets of pathways that emerge. In general there are two main cell types within the cortex: pyramidal cells, and non-pyramidal cells. Layer 1 is composed primarily of axons running laterally through the layer, which synapse on to apical dendrites of deeper lying pyramidal neurones. Layer 2 contains small pyramidal neurones, while layer 3 contains larger pyramidal neurones. Layers 2 and 3 provide most of the output to other cortical regions. Layer 4 receives its major input from the thalamus and consists primarily of non-pyramidal cell types. The largest pyramidal cell types are seen in layer 5, and are responsible for projections to sub-cortical regions. Layer 6 also contains pyramidal neurones, which are responsible primarily for projections to the thalamus and other regions of the brain (figure 1.2). Although this 6 layered structure is characteristic of the entire neocortex, the thickness of the individual layers varies throughout the whole structure depending on functional constraints.

1.2 Evolution of the cerebral cortex

The cortex that is visible on the external surface of the brain is called the neocortex, which as the name suggests is the most recent evolutionary addition. The folded nature of the neocortex has arisen due to evolutionary demands requiring greater processing power to interpret and pre-empt the environment. This greater processing power comes from an increase in cortical cell number and increase in complexity of connections. The volume of the cerebral cortex has increased much more rapidly than the volume of the cranium, resulting in folding of the neocortical sheet into *sulci* and *gyri.* This aspect is seen most easily when comparing the neocortices of several different mammals. For example, the neocortex of the rat is smooth and unfolded; in the cat there is an obvious appearance of *sulci* and *gyri,* and the caudal end extends downwards; in the monkey and human the folding is extremely pronounced and even more prominent is the horse-shoe shaped folding of the entire cortex (figure 1.3).

Figure 1.2

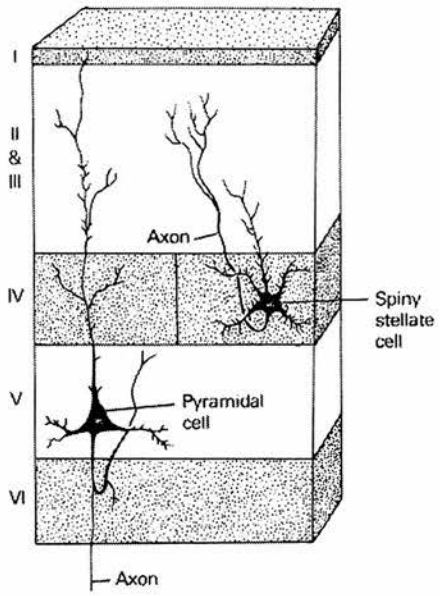

Figure 1.2.

A general overview of the cortical layers, showing pyramidal and non-pyramidal neurones (Stellate). Each layer of the cortex contains both types of these cells although the proportions of these cells vary from layer to layer. (Diagram taken from Kandel *et al.*, 1991)

Figure 1.3

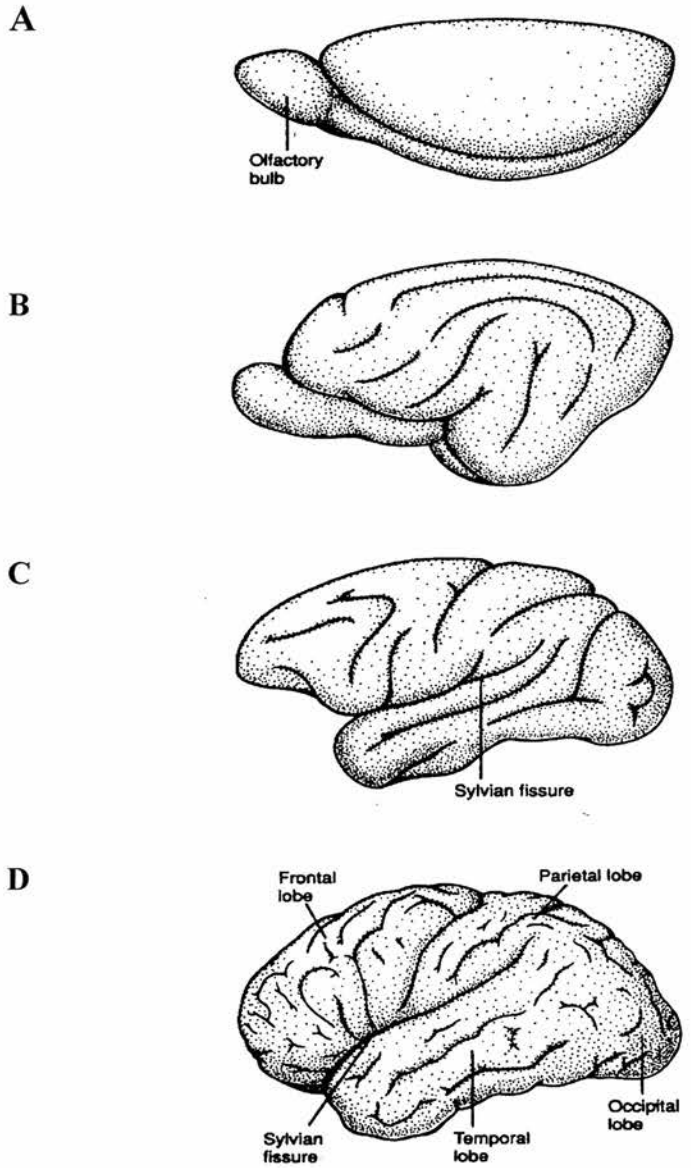

Figure 1.3.

A diagram illustrating the phylogenetic changes of the cerebral cortex. In the rat **(A)** the hemisphere is not folded. In the cat **(B)** the folding is more obvious. In the monkey **(C)** and man **(D)** the folding is very pronounced and the cerebral hemisphere curves from the frontal lobe into the temporal lobe. (Diagram taken from Kandel *et al.*, 1991).

1.3 History of neocortical research

As mentioned above, the neocortex is divided into a variety of functional sub units. This observation was made over 200 years ago. In fact one of the first recorded descriptions of substructures within the brain can be traced back to the eighteenth century. With the unaided eye, Gennari (1782) described a white line within the occipital lobe of the cortex in human brain samples. This layer was later shown to lie within the visual cortex corresponding to the highly myelinated layer IV of primary visual cortex, which receives input from the thalamus. Baillarger (1840) is credited as being the first person to describe the 6 layered nature of the cortex that we refer to today. He noted variations in the form of layers depending upon the different areas of cortex examined, although individual neurones were probably not observed. Using the silver stain method of Camillo Golgi, Ramon y Cajal (1899) in his now classical experiments, identified many CNS structures for the first time and it was at the turn of the century that Korbinian Brodmann (1903) produced the first map of the primate cortex. Using primarily the Nissl stain for cell bodies and myelin stain for axons he was able to identify fifty cytoarchitectural areas, according to cell size, cell density, the number of layers in each region, and the density of myelinated axons. He assigned a number to each structural area. The descriptions of Brodmann have been retained today (figure 1.4).

1.4 Mammalian brain development

The vertebrate embryo begins as a flat disc (embryonic disc) consisting of three layers: the endoderm (innermost layer) which gives rise to the gut, lungs and liver; the mesoderm (middle layer) which gives rise to the connective tissues, muscle and vascular system and the ectoderm (outermost layer) which forms the epidermis and its derivatives (the outer part of the skin) and, more importantly for the purpose of this thesis the nervous system.

Figure 1.4

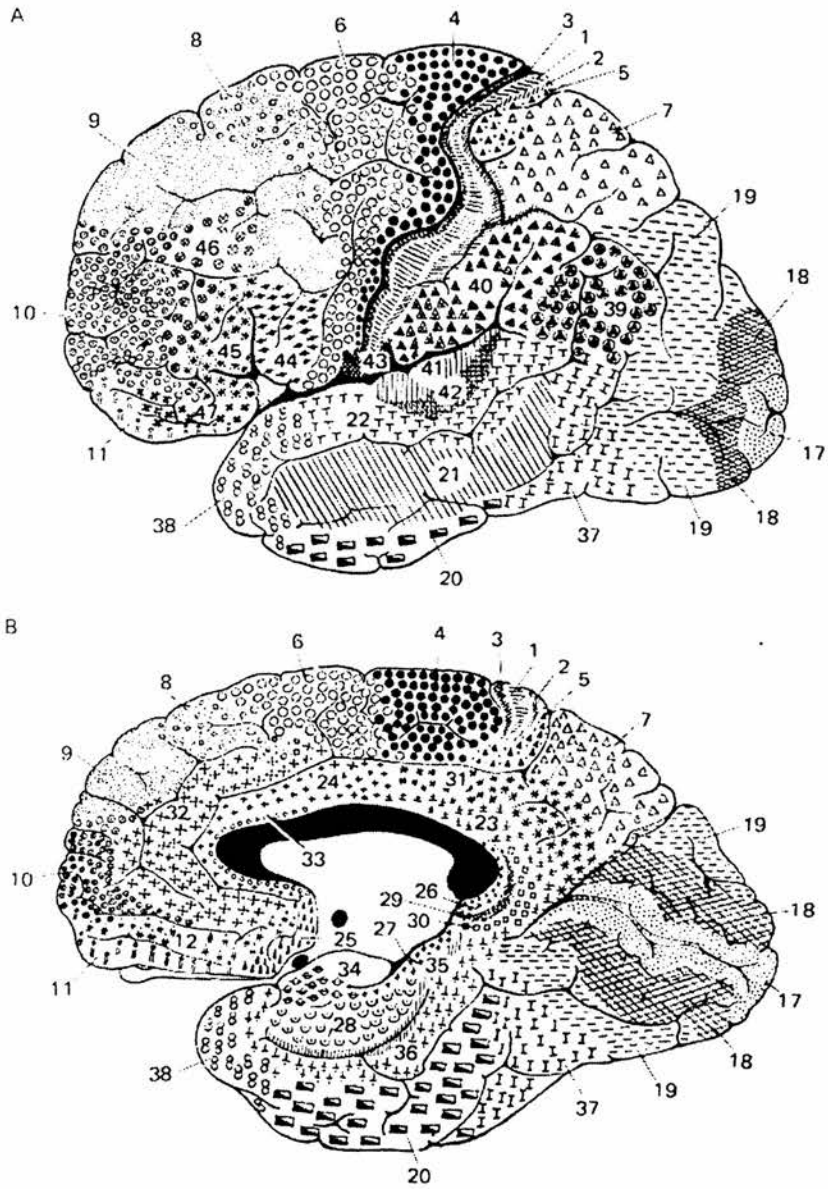

Figure 1.4.

Cortical maps showing the cerebral cortex divided up into discrete cytoarchitectonic areas as described by Brodmann. **(A)** Lateral view **(B)** Medial view. Numbers refer to distinct regions e.g. Brodmanns area 17 is primary visual cortex.

The axial mesoderm plays an important role in that it induces the overlying ectoderm to change structurally, forming a plate of multi-layered newly differentiated cells called the neural plate. The neural plate gives rise to the entire nervous system. At the beginning, the neural plate indents to form a groove along the rostral-caudal axis of the ectoderm known as the neural groove. The edges of the neural groove are known as the neural folds, and these eventually fuse together due to the deepening of the groove to from the neural tube. The neural tube pinches away from the overlying ectoderm. It is the neural tube which gives rise to the entire central nervous system, except for the microglia. The peripheral nervous system derives from the neural crest cells, which are a specialised group of cells that delaminate from the neural folds during the formation of the neural tube. These cells lie dorsal and lateral to the neural tube (figure 1.5).

The early mammalian neural tube is a uniform cylindrical structure. Before the caudal end of the neural tube has formed properly, the rostral end of the tube undergoes several changes. The anterior end of the tube balloons out to form three swellings known as primary vesicles. The most rostral vesicle is the prosencephalon or forebrain, followed by the mesencephalon or midbrain, followed finally by the rhombencephalon or hindbrain. By the time the posterior end of the neural tube closes, secondary bulges, the optic vesicles, have extended laterally from each side of the developing forebrain. The rhombencephalon joins with the rostral part of the neural tube and forms the spinal cord.

The prosencephalon further divides into the telencephalon (the two lateral swellings) and the more caudal diencephalon. The telencephalon eventually gives rise to the two cerebral hemispheres, whereas the diencephalon gives rise to the thalamus, hypothalamus, epithalamus and the subthalamus. The mesencephalon does not undergo any subsequent divisions, and its lumen finally becomes the cerebral aqueduct. The rhombencephalon undergoes further sub divisions into the myelencephalon, which later becomes the medulla oblongata, and the metencephalon that gives rise to the cerebellum. The hindbrain develops a segmental pattern, the swellings that are known as rhombomeres.

Figure 1.5

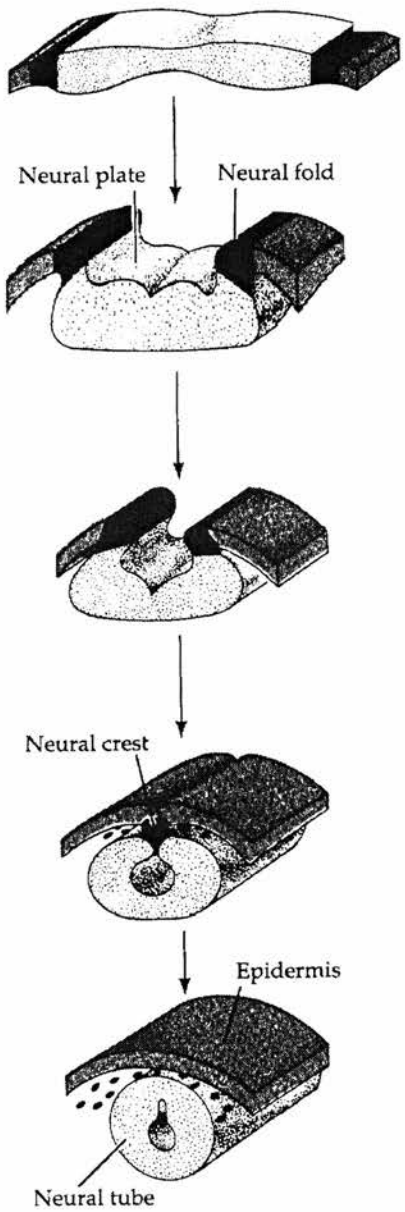

Figure 1.5.

Schematic illustration of the formation of the neural tube. See main text for a detailed description of events.

This thesis is concerned primarily with the development of the telencephalon, which gives rise to the cerebral cortex. Therefore I will concentrate primarily on the development of the telencephalon.

1.5 The developing telencephalon

Telencephalic development is similar in all species of mammal, although the timing of this process may vary between species. In rodents the process is much faster than in carnivores and primates. Since most of our understanding of cortical development comes from rodents, the following descriptions are all of rodents. When the telencephalic vesicles bulge from the prosencephalon, they consist solely of a single layer of neuroepithelial cells. This apparently homogenous population of cells gives rise to all the neurones and glial cells of the neocortex (Fujita, 1963; Stensaas, 1968; Hinds and Ruffet, 1971; Takahashi *et al.*, 1992; Sidman and Rakic, 1982; Bayer and Altman, 1991). Subsequent development of the cortex involves the production of at least three main cell types within the proliferative zone. These include neurones, glial cells and new progenitor cells. Neurogenesis and gliogenesis occur sequentially during development. These processes are described in more detail in the next section.

The sequence of events that leads to the production of the six layered cerebral cortex is summarised in figure 1.6. During development, the telencephalic wall becomes divided up into a number of zones. The exact role of these different zones during development has been shrouded in some confusion. This is mainly due to the fact that many different names have been given to any one particular area. A self appointed committee took it upon themselves to go some way to solve this problem by deciding, definitively, on the terminology that should be employed when describing different developmental areas of the neocortex (Boulder committee, 1970).

Figure 1.6

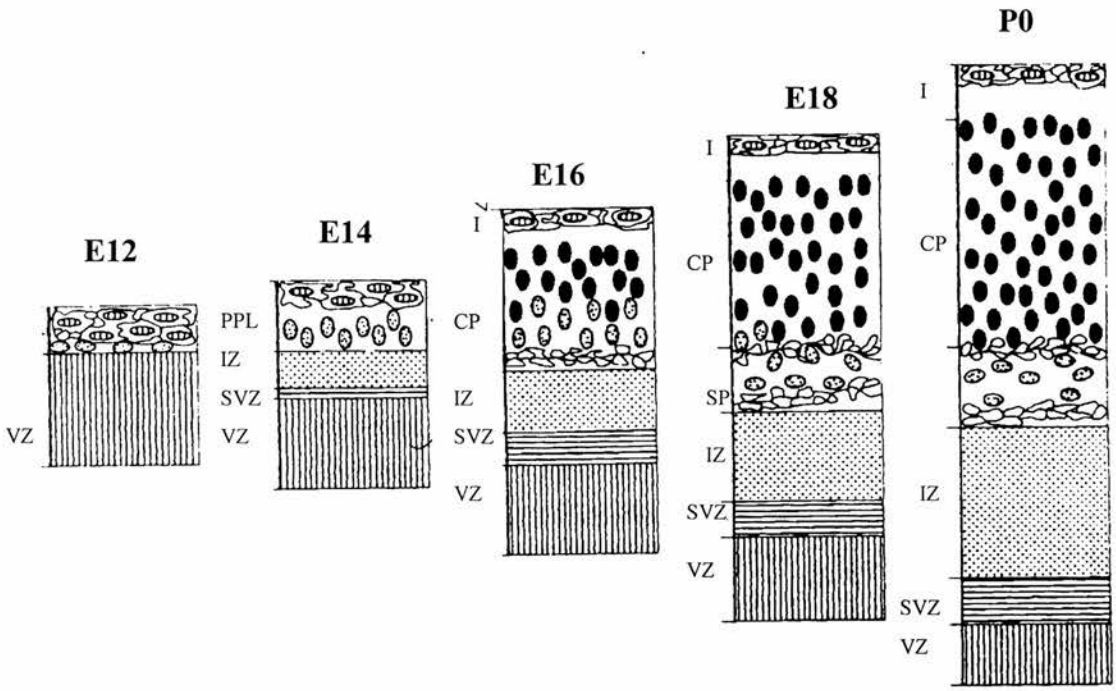

Figure 1.6.

Diagrammatic representations of how the cortical layers are formed. VZ cells dividing on E12 give rise to the PPL cells. This is split into the marginal zone (future layer 1) and the subplate by the insertion of later born cortical plate cells. Later born cells migrate through the earlier born CP cells and reside under the MZ. See main text for detail. **VZ**: ventricular zone, **SVZ**: subventricular zone, **IZ**: Intermediate zone, **CP**: Cortical plate, **PPL**: preplate, **MZ**: marginal zone. Adapted from Neocortical development by Bayer and Altman, Raven press (1991).

The first step in the lamination of the cortical wall is the division of the telencephalon into two regions, the ventricular zone (VZ) (Boulder committee, 1970) and the primordial plexiform layer (PPL) (Marin-Padilla, 1971;1978). The VZ consists of a layer of proliferating cells that lie directly above the lateral ventricle, and the PPL contains prospective Cajal-Retzius cells. Cajal-Retzius cells are born in the VZ and begin to differentiate before other cortical layers have started to form (Cajal, 1911; Uylings *et al.*, 1990). As development proceeds, cells of the VZ migrate radially towards the PPL through a region known as the intermediate zone (IZ). This is a cell sparse region containing cortical afferent and efferents.

The next zone to emerge is the sub ventricular zone (SVZ), which arises from cells of the VZ (Smart, 1972; Altman and Bayer, 1990; Halliday and Cepko, 1992; Takahashi *et al.,* 1993). The SVZ forms between the IZ and the VZ and consists of a secondary proliferative population of cells (SPP) (Takahashi *et al.,* 1995). The SVZ cells differ from the proliferative population of cells within the VZ in terms of their proliferative behaviour (see later section) and the cell type they produce. VZ cells give rise primarily to neurones whereas SVZ cells give rise primarily to glial cells. Early in embryonic development (embryonic day 12 (E12) in the mouse) the SVZ is thinner than the VZ but as development proceeds the VZ reduces in width and the SVZ increases in width. By E19, the SVZ is considerably thicker than the VZ (Bayer and Altman, 1991; Takahashi *et al.,* 1995).

Following the emergence of the SVZ cells, the VZ cells give rise to cortical plate (CP; future neocortex) cells. These cells migrate from the VZ radially through the SVZ/IZ and split the PPL into separate layers (Luskin and Shatz, 1985) by accumulating within it. The outer layer lies directly below the pia and is referred to as the marginal zone (MZ; future layer 1). The lower layer, the subplate (SP) is a transient structure (Kostovic and Molliver, 1974) containing differentiated neurones (Allendoerfer and Shatz, 1994) which lies just below the developing CP. The CP steadily thickens as subsequent waves of arriving neurones migrate through the existing cells and terminate in their final laminar position just underneath the MZ (Luskin and Shatz, 1985).

Autoradiographic experiments employing [^{3}H] thymidine have proved vital in studying the sequential manner in which the cortical layers are formed. These types of studies have shown that the earliest born neurones come to lie in the deepest layers of the cortex, while the latest born cells form the more superficial layers. Hence, the cortical layers are formed in an inside-first outside-last manner in the mouse (Angevine and Sidman, 1961) in the rat (Berry and Rogers, 1965), cat (Luskin and Shatz, 1985), ferret (Jackson *et al.,* 1984) and the monkey (Rakic, 1974). When neurones reach their appropriate laminar distribution, they complete differentiation and form the appropriate axonal connections with their target cells. There is one general exception to this inside-out rule and that is the cells of the PPL (Marin-Padilla, 1971;1978). As described earlier, cells of the PPL differentiate first out of the VZ and are split into the MZ and SP by subsequent waves of incoming neurones.

1.6 Cell proliferation and migration

The layered structure of the cortex is a result of neuronal cells at the ventricular edge migrating radially away from the VZ towards the pial edge where they differentiate into mature cell types (Angevine and Sidman, 1961; Rakic, 1972, 1974, 1988; Lund and Mustari, 1977; Smart and Smart, 1982; Jackson *et al.,* 1989; Gillies and Price, 1993; Rakic, 1977). Many techniques have been employed to study cell proliferation and migration, in particular the use of nucleotide analogues that are incorporated into newly synthesised DNA. Tritiated thymidine [^{3}H]Th and 5-bromodeoxyuridine (BrdU), which can be visualised using autoradiography or by specific antibodies (anti-BrdU), are two commonly used chemicals for these experiments.

1.6.1 Cell Proliferation

The cell cycle of eukaryotic cells consists of four distinct stages. These are (i) M phase, (ii) G1 phase, (iii) S phase and (iv) G2 phase. Sauer (1935) made the first observation that cells of the VZ were continuous from the edge of the ventricle to the lateral edge of the VZ, although the nuclei of these cells were at different heights. During the cell cycle, ventricular nuclei migrate to the outer edge of the ventricular zone during the first gap phase (G1) (Sidman et al.,1959), DNA synthesis (S phase) occurs while the nucleus is at the outside edge and the nucleus then migrates down to

the ventricular edge during the second gap phase (G2). The nucleus then undergoes mitosis (M phase). The daughter cell then either re-enters the cell cycle and migrates to the outer edge during G1 phase or becomes terminally postmitotic and migrates out to its specific laminar position within the CP. This process by which the nucleus moves throughout the cell cycle is known as interkinetic nuclear migration (Takahashi *et al.,* 1993; Berry *et al.,* 1964; Boulder committee, 1970; Misson *et al.,* 1988; Takahashi *et al.,* 1992) (figure 1.7).

Waechter and Jaensch (1972) used [^{3}H]Th in a cumulative labelling study to estimate the total length of the cell cycle. Takahashi *et al.,* (1995) did a series of complex experiments using BrdU to study the lengths of the different phases of the cell cycle within the mouse neocortex. These studies showed that there was a more than two fold increase in length of cell cycle throughout neurogenesis. Cells undergo eleven cell cycles in the cortex, which increase from 8.1 hours at E11 to 18.4 hours at E16. The only phase of the cell cycle to actually increase in length was G1 phase. The other 3 phases of the cell cycle (S, G2 and M) all remained constant throughout the period of neurogenesis.

1.6.1.2 Symmetric and asymmetric division

The concept of symmetric and asymmetric divisions within the cortex has been assumed for some time (Mione *et al.,* 1997). Symmetric cell division results in the progenitor cell dividing into two similar daughter cells (progenitor cells), whereas asymmetric cell division produces two different daughter cells (a progenitor cell and a post-mitotic cell). During embryonic development it is believed that the progenitor pool in the VZ is expanded through a series of symmetric divisions in which both the cells re-enter the cell cycle after mitosis (stem cell behaviour) (Caviness *et al.,* 1995). This stage is primarily a cell amplification stage for which a mathematical model has been proposed (Caviness *et al.*, 1995). Following the amplification step, progenitor cells undergo asymmetric divisions, with the resultant production of post-mitotic cells and new progenitor cells. This was first observed in Drosophila (reviewed in Huttner and Brand, 1997), although it has been more recently supported in the ferret by Chenn and McConnell, (1995).

Figure 1.7

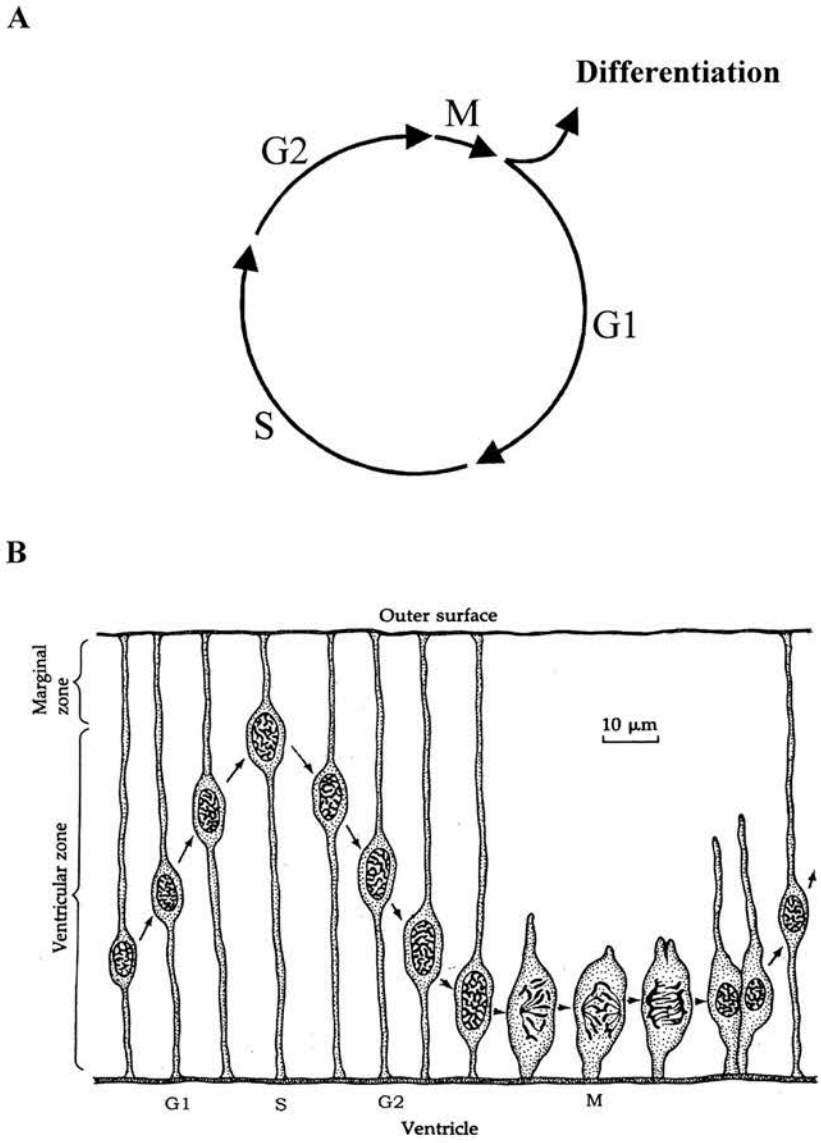

Figure 1.7.

(A) Diagram illustrating the 4 different stages of the cell cycle. The lengths of the arrows are a proportional representation of the length of each stage of the cycle.

(B) The cell cycle occurs in the neural epithelium lining the lumen of the telencephalon. During G1, progenitor cell nuclei migrate to the outer edge of the epithelium where they undergo S phase at the outer edge. During G2, the nucleus moves back to the ventricular edge where mitosis occurs (M phase) (reproduced from Purves and Lichtman).

These experimenters imaged living cells by time-lapse confocal microscopy and recorded the plane of direction in which the cells divided. Cells that divided in a vertical plane (symmetric division) had the basal part of their cell in contact with the lumen. The two daughter cells from this division gave rise to two identical stem cells. In contrast to this, cells that underwent division in the horizontal plane gave rise to two morphologically different cell types. The cell that remained in contact with the lumen gave rise to another stem cell whereas the basal cell that no longer had any contact with the ventricular edge gave rise to a migratory neurone (figure 1.8).

Recent studies have addressed the molecular consequences of asymmetric and symmetric cell divisions. Differential segregation of various genes have been shown to have important implications in specifying a cell fate. For example, in the mouse differential segregation of *M-numb* is necessary for daughter cells of asymmetric divisions to adopt distinct fates (Zhong *et al.,* 1996). Furthermore, *Notch-1* has been shown to be segregated to the post-mitotic daughter cells of asymmetric cell divisions (Chen and McConnell, 1995). However, while there is strong genetic evidence that *M-numb* directs the asymmetry of the division, there is no such strong evidence that *Notch 1* performs the same function in vertebrates.

Although the idea of symmetric and asymmetric divisions is fairly well established for early cortical neurogenesis, later neurogenesis and gliogenesis is less well understood. The idea of asymmetric versus symmetric division has important implications for the regulation of the size of specific cell populations, the generation of cell diversity among progenitors and their progeny, and the temporal sequences in which different cells are produced. For example, symmetric divisions could be used to expand certain types of cell, whereas asymmetric divisions could be used to generate cell diversity.

Figure 1.8

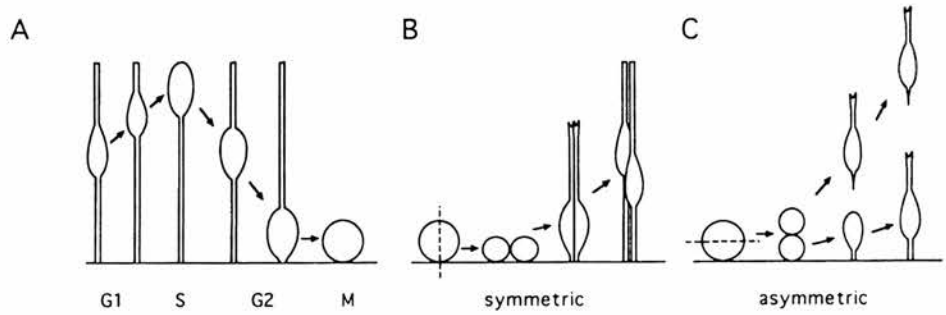

Figure 1.8.

Diagram illustrating asymmetric and symmetric cell division within the ventricular zone of the developing cortex. The orientation at which a progenitor cell undergoes its division, is a process involved in cell fate specification.

(A) Shows mitosis occurs at the ventricular edge.

(B) Shows a cell undergoing a symmetric division (cleavage plane is perpendicular to ventricular edge). Symmetric divisions replenish the progenitor pool.

(C) Shows a cell undergoing mitosis in the plane parallel to the ventricular zone. This is asymmetric division and gives rise to two daughters of different cell fates, usually a postmitotic neurone and an additional progenitor cell.

(Reproduced from Chenn and McConnell, 1995).

1.6.2 Cell migration

Mechanisms of cell migration have been hypothesised for over a hundred years but only with the development of techniques such as electron microscopy and tritiated thymidine autoradiography ([^{3}H]Th) has the processes begun to be fully understood. The majority of neurones reach their final laminar destination by migrating radially along radial glial processes (Rakic, 1972; 1988; 1990; Hatten, 1990). As cells become postmitotic, they attach to radial glial cells and migrate in a direction specific manner, the mechanism of which is unclear. Once neuronal migration is complete, radial glial cells transform into astrocytes (Schmeckel and Rakic, 1979; Levitt and Rakic, 1980; Voight, 1989; Cullican *et al.*,1990; Takahashi *et al.*, 1990; Misson *et al.*, 1991). Recent evidence has suggested that radial glial cells may also be precursors for neuronal cells (Gotz, 1999 unpublished observations).

1.7 Cell types

Within the CNS, there are 2 main classes of cells; neurones and glial cells.

1.7.1 Neurones

Neurones, although the minority in cell number throughout the cortex are much better understood than any other cell type. Originally neurones were thought to be the main cell type, and of greater functional importance (electrical transmission of information). Their stereotypical biochemical properties (MAP2 (micro-tubule associated protein 2) and tau) and anatomy (cell body, axon and dendritic processes etc), contributed to the ease with which they could be investigated. In general, within the cortex, the cell bodies of neurones have a variety of shapes, although two main types can be distinguished in all areas of the cortex: pyramidal and non-pyramidal. Individual layers of the cortex do not contain equal proportions of pyramidal and non-pyramidal cells, and the type of cell that predominates in a layer provides information about the specific function of that layer. For example, layers rich in pyramidal cells are predominantly output layers, whereas layers with more non-pyramidal cells are the principal sites of afferent inputs.

1.7.2 Glial cells

The second cell type within the CNS are the glial cells. There are more than ten times as many glial cells in the brain as there are neurones, yet they are very much less understood. Difficulty in studying these cells has contributed in part to this lack of understanding. Unlike neurones, glial cells do not have stereotypical biochemical properties (few early glial specific markers) and they continually proliferate and migrate making studying them with DNA analogues difficult. In addition to this the functions of glial cells have been very much underrated and hence perceived as less interesting to study.

The term glia is a greek word meaning "glue" which arose from the observation that glial cells surround and appear to bind the CNS together. It is now widely accepted that the main roles of glial cells are to provide a suitable environment for the development and maintenance of neurones. This includes processes such as myelination, support and guidance for migrating cells and control of ionic composition of cells.

There are two major classes of glial cells: microglia and macroglia. The microglia are phagocytes that are mobilised after injury, infection and disease. They are unrelated to the other cells of the nervous system in that they are derived from macrophages. The microglia are not considered any further throughout this thesis. The macroglia consist of two main types: astrocytes and oligodendrocytes (figure 1.9). Oligodendrocytes are the best characterised of the glial cells. These cells are the myelinating cells of the CNS, and they wrap themselves processes around axons to form a sheath, which is essential for promoting rapid nerve impulse conduction.
Astrocytes are the most numerous of the macroglial cells, yet the least understood. They are known to take up neurotransmitters, have a nutritive function, and are able to buffer K+ ions around highly active neurones. In addition to these functions, reactive astrocytes are also produced in response to injury, although their exact roles are not fully understood. Furthermore astrocytes may act as neural stem cells in the adult brain which could have important implications for the repair of damaged tissue (Doetsch *et al.,* 1999).

Figure 1.9

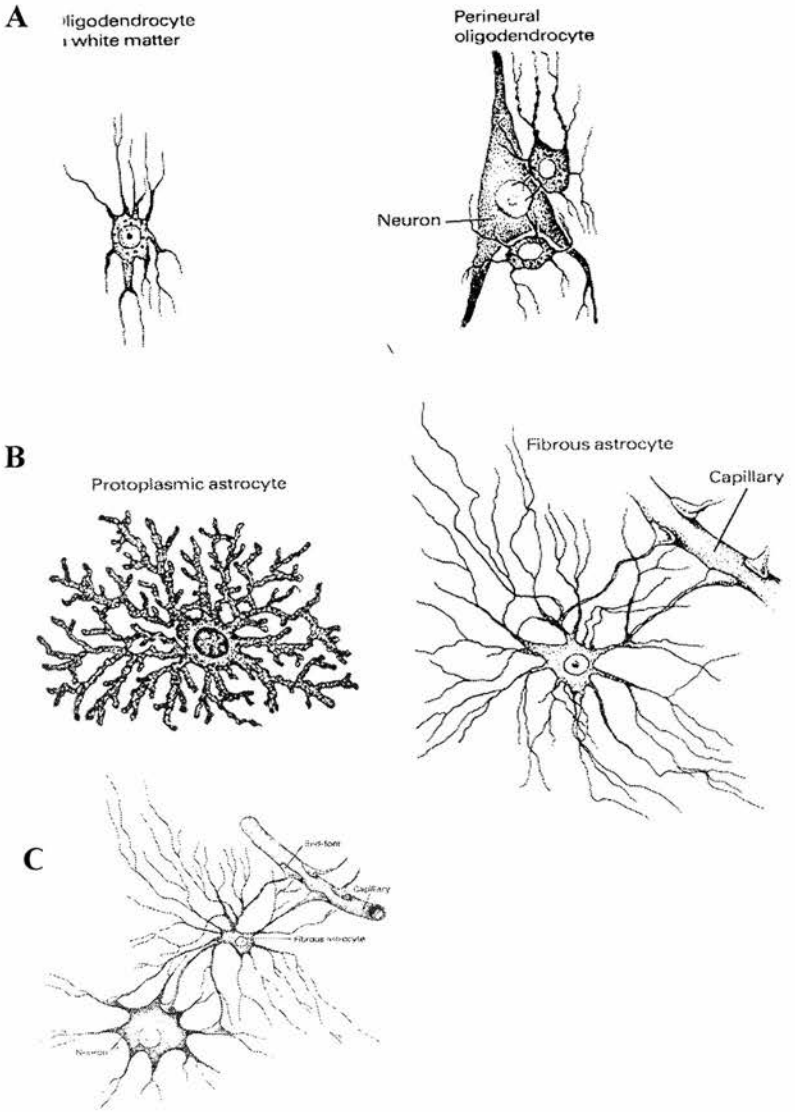

Figure 1.9. Diagram illustrating the two main types of macroglia in the nervous system, the oligodendrocytes and astrocytes.

(A) Oligodendrocytes have few processes, and they form myelin sheaths around the axons of nerve cells.

(B) Astrocytes are star shaped and can be either fibrous (white matter), or protoplasmic (grey matter).

(C) Astrocyte making contact with blood vessels and neurones showing its role of nutrient provision and support. (Taken from Kandel *et al.,* 1991).

1.8 Glial cell development

Unlike neurogenesis, the pattern of colonisation of the cerebral hemispheres by glial progenitors is not well understood. Glial cells share a common embryonic origin with neurones, both of which arise from undifferentiated neural precursors in the germinal layers of the developing brain (SVZ and VZ respectively). Therefore, as cells within the germinal layers proliferate, migrate and differentiate, a series of decisions have to be made in order for a cell to follow a specific developmental pathway (neuronal or glial).

Although many studies have examined neuronal cell lineages (see next section), glial cell lineage studies have been notoriously difficult to study. This is due partly to the lack of glial specific markers (Cameron and Rakic, 1991) and partly to the proliferative nature of glial cells which results in the dilution of cell dyes commonly used in these studies.

The traditional held belief is that the main wave of gliogenesis occurs after cortical neurogenesis is complete, occurring during late gestation in many species. In brief there are two stages of astrocyte production followed by a wave of oligodendrocyte production. After neuronal migration is complete radial glial cells transform into astrocytes (Goldman and Vayese, 1991; Cameron and Rakic, 1991; Misson *et al.,* 1991; Culican *et al.,* 1990; Takahashi *et al.,* 1990; Voight, 1989; Schmechel and Rakic, 1979). A second wave of astrocyte generation occurs when cells of the SVZ begin to proliferate and produce a population of astrocytic precursor cells (Zerlin et al., 1995; Levison and Goldman., 1993; Goldman and Vayese., 1991). Following this wave of astrocyte production, oligodendrocytes are generated from precursors in the SVZ (Levison and Goldman., 1993). These oligodendrocyte precursors migrate into the IZ and CP, divide again and then differentiate (Goldman and Vayese., 1991 Zerlin and Levison., 1995). Generally there appears to be a switch from the predominant production of neurones to the predominant production of glial cells.

1.9 Progenitor cells

For a better understanding of the development of cell diversity within the cortex it is important to characterise the different populations of neural progenitor cells within the VZ and SVZ. More importantly is to understand the different types of progeny that a progenitor cell can generate. In addition to this, identifying factors that regulate events of progenitor cell development such as proliferation, differentiation and death are important in allowing a fuller understanding of how these cells build up the mature nervous system.

1.9.1 Classification of neural progenitor cells

The process of generating distinct types of neurones and glial cells from progenitor cells at particular times is thought to involve a sequence of progenitor cell states that are controlled by environmental and cellular regulatory molecules.

Neural progenitors fall into three main categories:- 1) progenitors that produce only neurones (neuroblasts), 2) progenitors that produce only glial cells (glioblasts) and 3)progenitors that can generate both neurones and glial cells (multi-potential). Both neuroblasts and glioblasts have the capability to be multipotential in which case they can produce more than one type of neurone or glial cell (figure 1.10). The relationships between these types of progenitor cells and the timing of their generation is yet to be fully elucidated.

Different regions of the developing CNS are known to have different populations of the above three types of progenitor cells. Within the cerebral cortex the general belief is that multipotential neuronal/glial progenitors are rare, with the majority of progenitor cells producing clones consisting of either neurones, astrocytes or oligodendrocytes (Williams and Price, 1995; Reid *et al.,* 1995; Goldman and Vayesse, 1991; Grove *et al.,* 1995; Rao *et al.,* 1997).

1.9.2 Production of various cell types (lineage studies)

Much of the work done on the study of progenitor cells and the cell types which they produce has come from lineage studies. The lineage of a cell is a description of its

ancestry. In simple organisms such as the nematode *Caenorhabditis elegans* cell lineage can be traced by simple observations of the developing embryo. However, in more complicated organisms these simple observational studies of cell lineage are not possible.

Cell lineage studies within the cerebral cortex are far from straightforward. Firstly, progenitor cells cannot be directly observed *in vivo* as they can in simple organisms such as *C.elegans*. Secondly, there are no morphological differences between neuronal or glial progenitors, making identification of specific cell types difficult. Thirdly, continual mitosis of cells makes dye labelling of progenitor cells difficult due to the dilution of the dye. This begs the question "how do you follow the ontological fate of a progenitor cell?".

The earliest tools used for cell lineage studies within the cerebral cortex were genetic chimeras. Such studies involved mixing cells from different species and identifying them histologically (Fishell *et al.,* 1990). An improved method of this type of experiment was used by Tan and Breen (1993) who developed a transgenic mouse carrying a ß-galactosidase transgene in the X chromosome. An alternative method involves the use of retroviruses. These viruses integrate into the genome of specific mitotic cells (Varmus, 1988) and proteins are expressed in cell progeny. These types of study have suggested that progenitors produce either similar neuronal cells, (Parnavelas *et al.,* 1991; Grove *et al.,* 1993; Luskin *et al.,* 1993; Mione *et al.,* 1994), or glial cells (Luskin *et al.,* 1988, 1993; Goldman and Vayesse, 1991; Grove *et al.,* 1993). However, it has been shown that a proportion of cortical progenitors are multipotential and produce diverse cell types (Price and Thurlow, 1988; Walsh and Cepko, 1988).

In addition to the above experiments, lineage analysis studies have been important in studying the migratory pattern of cells. Some of the earliest studies in the cortex show that clones of cells that descended from a single progenitor cell can spread laterally over distances of 500µm (Luskin *et al.,* 1988; Price and Thurlow, 1988; Walsh and Cepko, 1988) or greater (Reid *et al.,* 1995).

1.9.3 Proliferative behaviour of progenitor cells

In addition to the cell type into which a progenitor cell differentiates, progenitor cells can also be classified according to their proliferative behaviour. *In vivo* (genetic manipulations, transplant studies) and *in vitro* studies (exposure to specific signals or co culturing techniques) have revealed that most progenitor cells go through a limited number of cell cycles before differentiating into their final phenotype. However, it has also been shown that a small number of cells continually divide (Stemple, 1997). A cell that continually divides and is capable of self renewal, is referred to as a stem cell.

Progenitor cells have been shown to have a range of phenotypic potentials, which range from highly restricted to multi-potential. Lineage restricted progenitors cells have been shown to derive from multi-potential stem cells, although the mechanism of this is unknown. Other studies have suggested that environmental signals may act to promote the differentiation of stem cells into neurones or glia by initially producing a mitotic, intermediate progenitor cell. However, it is not clear whether the generation of specific types of differentiated cells involves lineage-restricted intermediates or if it can occur directly from stem cells.

Figure 1.10

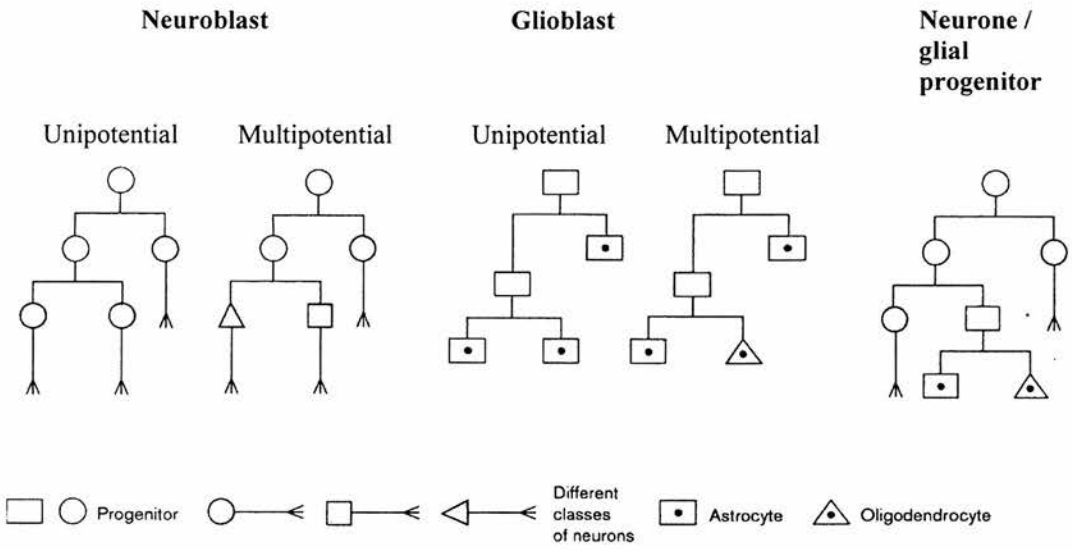

Figure 1.10.

Illustration of the different classes of neural progenitor cells in the developing nervous system. Neuroblasts and glioblasts can be either mulitpotential or unipotential. Neuro/glial precursors are multipotential and can produce either multipotential or unipotential neuroblasts or glioblasts. Diagram adapted from Temple and Qian, (1996).

1.10 What determines cortical cell fate?

Determining the factors involved in cell fate specification is vital to our understanding of how cell diversity is achieved within the brain. It is likely that the production of cell diversity is influenced by a combination of intrinsic and environmental factors (see reviews by Reh and Cagan, 1994; Jan and Jan, 1995). It is well established that progenitor cells within the proliferative regions of the developing cortex are able to generate neurones, astrocytes and oligodendrocytes. However, it is not clear to what extent these fates are specified intrinsically i.e. a particular neurone's genetic repertoire is selected very early in neurogenesis, or is specified extrinsically i.e. a nascent neurone or glial cell has the ability to alter its phenotype in response to local soluble factors.

For the purpose of this thesis, experiments focused on the study of cell fate decisions in relation to neuronal versus glial cell differentiation. There are a variety of questions that arise regarding cell fate specifications. Questions that remain unanswered include 1) how does a ventricular zone cell know to initially become a neurone and later become a glial cell? 2) are all progenitor cells predetermined? Although some studies have begun to elucidate the role of various environmental factors in neuronal and laminar specification there is very little known about the events that promote the differentiation of neural progenitors into neurones or glia. The main aim of this thesis is to try and elucidate the mechanisms by which a progenitor cell makes the decision to differentiate into either a neuronal or a glial cell.

1.11 Neuronal/glial switch

As described earlier all neurones and glia arise from a common ancestry within the VZ. It is likely that a combination of intrinsic and extrinsic processes is involved in neuronal/glial cell fate decisions. Furthermore, because neurogenesis and gliogenesis are traditionally thought to be sequential rather than concurrent, it is possible that the repertoire of cell fate determining factors that influence progenitor cells in their cell fate decisions are altered over time.

1.11.1 Intrinsic mechanisms

In Drosophila, much is known about the genes that control the development of the specific patterns and identities of neurones, but less is known about the genes that control of glial cell identity. Neurogenesis is known to require activation of neuronal determination genes and inactivation of other genes. Tanabe and Jessel, (1996) showed that for neuronal determination it was necessary for the activation of the *achaete-scute* complex whereas Schoenherr and Anderson, (1995) suggested that there was inactivation of neurone restrictive silencer factor (NRSF), a gene that negatively regulates the neuronal phenotype (Anderson 1995).

Schoenherr and Anderson (1995) suggested that gliogenesis is the result of two co-operative processes: 1)activation of a neuronal repressor and 2) activation of glial specific genes. In Drosophila both of these processes have been shown to be under the control of just one gene, glial cells missing (*gcm*) (Hosoya *et al.,* 1995; Jones *et al.,* 1995). The presence or absence of *gcm* determines the choice between neuronal and glial fates. Furthermore Vincent *et al.,* (1996) suggest a role for *glide* (glial cell deficient) in glial cell fate commitment, although this was later shown to be the same gene as *gcm*. The idea that a single gene can control a choice between neuronal and glial lineages is not unprecedented. Condron *et al.,* 1994 showed in the grasshopper CNS that the engrailed gene is required for early neuronal to glial fate transition of midline glia, whereas activation of protein kinase A is responsible for the glial to neuronal fate transition (Condron and Zinn, 1995).
Mammalian homologs of the Drosophila *gcm* gene have been characterised, *gcm1* and *gcm2* (Kim *et al.,* 1998). The expression pattern of these two genes appears to be non-neural, suggesting that the functions of the homologs have diverged and diversified.

Recently RNA binding proteins have been shown to play a possible role in neuronal/ glial cell fate decisions. Hardy (1998) has suggested a role for QK1, an RNA binding protein in the neuronal/glial switch. This QK1 protein is present in all neural progenitor cells of the spinal cord. QK1 expression is down regulated as the progenitor cells leaves the cell cycle and differentiates into a neurone. In contrast to

this, cells that follow the glial lineage maintain QK1 expression as they migrate away from the VZ. This paper not only suggests a role for QK1 in neuronal/glial switch cell fate decisions, but also implicates a role for QK1 as a marker of early glial cells (Hardy, 1998). Furthermore Sakakibara and Okano, (1997) have suggested that the M-msi family of RNA binding proteins have a regulatory role in neuronal/glial switch mechanisms.

1.11.2 Extrinsic mechanisms

Extrinsic mechanisms have also been implicated in neuronal / glial cell fate decisions. There is evidence to suggest a role of extrinsic cues/exogenous factors that influence the proliferation and differentiation of progenitor cells into neuronal rather than glial cell types. For example, basic fibroblast growth factor (bFGF) has been demonstrated to be mitogenic for multi-potential precursors in the forebrain Johe *et al.,* 1996; Gritti *et al.,* 1996; Qian *et al.,* 1997). Recently, it has been suggested that different concentrations of bFGF can determine whether neurones or glial cells are formed from the mulitpotential cells. Furthermore, Gross *et al,* 1996 showed that bone morphogenetic proteins (BMPs) promote glial cell differentiation rather than neural cell differentiation, likewise Bonni *et al.,* 1997 have shown a similar role for ciliary neurotrophic factor (CNTF).

1.12 Aims and objectives of this study

The main aims and objectives of this were to investigate mechanisms involved in neuronal/glial cell fate decisions. Although it is well established that neurogenesis occurs in early embryogenesis, whereas most gliogenesis occurs postnatally, there is no literature to state exactly when the last neurones are born and gliogenesis begins. This has been due in part to problems of identifying early progenitors destined for a glial fate. However, using the recently characterised QK1 antibody the embryonic timings of the switch over period between neurogenesis and gliogenesis were determined.

The first part of this study involved following the populations of cells born on E18, E19 and P0 using BrdU as a marker of cell proliferation and various antigenic markers of specific cell types. The migratory pattern and differentiation of these cells was followed in order to determine the exact time when neurogenesis ended and gliogenesis began in the mouse neocortex.

The second stage of the study was to determine if cortically derived soluble factors had an effect on the behaviour of progenitor cells. This was addressed *in vitro* using a cortical explant culture technique. This chapter was complimented by a transplant study in which the identity of glial progenitors was challenged by transplanting them into different environments and following their behaviour *in vivo.*

Finally the expression pattern of a novel RNA binding protein isolated from an oligodendrocyte subtractive library was characterised. RNA binding proteins have previously been shown to be involved in neuronal / glial cell fate decisions. Therefore it was important to characterise this novel RNA binding protein to determine if any insight could be gained into its role in cell fate decisions.

1.13 Standardisation of embryonic ages

Most of the work carried out in this thesis was done on embryonic mice. There are two different methods used to determine the exact age of the embryo. The day of the vaginal plug can be referred to as embryonic day 1 (E1) or embryonic day 0 (E0). In this study we deemed our mice E1 on the day of the plug. In studies that I have described throughout this thesis in which the animals were deemed E0 as the day of the plug, I have adjusted the ages accordingly to fit in with the system used here.

1.14 Overview of chapters

The following is a brief explanation of the work carried out in each chapter of my thesis.

Chapter 2

The main aim of this chapter was to determine the events that occurred at the end of neurogenesis and the beginning of gliogenesis in the developing mouse neocortex. This was achieved by labelling cells with BrdU between E18 and P0, and following 1) their migratory pathway and 2) determining the cell type into which they differentiated.

Chapter 3

The purpose of these experiments was to determine if cortically derived diffusible factors had an effect on the behaviour of progenitor cells in the neocortex. This was studied using an explant culture technique.

Chapter 4

In this chapter the role of the cellular environment on cell fate decisions was investigated *in vivo*. This was studied using a transplantation technique.

Chapter 5

Novel proteins that may be involved in cell fate specification were sought in an oligodendrocyte subtractive library. A novel clone was isolated and its expression pattern examined during embryonic development.

CHAPTER 2: THE TRANSITION FROM NEUROGENESIS TO GLIOGENESIS IN THE DEVELOPING MOUSE NEOCORTEX.

2.1 Abstract

In the developing mouse cerebral cortex, the process of neurogenesis is well characterised but the timing and location of proliferation of the glial cells is not. Radial glial cells are the earliest-born glial population and are present during neurogenesis. Other glial cell types such as astrocytes and oligodendrocytes are thought to appear after neuronal generation is complete.

To determine when astrocytes and oligodendrocytes first proliferate and differentiate in the mouse neocortex, cells proliferating at the end of cortical neurogenesis from embryonic day eighteen (E18) to birth were studied. These cells were labelled with 5-bromeodeoxyuridine (BrdU) and the density and distribution of these cells was studied over a 20 day period. Their fates were also examined using immunocytochemical markers of glia.

These data suggest that cells labelled on E18 give rise to both neuronal and glial precursors whereas cells born on E19 and the day of birth give rise solely to glial precursors. Based on their expression of specific markers the results suggest that these glial precursors give rise to both astrocytes and oligodendrocytes.

2.2 INTRODUCTION

To address the mechanisms of neuronal/glial cell fate decisions in the mouse neocortex, it is essential to know the time at which gliogenesis starts and neurogenesis finishes. Since the literature on the events during this transition period is very limited, this study was intended to provide a clear picture of events over this time period.

As described in the main introduction of this thesis, neuronal and glial progenitors are located in two proliferating zones, the ventricular zone (VZ), which directly lines the cerebral ventricles, and the adjacent subventricular zone (SVZ) (Boulder Committee, 1970; Schmechel and Rakic, 1979; Sidman and Rakic, 1982; Levison and Goldman 1993; Takahashi et al, 1993, 1994). Within these two proliferative regions there are two distinct populations of cells which for the purpose of this study are referred to as the pseudostratified ventricular epithelium (PVE) and the secondary proliferative population (SPP) (Takahashi *et al.,* 1995). The PVE lies immediately adjacent to the ventricle and is present from the outset of the evagination of the cerebral hemispheres. The position of the PVE corresponds closely to that of the VZ. Cells of the PVE give rise to the majority of neurones and also to radial glial cells. The SSP arises from the primordial PVE (Smart, 1972; Altman and Bayer. 1990; Halliday and Cepko, 1992; Takahashi *et al.,* 1993), but tends to have a much more widespread distribution than that of the PVE. The SPP extends from the interface of the VZ and SVZ outwards across the width of the intermediate zone (IZ) to the base of the developing cortical plate (Takahashi *et al.,* 1993), giving rise to the glial cells of the cerebral cortex (Smart, 1961; Smart and Leblond, 1961; Patterson *et al.,* 1973; Privat, 1975; Marres and Bruckner, 1978; Todd and Smart, 1982; Levine and Goldman, 1988; Levinson and Goldman, 1993).

Cells of the PVE undergo an interkinetic movement as they progress through different stages of the cell cycle (Sauer, 1935; Sauer and Walker, 1959; Sidman *et al.,* 1959; Fujita, 1960, 1963), whereas cells of the SPP do not (Takahashi *et al.,* 1992).

In the mouse the SPP arises out of the PVE by E14 and increases massively in size due to repeated cell division near the end of neurogenesis (Sturrock and Smart, 1980; Takahashi *et al.,* 1995). The increase in size of the SPP is coincidental with a corresponding decrease in size of the PVE. By E18 cells of the PVE undergo their final round of mitosis (Caviness *et al.*, 1995; Polleux *et al.*, 1997). This is reflected in the disappearance of the VZ. Hence, this period at the end of neurogenesis and the beginning of gliogenesis is one of great change. This can be clearly seen when considering the PVE and SPP at this time.

An understanding of the mechanisms that regulate the switch from neurogenesis to gliogenesis requires a detailed description of the events that occur at this time as well as reliable markers for the different cell types formed. Although there have been several studies on postnatal gliogenesis in the mouse (Smart, 1961) and the rat (Altman, 1966; Levison *et al.*, 1993; Zerlin *et al.*, 1995;Lewis, 1968; Patterson *et al.,* 1973; Privat and Leblond, 1972) there have been very few studies on embryonic gliogenesis. With the exceptions of Gressens *et al.* (1992) who studied this population of cells in the mouse and Berman *et al.* (1997) who reported findings in the ferret, there is very little literature on the development of cells that are undergoing mitosis towards the end of neurogenesis.

Early glial cell development is notoriously difficult to study, and information on this area is still deficient in many respects. Studies which have relied on morphological criteria to study developmental fates of immature glial cells proved largely unsuccessful because it was not possible to assign immature cells to specific lineages. Problems of identifying early progenitors destined for a glial fate have seriously hampered the study of gliogenesis. Most of the genes known to be specific for different glial subtypes are expressed at later stages of development, often in terminally differentiated cells. For the later stages of glial cell development when more cell specific markers are available, cell identification was possible, but it remained difficult to determine lineage relationships between the various cell types (Levine and Goldman, 1988; Levitt *et al,* 1981).

Studies that are involved in the successive timing of gliogenesis often involve the use of nuclear markers such as [^{3}H] thymidine. This has not been without problems. There is a long delay between the origin of cells and the time at which they reach their final state of differentiation. During this period cells normally undergo several rounds of cell division, resulting in dilution of the label to below detectable levels. Other difficulties stem from the fact that neuronal cells are in much greater numbers at this early stage. This had a shielding effect and tended to conceal the glial cell population. Additionally, migration of neuronal precursors into the cortical wall has been well documented (Angevine and Sidman, 1961; Berry *et al.,* 1964; Caviness and Sidman 1973; Luskin and Shatz, 1985), whereas glial cell migration has not (reviewed in McConnell, 1995). All of the above problems have seriously hampered our knowledge and understanding of the mechanisms by which glial cell differentiation occurs.

To overcome the lack of early marker problem the recently characterised anti-QK1 antibody (Hardy, 1998), was used to label early glial progenitor cells. QK1 proteins are expressed in postnatal glial cells (Hardy *et al,* 1996; Hardy, 1998) and also neural progenitors of the VZ. As cells start to differentiate and follow the neuronal cell lineage, QKI expression is down regulated, but if cells differentiate into cells of the glial lineage QKI expression is maintained (Hardy, 1998).

2.2.1 Study

5-bromo-2-deoxyuridine (BrdU) was used to label cortical cells in S phase and the distribution of the cells was compared with the distributions of cells labelled with BrdU on E16 - E19 and postnatal day 0 at one hour post-injection and at later postnatal ages. The antigenic properties of these cells was investigated by using a double labelling protocol with BrdU and either 1) glial fibrillary acidic protein (GFAP), a marker of cells of the astroglial lineage, (Choi, 1988) 2) CNPase, a marker of oligodendrocytes, (McEwan, 1996) 3) QK1, a marker of glial progenitors and mature glia (Hardy, 1998) and 4) MAP2, a neuronal specific cytoskeletal marker (Bernhardt and Matus, 1984; Caceres *et al.,* 1984).

2.2.2 Summary of results

The results showed that cells dividing on E18, E19 and P0 have different distributions patterns to those dividing on E16 and E17. The E16 and E17 cells proliferate almost entirely within the VZ, whereas those dividing on E18, E19 and P0 do so within the VZ/SVZ, the IZ and, to a small extent, the CP itself. In addition, cells labelled with BrdU on E16 and E17 undergo interkinetic migratory behaviour within the proliferative zone, whereas cells labelled on E18, E19 and P0 do not.

Cells labelled with BrdU on E18 gave rise to two separate populations of cells. A substantial proportion of these cells migrated to the upper cortex, just below the marginal zone (MZ) by early postnatal ages. These cells were negative for QK1, GFAP and CNPase, and along with their morphology this suggested that they were neurones. The remaining population of E18 labelled cells remained within the VZ/SVZ, white matter (WM) and deep cortical plate (CP). Some of these cells expressed GFAP and QK1, indicating that they were glia. The E19 and P0 labelled cells did not form a band of cells under the MZ, but were more diffusely distributed throughout the whole cortical width. The great majority of these cells were QK1 positive, although a few were GFAP positive. This chapter provides evidence that cells generated on E18 give rise to both neurones and glial cells whereas cells generated on E19 and P0 give rise almost exclusively to glial cells or glial progenitors.

2.3 MATERIALS AND METHODS

2.3.1 Animals

C3H mice from an inbred laboratory colony were mated overnight and the following day was deemed embryonic day 1 (E1). BrdU was injected (i.p.) in saline solution (50μg g^{-1}) into pregnant mice at midday on E16, E17, E18 or E19, or into P0 pups. The tissue was analysed at 1 hour, 2, 5, 9 and 20 days post-injection. At each of these times, four pups from two separate litters injected at each age were reacted immunohistochemically either singly for BrdU or for BrdU and one of the following: GFAP, CNPase, MAP2 or QK1.

2.3.2 Dissections and tissue preparation

Embryonic mice brains were obtained by Caesarean section from pregnant females deeply anaesthetised with 0.35 ml 25% urethane in saline (i.p). The brains were removed from the skulls and fixed in 4% paraformaldehyde in 0.1M phosphate buffered saline (PBS) overnight. Postnatal mice were deeply anaesthetised with sodium pentobarbitone (6μg g^{-1}, s.c) and were fixed by transcardial perfusion for 5 minutes with 4% paraformaldehyde followed by overnight immersion in the fixative. The brains were rinsed and stored in PBS at 4^{o}C.

2.3.3 Tissue processing

Brains were embedded in paraffin wax using an automated tissue processor. This was a 17 hour cycle in which brains were dehydrated through an alcohol series from 50% to 100% ethanol, followed by 4½ hours in xylene. The brains were sectioned at 10μm in the parasagittal plane and mounted onto poly-L-lysine coated slides.

2.3.4 Cortical stratification

The cortical wall changes throughout development. It increases in width and the width of individual zones alters over time. To examine the extent of these changes the parasagittal sections used in the cell distribution analysis were de-coverslipped (after the BrdU analysis had been done) and heavily counterstained with cresyl violet. Camera lucida drawings were made of the cortical wall and the specific zones

within it using a Leitz Laborlux S light microscope and camera lucida drawing tube at x10 magnification.

The different cortical zones (VZ, SVZ, IZ, WM, CP and MZ) were identified by their location and density of cells within them. At each age studied, three different brains, and three different parasagittal sections from each brain were drawn. In each section, three lines were drawn 250μm apart at 90^0 to the VZ and the individual zones were marked. The first line was drawn at the junction between the cortex and striatum, and the following two lines were drawn a further 250μm and 500μm in the caudal direction. The width of the individual zones was calculated using UTHSCASA image tool for Windows. The average width of each zone was taken to be the average width of the three animals. These measurements were plotted against age to reveal the changing stratification of the wall and the average width of each zone.

2.3.5 Cell distribution / counts

To estimate the number of BrdU labelled cells in each cortical region, camera lucida drawings were made of the positions of dark and light labelled cells (distinguished as described in Results) within a 0.5mm wide (in the parasagittal plane) radial strip through the cortex, as shown in figure 2.1A. Four non-consecutive parasagittal sections approximately one third of the distance from the midline to the lateral edge of the brain were chosen from the dorsal cortex of each brain corresponding to figure GD18 SAG 7 Shambra *et al.* (1992) in Atlas of the Prenatal Brain (appendix 1). These sections were easily identifiable due to the presence of the lateral ventricle, choroid plexus and striatum (globus pallidus and caudate putamen). This procedure was performed on E16, E17, E18, E19 and P0, one hour post injection and on E18, E19 and P0 injected animals 2 days, 5 days, 9 days and 20 days post injection (Table 1). In each of these strips, cell numbers were obtained from counts of cell profiles after correcting according to the method of Abercrombie (1946). To correct the cell profile number according to Abercrombie, the lengths of a random sample of BrdU labelled nuclei throughout the width of the cortex was measured at x100 magnification. For each age of injection approximately 500 cells were measured. The average number of cells per cortical zone was plotted against cortical zone. In

addition, the radial strips were divided into ten bins of equal depth, from ventricular edge to pial edge, and the average number of cells in each bin was plotted against bin number.

2.3.6 Expansion factor

Since total cell counts were made in a bin of constant width (500 μm) and thickness (10 μm), the rostrocaudal and mediolateral expansion of the cortex that occurs over time had to be accounted for. To do this, the expansion in these directions was calculated and the + 2d counts were divided by the expansion factor to predict an expected value for the + 5d, + 9d and + 20d counts.

To calculate the extent of expansion of the cortex in these directions the distance along the pial edge and ventricular edge (as illustrated in figures 2.1A and 2.1B) was measured in four equally spaced parasagittal sections and four equally spaced coronal sections at each age studied (figure 2.1C). The mean value of these distances was calculated at each age and used to calculate a series of expansion factors between the different ages of the brain studied. A similar method has been used by Price *et al.,* 1997).

2.3.7 Immunocytochemistry

2.3.7.1 BrdU

Sections were incubated for 25 minutes at 37^0 C in 0.1% trypsin in 0.1% $CaCl_2$, rinsed twice in tris buffered saline (TBS) containing 0.2% Triton X-100 (TBS-T) and then immersed in 1N HCl for eight minutes at 60^0 C. Sections were rinsed in dH_20, followed by TBS-T and incubated in a blocking solution of TBS-T containing 20% normal rabbit serum for 40 minutes. This was replaced with primary mouse anti-BrdU (Becton Dickinson; 1:200) for 1 hour at room temperature (RT). Following three washes in TBS-T the sections were incubated in biotinylated rabbit anti-mouse Ig antibody (Dako:1:200) for 30 minutes at RT. BrdU labelled cells were revealed using the peroxidase method and sections were counterstained in cresyl fast violet

Figure 2.1.

Schematic diagrams illustrating how measurements of cell distribution and cortical expansion were made.

(A) Cell distribution was measured in parasagittal sections in a 500μm wide bin spanning the entire width of the cortical wall. Cortical expansion was estimated by measuring the length of the ventricular and pial edges (as indicated between the lines) of the cortex in four equally spaced parasagittal **(A)** and four equally spaced coronal **(B)** sections as indicated in **(C).** See main text for details.

Ctx: Cortex; **cp**: caudate putamen; **Th**: Thalamus; **OB**: Olfactory bulb; **R**:Rostral; **C**: Caudal; **L**:Lateral.

Figure 2.1

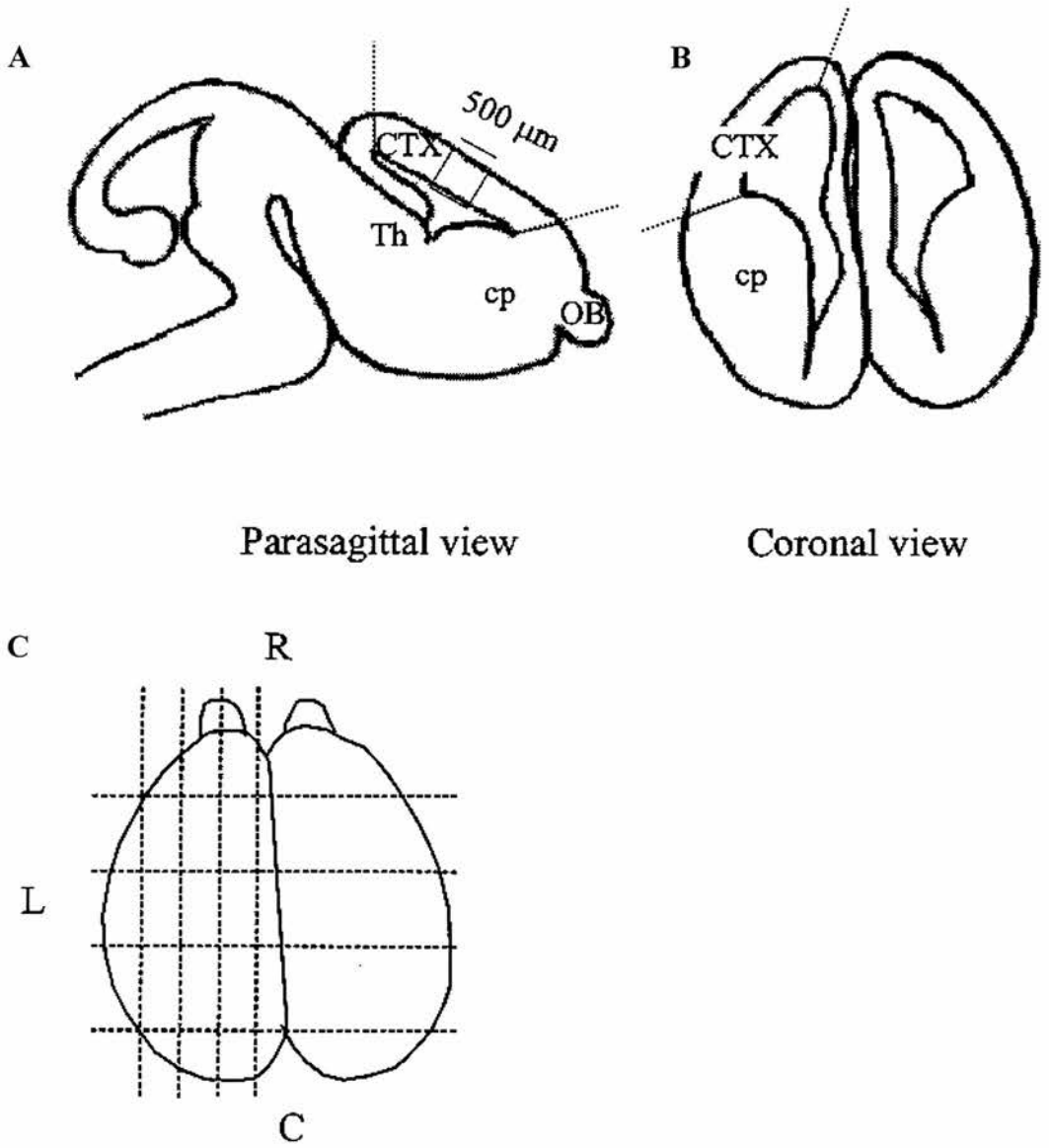
A
500 μm
CTX
Th
cp
OB
B
CTX
cp
Parasagittal view
Coronal view
C
R
L
C

TABLE 2.1

Age and time of BrdU injection	Time interval between injection and fixation	Number of litters	Number of brains analysed
E16 Midday	1 hour	3	5
E17 Midday	1 hour	2	3
E18 Midday	1 hour	4	6
E18 Midday	2 days	4	4
E18 Midday	5 days	4	4
E18 Midday	9 days	4	4
E18 Midday	20 days	4	4
E19 Midday	1 hour	4	4
E19 Midday	2 days	4	4
E19 Midday	5 days	4	5
E19 Midday	9 days	4	4
E19 Midday	20 days	4	4
P0 Midday	1 hour	3	4
P0 Midday	2 days	4	4
P0 Midday	5 days	4	4
P0 Midday	9 days	2	2
P0 Midday	20 days	4	3

Table 2.1. Summary of the experimental protocol, indicating the time at which the BrdU was administered, the time at which the tissue was fixed and processed, the number of litters that were used and the final number of brains that were analysed.

2.3.7.2 Brd-U and GFAP or QK1

Sections were incubated in 0.1% trypsin in 0.1% $CaCl_2$ for 25 minutes at 37^0C, rinsed twice in PBS-T (PBS/0.2% Triton X-100), before being immersed in 50% HCl containing 1% Triton X-100 for 12 minutes at room temperature. Sections were rinsed in PBS-T and incubated in the same solution containing 10% normal swine serum for 1 hour. The sections were then incubated overnight at 4^0C in a solution of polyclonal rabbit anti-GFAP (Sigma; 1:100) or anti-QK1 (gift from Dr. R Hardy; 1:500) and mouse monoclonal anti-BrdU (1:50).

Sections were rinsed in PBS-T (3x20mins) and incubated in biotinylated swine anti-rabbit (DAKO;1:100) and Texas red anti- mouse IgG (Vector;1:100) for 2 hours at room temperature. Sections were rinsed and treated with fluorescein avidin D (Vector F1205) 30μg/ml in 0.1M sodium bicarbonate, pH8.5, 0.15M NaCl.

2.3.7.3 BrdU and CNPase

Sections were trypsinised, washed and blocked as above. They were then incubated in anti-CNPase (mouse monoclonal; Chemicon; 1:20) overnight at 4^0C. Following application of the appropriate fluorescein conjugated secondary antibody, the sections were fixed in 50% ethanol / acetic acid for 10 minutes, washed in PBS and incubated in 50% HCl for 12 minutes. The BrdU protocol was then continued as described above for the BrdU and GFAP double labelled protocol.

2.3.8 Identification of double-labelled cells

Double labelled cells were identified on a Leica TCS NT confocal microscope using the Leica TCS NT version 1.6.551b software package. To ensure that cells were double labelled, the 10μm sections were optically sectioned (0.5μm to 1μm thick), and then superimposed. This allowed for clear identification of double-labelled cells. If there was any doubt that a cell was double-labelled a 3d reconstruction was made.

2.3.9 Cell death

Pyknotic cells were identified using DAPI (4,6-diamidino-2-phenylindole) as a nuclear marker. Pyknotic cells were identified by their small, rounded dark nucleus. In contrast to this, healthy cells were pale coloured with a clear nucleus showing the chromatin within the cells. To determine the proportion of BrdU labelled cells that

were dying, fluorescent BrdU immunocytochemistry in conjunction with DAPI was performed. BrdU immunocytochemistry was carried out as described above, although a secondary antibody conjugated to TRITC (DAKO:1;200) was used. Sections were mounted in vectashield with DAPI (Vector code number) and the number of BrdU labelled and pyknotic cells were identified using a fluorescence microscope. The counting procedure was identical to the technique as described above.

2.4 RESULTS

In this study the changing stratification of the cortical wall between E16 and P18 was investigated. Following this, proliferating cells were labelled with BrdU on E16, E17, E18, E19 and P0 and their distribution studied over time. In addition to this, the distribution of E18, E19 and P0 labelled cells was compared with the distribution of cells labelled on E16 and E17 after a 1 hour BrdU pulse to investigate the locations and numbers of proliferating cells at each of these ages. Subsequently the fates of E18, E19 and P0 labelled cells were followed in terms of their distribution patterns and their antigenicity during the neonatal period.

2.4.1 Development of the cortical wall / Changes in stratification

Figure 2.2 shows the changing stratification of the cortical wall over time. At E16 the total cortical width is approximately 200μm wide. The proliferative zones, which consist of the VZ and SVZ at this age, constitute half the total width of the cortical wall. The remaining width of the wall is made up of the IZ, which lies just above the proliferative zones and the CP. At this age the CP is only just starting to emerge and is relatively thin. Over the next 48 hours the full stratification of the cortical wall start to emerge. The proliferative zone starts to decrease in width and by P8 all that remains of it is a single layer of cells. This reduction in width of the proliferative zone is coincidental with an increase in the width of the IZ/WM, SP and CP. The SP is a transient increase and subsequently it had disappeared by about P4-P5. The IZ reached its maximum thickness by P1 and remained at this width over the period of study. The CP/CTX increased rapidly in width from P0 and reached its maximum thickness by P9. At this age the CP/CTX accounts for over 90% of the thickness of the cortical wall. Although the graph suggests that the cortical width reduces after P9, this is likely this is due to shrinkage of the tissue from the processing method that was used.

Figure 2.2

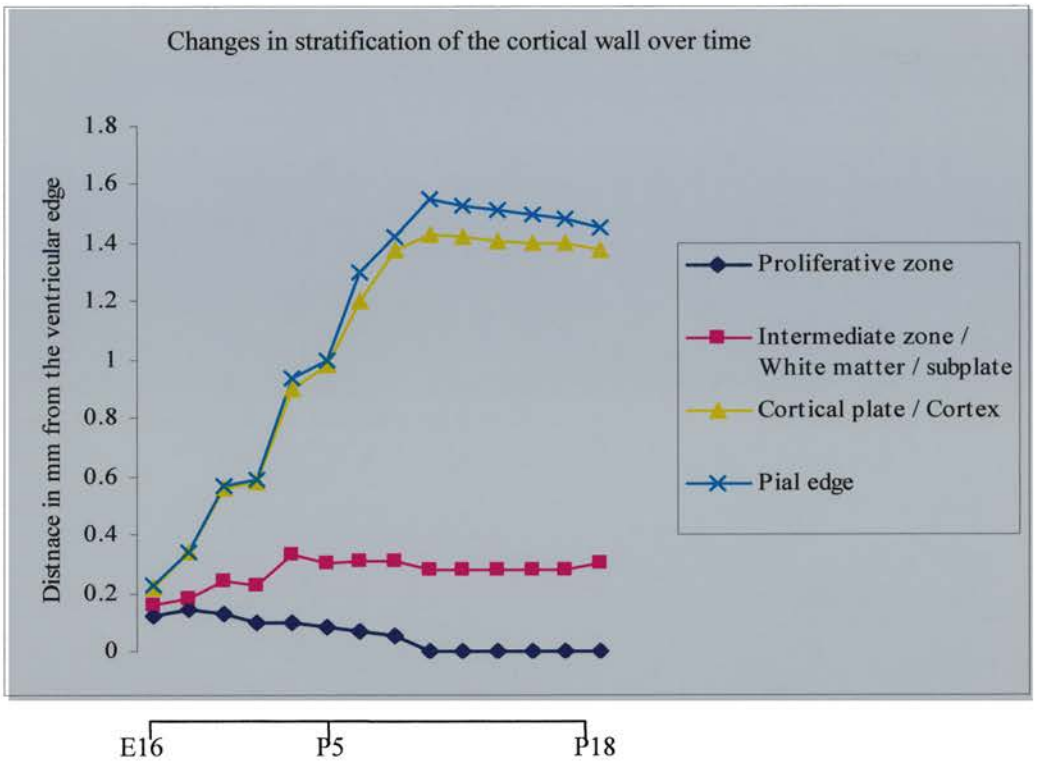

Figure 2.2.

The changing stratification of the developing cortical wall from E16 to P18. The points plotted represent the average distance from the outer limit of the cortical zones to the ventricular edge at each of the ages indicated on the X axis.

2.4.2 Classification of dark and light labelled BrdU cells

Previous experiments (Del Rio and Soriano, 1989; Gillies & Price, 1993) have shown that BrdU labelled cells can be categorised into two groups after long survival times: (1) densely labelled cells, in which more than half of the nucleus is labelled and (2) lightly labelled cells, which have lighter labelling of the nucleus (figure 2.10). The amount of BrdU that a cell contains reveals something of the cell's mitotic history. Densely labelled cells were assumed to have undergone only one round of cell division after the BrdU pulse (Del Rio and Soriano, 1989; Gillies & Price, 1993). The great majority of light labelled cells are likely to be the result of several rounds of cell division of labelled cells. In addition to these lightly labelled cells, a few cells would have been entering or leaving S phase at the time of the BrdU pulse, resulting in the production of lightly labelled cells. In this latter case, the birth dates of these cells remains unclear. However, there would have been no cells of this second type obtained from the 1-hour BrdU pulse in this study. In view of this, all the labelled cells were counted together and no distinction between the dark and the light labelled cells was made in brains fixed after 1 hour, thus assuming that all cells were the products of a single cell cycle. However, in cell counts obtained 2-20 days post-injection dark and light cells were considered separately.

2.4.3 Cell densities

The total densities of BrdU labelled cells within a central region of cortical wall (see methods) at 2 days post-injection were compared with cell densities obtained at 5, 9 and 20 days post injection. Cell counts from the acutely labelled animals (1 hour post injection) were not used in this comparison because the periods of exposure to BrdU were not compatible. In acutely labelled brains the BrdU was only present for 1 hour. In animals that were allowed to survive longer the cells were exposed to BrdU for approximately 3.5 hours. This is the time that it takes for the BrdU to be metabolised (Takahashi *et al.,* 1992). Results are shown for all labelled cells in figure 2.3 and then for light and dark labelled cells separately in figure 2.4. In all cases, the densities of cells decreased between 2 and 20 days.

Cortical expansion in both the rostrocaudal and mediolateral directions is one factor that will affect the cell counts, and to compensate for this, the amount by which the cortex expands in these directions was calculated between 2, 5, 9 and 20 days post injection (see methods; Price *et al.,* 1997). To assess the contribution of neocortical expansion to the observed changes in cell densities between 2 and 20 days, a series of expected cell counts were calculated using the expansion factor (i.e. the 2 day cell counts were divided by the appropriate expansion factor to produce an expected cell count). These expected cell counts were compared with the actual cell counts (figures 2.3 and 2.4).

For the counts obtained following E18 injections, the observed densities were close to the expected densities at all later ages for the total cell densities (figure 2.3A), and for light and dark labelled cell densities (figure 2.4A). These results suggest that the observed decrease in cell density between 2 and 20 days be due largely or completely to the expansion of the cortex.

Following E19 injections, the observed densities of cells (total cells, light and dark labelled cells) were similar to their respective expected values up until 5 days post injection, suggesting that up until 5 days post injection the observed decrease in cell densities could be explained by cortical expansion alone (figures 2.3B and 2.4B). However, by 9 days post-injection the actual cell densities in the three categories (total, dark and light) were significantly lower than their respective expected values as predicted by the expansion factor (figures 2.3B and 2.4B: Table 2.2).

The observed densities of the P0 labelled cells, in contrast to the E19 labelled population, had decreased more dramatically than their respective expected cell densities by 5 days post injection. By 9 and 20 days post-injection, the actual cell densities remained significantly lower than their respective expected cell densities. This was true for total, dark and light labelled cell populations (figures 2.3C and 2.4C).

Interestingly, the observed densities (total cells, light and dark labelled cells) obtained between 9 and 20 days following an E19 or P0 injection, showed a slight increase.

For all the ages studied, the density of cells as a percentage of the expected cell density is shown in Table 2.2.

Figure 2.3.

Line graphs illustrating total densities of labelled cells on **(A)** E18, **(B)** E19, **(C)** and P0 after 2, 5, 9 and 20 days post injection. Broken lines represent the respective expected cell density as calculated by the expansion factor. Values are mean densities of BrdU cells ± SEM.

Figure 2.3

A

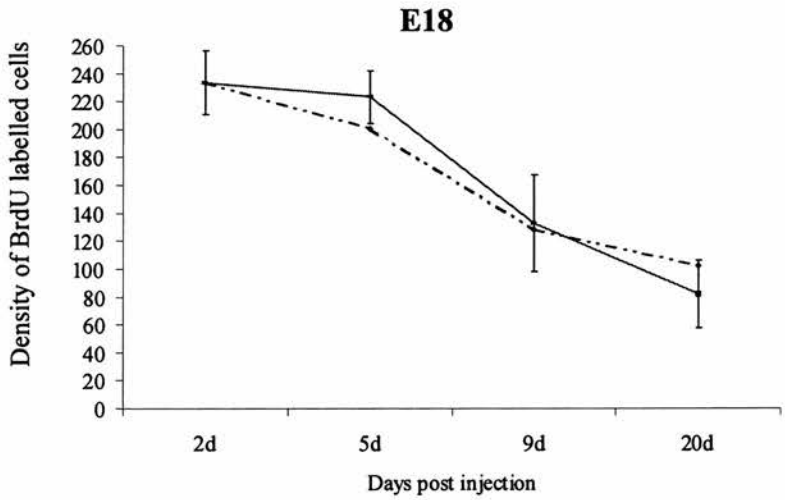

B

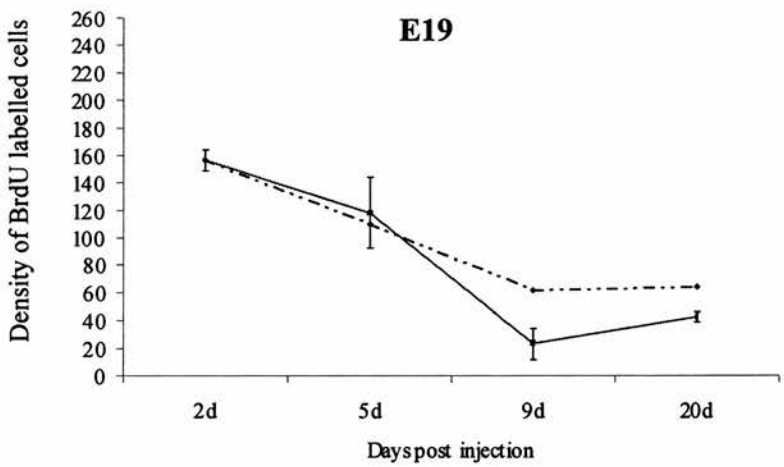

C

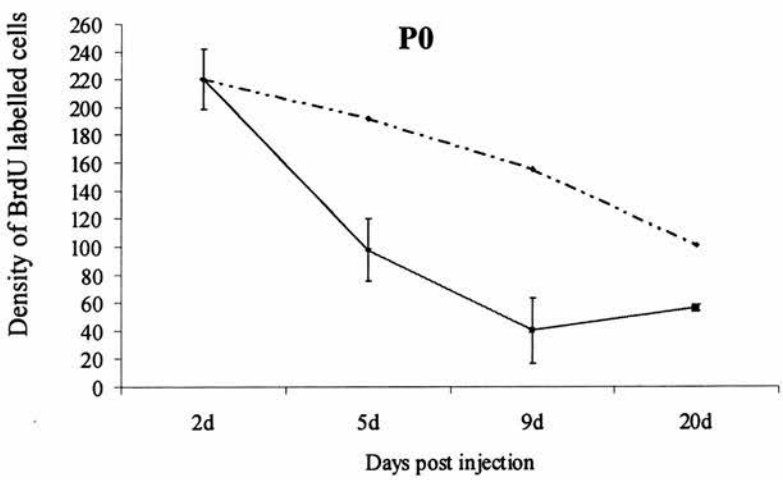

Figure 2.4

Line graphs illustrating the densities of dark (blue lines) and light labelled (pink lines) cells, labelled on **(A)** E18, **(B)** E19 and **(C)** P0 after 2, 5, 9 and 20 days. Broken lines represent the respective expected cell densities as calculated by the expansion factor. Values are mean densities ± SEM.

Figure 2.4

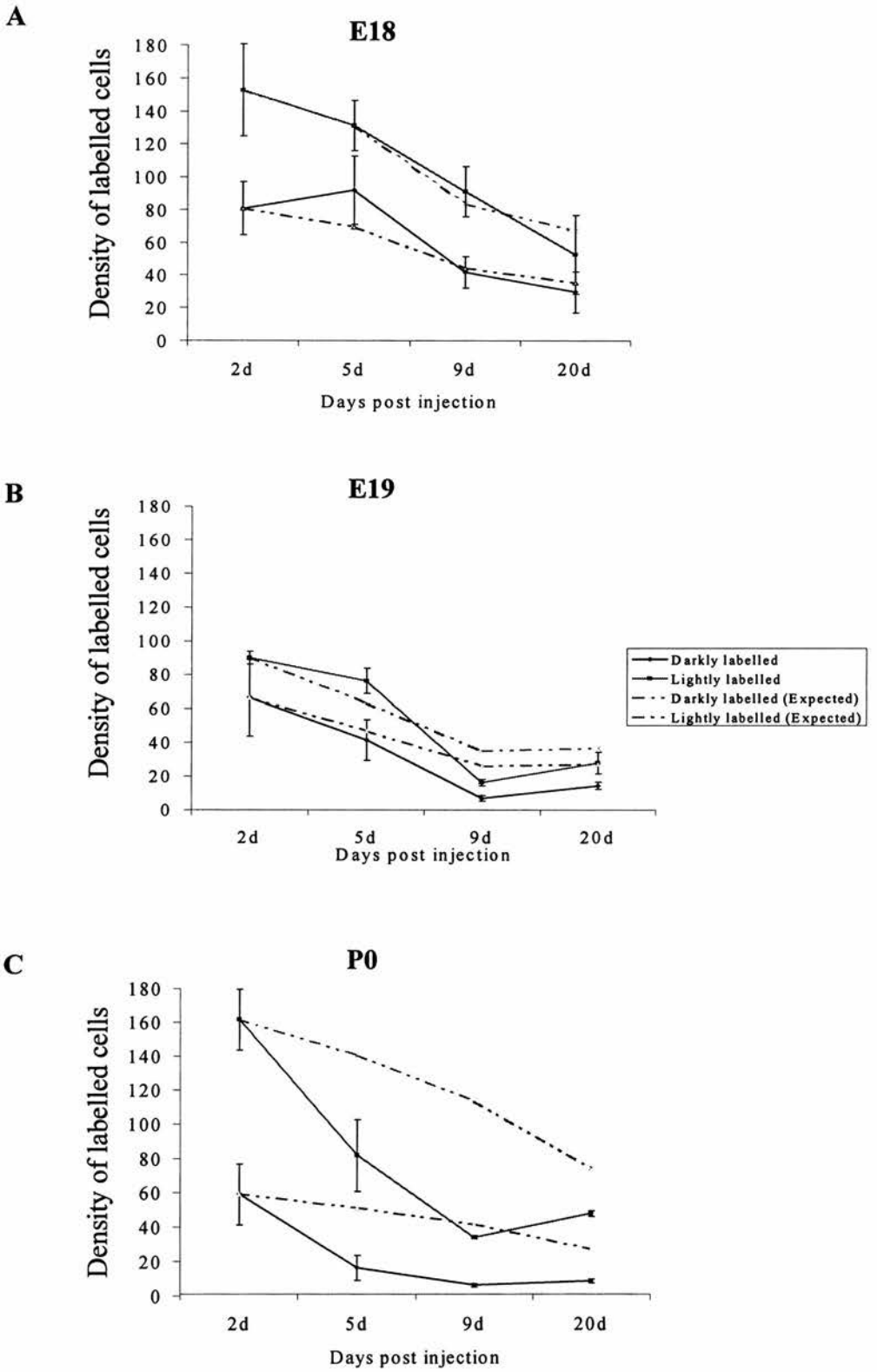
A
E18
Density of labelled cells
180
160
140
120
100
80
60
40
20
0
2d
5d
9d
20d
Days post injection
B
E19
Density of labelled cells
Darkly labelled
Lightly labelled
Darkly labelled (Expected)
Lightly labelled (Expected)
Days post injection
C
P0
Density of labelled cells
Days post injection

Table 2.2

	Age of animal at time of BrdU injection		
	E18	**E19**	**P0**
+ 2 days	100%	100%	100%
+5 days (dark label)	133%	89%	32%
+5 days (light label)	100%	121%	58%
+5 days (total label)	111%	107%	51%
+9 days (dark label)	94%	26%	15%
+9 days (light label)	108%	46%	30%
+9 days (total label)	104%	38%	26%
+20 days (dark label)	84%	53%	32%
+20 days (light label)	78%	76%	65%
+ 20 days (total label)	80%	66%	56%

Table 2.2.

This table shows the actual density of BrdU labelled cells at the various ages as a percentage of the expected density as calculated by the expansion factor.

2.4.4 Cell positions

2.4.4.1 1 hour post injection

The location and distribution of BrdU labelled cells in E16 and E17 embryos after a 1 hour BrdU pulse were compared with the distribution patterns of E18, E19 and P0 injected animals after a 1 hour BrdU pulse. Camera lucida drawings illustrating the main findings are shown in figure 2.5 and graphical representations for all animals studied are shown in figure 2.6.

At E16 and E17, BrdU labelled cells were found primarily in the PZ (VZ/SVZ) (figures 2.5A and 2.6A&B). At E18, BrdU labelled cells were mainly in the PZ (65% of the total labelled cells) although a few labelled cells were observed in the IZ/WM. Occasionally labelled cells were seen in the SP and CP (figures 2.5B and 2.6C). Cells labelled on E19 and P0 were found mainly in PZ and IZ/WM, although a small proportion of cells was observed in the SP, CP and very occasionally in the MZ (figures 2.5C and 2.6D&E).

The pattern of distribution of these cells also differed within the PZ between all the ages studied. The populations of cell labelled on E16 and E17 formed a relatively tight band with a peak at a short distance away from the ventricular zone (figure 2.6A&B:bins 2-4) whereas cells labelled on E18-P0 remained in a position close to the ventricular edge (figure 2.6C, D &E: bins 1-2).

Figure 2.5

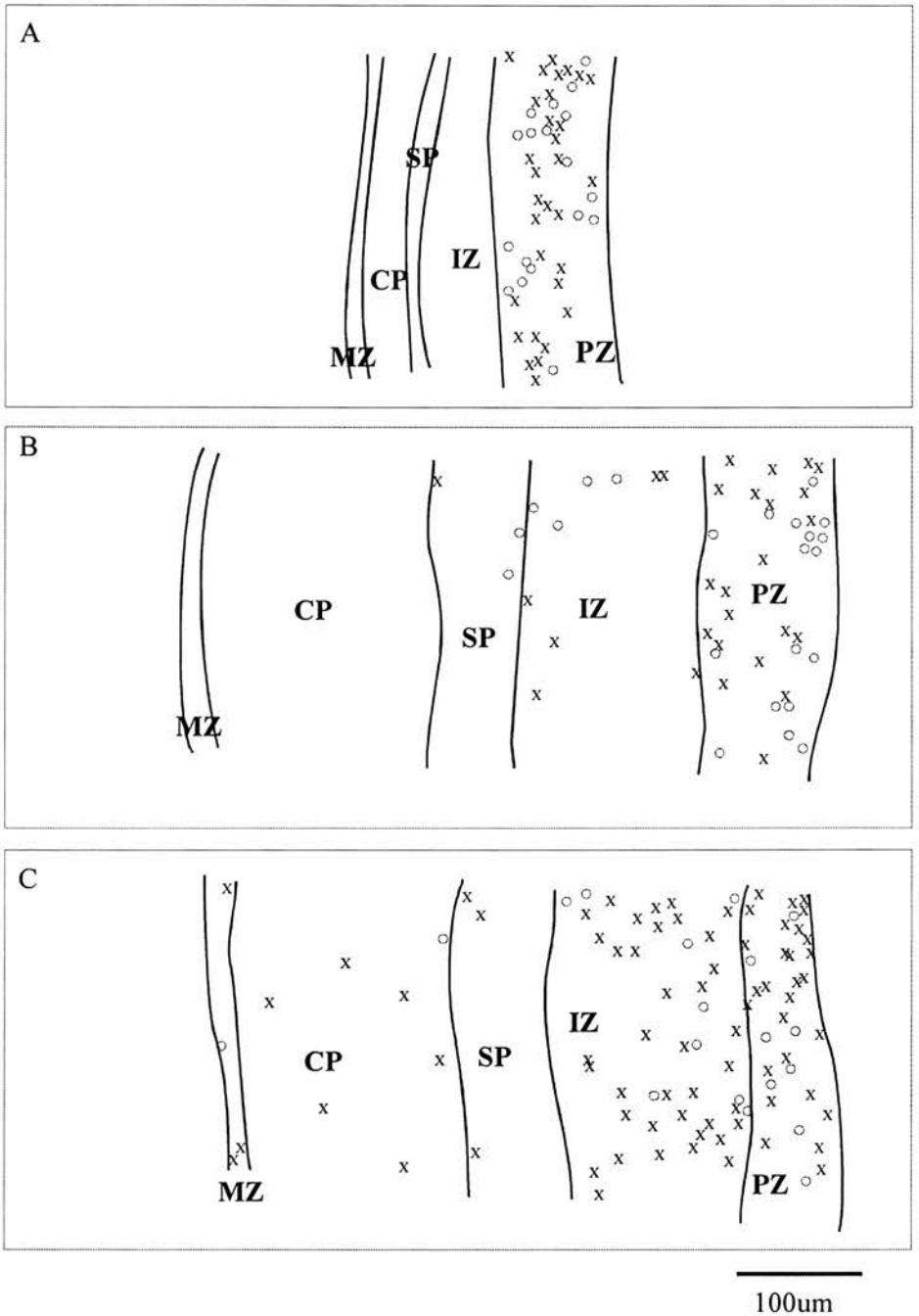

Figure 2.5.

Computer generated camera lucida drawings of the cortical wall at **(A)** E16 **(B)** E18, **(C)** P0 showing the location of dark and light labelled BrdU cells 1 hour after injection. Each cross represents a darkly labelled cell, and each circle represents a lightly labelled cell. **PZ**: Proliferative zone, **IZ**: Intermediate zone, **SP**: Subplate, **CP**: Cortical plate, **MZ**: Marginal zone.

Figure 2.6

Histograms illustrating the relative distribution of BrdU labelled cells 1 hour after BrdU injection on **(A)** E16, **(B)** E17, **(C)** E18, **(D)** E19 and **(E)** P0. The cortical wall was divided into 10 equal size bins, numbered 1-10 from ventricular to pial edge. The positions of the cortical zones and the average total cortical width are indicated above each graph. BrdU cells are located primarily in bins 2-4 following E16 and E17 injections, and in bins 1-2 following E18-P0 injections. Values are mean densities ± SEM.

PZ: Proliferative zone; **IZ**: Intermediate zone; **SP**: Subplate; **CP**: Cortical plate; **MZ**: Marginal zone.

Figure 2.6

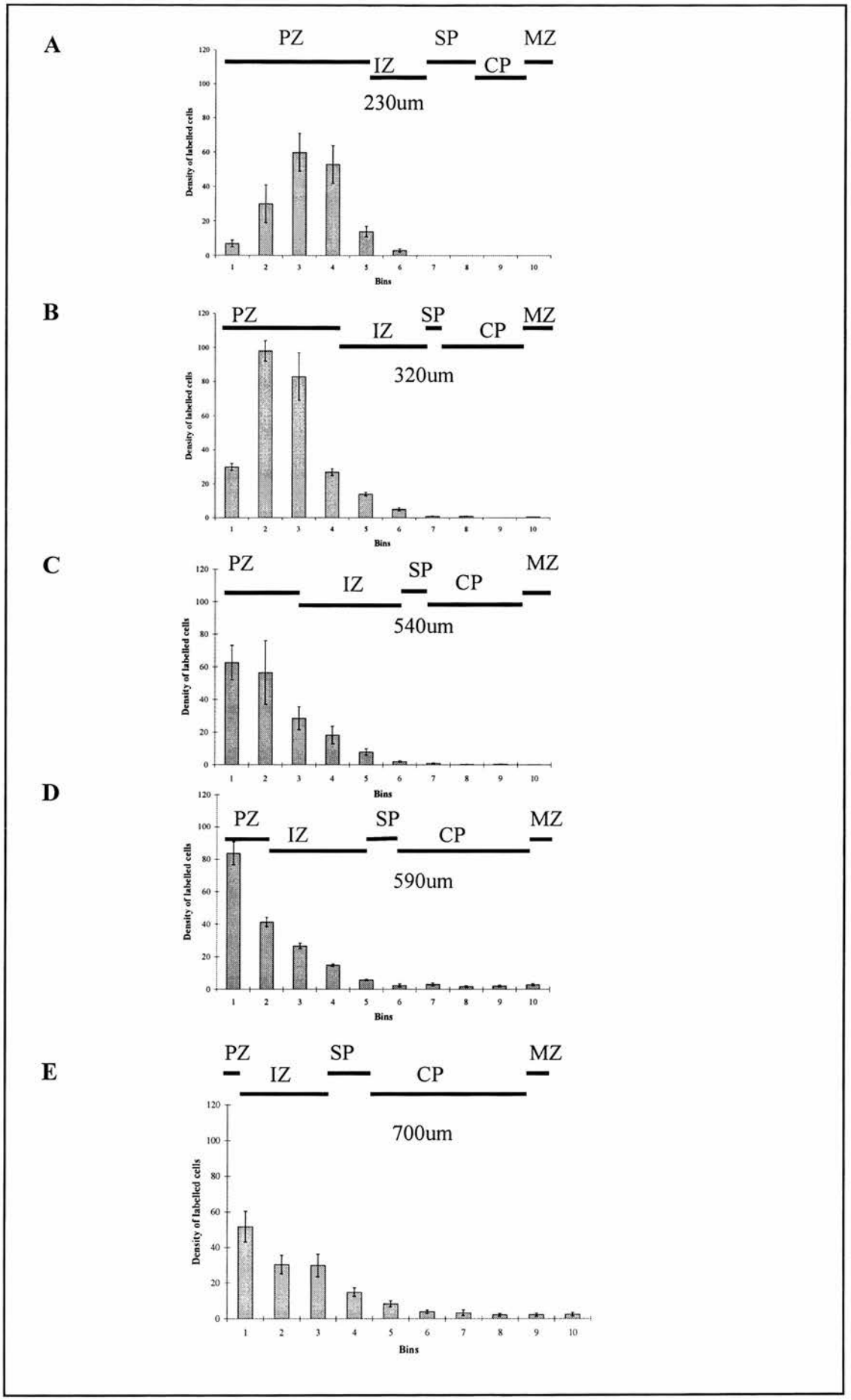
A
PZ
SP
MZ
IZ
CP
230um
Density of labelled cells
Bins
B
PZ
IZ
SP
CP
MZ
320um
Density of labelled cells
Bins
C
PZ
IZ
SP
CP
MZ
540um
Density of labelled cells
Bins
D
PZ
IZ
SP
CP
MZ
590um
Density of labelled cells
Bins
E
PZ
IZ
SP
CP
MZ
700um
Density of labelled cells
Bins

2.4.4.2 2 – 20 days post injection

Although the distributions of darkly and lightly labelled cells were analysed separately, only the darkly labelled cells were illustrated graphically (figures 2.7 and 2.8). As outlined earlier this was because of the difficulties in determining the exact birth dates of the lightly labelled cells. Figure 2.7 illustrates the proportional distribution of E18, E19 and P0 BrdU labelled cells within the cortical wall between 2 days and 20 days post injection. Figure 2.8 represents the actual cell densities of E18, E19 and P0 BrdU labelled profiles within the cortical wall at the same time points. The data obtained after a 1 hour BrdU pulses were also included in figures 2.7 and 2.8 for comparison. In addition figure 2.8 also includes the distributions of E16 profiles after 1hour and after 2 and 5 days. Finally, the data obtained between 9 and 20 days showed similar patterns, therefore only the 20 day data was included.

E18 labelled cells

The E18 labelled cells were mainly in the PZ and IZ/WM after 2 days, although a small proportion was in the SP and CP (figure 2.7B:blue bars). A similar pattern was observed after a 1 hour BrdU pulse (Figure 2.7A:blue bars), although their was a small but significant increase in the proportion of cells within the CP at 2 days compared with a t 1 hour ($p< 0.05$; Student *t* test). The proportion of labelled cells within the CP (the SP had disappeared by P4) further increased over time (Figures 2.7C and D:blue bars). At all ages investigated the proportion of labelled cells within the CP was significantly larger than the proportion at the start (1 hour) ($p<0.05$; Students *t* test). By 20 days post-injection the population of cells within the CP accounted for approximately 40% of the total population of E18 labelled cells and was found in a tight band under the MZ. Camera lucida drawings illustrating these findings are shown in Figures 2.9 and 2.10.

The increase in proportion of cells within the CP was accompanied by a corresponding decrease in proportion of cells within the PZ. This decrease in proportion of cells within the PZ was significantly different than the starting point (1 hour) by 5, 9 and 20 days post-injection ($P< 0.05$; Student *t* test). The proportion of labelled cells in the IZ/WM did not significantly alter over time.

The distribution pattern of actual cell densities at 1hour, 2 and 5 days was similar to the proportional distribution pattern at similar time points (figure 2.8A, B and C;blue bars). After 5 days post-injection there was a significant decrease in cell number within each cortical zone, which held true up until at least 20 days post-injection (Figure 2.8D).

E19 labelled cells

By 2 days post injection the E19 labelled cells had a proportional distribution pattern similar to the proportional distribution observed at 1 hour, although a small but significant increase in the proportion of cells observed in the CP was observed by 2 days ($P<0.05$; Students *t* test) (Figures 2.7A and B; white bars). The proportion of cells within the CP further increased over time (up until 20 days), and was accompanied by a corresponding decrease in proportion of cells within the PZ at all ages studied (Figures 2.7C and D; white bars). These changes in cell proportions within the PZ and CP are all significant in relationship to the start (1 hour) ($p<0.05$; Student *t* test). No significant difference in the proportion of cells in the IZ/WM was observed at any of the ages studied in comparison with the proportion at the start.

The actual densities of labelled cells within the CP and the IZ were higher at 5 days than the corresponding densities at 2 days although these values were not significant. The density of cells within the PZ decreased significantly between 2 and 5 days ($P<0.05$; Students t test) (Figure 2.8C;white bars). After 5 days, the density of cells within all cortical zones decreased dramatically (Figure 2.8D;white bars).

In summary, there was an increase in the proportion and density of cells in the CP up until 5 days post-injection, which was accompanied by a corresponding reduction in the density and proportion of cells within the PZ. After 5 days the density of cells in all zones fell dramatically, leaving few remaining cells by 9 and 20 days post-injection.

P0 labelled cells

The P0 labelled population of cells was also primarily in the PZ and IZ/WM, and to a small extent in the SP and CP by 2 days post-injection (figures 2.7B and 2.8B: Yellow bars). The proportion of cells in the SP and CP were significantly higher at 2 days than they were at the starting value ($p<0.05$;student *t* test). This proportional significant increase within the CP was observed up until 20 days ($p<0.05$; Student *t* test). In the PZ, the proportion of cells at 2 and 5 days post injection was similar to the proportion observed at the start, but fell dramatically by 9 and 20 days (Figure 2.7D;Yellow bars). This decrease in proportion of cells within the CP was significant by 20 days ($p<0.05$;students *t* test). In the IZ/WM, there was a small but significant decrease in the proportion of cells from the start up until 5 days post-injection. This was not significant at 20 days post-injection.

A large decrease in cell density was observed in the PZ, IZ and CP by 5 days post-injection. These decreases in cell density were significantly lower at 5 days in comparison with the densities observed at 2 days. This significant decrease was further enhanced by 20 days.

In summary, all three populations of labelled cells were present in the PZ and IZ/WM and to a smaller extent the SP and CP by 2 days post-injection. In all three cell populations, the proportions of cells within the CP significantly increased from their respective starting proportions at 1 hour post-injection. The proportion of E18 labelled cells within the CP further increased overtime, and was accompanied by a corresponding decrease in cell proportion within the PZ. The E19 population behaved similarly to the E18 population although the increase in proportion of cells within the CP was slightly smaller. A corresponding decrease in proportion of cells in the PZ was also observed. For the P0 population, the increase in proportion of cells within the CP was slightly larger than for both the E18 and E19 populations, although the decrease in proportion and density of cells in the PZ was much more dramatic.

2.4.4.3 E16 labelled cells

For comparison purposes data from the E16 labelled cells (figures 2.8E-G) was included. After 1 hour post-injection, the majority of E16 labelled cells were within the PZ, although a few cells were observed in the IZ. This distribution pattern was similar to the distribution patterns of the E18, E19 and P0 labelled populations after 1 hour, although the density of cells within the PZ at E16 was greater than the densities at E18, E19 and P0.

By 2 days post-injection the density of cells within the PZ had decreased in comparison with the density at the start. This decrease was accompanied by an increase in cell density within the IZ, SP and CP. By 5 days post-injection a further reduction in cell density within the PZ and a reduction in cell density within the IZ was observed. A further corresponding increase in cell density within the CP was observed. The distribution pattern of the E16 labelled cells by 5 days post-injection was very different than the distribution patterns of the E18, E19 and P0 labelled cells by 5 days post-injection.

Figure 2.7

Histograms illustrating the proportional distribution of E18 (blue bars), E19 (white bars) and P0 (yellow bars) darkly labelled BrdU cells after **(A)** 1 hour **(B)** 2 days, **(C)** 5 days and **(D)** 20 days post injection. The asterisks indicate a significant change in the proportion of cells within a particular zone, from the starting proportions, 1 hour after BrdU injection (student t test; $P<0.05$). Values are mean percentages ± SEM. **PZ**: Proliferative zone; **IZ**: Intermediate zone; **SP**: Subplate; **CP**: Cortical plate; **MZ**: Marginal zone.

Figure 2.7

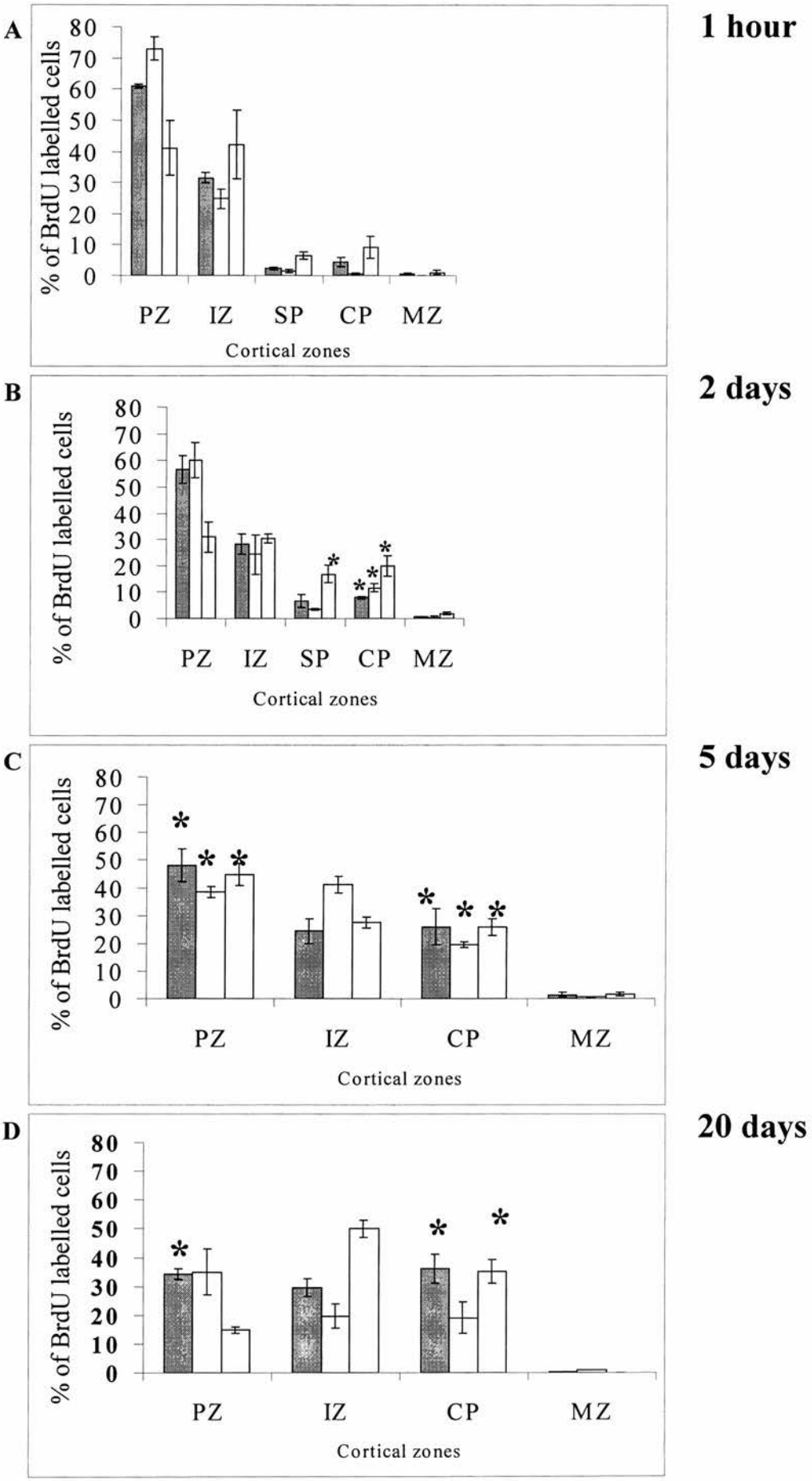
A
1 hour
% of BrdU labelled cells
80
70
60
50
40
30
20
10
0
PZ
IZ
SP
CP
MZ
Cortical zones
B
2 days
% of BrdU labelled cells
80
70
60
50
40
30
20
10
0
PZ
IZ
SP
CP
MZ
Cortical zones
C
5 days
% of BrdU labelled cells
80
70
60
50
40
30
20
10
0
PZ
IZ
CP
MZ
Cortical zones
D
20 days
% of BrdU labelled cells
80
70
60
50
40
30
20
10
0
PZ
IZ
CP
MZ
Cortical zones

Figure 2.8

Histograms illustrating the numerical distribution patterns of E18 (Blue), E19 (white) and P0 (yellow) labelled BrdU cells after **(A)** 1 hour, **(B)** 2 days, **(C)** 5 days and **(D)** 20 days post injection. The distribution patterns of E16 labelled cells are shown after **(E)** 1hour, **(F)** 2 days and **(G)** 5 days post injection. **Prolif:** Proliferative zone; **IZ**: Intermediate zone; **SP:** Subplate; **CP:** Cortical plate **MZ**: Marginal zone

Figure 2.8

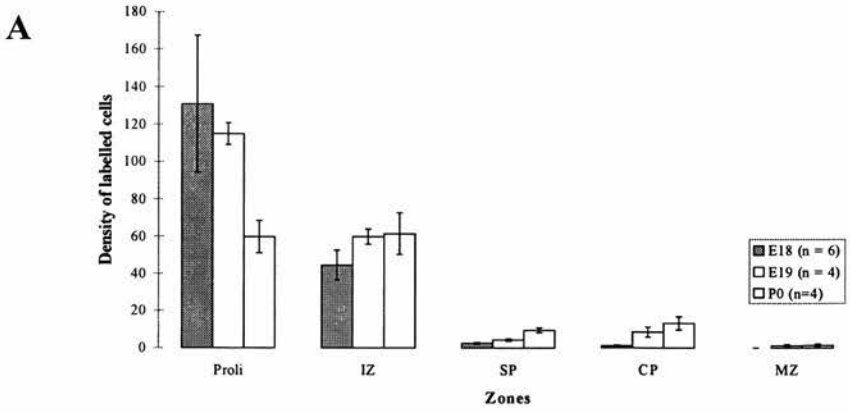
A
Density of labelled cells
Proli
IZ
SP
CP
MZ
Zones
E18 (n = 6)
E19 (n = 4)
P0 (n=4)

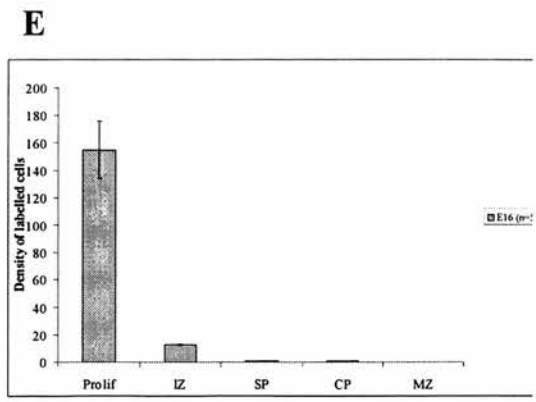
E
Density of labelled cells
Prolif
IZ
SP
CP
MZ

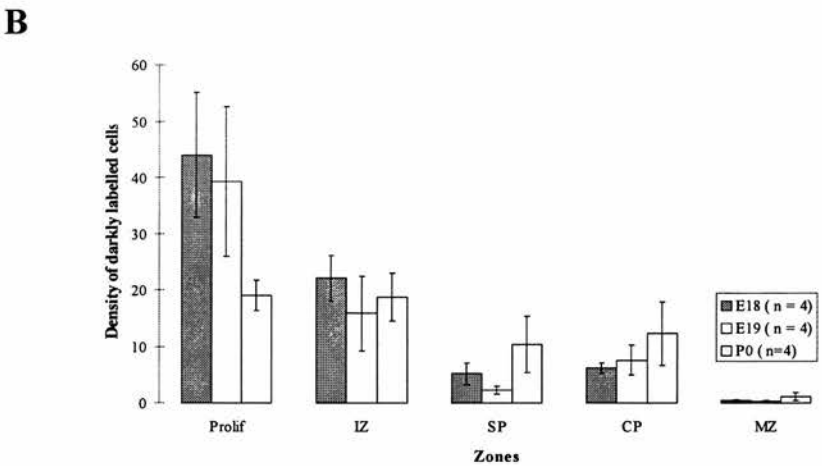
B
Density of darkly labelled cells
Prolif
IZ
SP
CP
MZ
Zones
E18 (n = 4)
E19 (n = 4)
P0 (n=4)

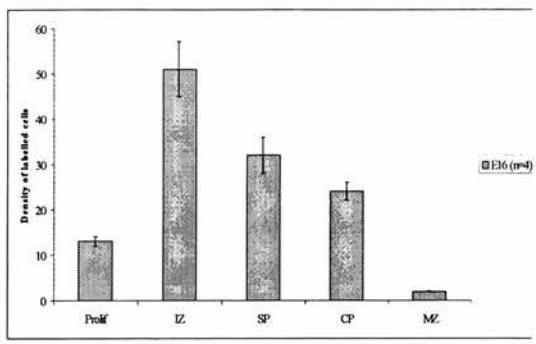
F
Prolif
IZ
SP
CP
MZ

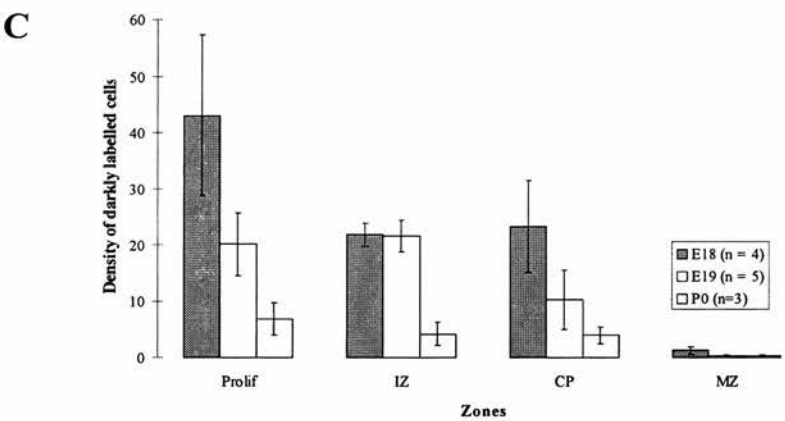
C
Density of darkly labelled cells
Prolif
IZ
CP
MZ
Zones
E18 (n = 4)
E19 (n = 5)
P0 (n=3)

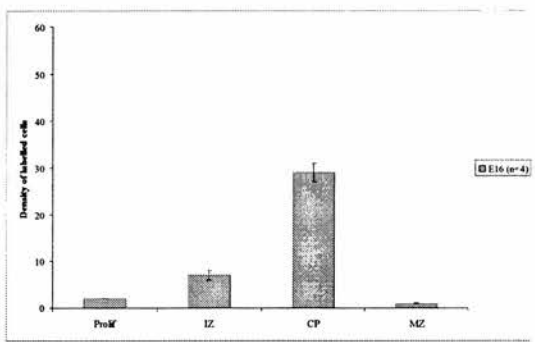
G
Prolif
IZ
CP
MZ

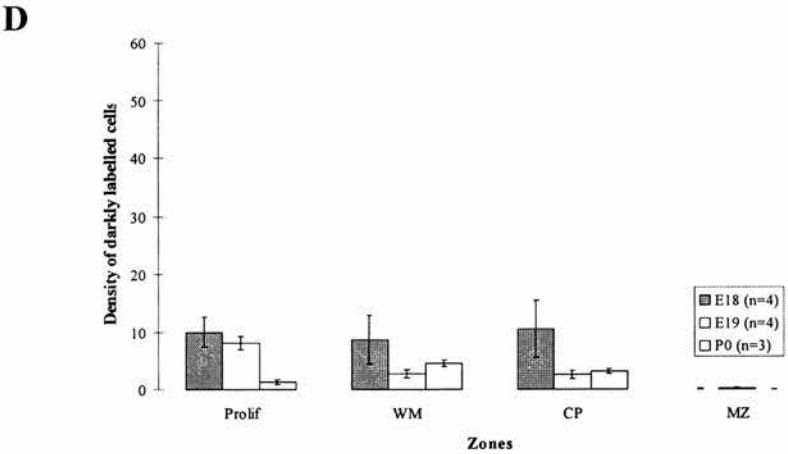
D
Density of darkly labelled cells
Prolif
WM
CP
MZ
Zones
E18 (n=4)
E19 (n=4)
P0 (n=3)

Figure 2.9

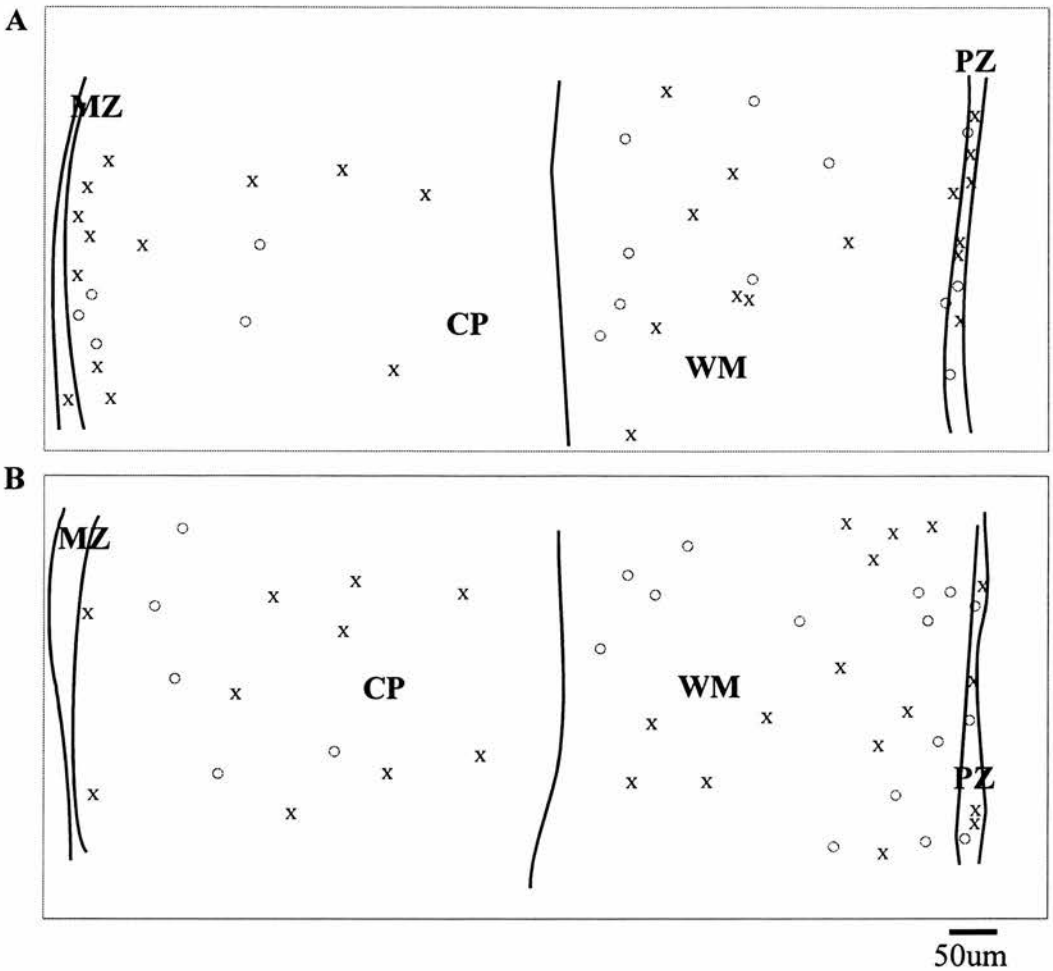

Figure 2.9
Camera Lucida drawings of the cortical wall on **(A)** P18 (E18+20 days) and **(B)** P20 (P0+20 days) showing the location of dark (crosses) and light (circles) labelled BrdU cells.

Figure 2.10

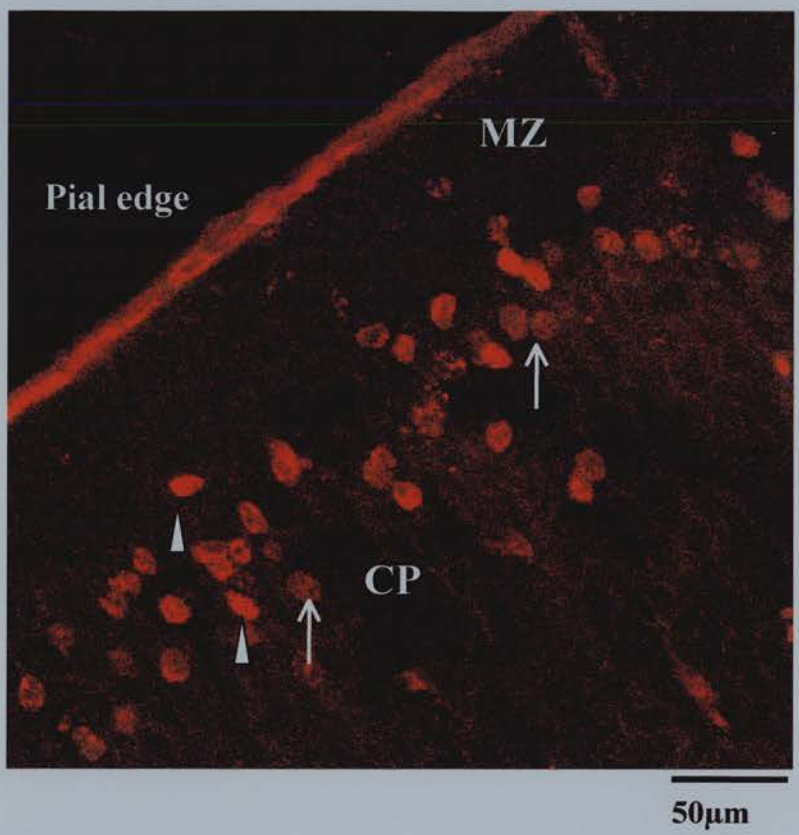

Figure 2.10

Photomicrograph illustrating E18 labelled BrdU cells, 20 days post injection. The cells are in a tight band in the upper region of the cortical plate just beneath the MZ. Darkly labelled cells are indicated by the arrow heads and lightly labelled cells by the arrows.

MZ: Marginal zone; **CP:** Cortical plate.

2.4.5 Identification of BrdU labelled cells

Antibodies against GFAP, CNPase, QK1 and MAP2 were used to identify the phenotype of the E18, E19 and P0 populations of BrdU labelled cells. GFAP expression was first seen at P1 (E19 + 2 days) (figure 2.11A), and was present within the PZ (VZ/SVZ) and WM. A similar staining pattern was maintained until at least P18 (figure 2.11B). A small amount of staining was observed right at the pial edge (figure 2.11C).

CNPase immuno-labelling was first seen at P3 (E18 + 5 days), and was restricted to the WM although a small amount of staining was scattered throughout the grey matter (SP and CP) (figure 2.12). QK1 staining however was much more widespread. At the earliest ages studied (E18) QK1 staining was very strong in the proliferative regions. Strong staining was also seen throughout the IZ and CP at all ages studied (figure 2.13). MAP2 staining was also present at all ages studied and was located within the cortical plate (not shown).

Double-labelled cells were identified on a confocal microscope by imaging cells in 3D. A small proportion of E18, E19 and P0 labelled BrdU positive cells were double labelled with GFAP between 5 and 20 days post injection. By 5 days post-injection 9.2% (n=4(4 brains, 16 sections)), 10.1% (n=5) and 15.4% (n=5) of the E18, E19 and P0 BrdU labelled population were expressing GFAP (figure 2.14). Double-labelled cells were located within the IZ/WM and lower cortex, and occasionally in the upper cortex. Figure 2.15 shows a high magnification view of a P0 double-labelled cell in the lower cortex. Similar proportions of double-labelled cells were observed by 9 and 20 days post injection for all three populations of labelled cells.

The 40% of the E18 BrdU labelled cell population that formed a tight band under the marginal zone (figure 2.10)did not express GFAP.

Because CNPase labelled the fibre tracts it was difficult to clearly identify if individual BrdU labelled cells were labelled with CNPase. However CNPase expression coincided with the location of BrdU positive cells within the IZ/WM,

suggesting that these BrdU cells were labelled with CNPase. This holds true for E18, E19 and P0 labelled cells.

A substantial proportion of E18, E19 and P0 labelled BrdU cells were double labelled with the QK1 antibody (figures 2.16 and 2.17). After 1 hour and 2 days post BrdU injection, the proliferative region was so intensely stained with QK1 that accurate quantification of the proportion of BrdU and QK1 double labelled cells was not possible (figure 2.17A). This was true for the E18, E19 and P0 labelled cell populations. In addition to the staining in the proliferative regions, staining was also present in the WM and CP. This pattern of staining was observed for all three populations of cells.

Figure 2.16 summarises the proportions of BrdU cells that were also labelled with QK1 between 5 and 20 days post injection. By 5 days post injection, approximately 90% of the E18, E19 and P0 labelled BrdU cells were double labelled with QK1 within the IZ/WM (figure 2.16A, B and C). Similar proportions of double labelled cells were observed in the IZ/WM after 20 days post-injection (Figure 2.16D, E and F).

In the CP, only 54% of E18 labelled cells were immunolabelled with QK1 by 5 days post-injection (figure 2.16G). This proportion was further reduced to 40% by 20 days post-injection (figure 2.16J). The 40% of BrdU labelled cells that formed a tight band under the MZ did not double label with QK1 (figure 2.17B). The E19 and P0 labelled populations had significantly higher proportions of cells double labelled with QK1 than the E18 labelled population had within the CP at 5 days post-injection (figure 2.16H and I). By 20 days post injection similar proportions of double-labelled cells were seen for the E19 and P0 labelled cell populations as was observed at 5 days (figure 2.16K and L).

Only a small proportion of E18 labelled cells were colocalised with MAP2. These were the cells present in the upper region of the cortical plate just beneath the MZ. These cells were GFAP, QK1 and CNPase negative. Furthermore the nuclei of these

cells were similar in terms of size, location and appearance to that of neuronal cells born during the peak of neurogenesis (own observations). Hence it is likely that these E18 labelled cells were neurones.

2.4.6 Cell death

Pyknotic cells were identified by their nuclear morphology using DAPI. For all three populations of cells (E18, E19 and P0) the density of BrdU labelled cells that were pyknotic at 2,5, 9 and 20 days post-injection were annalysed. At all ages studied, pyknotic cells were visible in every zone throughout the cortical wall. Only 1 or 2 BrdU labelled cells were pyknotic at any of the ages studied.

Figure 2.11

Photomicrographs illustrating GFAP immunostaining throughout the developing cortical wall. **(A)** GFAP staining in the cortex of a P3 mouse brain. GFAP positive cells are primarily in the WM, although a few cells are also present in the lower CP. **(B)** GFAP staining in the WM of the cortex in a P18 mouse brain. **(C)** GFAP expression at the pial edge of the cortex in a P18 mousse brain.

CP: Cortical plate; **WM:** White matter. Arrows show GFAP staining (green); Arrow heads show BrdU labelling (red).

Figure 2.11

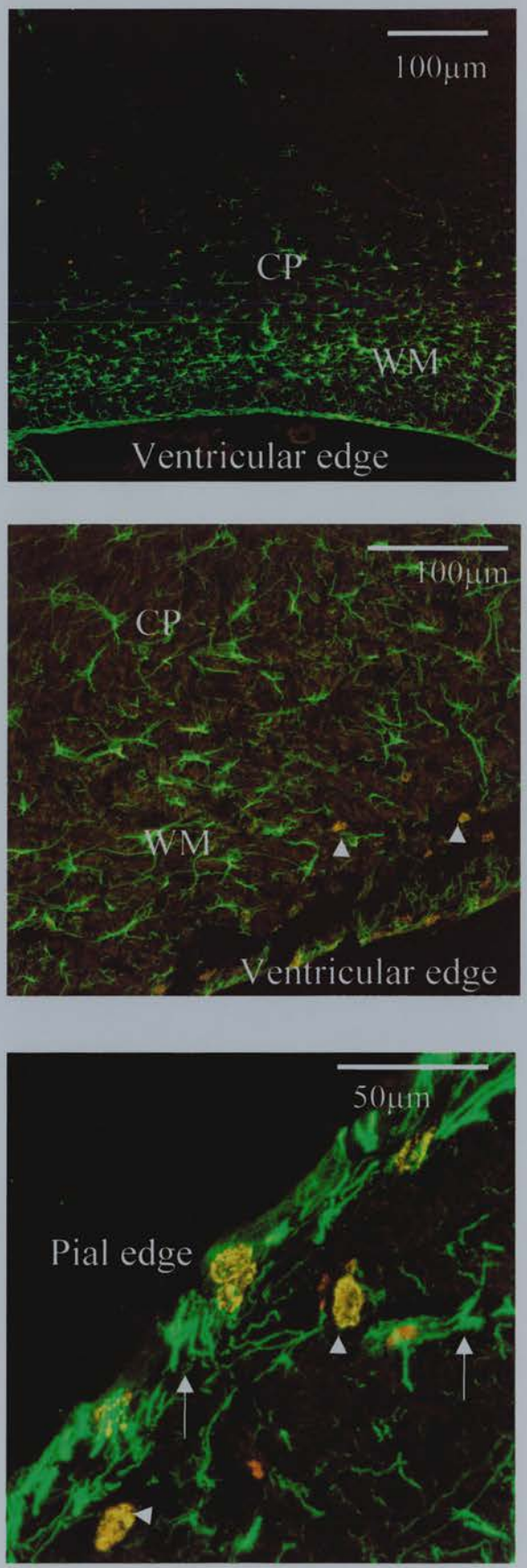
A
100μm
CP
WM
Ventricular edge
B
100μm
CP
WM
Ventricular edge
C
50μm
Pial edge

Figure 2.12

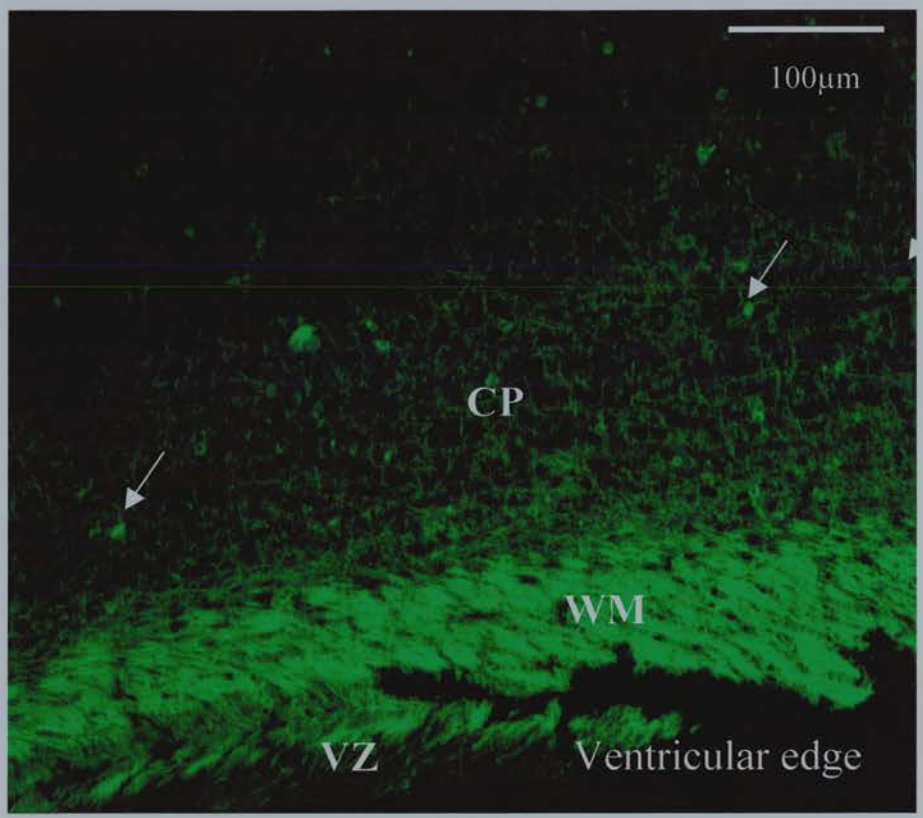

Figure 2.12.

Photomicrograph illustrating CNPase expression in the WM at P5. The arrows indicate staining in the CP.

CP: Cortical plate; **WM**: White Matter; **VZ**: Ventricular Zone.

Figure 2.13

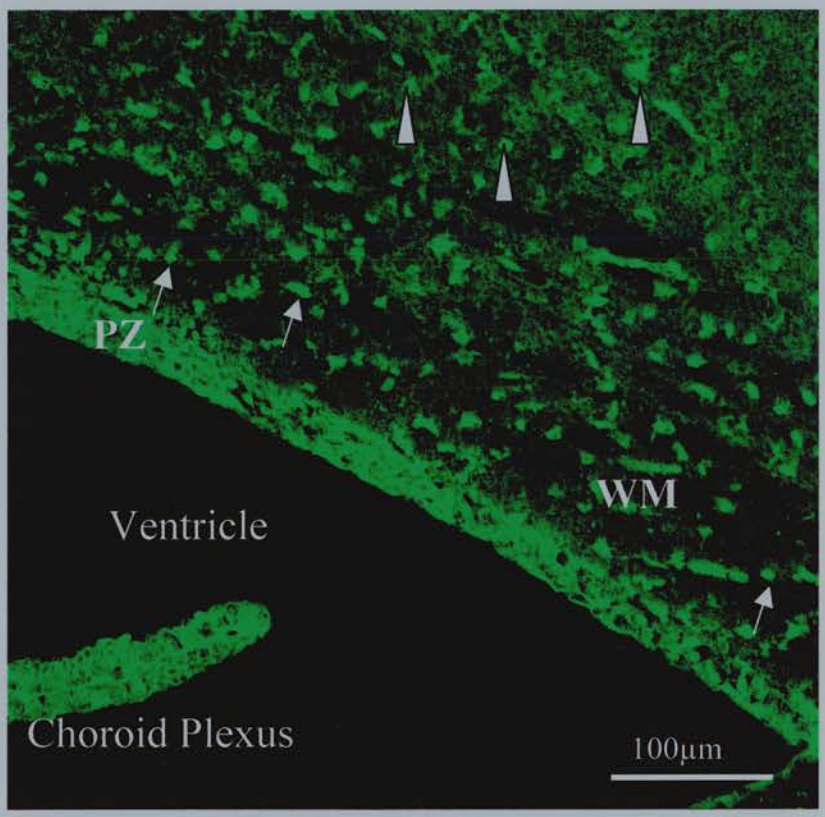

Figure 2.13.

Photomicrograph illustrating QKI immunostaining at P3 in the mouse cortex. The PZ was stained strongly with QK1. Staining was also observed in the WM (arrows) and the CP (arrowheads).

PZ: Proliferative Zone; **WM**: White Matter; **CP:** Cortical plate

Figure 2.14

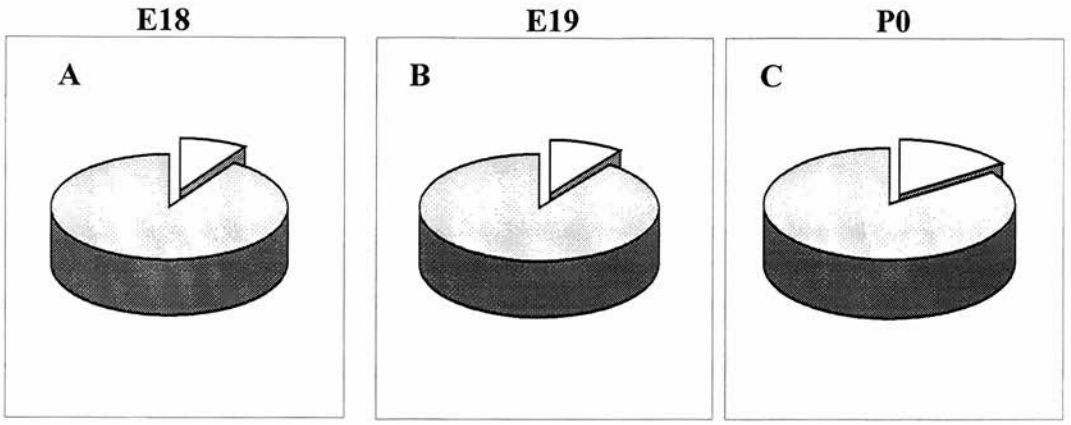

Figure 2.14.

Pie charts illustrating the proportion of BrdU cells labelled on **(A)** E18, **(B)** E19 and **(C)** P0, 5 days post-injection that were double labelled with GFAP. Yellow segments represent the proportion of BrdU cells that were also labelled with GFAP, while the blue segments represent the remaining proportion of BrdU cells that did not express GFAP.

Figure 2.15

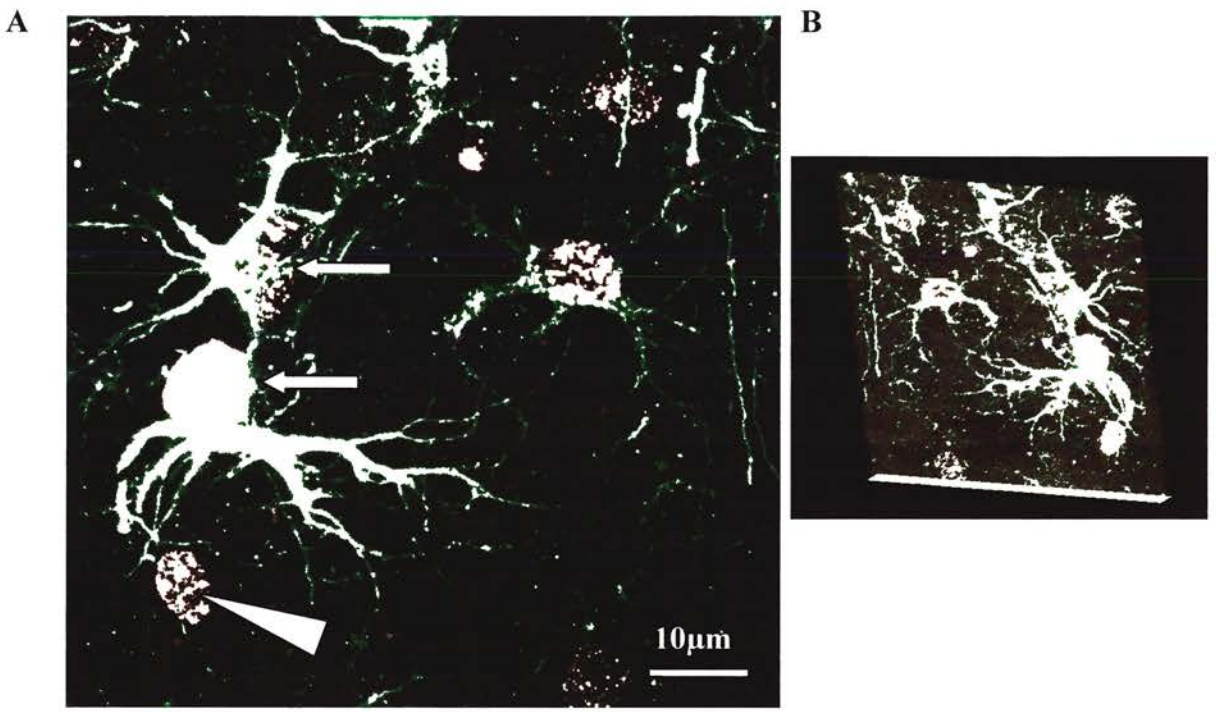

Figure 2.15.

(A) Confocal image illustrating a cell in the lower cortex labelled with an antibody to BrdU (red) and GFAP (green), 5 days after a BrdU injection on P0.

(B) Confocal image illustrating the same cell rotated through 180^0 to ensure that the cells were double-labelled and not overlying each other. Arrows indicate double-labelled cells; Arrowhead indicates BrdU labelled cell.

Figure 2.16.

Pie charts illustrating the proportion of BrdU labelled cells that are double labelled with QK1. (**A-F**) represent cells within the IZ; **(G-L)** represent cells within the CP. Yellow segments represent the proportion of BrdU labelled cells that are expressing QK1, while the blue segments represent the remaining proportion of BrdU cells that are not double labelled with QK1. **(A, D, G & J)** represent the E18 labelled population, **(B, E, H & K)** represent the E19 labelled population and **(C, F, I & L)** represent the P0 labelled population. Mean percentage of double labelled cells and their corresponding SEM values are indicated on the figure.

n: Number of brains analysed (at least 3 sections per brain);

Figure 2.16

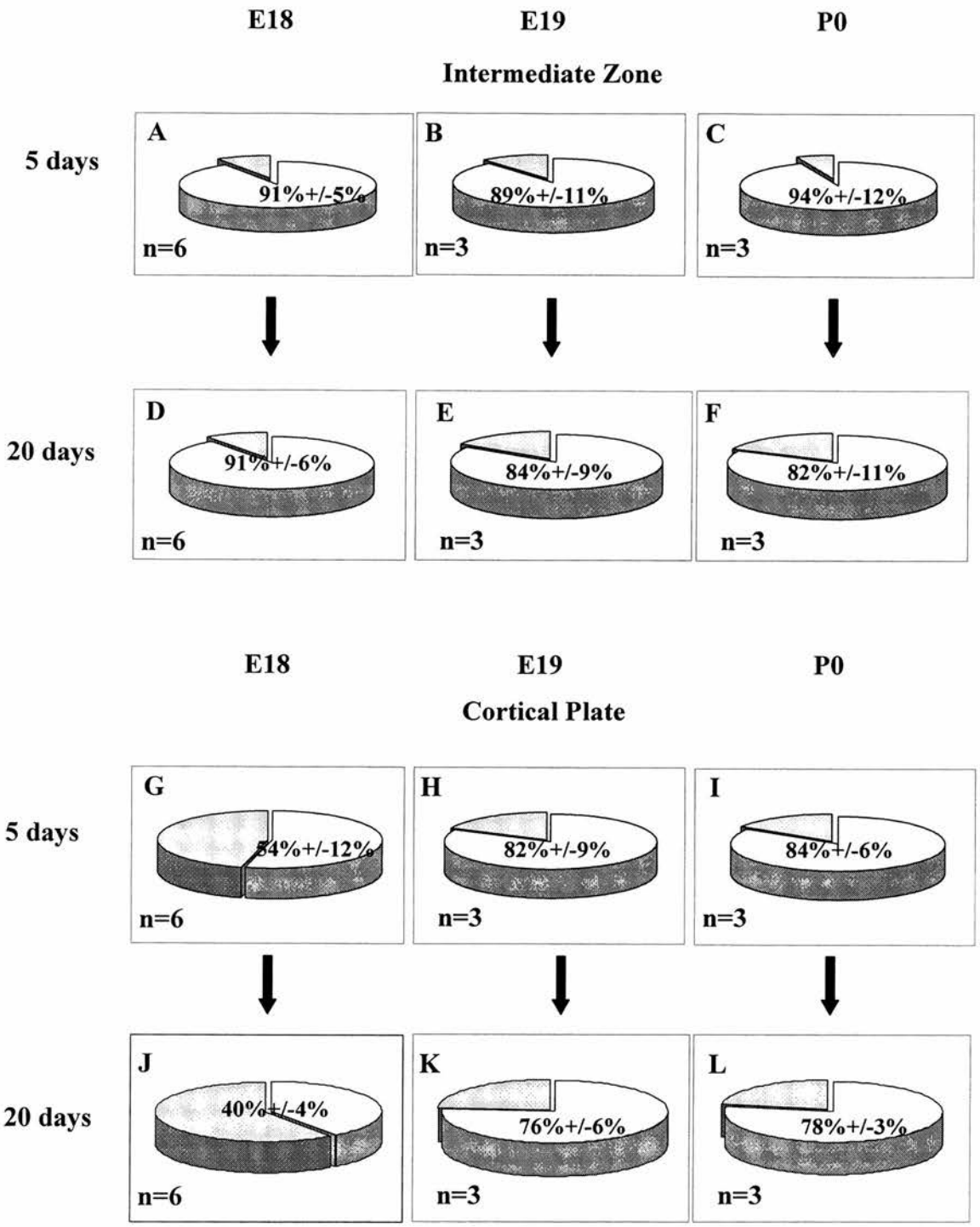
E18
E19
P0
Intermediate Zone
5 days
A
91%+/-5%
n=6
B
89%+/-11%
n=3
C
94%+/-12%
n=3
20 days
D
91%+/-6%
n=6
E
84%+/-9%
n=3
F
82%+/-11%
n=3
E18
E19
P0
Cortical Plate
5 days
G
84%+/-12%
n=6
H
82%+/-9%
n=3
I
84%+/-6%
n=3
20 days
J
40%+/-4%
n=6
K
76%+/-6%
n=3
L
78%+/-3%
n=3

Figure 2.17

Confocal images illustrating BrdU and QK1 double immunolabelled cells **(A)** E19 (E19 + 1 hour) cortex showing strong staining in the PZ. BrdU and QK1 double-labelled cells are indicated by the arrowheads, while single BrdU labelled cells are indicated by the arrows. The intensity of the QK1 staining within the PZ, made identification of double labelled cells difficult.

(B) The E18 labelled BrdU cells in the upper CP after 20 days post-injection do not double label with the QK1 antibody. Arrowheads indicate double-labelled cells in the CP; Arrows indicate BrdU cells in the upper CP that are not expressing QK1. **MZ**: Marginal zone; **CP**: Cortical plate; **IZ**: Intermediate zone.

Figure 2.17

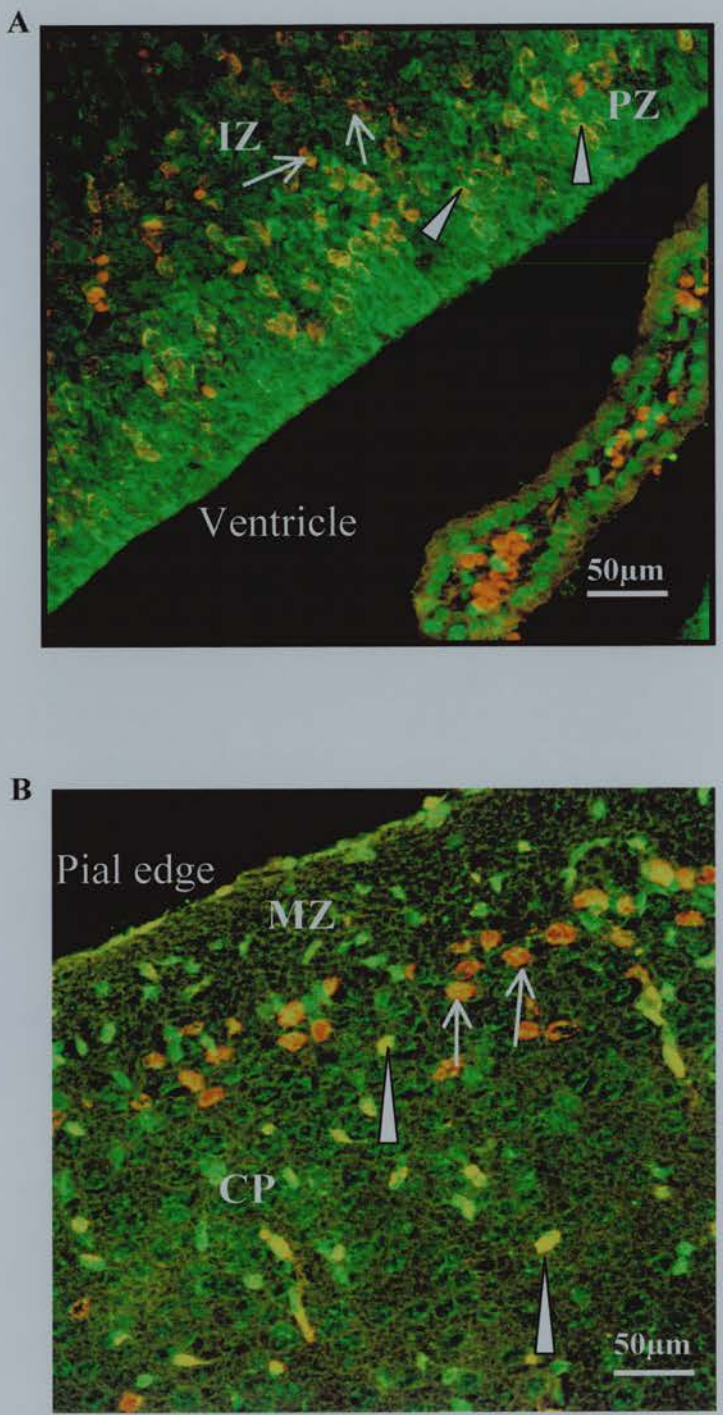

2.5 DISCUSSION

The purpose of this study was to characterise the proliferative behaviour, migration and antigenic properties of cells born in the transition period between neurogenesis and gliogenesis. The timing and location of neuronal proliferation within the cortex is well understood, whereas the timing of events of glial cell proliferation is much less well understood.

Initially the distribution patterns of E16 and E17 BrdU labelled cells (neuronal progenitors) were compared to the distribution patterns of E18, E19 and P0 labelled BrdU cells after a 1 hour BrdU pulse. The results suggested that E18, E19 and P0 labelled BrdU cells had different distribution patterns than the E16 and E17 BrdU labelled populations.

Secondly, the results suggested that the E18, E19 and P0 labelled cell populations decreased in density between 2 and 20 days post BrdU injection. For the E18 labelled population the decrease in density could be accounted for by cortical expansion alone. The E19 and P0 populations however, decreased in density more than could be accounted for by cortical expansion alone. Finally, this study showed that E18 born cells within the mouse cerebral cortex gave rise to both neuronal and glial cells, whereas cells labelled on either E19 or P0 with BrdU gave rise to glial cells.

2.5.1 Technical considerations

Although the process of gliogenesis during post-natal development has been well studied, pre-natal gliogenesis has been less well studied and is therefore poorly understood (Levison and Goldman, 1993). This is in part due to the fact that early glial cells are notoriously difficult to study. There are two main reasons for this. Firstly, glial cells continually divide throughout life (Sturrock, 1979), thus making BrdU and [^{3}H]-thymidine studies difficult to interpret over time due to the dilution of the label (Levison *et al.,* 1993). Secondly, very few antibodies are available that specifically label glial progenitors (Gonye *et al.,* 1994), hence making early identification difficult.

In addition to the above previously reported problems further technical difficulties were experienced during this study when attempting to label the BrdU cells with specific neuronal markers. MAP2 staining was employed, but the observed immunostaining pattern was so intense throughout the cortical plate that identification of individual BrdU cells that were also expressing MAP2 was difficult. Furthermore, this study was performed on paraffin embedded tissue. Many antibodies are unable to penetrate through paraffin embedded tissue, hence the number of antibodies available for use in this study is restricted.
However, in view of these difficulties, conclusions were still made regarding the behaviour of E18, E19 and P0 BrdU labelled cells based upon the densities and positions of the cells over a 20 day period and immunohistochemically using the recently characterised QK1 antibody as a marker for glial progenitor cells.

2.5.2 Stratification of the cortical wall

Throughout this study the locations of cells were classified according to the cortical zone in which they resided in over a 20-day time period. Throughout this period the thickness of the cortical wall increased and the individual cortical zones within it altered in width over time. Therefore the first part of this study involved examining the changing stratification of the cortical wall over time. Although this has previously been done by Takahashi *et al.,* (1995), this present study employed a different processing technique than that used by the above experimenters. I therefore felt it was important to determine how the tissue processing method used in this study affected the cortical stratification over time.

Generally, a reduction in the width of the proliferative zones was accompanied by an increase in width of the cortical plate (Smart, 1961; Lewis, 1968; Privat and Leblond, 1972; Paterson *et al.,* 1973). These changes are due largely to cells of the proliferative zones migrating radially to populate the cortical wall. Although the cortex appeared to attain its maximum thickness by P8, this was unlikely a true reflection of the actual width of the cortex, because the P18 and P19 brains were visibly larger than P8 brains. The most likely explanation for this is that the neuropil (which contributes most to the expansion of the cortex once neurogenesis is

complete) (Angevine, 1965), preferentially shrinks due to the processing used for paraffin wax embedding. The IZ/WM expanded initially until P3 when it attained a stable thickness. This is consistent with the theory that glial progenitors at about the time of birth migrate away from the PZ and populate the IZ where they differentiate into oligodendrocytes. The reduction in width of the SP can be explained by the transient nature of this structure, which has been shown to disappear by early postnatal life (Price *et al.,* 1997).

2.5.3 A comparison of the distribution patterns of E16 and E17 BrdU labelled cells with E18, E19 and P0 labelled BrdU cells.

Although this study was primarily involved in characterising the behaviour of E18, E19 and P0 labelled cells, comparisons were made with E16 and E17 labelled cell populations after a 1 hour BrdU pulse as the behaviour of these cells is more clearly understood. It is clear from the literature that cells that uptake BrdU on E16 and E17 are neuronal precursors (Angevine and Sidman, 1961: Caviness and Sidman, 1973; Caviness, 1982). A distinguishing feature of neuronal precursors is that they undergo interkinetic migration during the different stages of the cell cycle (Sauer, 1935; Sauer and Walker, 1959; Sidman *et al.,* 1959; Fujita, 1960, 1963; Hinds and Ruffett, 1971). To assess if the E18, E19 and P0 BrdU labelled cell populations behaved similarly to the E16 and E17 labelled populations their distribution patterns were examined 1 hour post BrdU injection. The distribution patterns of E16 and E17 labelled cells were as expected for cells that undergo interkinetic migration (figure 2.6). Cells were observed in a band at a small distance away from the ventricular edge, presumably representing the region of the VZ where cells were in S phase (Chapter 1; figure 1.7). A few cells were also seen above and below this band of cells, representing cells that were leaving S phase and entering G2 phase (Takahashi *et al.,* 1992). Similar results for E14 labelled cells have been reported previously (Takahashi et al., 1993).

By E18 the VZ has largely disappeared and the proliferative zone consisted mainly of the SVZ (Takahashi *et al.,* 1995). The distribution patterns of the E18, E19 and P0 labelled cells differed from the observed patterns of the E16 and E17 labelled

populations. BrdU labelled cells were evenly positioned throughout the whole width of the PZ (figure 2.6C, D and E). In addition to this E18, E19 and P0 labelled cells were observed within the overlying IZ/WM, SP, CP and occasionally the MZ after a 1 hour BrdU pulse. Since neuronal precursors do not normally divide in these regions it is most likely that these cells were glial precursors or glial cells that were undergoing further rounds of cell division after they had left the proliferative zone. The IZ as a proliferative region for glial cells has previously been reported (Berman et al., 1997).

In view of the observed differences in distribution patterns between the E16/E17 labelled cells and the E18, E19 and P0 labelled cells after a 1 hour BrdU pulse, it is likely that E18, E19 and P0 labelled cells do not give rise primarily to neurones. Hence the difference in the distribution patterns after a 1 hour BrdU pulse of the different labelled cell populations provides the first evidence in this chapter that the E18, E19 and P0 labelled cells are of the glial lineage.

2.5.4 Do E18, E19 and P0 labelled cells belong to the PVE or the SPP?

As described in the introduction to this chapter, proliferating cells belong either to the PVE or the SPP which give rise to neurones or glial cells respectively. Previous studies by Takahashi *et al* (1995) have shown that by E14, the SPP accounts for 10% of the proliferative population and by E16 35% of the proliferative population. In this study, approximately 30-40% of E18 labelled cells gave rise to cells that behaved like neurones (presumably derived from the PVE). Therefore it was speculated that the remaining 60-70% of the E18 labelled cells were from the SPP. According to Takahashi *et al.,* (1995), the PVE has reduced totally by E19, suggesting that the cells labelled on E19 and P0 in these experiments consist entirely of cells of the SPP.

2.5.5 Cell density

The first observation made from the study of the E18, E19 and P0 labelled cell populations was that all three cell populations decreased in density between 2 and 20 days (Figures 2.3 and 2.5). The four most likely explanations to account for these

reductions in cell densities are 1) expansion of the cortex, 2) dilution of the BrdU label due to successive mitosis, 3)cell death and 4)cell migration. It is possible that just one or a combination of these processes contribute to the observed reduction in cell density over time.

To assess the contributing role of cortical expansion to the reductions in cell density, an expansion factor was calculated (see methods). This expansion factor was used to calculate from 2 days the expected density of cells at five, nine and twenty days post-injection. The expected cell densities were compared with the actual densities.

For the E18 labelled cell population, the actual cell density plots and the expected cell density plots were both similar (both light and dark labelled cells) (figure 2.3A and 2.4A). This was a strong indication that the reduction in cell density between 2 and 20 days was due purely to cortical expansion. These finding are perhaps not that surprising as Caviness *et al.,* (1995) and Polleux *et al.,* (1997) have shown that cells of the PVE undergo their final round of cell division on E18. Therefore it is likely that the labelled cells in this study were the last cells of the PVE and form a relatively stable population of cells that don't divide or migrate to other regions of the brain.

However, the possibility of net migration in which BrdU labelled cells migrate into the cortex at the same rate as BrdU cells migrate out cannot be ruled out. Numerous studies have demonstrated that during cortical development radial as well as tangential migration occurs (Rakic, 1972; 1988; O'Rourke *et al.,* 1992; 1995). Of particular interest is the migration of cells between the cortex and the LGE (lateral ganglionic eminence) in the adjacent striatum. The traditional held belief is that migration of cells between these two regions is a one-way procedure, in which cells from the LGE can migrate into the cortex (Rakic, 1972; 1988; O'Rourke *et al.,* 1992; 1995) whereas cortical cells are unable to migrate into the LGE. In view of the results in this chapter and the reported literature the E18 labelled cells are suggested to form a relatively stable population of cells. This is true up until at least 20 days.

The E19 labelled cell population of decreased in density as predicted by the expansion factor up until 5 days post injection. For reasons explained above this population of cells is suggested to be in a state of stable equilibrium. However, by 9 days post-injection the actual density of cells (light and dark labelled populations) had fallen to a significantly lower value than the expected density implying that cells were either dying, diluting out or migrating out of the counting area between 5 and 9 days after the BrdU injection.

Cell death is an important and necessary process that occurs during cortical development to ensure the correct numbers of cells and the correct connections are made at the correct developmental time (Finlay and Slattery, 1983; Blaschke *et al.*, 1996). Recently, Blaschke *et al.,* (1998) have shown that over 50% of proliferative cells die during development. In view of the results shown by Blaschke *et al.,* (1998) the results from this study are surprising. Only 1 or 2 BrdU cells at any one age were pyknotic, leading to the conclusion that the E19 labelled BrdU cells were not dying. The difference between the results in this study and the results of Blaschke *et al.,* (1998) can be explained in terms of the sensitivity of the techniques employed. Alternatively, the dying cells could be cleared away so rapidly that an inaccurate representation of the amount of cell death is recorded in this study.

The reduction in density of the E19 BrdU labelled cells (both light and dark labelled populations) between 5 and 9 days could be explained by cell division, although without a more comprehensive study no more further suggestions about the proliferative behaviour of these cells can be made. Finally, cell migration out of the counting region of the cortex could account for the observed reduction in cell density. For reasons outlined above it is unlikely that these cells are migrating to the LGE. However, Luskin *et al.* (1994, 1995) have shown that cells migrate tangentially from the SVZ to the olfactory bulb. It is possible that the E19 labelled cells represent a similar population of cells which are previously unreported in the literature. Between 9 and 20 days the densities of both dark and light labelled cells slightly increased. This could be explained in terms of tangential migration of cells

into the cortex (Rakic, 1972; 1988; O'Rourke *et al.,* 1992; 1995; Luskin *et al.,* 1994, 1995).

The P0 labelled cell population (both light and dark) decreased in density more dramatically than could be explained by cortical expansion alone between 2 and 20 days. There is some evidence to suggest that that the reduction in density is due to cell proliferation. The lightly labelled cell population (many of which are the products of one or more subsequent rounds of cell division) represented a much larger proportion of the total cell density in comparison with the E18 and E19 labelled cell populations. Previous experiments by Morshead and Van der Kooy (1992) have shown that adult mouse subependymal cells dilute BrdU out by 8 days after injection. If proliferation does account for the reduction in cell density, the P0 labelled cells must have a relatively short cell cycle time since they begin to dilute out by 5 days after the injection. In addition to cell proliferation the reductions in cell density could be accounted for by cell migration or cell death as described above.

The results from this analysis provide evidence that the E18 labelled population behave differently than the E19 and P0 population. The E18 labelled cells form a stable population of cells, whereas the E19 and P0 labelled cell populations migrate, proliferate or die over the period of study.

2.5.6 Distribution and fate of BrdU labelled cells

2.5.6.1 E18 labelled population

The results of the distribution study suggested that 30-40% the E18 labelled cells behaved like neuronal precursors in that they migrated from the proliferative zone to the upper CP just under the MZ. The nuclei of these cells were similar in terms of size and appearance to neuronal cells born during the peak period of neurogenesis (own observations). The remainder of the E18 labelled cells remained within the proliferating zones and the WM. The nuclei of these cells were smaller than those found at the upper cortical plate and were presumably from the SPP. Unlike Gressons *et al,* (1992), who showed that this population of cells differentiated into

GFAP positive astrocytes, only a small percentage of the E18 labelled cells differentiated into GFAP positive astrocytes, but the majority of them were labelled with the QK1 antibody. QK1 proteins have previously been shown to be expressed by differentiated glia and neuronal and glial progenitors (Hardy et al., 1996; Hardy, 1998). As progenitor cells undergo the neuronal cell fate decision, QK1 expression becomes restricted whereas if a progenitor cell differentiates into a glial cell QK1 expression in maintained (Hardy 1998). Therefore in view of the distribution pattern of these cells, and the expression of QK1 it is likely that these cells were of the glial lineage.

A simple explanation for the discrepancies in results between this study and the work of Gressens *et al.,* 1992 could be explained in terms of sub optimal GFAP labelling in this study for reasons outlined at the beginning of this discussion. However, it is important to note, that the above experimenters did not quantify their findings, and hence it is unclear as to the exact proportions of GFAP labelled cells that they observed.

A comparison of the E18 labelled cell distribution pattern with the E16 labelled cell distribution pattern revealed that the distribution patterns were very different. The majority of E16 labelled cells after 5 days were found within the CP. Very few remained in the PZ. No E16 labelled cells in the CP labelled with either QK1 or GFAP, suggesting that the E16 population of labelled cells gave rise purely to neuronal cells whereas the E18 population gave rise to a split population of progenitor cells, giving rise to neurones and glia.

2.5.6.2 E19 labelled cells

Unlike the E18 population, no cells were observed in a band underneath the MZ. A decrease in cell density within the PZ and a corresponding increase in density within the CP, suggests that cells have migrated from the PZ to the CP over the time period of study. This is consistent with a retro-viral analysis of cells of the glial lineage by Parnavelas, (1999). Similarly to the E18 labelled cell population, only a small percentage of the E19 labelled cells were labelled with GFAP, yet the vast majority of these cells labelled with the QK1 antibody. Although it was not possible to

discern whether these cells were of the oligodendrocyte or astrocyte lineage, this study confirmed that they were of the glial lineage.

2.5.6.3 P0 labelled cells

The distribution of the P0 labelled cells was less easy to interpret due to the large loss of cells between 2 and 20 days, as described earlier. However, from these studies it was clear that these cells were of the glial lineage. A similar proportion of double-labelled cells with QK1 and GFAP were seen as for the E19 labelled cell population.

2.5.7 Conclusions

The aim of this study was to characterise the proliferating population of cells at the end of neurogenesis / beginning of gliogenesis. These results suggest that E18 labelled cells and the E19 and P0 labelled cells form two distinct proliferative populations. The E18 labelled population consists of cells of the PVE and SPP giving rise to both neurones and glial cells, whereas the E19 and P0 labelled cell populations consist of cells of the SPP giving primarily to glial precursors.

In summary this chapter provides quantitative information on the proliferating cells born during the transition period between neurogenesis and gliogenesis. This is the first evidence to indicate the exact transition time between neurogenesis and gliogenesis in the mouse neocortex. This data is of importance when considering experiments involved in determining specific factors involved in cell fate determination. Future investigations arising from this work are described in more detail in the summary chapter at the end of this thesis.

CHAPTER 3: A TISSUE CULTURE APPROACH TO STUDYING CELL FATE

3.1 ABSTRACT

In the cerebral cortex glial progenitors receive information from neighbouring cells and soluble factors as well as their own intrinsic developmental signals. To identify the role of soluble factors upon the survival, proliferation, migration and differentiation of cells of the glial lineage, a tissue culture technique was devised.

The identity and behaviour of subpopulations of cells within E19 cortical explant cultures were challenged by culturing cortical slices in culture medium, preconditioned with E15 cortical derived soluble factors. The survival, proliferation, migration and differentiation of sub-populations (BrdU, GFAP and O4 labelled cells) of cells were examined.

The results suggest that E15 and E19 cortical derived factors have multiple effects upon the behaviour of these subpopulations of cells. These results fit in with a general consensus for the regulatory role of extrinsic factors during cortical development.

3.2 INTRODUCTION

The previous chapter shows that E19 born cells give rise to either glial progenitor cells or more committed glial cells within the developing mouse neocortex. Following on from the study in chapter 2, this study was designed to investigate the role of diffusible factors upon the survival, migration, proliferation and differentiation of sub-populations of cells in E19 cortical explant cultures. Although previous studies have investigated the role of diffusible factors on the behaviour of neuronal progenitor cells (Ghosh and Greenberg, 1995; McKay, 1989; Cataneo and McKay, 1990) and glial progenitor cells (Hughes *et al.,* 1988; Lillien and Raff, 1990: Lillien *et al.,* 1990; Gard *et al.,* 1995; Barres and Raff, 1994) in dissociated cell cultures very few studies have investigated the role of diffusible factors on progenitor cell behaviour in cortical explant cultures.

As described in the main introduction, the neocortical epithelium consists of a thin layer of proliferating cells. As development proceeds cells migrate radially away from the proliferative zones towards the pial surface below which they form the CP and differentiate into neurones. The main phase of gliogenesis occurs sequentially after neurogenesis is complete and continues throughout the early postnatal period (with the exception of radial glial cells). The mechanisms that regulate neural diversity and the appropriately timed differentiation of neurones and glia during corticogenesis are poorly understood. There is substantial evidence to suggest that cells within the neuroepithelial layers can generate different phenotypes depending upon their local cellular microenvironment (Reviewed in Stemple and Mahanthappa, 1997). Due to the sequential development of different cell types, it is possible that different factors are expressed at various stages in development.

Understanding the mechanisms by which extrinsic factors control proliferation and differentiation of neural precursors will elucidate the cellular and molecular mechanisms that control these processes. To date, a variety of factors have been implicated in regulatory roles during development. The two main classes of factors that are involved in regulation of CNS development are the peptide growth factors and the neurotransmitters. The main members of the peptide growth factor family include fibroblast growth factor (FGF), transforming growth factor-α (TGF-α),

epidermal growth factor (EGF), Insulin-like growth factor-1 (IGF-1), bone morphogenetic proteins (BMP), Ciliary neurotrophic factor (CNTF), leukemia inhibitory factor (LIF) and platelet derived growth factor (PDGF). These factors all have a variety of different effects during CNS development, which are reviewed in Cameron et al., (1998). In addition to these growth factors a variety of neurotransmitters have been implicated in regulatory roles during CNS development, the main ones reported being GABA and glutamate which have been implicated a playing role in cell proliferation (reviwed in LaMantia, 1995).

The assessment of the role of extrinsic factors during cortical development requires the development of an appropriate *in vitro* system in which survival, proliferation, migration and differentiation can be examined under controlled conditions. In this study an explant tissue culture technique was employed.

3.2.1 Culturing brain slices

To date four different culture methods have been employed to study living brain slices. These include 1) the Maximow depression-slide technique in which slices are maintained in a drop of culture medium within a small glass enclosed chamber, 2) the roller tube method in which the tissue is embedded in a collagen matrix and undergoes slow rotation, 3) the poly-acylamide/gauze method, in which several explants are placed on a piece of gauze in a culture dish and intermittently exposed to air by slow rocking of the cultures and 4) the air/medium interface method, in which explants are placed on a porous membrane/filter at the interface between the medium and the air (Stoppini *et al.,* 1991). Techniques 1- 3 are reviewed in Humphreys *et al.* (1996).

Each of the above four techniques are effective methods for culturing brain slices. The specific culture technique employed in an experiment depends very much on the specific questions that are being addressed. For example brain slices cultured using the rollerdrum method have been shown to flatten to a monolayer, which is useful in experiments which require optimal optical conditions. The air/interface method (Stoppini *et al.,* 1991) has been shown to be important in experiments in which the

three dimensional structure of the cortex is desired. Using this latter technique Gillies and Price (1993) have shown that tissue only flattens by approximately 20%.

3.2.2 Previous studies

Explant cultures have proven to be a useful tool for studying processes such as cell migration and differentiation. Roberts et al (1992), Gotz and Bolz (1992), Price and Lotto, (1996). Wolburg and Bolz (1991) and Gillies and Price (1993) have all shown that cells behave normally in terms of their migratory behaviour in cortical explant cultures. Furthermore Gotz and Bolz (1992) have shown that the six layered structure of the cortex is maintained *in vitro* and that radial glial cells are present and act as the substrate for neuronal migration, as they do *in vivo*. Therefore explant cultures provide a suitable, realistic assay in which to study extrinsic cues in cell fate decisions.

3.2.3 Study

In this study a tissue culture technique was developed, based on the method by Stoppini *et al.* (1991) to assess the role of environmental influences upon the behaviour of cells in E19 cortical slice cultures. More specifically, the identity and behaviour of specific subpopulations of cells (proliferating cells (BrdU), cells of the astrocyte lineage (GFAP) and cells of the oligodendrocyte lineage (O4)) were challenged by growing the cortical slices in culture medium that had been preconditioned with E15 cortex.

Two different methods of analysis were employed in this study. When studying the BrdU and GFAP subpopulations of cells, the densities and distributions of these cells after 3 days in culture were compared to their respective densities and distribution patterns after 1 hour in culture. However, when analysing the O4 subpopulation of cells it was not possible to make similar types of comparison because no O4 staining was observed in E19 cortical slices after only 1 hour. Therefore the O4 staining after 3 days in cultures was compared between the three different culture conditions that were employed.

3.2.4 Summary of results

The results from these experiments show that sub populations of cells in E19 cortical explant cultures are responsive to E15 and E19 cortically derived soluble factors. In general the E19 derived soluble factor had a positive effect on cell proliferation or survival, whereas the E15 derived soluble factor had a negative effect on cell survival or proliferation. Isolating and identifying these factors will have profound importance in the understanding of mechanisms involved in glial cell development.

3.3 MATERIALS AND METHODS

3.3.1 Conditioning cortical medium

The forebrain of E15 and E19 pups were dissected in ice cold Earles balanced salts solution (EBSS) under sterile conditions. The meninges were removed and the presumptive neocortex isolated. The tissue was chopped on a MacIlwain tissue chopper at 500μm in the horizontal plane and 500μm in the vertical plane. Approximately 30 pieces of tissue were placed onto a filter in a 24 well plate containing 500μl of culture medium. The tissue was cultured for 24 hours at 37^0C in 95% O_2/5% CO_2. The culture medium was then removed and stored at -70^0C until required (figure 3.1).

3.3.2 Explant cultures

C3H mice from an inbred colony were mated overnight and the following day was deemed embryonic day 1 (E1). Pregnant mice were anaesthetised on E19 with 0.35ml of 25% Urethane in saline (i.p). Embryonic mice brains were obtained by caesarean section. Brains were dissected in ice cold EBSS, and stored in pre-warmed culture medium for 45 minutes. Following incubation, brains were sliced on a Macilwain tissue chopper at 350μm in the parasagital plane. The presumptive neocortex was teased away from the rest of the brain using forceps (figure 3.2A). Cortical slices were incubated for 4 hours in either 1.5ml pre warmed (37^0C) culture medium (appendix 1) or 1ml of culture medium + 0.5ml of conditioned medium.

BrdU was added to the culture medium at a concentration of 40μg ml^{-1} for 1 hour, after which the tissues were removed and placed in pairs on collagen coated filters (Costar), containing either 2.2ml of culture medium or 1.7mls of culture medium + 0.5 ml of conditioned medium (E15 or E19) (figure 3.2B).

To reveal the starting conditions explant cultures were fixed one hour after BrdU administration to reveal the pattern of BrdU staining and the morphology of GFAP and O4 positive cells at the beginning of the culture. The remaining slices were cultured for 3 days at 37^0C in 95% O_2/5% CO_2.
All procedures were performed under sterile conditions.

3.3.3 Cell distribution / number analysis

To reveal the distribution patterns of BrdU labelled cells within the cortical slice, camera lucida drawings were made of the BrdU labelled cells within a 500μm wide strip spanning the entire width of the cortical wall. This has been described in chapter 2. Four alternate sections were drawn from each slice, although in some cases it was only possible to draw three sections. Cell counts were performed in the centre of each slice. To determine the relative position of the cells within the cortical wall, the camera lucida drawings were divided into 10 equal size bins, from the ventricular edge to the pial edge (Figure 3.2C). The average number of cells (dark and light) in each bin were calculated and plotted as a proportion of the total cell number against the relative bin number.

3.3.4 BrdU and O4 immunocytochemistry

3.3.4.1 Fixation and processing of slices

Slices were fixed in 4% paraformaldehyde in 0.1M phosphate buffered saline (PBS;pH 7.4) for 1 hour. The slices were washed three times in PBS and stored overnight at 4^0C. Slices were dehydrated in a series of alcohols: 70% ethanol (2x15 minutes), 90% ethanol (2x15minutes), 100% ethanol (2x 15 minutes), and cleared in chloroform for 2 hours. Slices were removed from the collagen filters with a scalpel blade and transferred to paraffin wax for 3 hours (60^0C). Tissues were sectioned at 10μm on a microtome, mounted onto poly-L-lysine coated slides and incubated at 37^0C overnight. Sections were dewaxed by immersing in Xylene for 12 minutes and then rehydrating through a decreasing series of alcohols: 100% ethanol (3 minutes), 90% ethanol (3 minutes), 70% ethanol (3 minutes) and into water (3 minutes).

3.3.4.2 Antibody reaction

Slices were either reacted for BrdU alone or double immunostained for BrdU and GFAP. The methods for both of these techniques have been described in chapter 2. Double-labelled cells were identified on a Leica TCS NT confocal microscope as indicated in chapter 2.

3.3.5 O4 Immunocytochemistry

Slices were fixed as above. Following three washes in PBS, slices were blocked for 30 minutes in 10% normal goat serum, 1% gelatin, 5% BSA in PBS and incubated overnight in O4 (see below) diluted in the same buffer (1:10). Slices were incubated in a biotin-conjugated secondary antibody (DAKO;IgM 1:200) for 2 hours, followed by a 1 hour incubation in flourescein avidin (Vector 30μg/ml). All stages were followed by three washes in PBS (20 minutes each).

3.3.6 O4 Hybridoma cells

Mouse hybridomas producing O4 IgM mAb (Sommer and Schachner, 1981) were a gift from Dr R Hardy, University of Edinburgh. Hybridoma cells were grown in Optimem (Gibco, Paisley, Scotland) with 10% FCS, penicillin (100 IU/ml), and streptomyocin (100μg/ml) at 37^0C. When cells were approximately 80-90% confluent, the medium was isolated, centrifuged and the supernatant was stored at – 70^0C until required.

Figure 3.1.

A schematic diagram illustrating the method for conditioning culture medium with cortical derived soluble factors. The presumptive neocortex was isolated from mouse brain (E15 and E19) and chopped into 500μm squares on a Macilwain tissue chopper. Tissues were cultured overnight in standard serum free culture medium. Soluble factors released from the cortex diffused into the surrounding culture medium. This medium was collected and stored ready for use.

SF: Soluble factors.

Figure 3.1

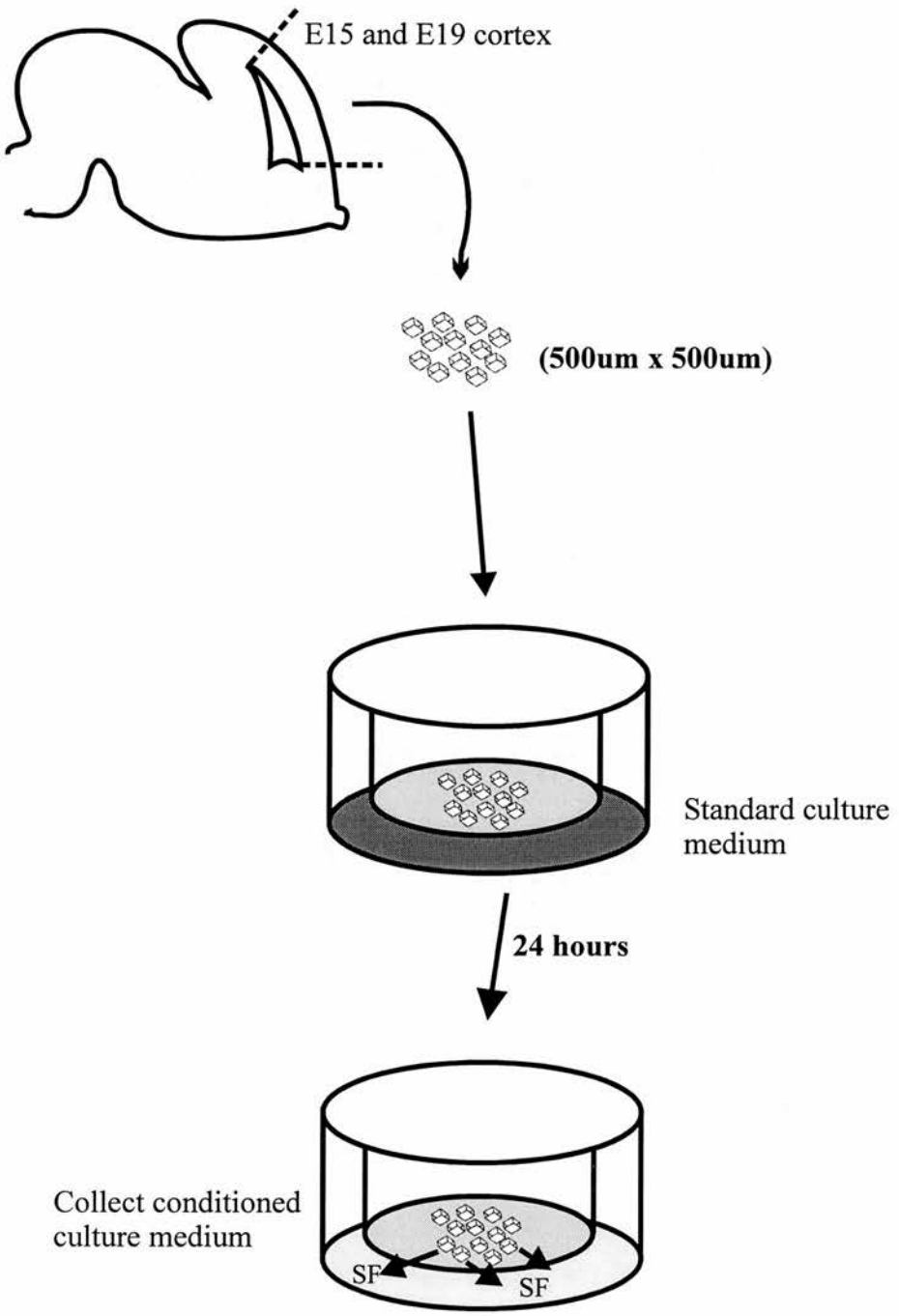
E15 and E19 cortex
(500um x 500um)
Standard culture medium
24 hours
Collect conditioned culture medium
SF
SF

Figure 3.2

(A) Diagrammatic representation of a parasagittal section of an E19 cortex. Cortical slices were obtained from the region indicted between the dotted lines.

(B) Cortical slices were cultured in (i) normal culture medium, (ii) E15 conditioned cortical medium or (iii) E19 cortical conditioned medium.

(C) Camera lucida drawings were made of the cells within a 500μm wide strip of the cortex. Drawings were divided into ten equal size bins, enabling the relative position of cells throughout the cortical width to be established.

P:Pial edge**; V:** Ventricular edge**; Ctx:** Cortex

Figure 3. 2

A

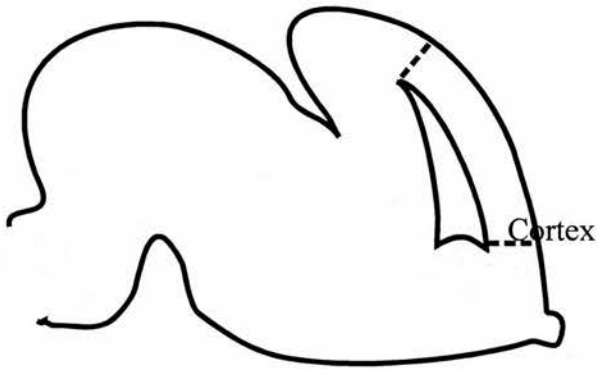

B

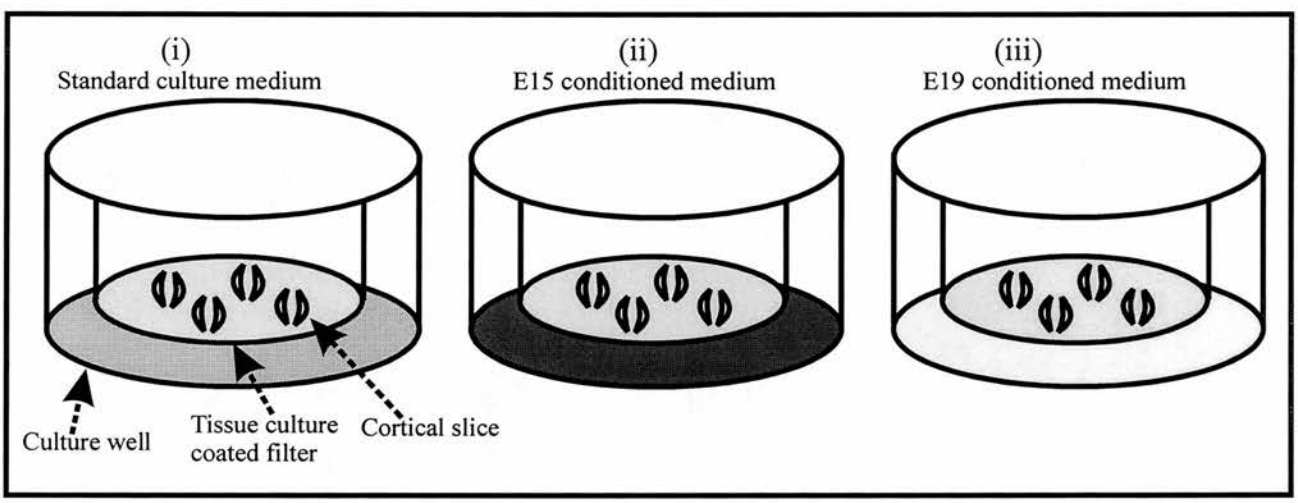

C

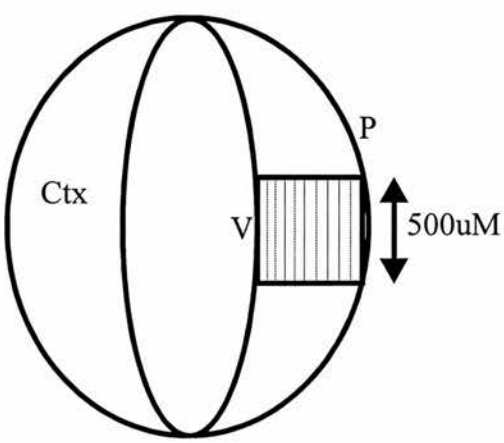

3.4 RESULTS

The aim of this study was to examine the behaviour (survival, migration, proliferation and differentiation) of subpopulations of cells in E19 cortical slice cultures. This was achieved by growing E19 cortical slices in E15 cortical conditioned medium to determine if extracellular factors were involved in glial cell development. BrdU, GFAP and O4 antibodies were used to label subpopulations of cells within the cortical slice and their position, morphology and density examined 1 hour and 3 days after BrdU administration for GFAP and BrdU immunocytochemistry and after just 3 days for O4 immunocytochemistry. For comparison purposes E19 cortical slices were also cultured in NM and E19CM for the three-day period.

3.4.1 Distribution of BrdU labelled cells

To determine if extrinsic cues effect the behaviour of subpopulations of cells undergoing S phase on or after E19, cortical slices were grown in three different conditions and BrdU uptake and distribution was examined after 1 hour and 3 days in culture. Figure 3.3A are camera lucida drawings illustrating the distribution of cells labelled with BrdU one hour after administration in normal culture medium (NM), E15 conditioned culture medium (E15CM), and E19 conditioned culture medium (E19CM). These results are presented in a graphical and photographical format in figures 3.3B and 3.3C respectively. In all three culture conditions cells were seen primarily in bins 1 and 2 (figure 3.3B) although a small percentage of the cells were seen in the other bins across the cortical width. These distribution patterns were similar to the distribution patterns obtained *in vivo* at E19 after a one hour BrdU pulse (Chapter 2; Figures 2.5 and 2.6C). No difference was observed in either the total number or the position of the BrdU labelled cells within the cortical width between the three-culture conditions. All dark and light labelled cells were counted together for reasons stated in chapter 2.

Figure 3.4A are camera lucida drawings illustrating the position of BrdU cells after three days in culture. These results are also illustrated in a graphical (figure 3.4B) and photographical format (figure 3.4C). The positions of the cells in all three-

culture conditions were compared to their respective positions after 1 hour in culture. BrdU labelled cells were more evenly distributed throughout the width of the cortex after three days in culture, and not located primarily in bins 1 and 2 as they were after one hour when cultured in either NM or E19CM. Furthermore a greater proportion of cells in the E19CM were seen in the region under the pia (Bins 8, 9 and 10) than was observed in slices cultured in NM. The distribution of cells in cortical slices cultured in E15CM for 3 days did not differ in comparison with their observed distribution after only 1 hour in culture. Cells were primarily located in a band along the ventricular edge (mainly bins 1-3), with a few cells scattered throughout the width of the cortex. Cortical slices were also grown in P3 and P5 conditioned culture medium, and similar distribution patterns were observed to the distribution patterns of the cells grown in E19 conditioned medium (data not shown).

The actual numbers of BrdU cells within a 500μm strip of cortex in each culture condition were all similar to each other after 1 hour (figure 3.5). However by 3 days in culture the densities of BrdU labelled cells in both the NM and E19CM significantly increased (Student *t* test, $p<0.05$) in comparison with their respective densities after 1 hour. A greater increase in density was observed for cells grown in E19CM than for cells grown in NM. In this study total number of BrdU cells were counted, so the observed increase in cell densities were likely the result of further cell division (i.e. an increase in number of lightly labelled cells). Interestingly, the density of BrdU cells in cortical slices cultured in E15CM for three days was similar to the respective density obtained after 1 hour, suggesting that these cells were not undergoing any further cell division.

In summary, these data show that the density and distribution of BrdU labelled cells in NM and E19CM are similar to each other after 1hour and 3 days in culture. In both of these culture conditions the density of cells increased between 1 and 3 days, and their distribution patterns altered over 3 days. Initially (1 hour) cells were primarily in the VZ and by 3 days in culture the cells were evenly distributed throughout the whole width of the cortex. In the E15CM the density and distribution of cells remained the same after 1 hour and 3 days in culture. These observations

Figure 3.3.

The distribution of BrdU labelled cells in E19 cortical explant cultures when cultured in three different culture conditions (NM, E15CM and E19CM) for 1 hour.

(A) Camera lucida drawings illustrating the position of BrdU labelled cells 1 hour after BrdU administration in NM, E15CM and E19CM. Cells were seen primarily at the ventricular edge of the cortex in all three-culture conditions.

(B) The proportion of BrdU cells per 10μm bin as a percentage of the total number of BrdU cells. Bin1 corresponds to the ventricular edge of the cortex, while bin 10 corresponds to the pial edge. In all three culture conditions cells were located primarily in bins 1 to 3.

(C) Photomicrograph illustrating the position of BrdU cells in an E19 cortical slice cultured in NM.

NM: Normal medium; **E15CM**: E15 conditioned medium; **E19CM**: E19 conditioned medium; **VZ**: Ventricular zone.

Figure 3.3

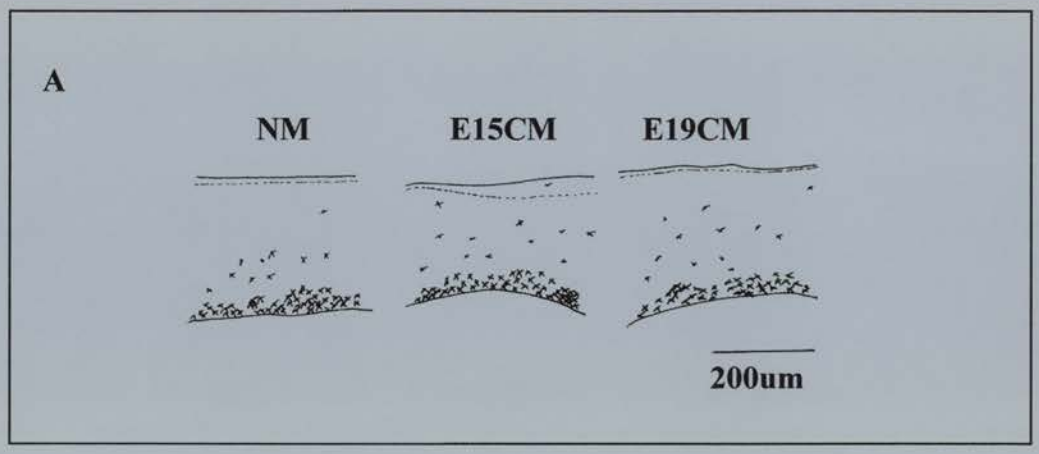
A
NM
E15CM
E19CM
200um

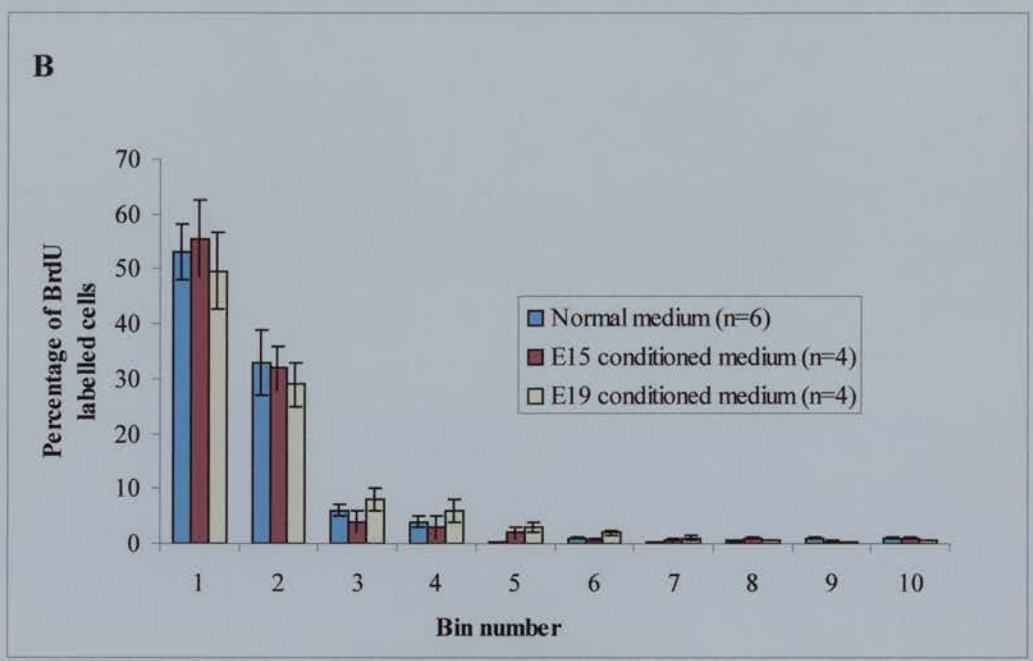
B
Percentage of BrdU labelled cells
70
60
50
40
30
20
10
0
1
2
3
4
5
6
7
8
9
10
Bin number
Normal medium (n=6)
E15 conditioned medium (n=4)
E19 conditioned medium (n=4)


C
PIA
VZ
100um

Figure 3.4.

The distribution of BrdU labelled cells in E19 cortical explant cultures when cultured in three different culture conditions (NM, E15CM and E19CM) for 3 days.

(A) Camera lucida drawings illustrating the position of BrdU labelled cells within an E19 cortical slice after culturing in NM, E15CM and E19CM for 3 days.

(B) The proportion of BrdU cells per 10μm bin as a percentage of the total number of BrdU cells. Bin1 corresponds to the ventricular edge of the cortex, while bin 10 corresponds to the pial edge.

(C) Photomicrographs illustrating the position of BrdU cells in all three culture conditions. See main text for details.

NM: Normal medium; **E15CM**: E15 conditioned medium; **E19CM**: E19 conditioned medium; **VZ**: Ventricular zone.

Figure 3.4

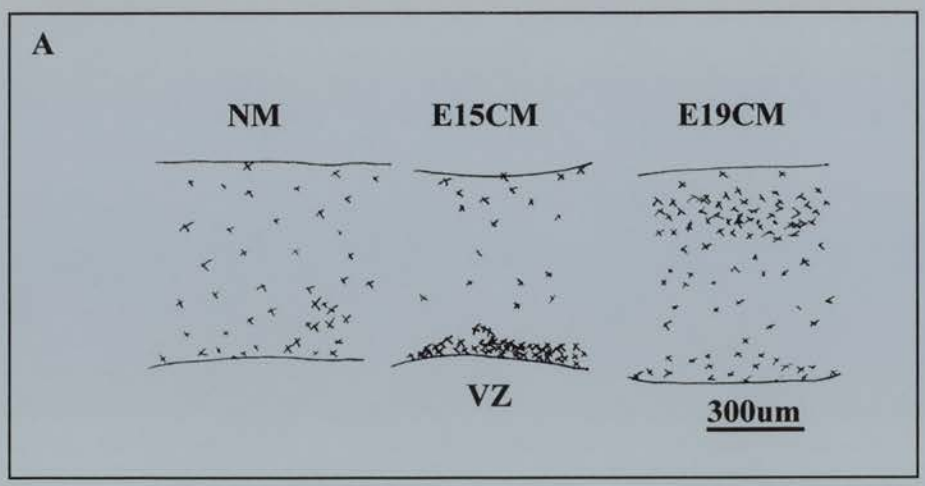
A
NM
E15CM
E19CM
VZ
300um

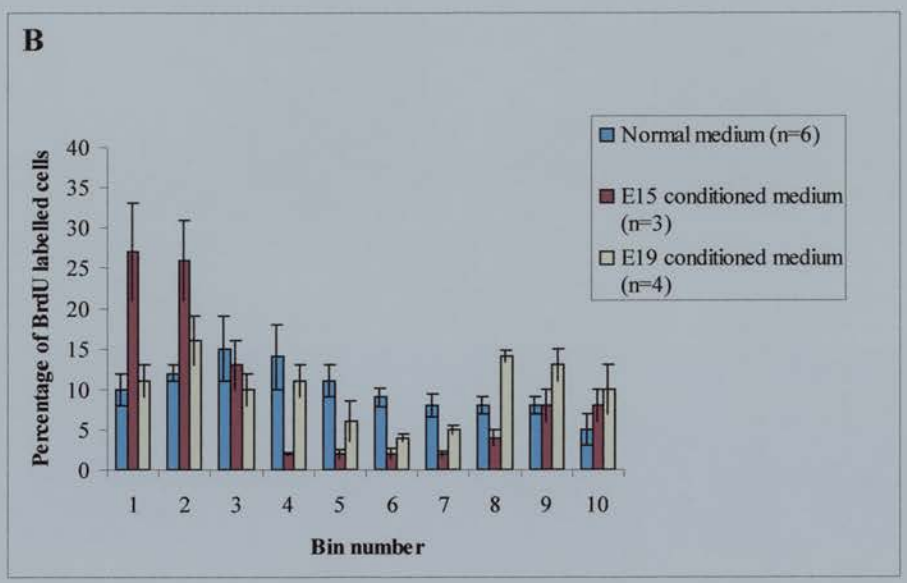
B
Normal medium (n=6)
E15 conditioned medium (n=3)
E19 conditioned medium (n=4)
Percentage of BrdU labelled cells
0
5
10
15
20
25
30
35
40
1
2
3
4
5
6
7
8
9
10
Bin number

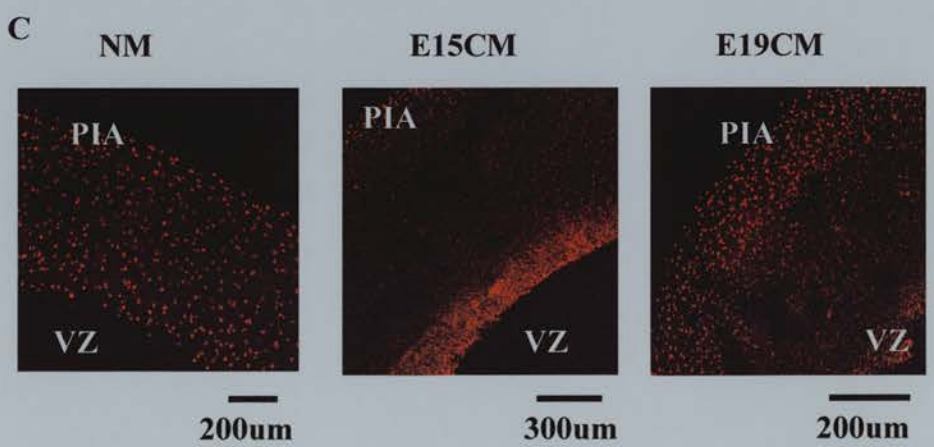
C
NM
E15CM
E19CM
PIA
VZ
PIA
VZ
PIA
VZ
200um
300um
200um

Figure 3.5

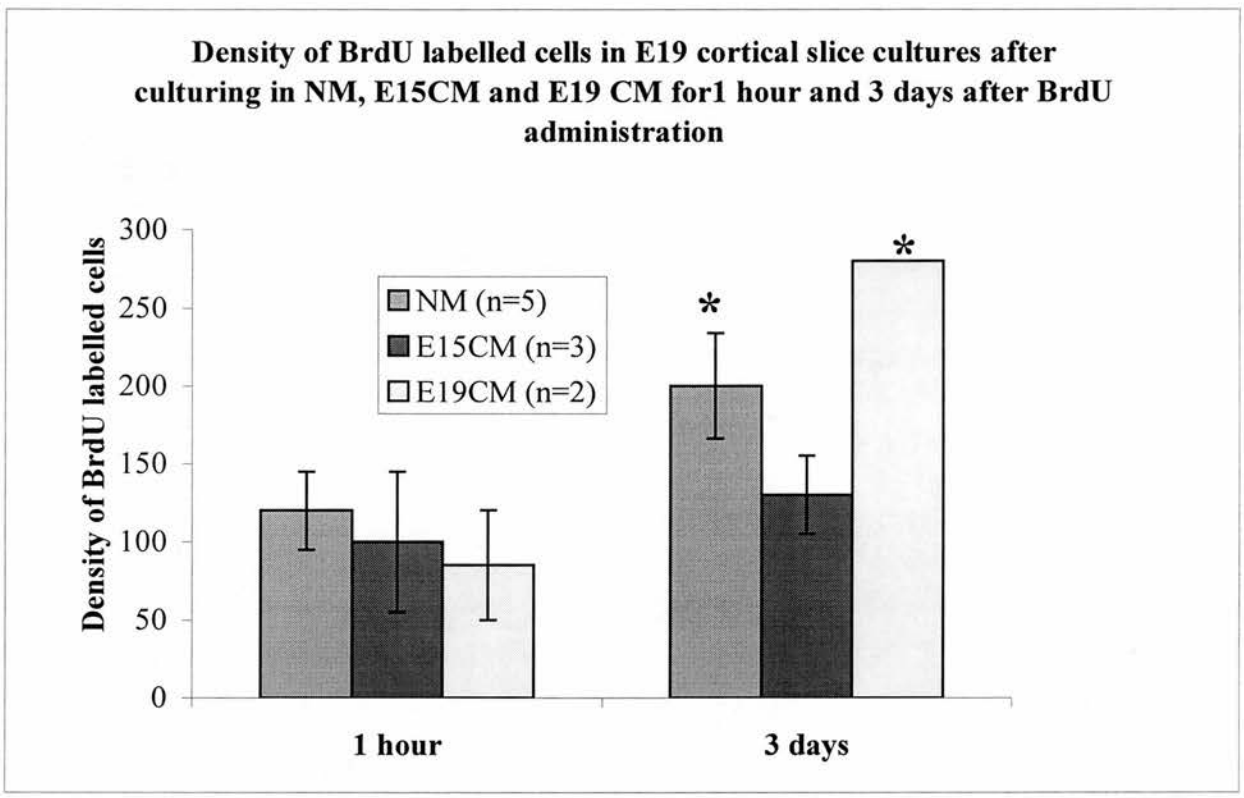

Figure 3.5

Histogram illustrating the density of BrdU labelled cells in a E19 cortical slice width of the cortical slice, after culturing in three different culture conditions for 1hour and 3 days after BrdU administration. See main text for details. Values are mean densities +/- SEM. The asterisks indicate a significant difference ($p<0.05$: Students *t* test).

show that soluble factors released from E15 and E19 cortex alter the migration and proliferation or survival (or both) of cells undergoing S phase in E19 cortical slice cultures.

3.4.2 Analysis of GFAP positive cells

To determine if cortically derived soluble factors affected cells of the astrocyte lineage, the number of GFAP positive cells were counted (within a 500μm strip) in each of the three different culture conditions. These results are shown graphically in figure 3.6. After only 1 hour in culture many GFAP positive cells (approx. 100 in a 500μm bin) were present in all three-culture conditions, the densities of which were all similar to each other. However, by three days in culture some obvious differences were apparent. When slices were cultured in NM for 3 days, there was a significant increase in the density (almost doubled) of GFAP positive cells in comparison with the observed density after 1 hour ($p<0.05$; Students *t* test). In contrast to this, the density of GFAP positive cells in cortical slices cultured in E15CM remained similar between 1 hour and 3 days in culture. Dramatic differences were seen in slices cultured in E19CM. Individual astrocytes were not clearly seen, but instead an immense array of GFAP positive fibres were observed resembling the morphology of radial glial cells. This data was not quantifiable. Photomicrographs of GFAP labelled cells in cortical slices grown in NM and E19CM are shown in figures 3.7 and 3.8 receptively.

3.4.3 BrdU and GFAP double labelled cells

In addition to analysing GFAP positive cells alone, the number of BrdU and GFAP double-labelled cells were counted and expressed as a proportion of the total number of BrdU cells. This enabled the role of soluble factors to be investigated upon E19 born cells (and their daughter cells) of the astrocytic lineage *in vitro*.

Figure 3.9 illustrates the proportions of BrdU cells that are double labelled with GFAP in each of the three-culture conditions after 1 hour and 3 days in culture. Only 1 hour after the BrdU pulse, 33% of BrdU cells were double labelled with GFAP when cultured in NM. Similar proportions of double-labelled cells were seen when slices were cultured in E15 and E19 CM after 1 hour (figure 3.10).

Figure 3.6.

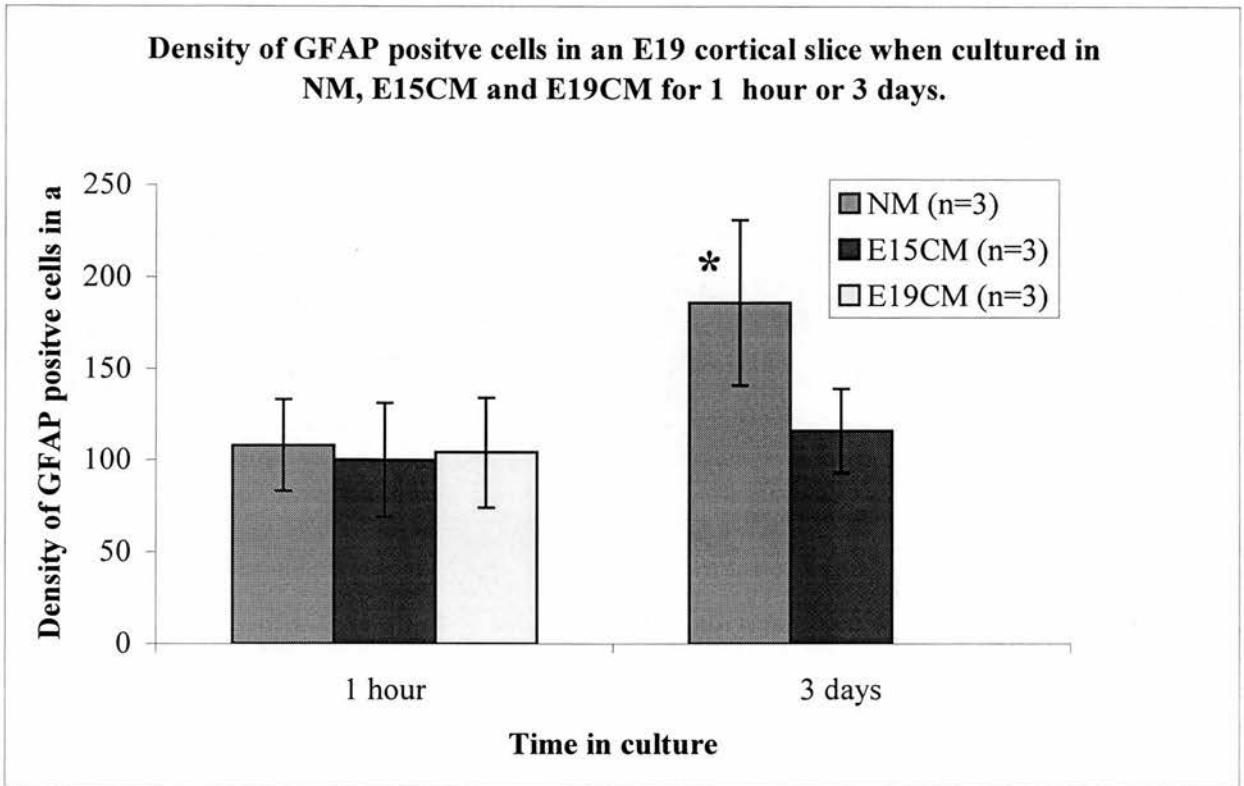

Figure 3.6.

Histogram illustrating the density of GFAP labelled cells in E19 slice cultures when grown in either NM, E15CM or E19CM for 1 hour or 3 days. The number of cells was recorded in a 500μm bin through the width of the cortex. No data is shown for E19CM after 3 days (not quantifiable). Values are mean densities +/- SEM. Asterisk demonstrates a significant difference ($p<0.05$; Students *t* test)

NM: Normal medium; **E15CM**: E15 conditioned medium; **E19CM**: E19 conditioned medium.

Figure 3.7

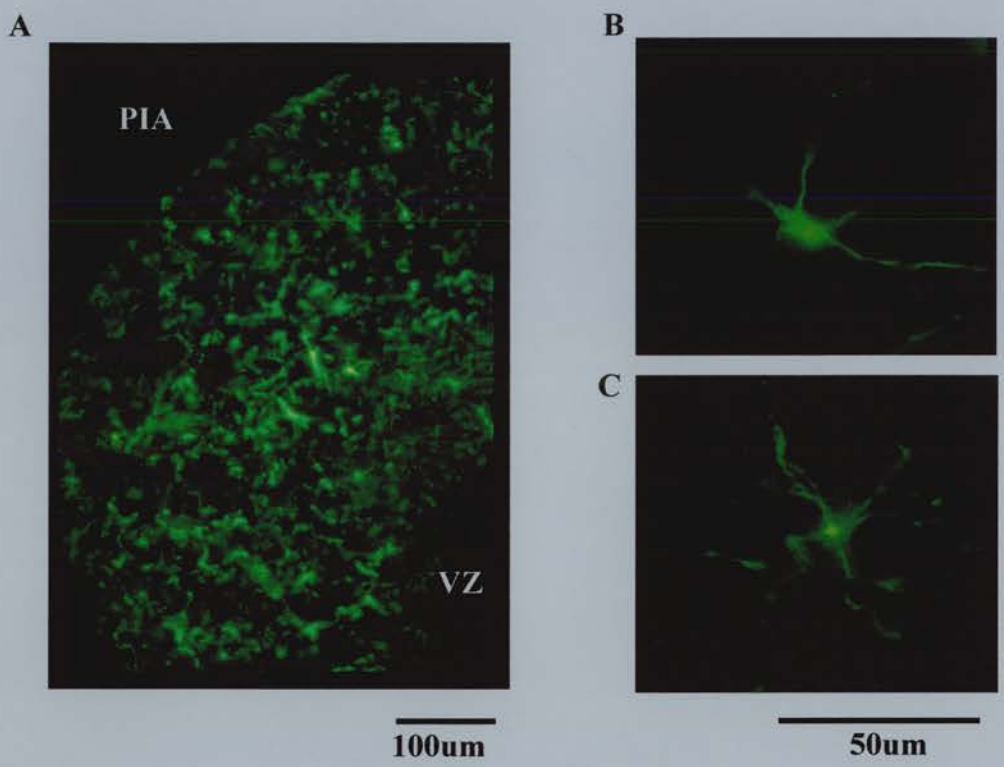

Figure 3.8
(A) Photomicrograph illustrating GFAP immunocytochemistry in an E19 cortical slice culture after culturing in NM for 3 days.
(B) and **(C)** High power photomicrographs illustrating the morphology of GFAP labelled cells in E19 cortical slice cultures.
VZ: Ventricular zone; **NM:** Normal medium.

Figure 3.8

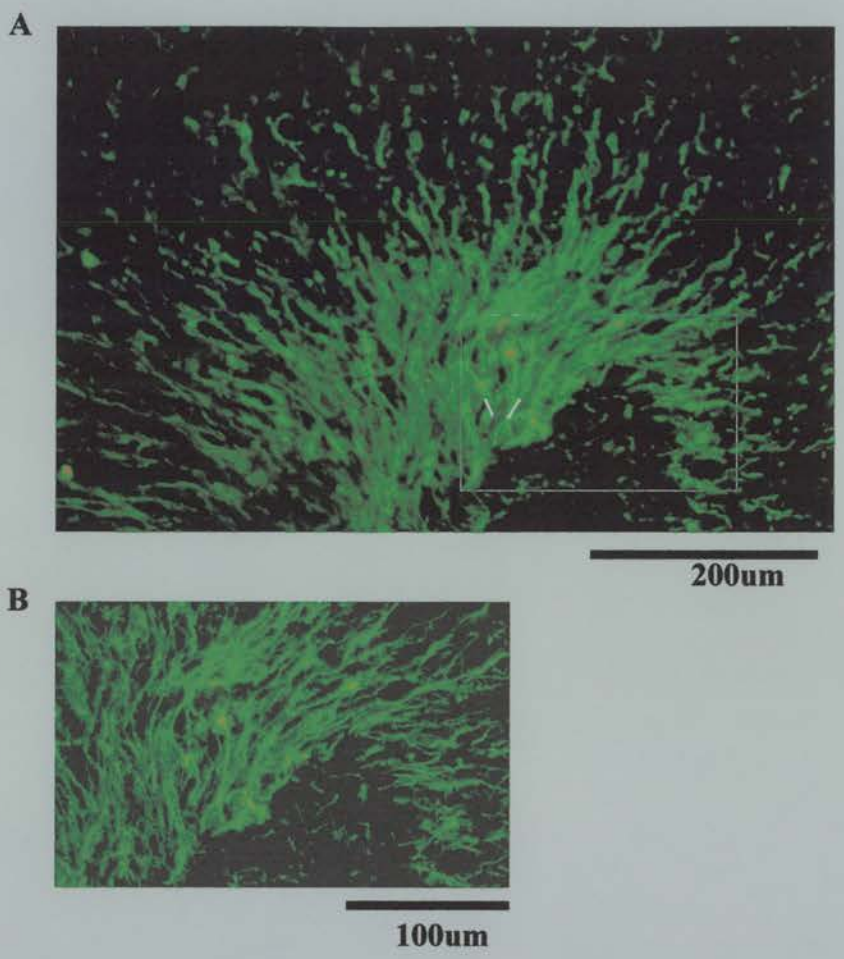

Figure 3.8

Illustrates GFAP immunoreactivity in E19 cortical slice cultures after culturing for 3 days in E19CM.

(A) No individual astrocytes were seen but instead, a massive array of cells with morphologies resembling radial glial cells were observed.

(B) High power photomicrograph of the insert in (A).

VZ: Ventricular zone; **E19CM:** E19 conditioned medium.

Figure 3.9

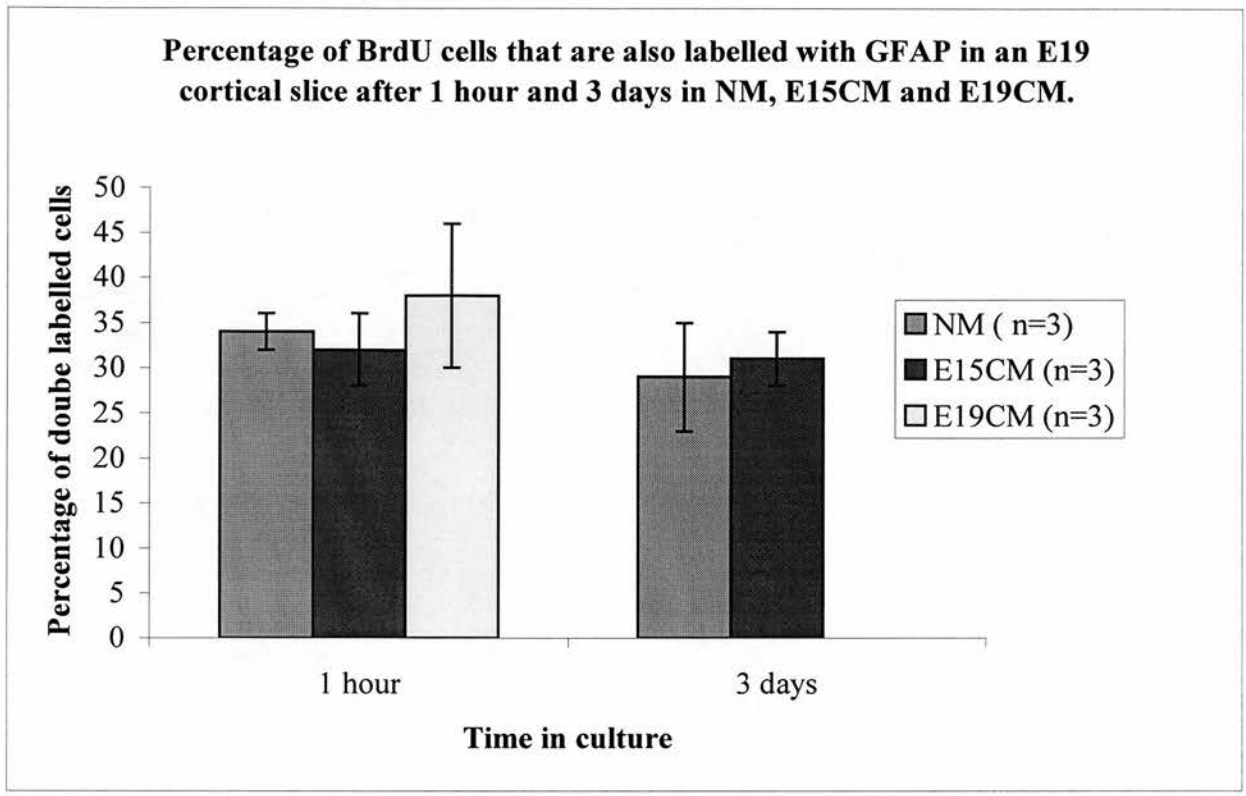

Figure 3.7

Histogram illustrating the proportion of BrdU cells that are labelled with GFAP labelled in E19 cortical slice cultures after 1 hour and 3 days. Slice cultures where grown in NM, E15CM and E19CM. Cell counts were recorded from a 500μm bin through the width of the cortex. See main text for details. No data is shown for E19CM after 3 days as this was not quantifiable. Values are mean percentages +/- SEM.

NM: Normal medium; **E15CM**: E15 conditioned medium; **E19CM**: E19 conditioned medium.

Figure 3.10

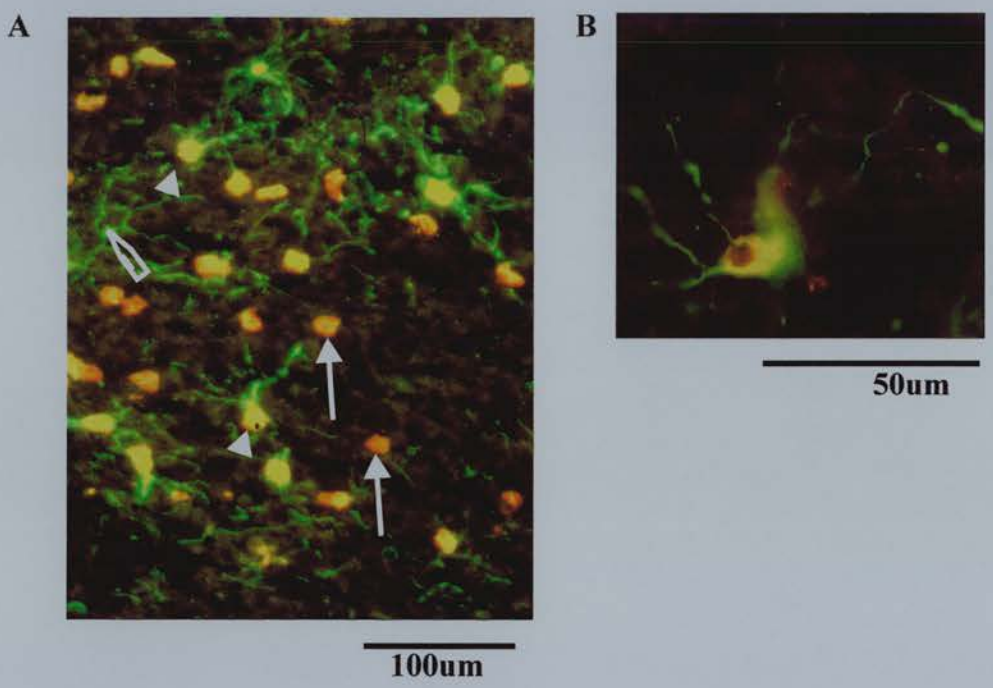

Figure 3.10
Photmomicropgraphs of E19 cortical slice cultures grwon in E15CM for 3 days..
(A) Illustates BrdU and GFAP labelled cells throughout the cortical width. VZ is to the bottom right and Pial edge is to the top left in the photpmigrograph. Red cells are BrdU positive (arrows) and green cells are GFAP postive (open arrow). Yellow cells indicate cells that are labelled with both antibodies (Arrow head).
(B) High power photomicrograph of a double labelled cell.
E15CM: E15 conditioned medium; **VZ:** Ventricular zone.

After 3 days in culture the proportion of double-labelled cells in both NM and E15CM were similar to their respective values observed after 1 hour. For reasons explained above, the data obtained from slices grown in E19 conditioned medium were not quantifiable.

In summary, the densities of GFAP positive cells after 1 hour in each culture condition were similar to each other. These values were much higher than the observed values *in vivo*. By 3 days in culture the density of GFAP cells in NM increased in comparison with its respective density at the start (1 hour) whereas the density of GFAP positive cells in the E15CM remained similar to its respective value after 1 hour. In terms of double-labelled cells the proportions between NM and E15CM remained similar to each other after 1 hour and 3 days. The E19CM data was not quantifiable.

3.4.4 Analysis of O4 positive cells

To determine the effect of environmental signals on the behaviour of cells of the oligodendrocyte lineage, the morphology and density of O4 positive cells was examined in all three-culture conditions. As described in the introduction these results were analysed differently than the earlier experiments in this chapter. This was because no starting data (1 hour) was available (no O4 positive cells were present in the cortical slices after only 1 hour). However, there were some noticeable morphological differences of the O4 labelled cells between the three different culture conditions. These are summarised in figure 3.11. Figures 3.11A and 3.11B illustrate the morphology of O4 labelled cells when cultured for 3 days in NM. Processes can be seen radiating away from the cell body. When slices were cultured in E15CM (Figure 3.11C and 3.11D), the O4 labelled cells adopted a more immature phenotype (defined by fewer processes) than was observed in slices grown in NM. O4 labelled cells in slices grown in E19CM (Figure 3.11E and 3.11F) had similar morphologies to O4 positive cells cultured in NM, whereas O4 positive cells grown in older ages of conditioned medium adopted a more mature phenotype in which many more processes were seen radiating away from the cell body (Figure 3.11G and 3.11H).

Figure 3.12 illustrates the densities of O4 positive cells after 3 days in culture in a variety of different conditioned culture mediums (NM, E15, E19, P3, P5 and P7). The number of cells within a 500μm bin spanning the width of the cortex was analysed. In NM approximately 140 O4 positive cells were seen within the analysed area. When slices were grown in E15CM and E19 CM a 58% and 72% reduction from the density in NM was observed. Slices were also grown in P3, P5 and P7 conditioned medium, and the density of O4 positive cells were similar to the observed densities in E19 CM.

In summary, oligodendrocyte precursors *in vitro* are susceptible to change by soluble factors derived from various ages of cortex. These cortically derived factors can alter the differentiated state of the O4 positive cells, and can also reduce the number of O4 positive cells within the cortical slice.

Figure 3.11: Photmicrographs illustrating the morphology of O4 positive cells in E19 cortical explant cultures when grown in different conditioned culture mediums.

A and B: Show the morphology of O4 cells in an E19 slice culture when grown in NM for 3 days.

C and D: Illustrate the immature phenotype of O4 positive cells when grown in E15CM for 3 days.

E and F: O4 positive cells in an E19 slice culture in E19 conditioned medium. The morphology of these cells resembles the morphology of cells grown in NM.

G and H: Mature O4 cells showing extensive branching when grown in P5 conditioned medium.

Scale bar corresponds to all photomicrographs.

NM: Normal medium; **E15CM:** E15 conditioned medium; **E19CM:** E19 conditioned medium.

Figure 3.11

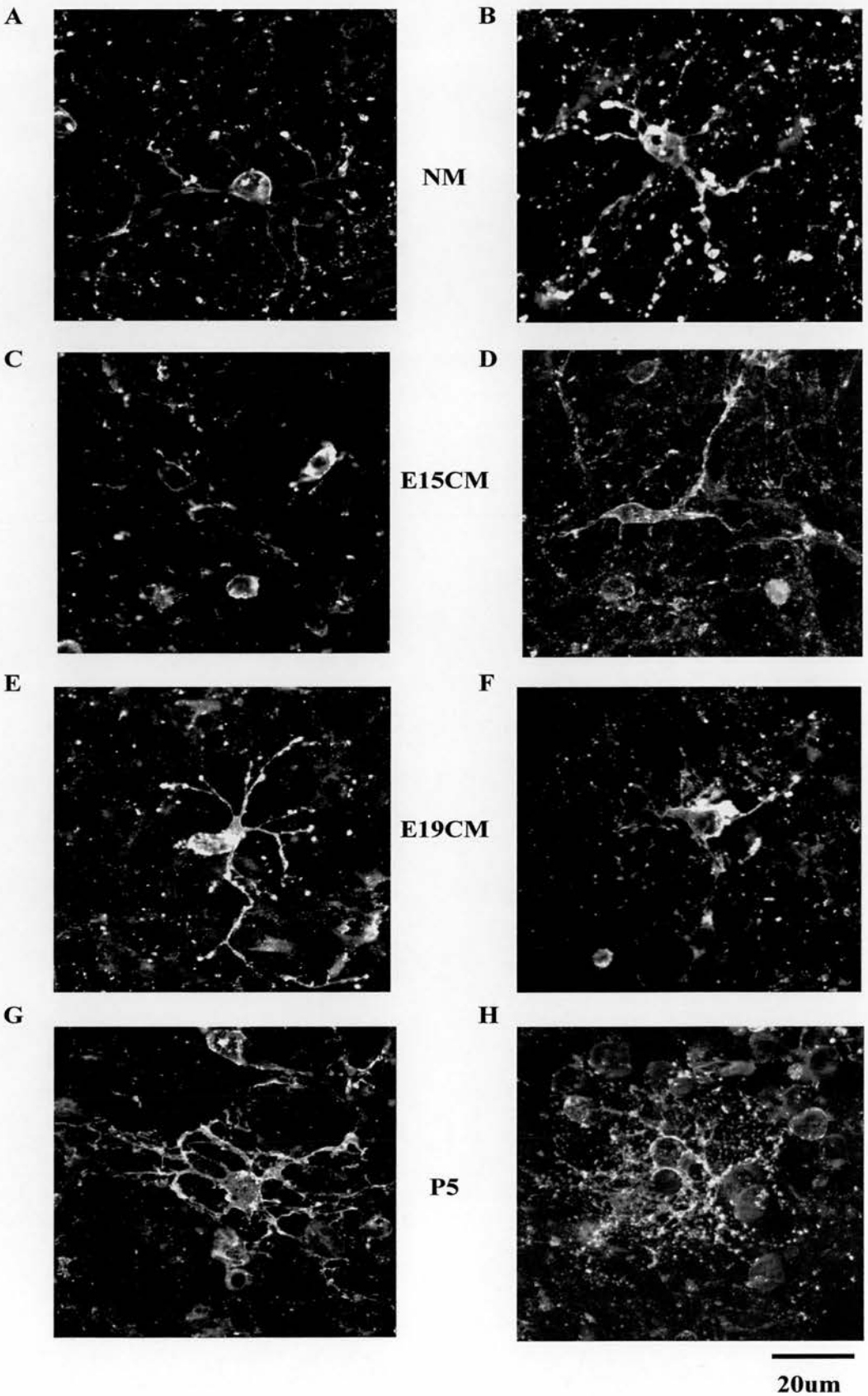

Figure 3.12

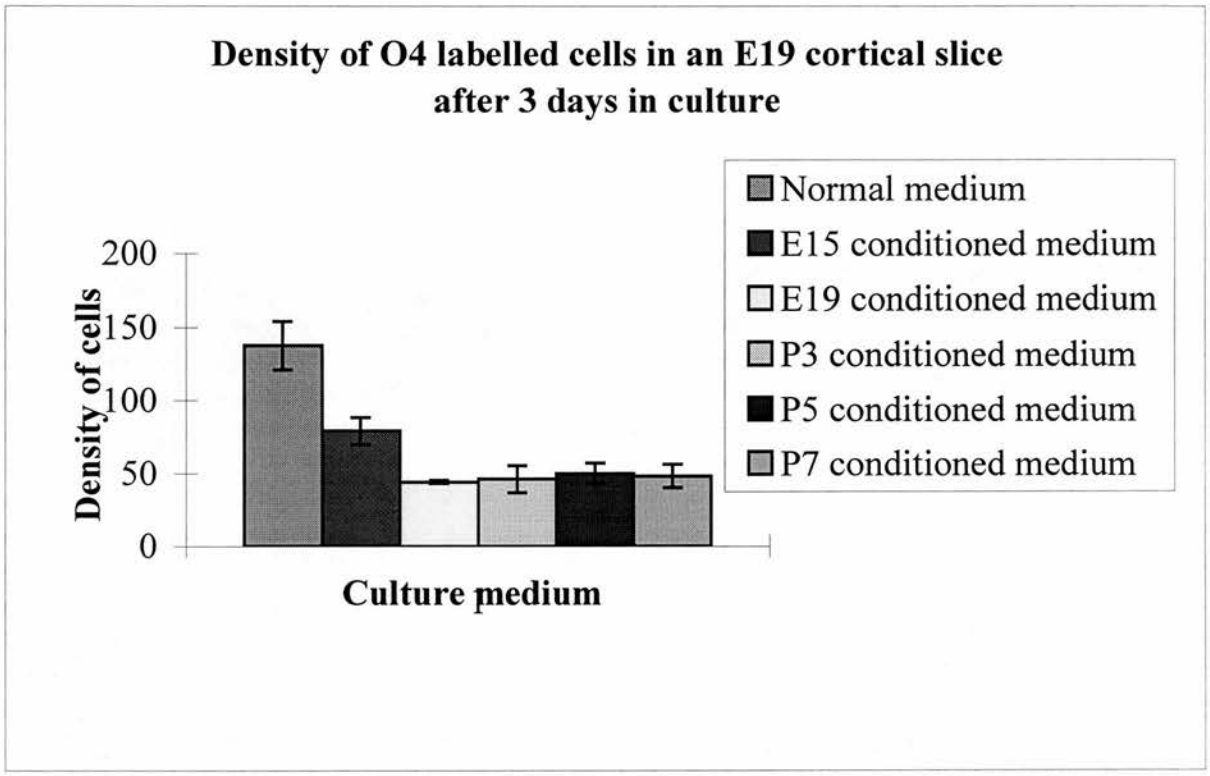

Figure 3.12:

Histogram illustrating the density of O4 positive cells in an E19 slice culture when grown in various conditioned mediums. Values are mean densities +/- SEM.

3.5 DISCUSSION

These experiments were designed to determine if sub-populations of cells (indicated by birth date, GFAP immunoreactivity, and O4 immunoreactivity) in E19 slice cortical cultures were responsive to diffusible cortical derived factors. A culture system was employed in which the proliferation, migration and differentiation of cells in E19 cortical explant cultures was challenged when grown in culture medium containing soluble factors derived from E15 cortex.

The results from these experiments suggest that cortical derived factors play multiple roles in regulating cortical development in E19 cortical slice cultures. The main findings from this study were 1) E15 cortical derived factors inhibit the proliferation or reduce the survival of BrdU and GFAP positive cells within an E19 cortical slice *in vitro* and 2) E19 cortical derived factors have a positive proliferative or survival effect on BrdU and GFAP positive cells *in vitro*. It was not possible to determine from these experiments whether this is an instructive or permissive effect.

The first part of this discussion will cover the effects of the conditioned medium upon BrdU and GFAP positive cells. The O4 data will be considered in the final section at the end of the discussion.

3.5.1 The effect of E19 cortical conditioned medium upon the behaviour of BrdU and GFAP positive cells in E19 cortical slice cultures

The results of this study showed that when E19 cortical slices were cultured in medium conditioned with their own factors, BrdU positive and GFAP positive cells were able to survive migrate, proliferate and differentiate. The behaviour of the BrdU labelled cells to an extent mimics the behaviour of these cell populations *in vivo*. In chapter 2, the BrdU distribution analysis showed that after a 1 hour BrdU pulse the majority of cells were seen within the proliferative regions of the cortex. By 2 days post injection the density of cells in the PZ had reduced but was accompanied by a corresponding increase in density within the cortex, suggesting that cells had migrated from the PZ into the CP. *In vitro* a similar pattern of BrdU distribution was observed.

In contrast to the *in vivo* situation, an increase in total BrdU cell density was observed between 1 and 3 days in culture. This was presumably the result of cells dividing and producing second generation cells. The difference between the *in vivo* and *in vitro* situation presumably could be explained in terms of cortical expansion. *In vivo,* the decrease in cell density was due entirely to cortical expansion until 5 days post-injection. Although the expansion of the cortex in culture was not measured it is unlikely that the cortex expands to the same extent as observed *in vivo*. Therefore the differences in cell densities between the *in vivo* and *in vitro* situation could be explained in terms of less cortical expansion.

The idea of soluble factors affecting cell proliferation is not unprecedented. For example, bFGF has been previously reported to positively regulate cell proliferation (Cattaneo and McKay, 1990; Kilpatrick and Bartlet, 1993; Ghosh and Greenberg, 1995; Vaccarino *et al.,* 1999) of neural precursor cells, whereas Canoll *et al.* (1996) show that GGF is mitogenic for oligodendrocyte precursors. To gain a clearer understanding of the possible proliferative effect caused by the E19CM, a more comprehensive BrdU study is required in which the density and positions of dark and lightly labelled BrdU cells are examined (similar to the study in chapter 2).

In view of the similarities between the *in vivo* and *in vitro* situations the likely explanation is that the factor or factors released from E19 cortex allows normal cortical development to proceed. It is unclear from these experiments whether this factor is permissive or instructive to the behaviour of BrdU and GFAP cells in E19 cortical slice cultures.

The effects of E19CM upon cells of the astrocytic lineage were dramatic after 3 days in culture. Very few individual astrocytes were observed but instead a massive array of fibres were seen, which appeared to have the morphology of radial glial cells. This finding can be explained in two different ways, 1) the E19 cortical derived factor could instruct the differentiation of radial glial cells from neural precursors within the VZ or 2) the factor instructs the transformation of astrocytes back into radial glial cells.

In vivo radial glial cells are known to support neuronal migration (Angevine and Sidman, 1961; Caviness and Sidman, 1973; Rakic, P, 1972; Levitt and Rakic, 1980). Neurones attach to radial glial fibres and migrate along the fibres until they reach their appropriate laminar destination where they detach from the fibre and differentiate into a specific cell type (Hatten, 1990; Rakic, 1972; 1974). After neuronal migration is complete, radial glial cells are transformed into astrocytes *in vivo* by birth (Cajal, 1911; Akers, 1977; Schmeckel and Rakic, 1979; Levitt *et al.,* 1981; Pixley and deVellis, 1984) and *in vitro* (Culican *et al.,* 1990; Hunter and Hatten,1995).

The physiological significance of this radial glial like cell production is unclear. Previous studies have suggested that radial glial to astrocyte transformation is a bi-directional process. Hunter and Hatten (1995) suggest that an extrinsic soluble factor within the embryonic forebrain (E15) instructs the transformation of astrocytes back to radial glial cells in dissociated cell cultures. The results obtained in this study are in agreement with the presence of a soluble factor in the embryonic mouse brain causing transformation of astrocytes to radial glial cells. However as mentioned above it is equally as possible that the radial glial like cells did not arise from the transformation of astrocytes but have differentiated directly from precursor cells within the VZ/SVZ.

To determine which of these processes occurs in E19 cortical slice cultures it would be interesting to label the cells with a specific marker of radial glial cells RC1 (Edwards *et al.,* 1990; Misson *et al.,* 1988). Radial glial cells *in vitro* label with RC1. They do not label with GFAP initially, but after several days in culture will label with both RC1 and GFAP. As the cells take on the morphological and immunocytological features of astrocytes, they retain GFAP immunoreactivity but lose immunoreactivity to RC1. Although no RC1 staining was performed on these cultures it is likely that if the cells were transforming from astrocytes into radial glial cells they would also be immuonreactive to RC1, suggesting that they were a transitory intermediate between astrocytes and radial glial cells. Interesting future studies would be to leave these cells in culture for longer time periods and determine

if they loose GFAP immunoreactivity altogether and maintain RC1 immunoreactivity. These experiments it would also allow confirmation that the GFAP positive fibres were actually radial glial cells rather astrocytes with an abnormal morphology.

In summary, BrdU cells in E19 cortical slices behave normally (as *in vivo*) in terms of their proliferative and migratory behaviour when grown in an environment conditioned with soluble factors released from their own environment. These results were comparable with the *in vivo* results shown in chapter 2. The effect of the E19 derived cortical factor upon cells of the astrocytic lineage produced an unusual result, which did not compare to the *in vivo* situation. The physiological consequence of this remains unclear.

3.5.2 The effect of normal culture medium upon the behaviour of BrdU and GFAP positive cells in E19 cortical slice cultures

The behaviour of BrdU and GFAP labelled cells in cortical slices grown in NM were similar to the observed behaviours of BrdU and GFAP labelled cells when slices were grown in E19CM, although the results were not so extreme. A relatively straightforward explanation for this similarity can be described in terms of a concentration effect of the E19 cortical derived factor. For example, E19 cortical slices when grown in NM will release E19 derived factors into the medium over the time of culture, whereas the E19 cortical slices grown in E19CM will release E19 derived factors to the all ready present E19 factors within the conditioned medium, thus resulting in an increase in the concentration.

The concept of different concentrations of factors having different regulatory roles has been described previously (Mabie *et al.,* 1997; Kessler *et al.,* 1999). These experimenters showed that low concentrations of BMP2 (1-10ng.ml) promoted neuronal differentiation and astroglial differentiation but inhibited oligodendroglial differentiation, whereas higher concentrations (100ng/ml) promoted cell death and inhibited proliferation.

The observed differences in behaviour of cells of the astrocytic lineage between NM and E19CM could be explained in terms of a concentration effect. For example, low concentrations of the E19 derived cortical factor may enhance proliferation of GFAP positive cells, whereas higher concentrations (as observed in the E19CM) may stimulate radial glial cell differentiation either from precursor cells or from the transformation of astrocytes. To determine if the observed differences between the NM and E19CM were due to differences in concentration the morphology of GFAP positive cells could be examined after longer culture periods in NM, which will have the resultant effect of increasing the concentration of the E19 derived cortical factor.

3.5.3 The effect of E15 conditioned medium upon the behaviour of BrdU and GFAP positive cells in E19 cortical slice cultures

When E19 cortical slices were grown in E15CM, the observed behaviour of BrdU and GFAP positive cells were different than their respective behaviours when slices were grown in NM and E19CM. After 3 days in culture the density and the distribution of BrdU cells remained similar to the density and distribution observed after only 1 hour in culture. These findings suggest that that the E15 derived soluble factor either inhibits cell proliferation, instructs cell death and/or impairs cell migration. Any one or a combination of these processes could occur.

To determine if the effect is upon cell proliferation a more comprehensive BrdU study is required. In addition to cell proliferation it is equally likely that the E15 derived factor may be instructing cell death. During normal cortical development many cells are programmed to die. Cell death is of profound importance in the development of the nervous system in ensuring that the correct number of cells and connections are established. Recently it has been estimated that up to 70% of cells in the proliferative regions of the cortex undergo programmed cell death during development (Blaschke *et al.,* 1996, 1998). Exactly how and what determines the death of these cells remains unclear. However, studies in which death of subplate cells has been examined suggest that the process is not cell autonomous but rather under the control of environmental signals (Wood *et al.,* 1992; Gillies and Price,

1993; Price and Lotto, 1996). It is possible that the E15 derived cortical factor instructs cells to die by similar mechanisms involved in the death of subplate cells.

In addition to inhibited cell proliferation and increased cell death, these results could be explained by impaired cell migration. In contrast to the distribution of cells in NM and E19CM, the BrdU cells remained primarily at the ventricular edge of the tissue. Although the process of neuronal migration along radial glial cells is well established very little is known about the mechanisms of glial cell migration. Therefore understanding how cortical derived factors may influence glial cell migration is unclear.

In E15CM, the density of GFAP cells observed within the slice after 3 days was similar to the observed density after 1 hour. In chapter 2, the results showed that astrocytes start to appear by P3 *in vivo*. Although the GFAP data was not quantified in chapter 2, it is clear from the literature that as development continues astrocytes are continually produced into adulthood. Hence, because a reduction in cell density it not observed it is possible that the E15CM is either inhibiting the differentiation of astrocytes or instructing cell death of some astrocytes *in vitro*.

The results so far suggest that E15 cortex releases a soluble factor which either inhibits cell proliferation or survival and differentiation of BrdU and GFAP positive cells. In contrast to this the E19 derived cortical factor has a positive effect upon cell proliferation and differentiation which is possibly concentration dependent. It is unclear whether these factors are permissive or instructive to cell behaviour.

3.5.4 How do cortically derived factors affect the behaviour of O4 positive cells?

As described earlier O4 data was not so straightforward to interpret. The morphology of O4 labelled cells within E19 cortical slice cultures differed when slices were grown in different culture conditions (figure 3.11). O4 labelled cells adopted an immature phenotype (as defined by the number of processes) when cultured in E15CM, and a more mature phenotype when cultured in older cortical conditioned medium. These results imply that extrinsic factors released from the

cortex of the developing mouse brain have an instructive effect upon cell differentiation.

As progenitor cells differentiate down the oliogdendrocyte lineage they express a variety of stage specific markers (figure 3.13). *In vitro* there are two major stages of oligodendroglial differentiation. Initially, G_{D3}^{+}/A2B5^{+} mitotic oligodenroglial progenitors exhibit a bipolar morphology. As the cells begin to differentiate they become increasingly mulitpolar and acquire the ability to bind to O4. As differentiation proceeds O4^{+} cells cease to proliferate and begin to express galactocerebrosidase (GC). Differentiated glia shortly cease to express G_{D3} and A2B5 but continue to bind O4 (Gard and Pfeiffer, 1990). One possible interpretation of these results is that the E15 and E19 derived cortical factors are acting at different stages of the oligodendroglial developmental pathway. For example, the E15 derived cortical factor may inhibit cell differentiation at an early stage of the developmental pathway, whereas the older derived soluble factors may enhance differentiation by acting at later stages of the pathway allowing normal maturation into differentiated oligodendrocytes. Again the presence of these factors may be permissive or instructive.

This theory is consistent with the earlier findings that factors derived from E15 CM have a negative effect on cell proliferation and differentiation within E19 cortical slice cultures, whereas E19 cortical derived factors have positive effects upon cell proliferation and differentiation.

The density of O4 positive cells within the cortical slices produced some intriguing data. Unfortunately these results cannot be explained in terms of the hypotheses proposed above. The reduction in density of O4 cells between NM and E15CM in the cortical slices fits in with the general hypothesis that the E15 derived factor reduces cell proliferation or survival. Surprisingly an even further reduction in cell density (from NM) was observed when slices were grown in older conditioned medium, suggesting that the older cortical derived factors also have an inhibiting

Figure 3.13

Schematic diagram illustrating the different stages of oligodendrocyte development and the specific markers that are expressed at each stage. The arrows indicate possible stages in the developmental pathway at which the cortical derived factors may exert their effects. The red arrow indicates the stage at which the E15 derived factor may inhibit cell differentiation, and the yellow and green arrows indicate the stages at which E19 and older derived factors may be enhancing differentiation.

GC: Galactocereobroside.

Figure 3.13

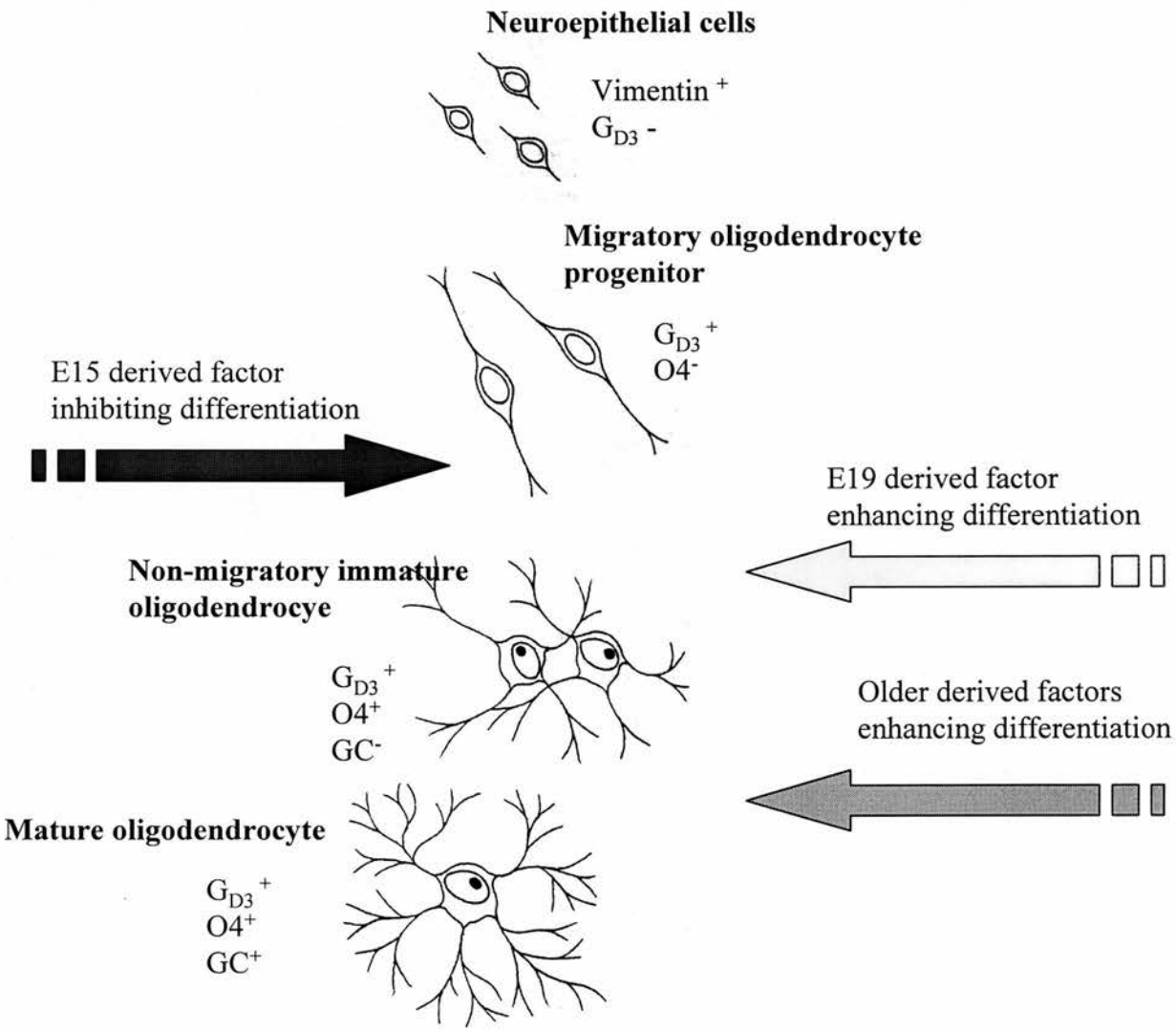
Neuroepithelial cells
Vimentin +
GD3 -
Migratory oligodendrocyte progenitor
GD3 +
O4-
E15 derived factor inhibiting differentiation
E19 derived factor enhancing differentiation
Non-migratory immature oligodendrocye
GD3 +
O4+
GC-
Older derived factors enhancing differentiation
Mature oligodendrocyte
GD3 +
O4+
GC+

effect on cell proliferation or survival. Without further experiments these data are difficult to explain.

3.5.5 Conclusions

In summary these data suggest that E15 derived cortical factors have mainly an inhibitory or negative effect upon on cell proliferation, migration, survival and differentiation (or a combination of these), whereas E19 cortical derived factors have positive effects on these behaviours within E19 cortical slices *in vitro*. Interestingly the E19 derived factors appeared to exert different effects in a dose dependant manner upon different subpopulations of cells. Whether these factors are permissive or instructive remains unclear, but one likely explanation is that the factors within the E19 cortex act permissively allowing normal development to proceed, while the E15 derived factor antagonises the effect of the E19 derived cortical factor. These results show that cortical derived factors play multiple roles in the regulation of CNS developmental and are consistent with a general role for extrinsic signals inducing CNS survival, proliferation, differentiation and migration within the developing brain.

CHAPTER 4: THE BEHAVIOUR OF OLIGODENDROCYTE PRECURSORS FOLLOWING TRANSPLANTATION INTO E16 AND P2 RAT BRAINS.

4.1 ABSTRACT

Following on from the *in vitro* study in chapter 3, this study challenged the behaviour of oligodendrocyte precursors upon transplantation into an earlier age of host tissue. Oligodendrocyte precursor cells were isolated from the telencephalon of P2 rat brains and transplanted into the lateral ventricles of E16 and P2 rat brains (control). The position and morphology of these cells was examined between 24 and 66 hours after transplantation.

The results from this study showed that isolated oligodendrocyte precursors were able to integrate into specific regions of E16 and P2 host brains. The morphology of transplanted cells in the E16 environment resembled the morphology of proliferating cells whereas the morphology of cells in the P2 environment resembled migratory and differentiated cell morphologies typical of normal P2 morphology.

Due to unforeseen circumstances this study remains incomplete. The data presented in this chapter gives an indication of the effect of environmental signals upon glial progenitor cell behaviour. In order to make more definite conclusions it would be necessary to map more accurately the position of cells (using the Nissl stain to identify specific regions) and also to determine the phenotype of the transplanted cells using a series of cell specific antibodies.

4.2 INTRODUCTION

Transplantation is a useful technique that has been employed by experimental biologists for over a century to examine mechanisms of neural development. Numerous studies have transplanted embryonic precursor cells into the adult CNS as a means of exploring the potential of cell replacement theories (see Martinez-Serrano and Björkland, 1997). However, it has been increasingly recognised that transplantation techniques can also be used as a means of investigating cell commitment within the developing CNS (McConnell, 1988; Dunnet *et al.*, 1991; Espinosa de Los Monteros *et al.,* 1993; Fishell, 1995; Brustle *et al.,* 1995; Campbell *et al.,* 1995).

Cell fate specification results from the interaction between extrinsic (signals within the local environment) and intrinsic (cell autonomous) factors. The relative contribution of cell-autonomous programs and environmental factors vary with cell type and developmental time. How these various extrinsic and intrinsic factors establish the identity of individual cells remains unclear. There are three main approaches for studying cell fate: **1)** *in vivo* lineage studies (see introduction), **2)** *in-vitro* differentiation studies (see chapter 3) and **3)** *in-vivo* cell transplantation studies. For the purpose of this study, I will concentrate primarily on the latter of these three categories.

4.2.1 What transplantation can tell us

In general there are two favoured methods of transplantation which involve either transplanting solid grafts of tissue or transplanting dissociated cells / cell lines. Both of these methods have proved successful, and the nature of the experiment being performed determines the choice of donor tissue. For example, studies in which intact pieces of tissue were transplanted between chick and quail have been important in making fate maps of the avian CNS (Couly and Le Douarin, 1985, 1987; Bronner-Fraser and Fraser, 1988; Lumsden *et al.*, 1994). Furthermore, our understanding of hindbrain regionalization has come from studies in which pieces of neural tube tissue have been heterotypically (see next section) grafted in terms of their dorsal/ventral and anterior/posterior position (Simon *et al.,* 1995).

Grafting experiments have also been performed on the mammalian CNS, although accessibility of the tissue has made this process more complicated. Heterotypic transplants (see below) in which E12-E17 rat cortical grafts were transplanted into neonatal cerebrum of a corresponding age has contributed to our understanding of cortical region formation. The results of these experiments suggest that some regions of the brain have made a cell fate choice prior to the transplant while other regions are plastic and can alter their cell fate in response to environmental signals. For example, when limbic cortex was transplanted into neocortex, the cells differentiated into limbic cortical cells, while neocortical cells when transplanted into limbic cortex, altered their fate and adopted the phenotype of limbic cortical cells (O'Leary and Stanfield, 1989; Schlagger and O'Leary, 1991; Barbe and Levitt, 1991, 1995).

Dissociated cells can be transplanted directly into brain tissue (McConnell, 1988; Dunnett *et al.*, 1991; Espinosa de Los Monteros *et al.,* 1993) or directly into the ventricles of the brain (Fishell, 1995; Brustle *et al.,* 1995; Campbell *et al.,* 1995). The latter technique of transplanting cells into the ventricle of the brain is not only less damaging than injecting directly into brain tissue, but also allows for widespread integration of the cells.

4.2.2 Heterochronic versus heterotypic transplantation

From the techniques and experiments described above it can be clearly seen that transplant studies have profound importance in increasing our knowledge of mechanisms involved in cell fate decisions and regional and cellular identity of neural progenitor cells. The two primary transplantation approaches to address such issues are heterochronic and heterotypic transplantation. Heterochronic transplantation looks at the variable of time on a particular place/area (donor and host tissues are different ages), while heterotypic looks at the variable of place at a particular age (host and donor tissues are from different regions).

4.2.2.1 Heterochronic transplants

An excellent example of the utility of heterochronic transplantation has been its application in studying laminar fate determination in the ferret neo-cortex

(McConnell, 1988; McConnell and Kaznowski, 1991; Frantz and McConnell, 1996). These experimenters transplanted E29 progenitor cells (normally destined to a deep neocortical layer fate) into E42 / P1 hosts (a time when superficial layer cells are being born) in an attempt to determine if the progenitor cells were committed to a deep layer. Their results showed that progenitor cells transplanted during S phase adopted a layer 2 and 3 morphology and position, but if they were transplanted later in the cell cycle, they adopted a deep layer fate appropriate for their origin. Hence the laminar fate of early progenitor cells can be modified by environmental cues during a specific time period that closes around the end of S phase. Complementary to this Frantz *et al.,* 1996 showed that later born cortical progenitors were not responsive to environmental cues and were restricted to a deep layer fate even if they were in S phase. These experiments lead to the conclusion that combinations of cell-intrinsic and cell-extrinsic cues are involved in specifying cells to specific laminar phenotype.

4.2.2.2 Heterotypic transplants

Heterotypic transplants are the favoured method of transplantation when considering questions of regional identity. Heterotypic transplants can be either isochronic (donor and host same age) or heterochronic. Brustle *et al.,* (1995), Fishell *et al.,* (1995) and Campbell *et al.,* (1995) isolated proliferating cells from neocortical and ventral telencephalic (developing globus pallidus and striatum) regions and examined the ability of these cells to integrate into specific brain regions. Furthermore, they determined that transplanted cells took on a phenotype characteristic of the new environment. The results from these experiments can be interpreted in different ways and have caused some confusion as to implications of the results (see Barbe, 1996).

All the studies described so far have involved challenging the identity of neuronal precursors and neurones. Studies on glial progenitors and mature glia have been less forthcoming (Lim *et al.*, 1997; Gates *et al.,* 1998). Therefore, this study was designed to examine the behaviour of one glial subtype (the oligodendrocyte precursor) following transplantation into two different ages of host tissue.

4.2.3Why use cultured O-2A progenitor cells as donor cells?

Cultured O-2A cells have been shown *in vitro* to develop into type 2 astrocytes or oligodendrocytes depending upon the different culture conditions to which they are exposed, whereas *in vivo*, they only differentiate into oligodendrocytes (Espinosa de Los Montereos *et al.,* 1993). The culturing conditions involved in isolating O-2A cells ensures that only cells of the glial lineage will be present, whereas if primary cells are isolated a mixed population of neuronal and glial progenitors will be present.

In this study, pure populations of O-2A cells were isolated and instructed to differentiate down the oligodendrocyte lineage. These early oligodendrocyte precursors were fluorescently labelled with a lipophilic dye (PKH26), and transplanted into E16 rat embryos (a time when neurogenesis is predominating) and P2 rat pups (a time when gliogenesis is predominating). The position and morphology of the transplanted cells was examined in the two different host environments.

4.2.4 Summary

The results from this study show that transplanted oligodendrocyte precursors can integrate into both E16 and P2 host tissue. The site of cell integration was similar between the E16 and P2 host although the morphology of the cells was different in the two ages of host tissues. The cells in the E16 environment had a round nuclear cell morphology whereas the cells in the P2 host adopted the morphologies of migrating or differentiated cells.

A small proportion of oligodendrocyte precursors adopted a neuronal morphology suggesting that some oligodendrocyte progenitors were not restricted to the glial lineage.

4.3 MATERIALS AND METHODS

4.3.1 Primary cell culture

Primary glial cultures were established from 2 day old Sprague-Dawley rats after removal of the meninges from the cerebral cortex. Cells were mechanically dissociated by passing through 19, 22 and 25 gauge needles and plated in 75cm^2 Falcon Flasks at 4 x 10^5 cells per cm^2 in DMEM containing 10% FBS. After 7-8 days in culture the flasks were shaken overnight (180rpm) to isolate the loose cells from the confluent monolayer. The loose cells (primarily O-2A progenitors and microglial cells) were concentrated by centrifugation and incubated for 15 minutes at room temperature with a 1:50 dilution of A2B5 ascites fluid in filtered MEM HEPES, 1% FBS. The cells were then diluted to 2 x 10^7 cells per ml in MEM HEPES, 1% FBS and plated on 100mm Falcon dishes. The dishes were left at room temperature for 7 minutes, and then swirled by hand. The non-adherant (A2B5 positive cells) were collected from the supernatant fluid. These cells were then plated in DMEM, 10% FBS onto 100mm Poly-D-Lysine-coated falcon dishes at a density of 2 x 10^6 cells per dish. Cells were re-fed after 24 hours with DMEM containing 4.5g/L of D-glucose, 25µg/ml gentamycin, 50µg/ml transferrin, 30nM sodium selenite, and 30nM triiodothyronine, 50ng/ml bovine insulin and 0.5% FBS. Cells were dislodged from the flasks after approximately 5 days using ATV trypsin. Following a 1 minute incubation in trypsin the cells were collected and resuspended in DMEM.

Using this method of isolation and selection, a pure population of oligodendrocyte precursors was obtained.

4.3.2 Labelling of cells

Cells were labelled *in vitro* with a fluorescent marker (PKH26; Sigma) according to the manufacturer's directions and then re-suspended in PBS. Briefly, the dissociated cells were incubated in HBSS containing PKH26 for 4 minutes and then washed in HBSS to ensure that any dye not incorporated into the cells was removed. Some cells were plated onto poly-lysine coated glass coverslips to check the efficiency of the PKH26 labelling.

4.3.3 Cell transplantation

4.3.3.1 P2 recipients

P2 rat pups were anaesthetised with halothane. 1 µl of cells (10 000 cells) were injected using a Hamilton 70 1µl syringe into the brain 1mm rostral from Bregma and 1mm right of the midline, to a depth of 3mm (figure 4.1). The animals were returned to their mothers after the procedure.

4.3.3.2 *In-utero* transplants (E16 recipients)

A caesarean section was performed on a pregnant rat, anaesthetised with Avertin. The uterine horns were exposed under sterile conditions. The cells were re-suspended in fast green dye (Sigma) and a single 1µl injection of 10 000 cells was injected into the lateral ventricle of the embryos. The dye was clearly visualised in the ventricles for a successful injection. The abdomen of the mother was sutured and the animal left to recover.

4.3.3.3 Tissue preparation

At the indicated time points after transplantation (66 hours for E16 recipients; 24, 48 and 66 hours for P2 recipients), recipient animals were anaesthetised with sodium pentobarbital (40mg/kg,i.p.;) and trans-cardially perfused with 1U/ml heparin in saline, followed by 4% paraformaldehyde in phosphate buffer, pH 7.4. The brains were removed, fixed in 4% paraformaldehyde overnight, equilibrated in 10% followed by 20% sucrose in PBS and frozen in OCT compound (TissueTek; Baxter Scientific). Frozen serial sections were cut with a freezing microtome (75µm), mounted onto poly-lysine coated glass slides and coverslipped. Transplanted cells were visualised using a Leica Confocal microscope under fluorescein and rhodamine optics.

4.3.4 Immunohistochemistry of sections from transplanted brains

After recording the position and morphology of the transplanted cells, coverslips were removed by immersing the slides in PBS overnight. Antibody reactions were performed using MAP2, GFAP, and QK1. A similar protocol as described in chapter 2 was followed, although the secondary antibodies were conjugated to fluorescein.

Figure 4.1

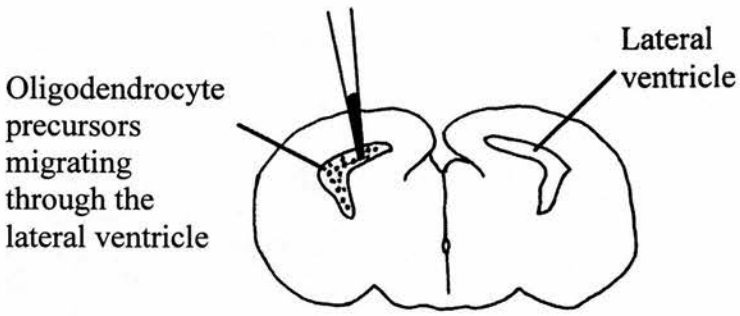

Figure 4.1

This schematic diagram shows the site of injection of the transplanted cells. Oligodendrocyte precursors were injected into the lateral ventricle of E16 and P2 host brains.

4.4 RESULTS

4.4.1 Culture efficiency

To ensure the cells for transplantation were a pure population oligodendrocyte progenitors, A2B5 (labels early oligodendrocyte progenitors) immunocytochemistry was performed and the proportion of A2B5 positive cells as a proportion of the total cell number was recorded. Over a 5-day culture period cells lost immunoreactivity to A2B5 but gained immunoreactivity to more mature markers of oligodendrocytes such as O4 and MBP (Chapter 3; figure 3.13). After only one hour in culture 100% of the live cells were expressing A2B5. This value reduced to 82% by 2 days and 54% by 5 days in culture (figure 4.2).

4.4.2 PKH26 efficiency

Cells were plated onto glass poly-lysine coated coverslips, and examined under the rhodamine filter. The number of red PKH26 positive cells were counted and expressed as a percentage of the total number. In each experiment a 75% (approximately) labelling efficiency was achieved. The total numbers of cells under bright field are shown in figure 4.3Aand PKH26 labelled cells under the rhodamine filter are shown in figure 4.3B.

4.4.3 Transplants

The behaviour of oligodendrocyte precursor cells obtained from P2 rat telencephalic hemispheres was examined *in vivo* by transplanting them into host brain tissue of two distinct developmental ages (E16 and P2). To enable as widespread an integration as possible the cells were injected into the ventricles of host animals. After the specified time points the location and morphology of the transplanted cells were examined, and comparisons between the two experimental groups (E16 and P2 recipients) were made. In both experimental groups (E16 and P2 recipients) the injection tract was easily identifiable, and a gliotic reaction was observed around the tract, detected by immunoreactivity for GFAP (data not shown).

Figure 4.2

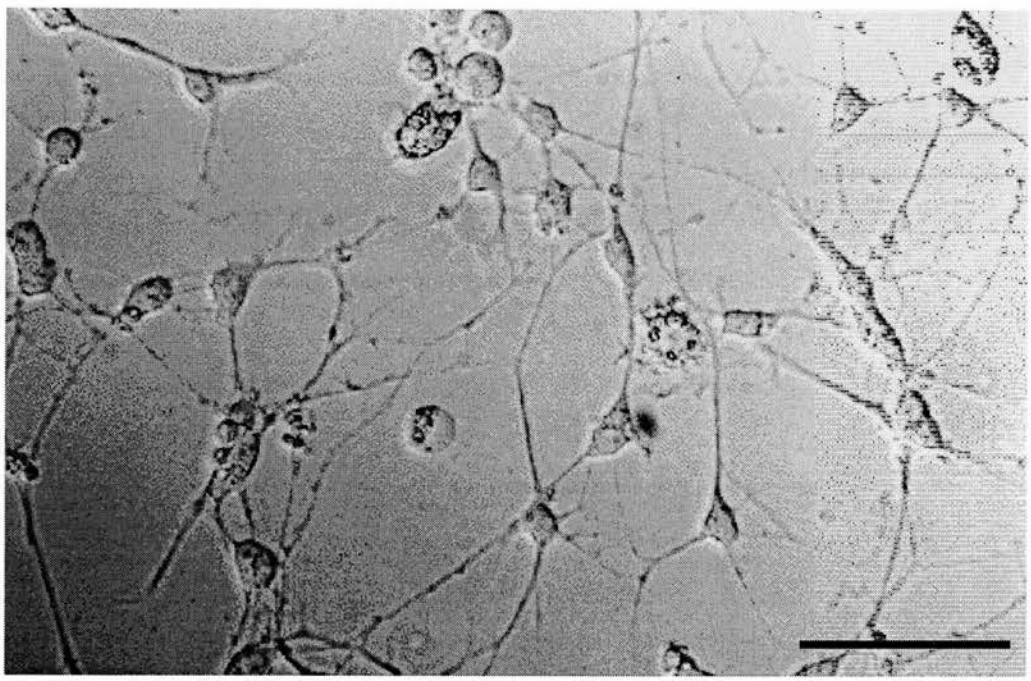

Figure 4.2

Photomicrograph illustrating the morphology of A2B5 immunolabelled cells after 2 days in culture in the absence of any mitogens. Scale bar = 50μm.

Figure 4.3

Photomicrographs show oligodendrocyte precursor cells after labelling with PKH26. **(A)** Bright field micrograph of oligodendrocyte precursor cells. **(B)** Red cells visualised under the rhodamine filter are PKH26 labelled. Arrows indicate cells that are not labelled with PKH26, arrowheads indicate cells that are labelled with PKH26. Scale bar: 50μm.

Figure 4.3

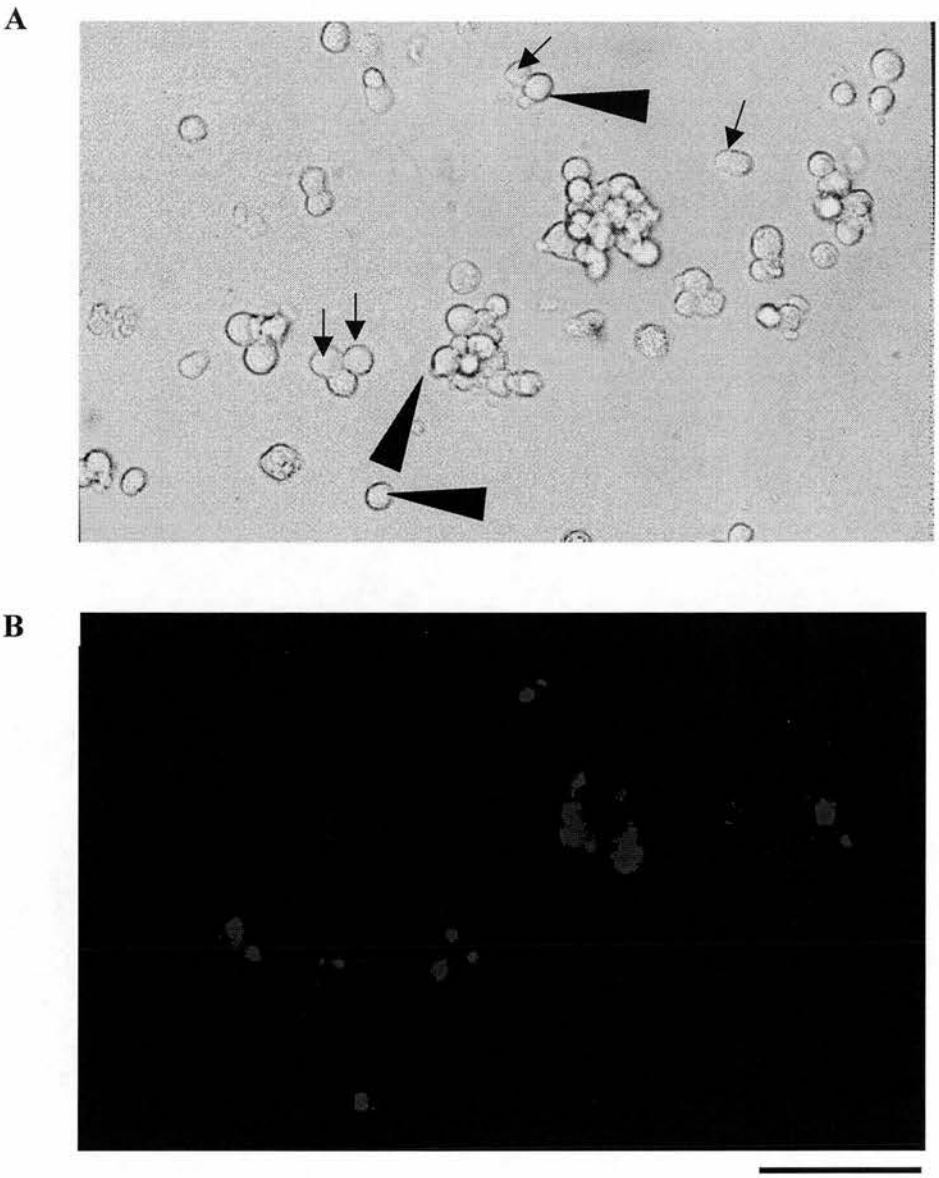

Figure 4.3
Photomicrographs illustrating oligodendrocyte precursor cells after labelling with PKH26. **(A)** Cells are shown in bright field . **(B)** Cells are shown under rhodamine optics. Arrows indicate precursor cells that are not labelled with PKH26; Arrowheads indicate precursor cells that are labelled with PKH26.
Scale bar = 50um.

4.4.3.1 Grafts into E16 recipients

The position of transplanted cells was examined 66 hours after transplantation. The majority of cells were in a region close to the injection site. The cells had integrated into the proliferative zone of the cortex and remained clumped together (figure 4.4). In addition to these cells, a small proportion of cells was seen in more ventral and lateral positions from the main group of cells. The more ventrally located cells were in a region corresponding with white matter tracts. A schematic diagram illustrating the position of the cells is shown in figure 4.4B.

To determine if transplanted cells integrated into all regions of the brain, the position of cells was examined throughout the rostro-caudal axis of the brain (figure 4.5). Schematic diagrams illustrating the positions of transplanted cells are shown in figure 4.5A-E. The most rostral sections are shown in figure 4.5A and the most caudal sections are shown in figure 4.5 E.

Cells were observed in both rostral and caudal regions of the brains. In all sections examined throughout the rostro-caudal axis of the brain, cells were located in the VZ of the developing cortex and striatum (ganglionic eminence). These cells remained close to the ventricle at all levels of the brain. These cells had a round symmetrical morphology and remained tightly grouped together (figure 4.5F).

In an attempt to determine the cell type into which the transplanted cells differentiated, their morphology and antigenicity (see later section) was examined. The majority of transplanted cells had a round cell morphology (figure 4.5F), although a small proportion of cells acquired the morphology of pyramidal cells (Figure 4.4A(insert)). Cells that adopted this morphology were only seen in the developing cortical plate (not in the VZ).

Figure 4.4

(A) Photomicrograph illustrating the integration of PKH26 positive cells into the VZ of the cortex in an E16 host brain. These cells were the closest to the site of injection. Arrows indicate cells that are in regions away from the main group of cells. Insert shows a high power view of a pyramidal neurone within the cortical plate. **(B)** Schematic representation of the positions of transplanted cells in an E16 host brain in a section closest to the site of injection.

VZ: Ventricular zone; **GE:** Ganglionic eminence

Figure 4.4

A

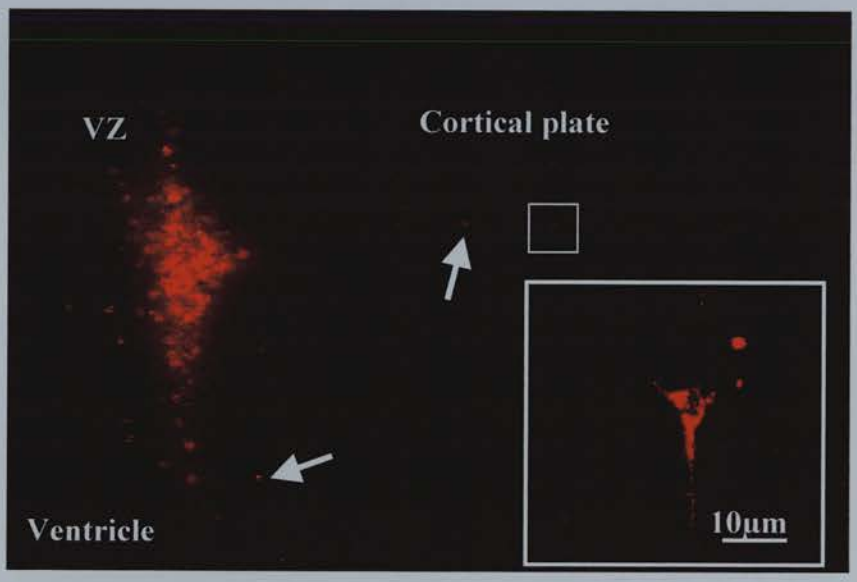

B

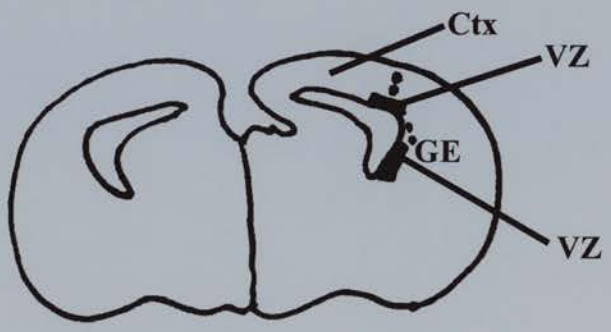

Figure 4.5

(A-E) Schematic diagram illustrating the position of transplanted cells in an E16 host brain throughout the rostro-caudal axis of the brain. Cells integrated into the VZ of the cortex and striatum throughout the rostro-caudal axis of the brain. **(B)** Photomicrograph illustrating the morphology of cells within the VZ of the E16 host brains. Scale bar = 50μm.

GE: Ganglionic eminence; **Hyp:** Hypothalamus; **Thal:** Thalamus; **Ctx:** Cortex

Figure 4.5

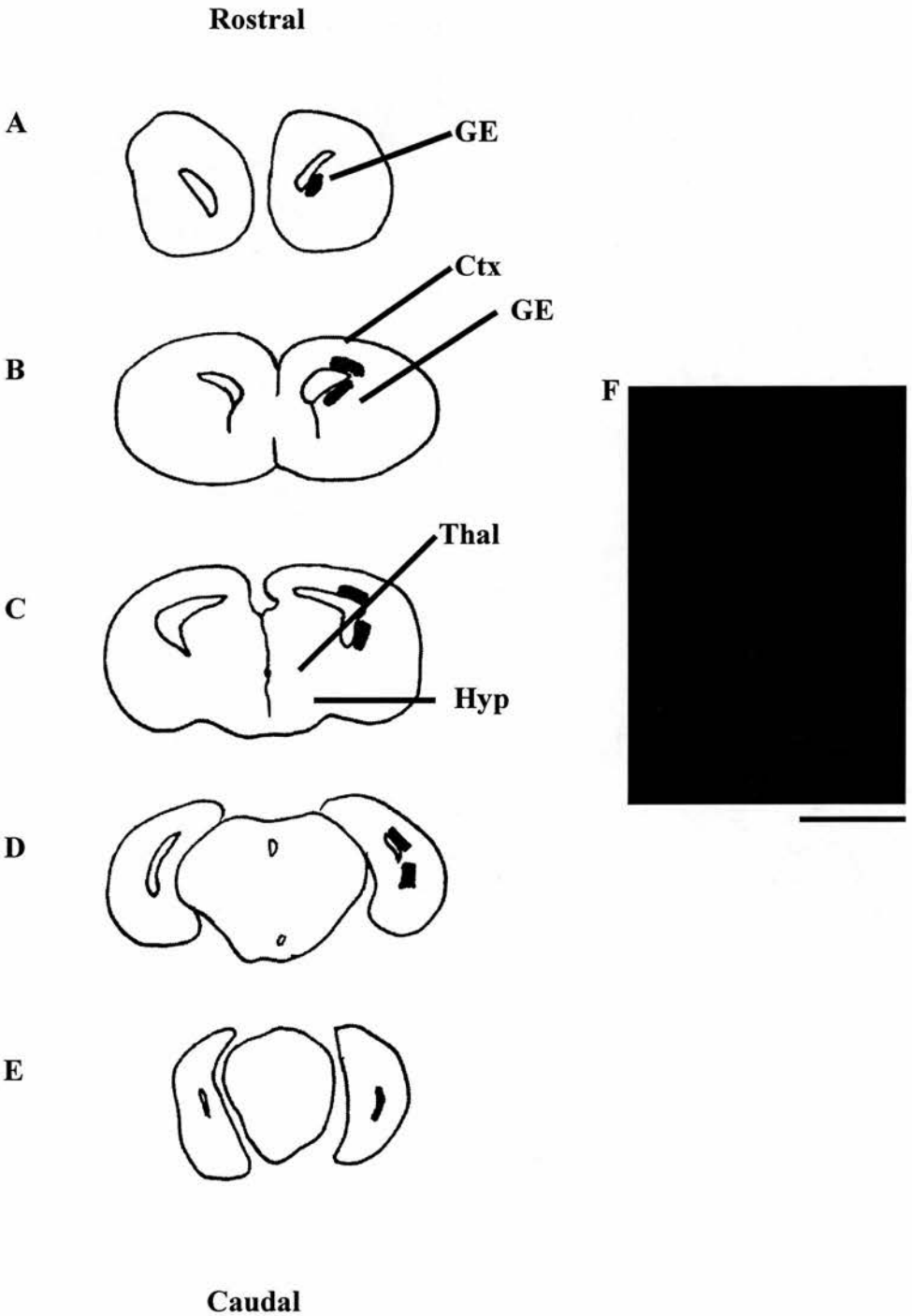

4.4.3.2 Grafts into P2 recipients

The distribution of cells transplanted into the P2 hosts were examined after 24, 48 and 66 hours. Similar to the E16 grafts, the position of cells in the rostro-caudal axis of the brain was recorded. 24 hours after transplantation, the needle tract was clearly visible and the cells were observed in the ventricle in close proximity to the end of the needle tract (data not shown). After this short time period, few cells had integrated into the tissue.

48 hours

By 48 hours post-transplantation the cells to a small extent had integrated into the tissue. A schematic diagram representing the position of the cells in the P2 host brains is illustrated in figure 4.6A. Transplanted cells were in the VZ of the cortex and striatum, still in relatively close proximity to the injection site. A few cells were observed in a position correlating to the white matter tracts. Furthermore, transplanted cells integrated into the diencephalon of the P2 host brains (ventral thalamus and hypothalamus). The morphology of cells within the P2 brains was different to the morphology of cells observed in the E16 host. The cells present in the cortex, striatum and white matter tracts had morphologies of migrating cells in which long thin processes extending from their cell bodies were present (figure 4.6B). The cells that had integrated into the diencephalon had the morphology of differentiated oligodendrocytyes (figure 4.6C).

66 hours

By 66 hours post-transplantation, cells were primarily seen on the white matter tracts and in the diencephalon. The morphology of these cells was similar to the morphologies of the cells observed after 48 hours. Cells that were present on the white matter tracts 48 hours after transplantation were more widely dispersed along the white matter tracts by 66 hours (Figure 4.7A and B).

Figure 4.6

(A) A schematic diagram illustrating the position of transplanted cells in a P2 rat brain 48 hours after transplantation. Cells were seen mainly in the cortex, striatum, white matter tracts and the diencephalon. **(B)** High power photomicrograph of a migrating cell on the white matter tract. **(C)** High power photomicrograph of a differentiated oligodendrocyte in the diencephalon. Scale bars = 10μm.
Hyp: Hypothalamus; **Thal:** Thalamus; **Ctx:** Cortex; **WM-T:** White matter tracts.

Figure 4.6

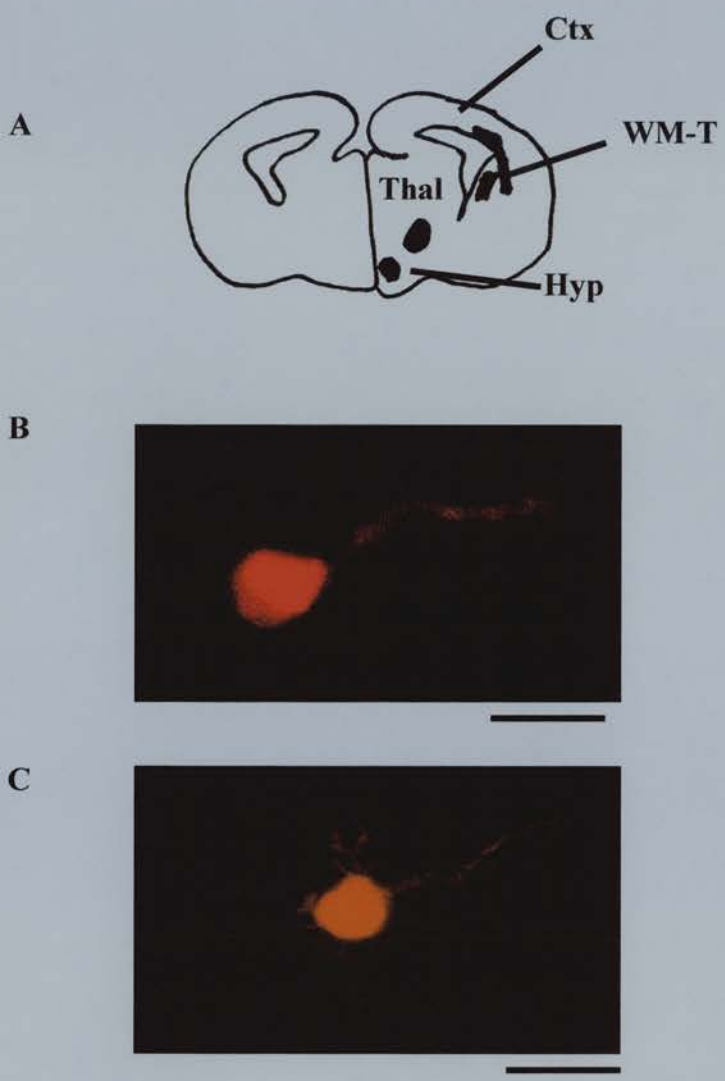

Figure 4.7

(A and B) Photomicrographs illustrating the position of cells on the white matter tracts in P2 rat brains, 66 hours after transplantation. Cells appeared to be migrating along the tracts away from the site of injection. Schematic diagrams illustrate the position of the cells. Scale bars = 100μm

Ctx: Cortex:; **Str:** Striatum

Figure 4.7

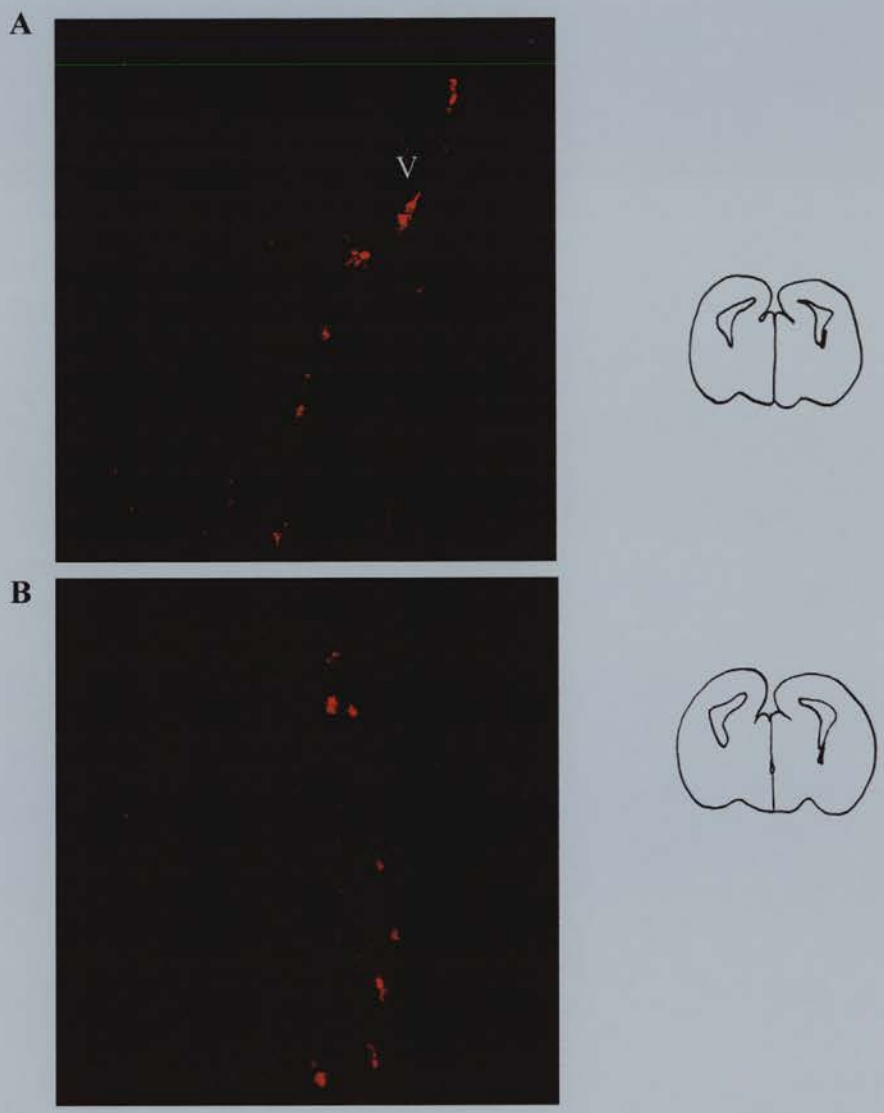

4.4.6 Immunoreactivity on transplanted cells

To ascertain the phenotype of transplanted cells in the two different host environments, antibodies against MAP2, β-Tubulin, GFAP, and QK1 were employed.

Unfortunately, due to technical difficulties (see discussion) very little information about the phenotype of the transplanted cells was obtained. GFAP immunocytochemistry was performed to assess if any of the transplanted cells were of the astrocyte lineage. No transplanted cells in either the E16 or the P2 host environment were labelled with GFAP.

A small percentage of the transplanted cells were seen to express QK1 in both the E16 and the P2 host environments. These data were not quantified, so an estimate of the proportion of transplanted cells expressing QK1 was not available. A small proportion of transplanted cells in the E16 host environment expressed MAP2. No transplanted cells in the P2 host expressed this protein.

In summary, oligodendrocyte precursor cells integrated into specific regions of the brain in both E16 and P2 host tissues. Transplanted cells within the E16 host brain integrated primarily into the ventricular zones of the developing cortical plate and future striatum, and adopted a round symmetrical cell morphology. In the P2 host brain, transplanted cells also integrated into the ventricular zones of the cortical plate and future striatum. However, these cells adopted the morphologies of migrating cells. Additionally, cells integrated into the diencephalon of the P2 host brains, where they adopted differentiated cell morphologies. The mechanisms by which these cells are instructed to integrate into specific regions of the brain remain unclear.

4.5 DISCUSSION

The results from this chapter demonstrate the capability of oligodendrocyte precursor cells to integrate into E16 and P2 host brains following transplantation into the forebrain ventricle. Cells were transplanted directly into the forebrain ventricle allowing for wide spread integration throughout the brain. Transplanted cells integrated into the ventricular zones of the cortex and striatum of E16 and P2 host brains and also into the diencephalon of P2 host brains.

4.5.1 Technical considerations

The interpretation of these results relies heavily on the ability to reliably identify donor cells within the host brain. Previous studies have shown that PKH26 remains in a cell for only 5 cell divisions (Fishell, 1995). During this study cells were examined after relatively short time periods, so dilution of the dye was unlikely to occur.

Secondly, it was important to establish that the donor cells were a pure population of oligodendrocyte precursor cells. Previous studies, which have employed this culture technique, have shown that a pure population of O-2A cells is produced (Raff *et al.*, 1983; McKinnon *et al.*, 1990, 1993). To confirm this, A2B5 immunocytochemistry was performed on the cells immediately after isolation. All of the living cells expressed A2B5, suggesting that a pure population had been isolated.

Finally, phenotypic identification of the cells relied on the use of specific antibodies. In this study, anti-GFAP, anti-CNPase, anti-QK1, anti-MAP2 and anti ß-TuJ1 were used. Unfortunately this part of the study remains incomplete. Problems of specific antibody labelling were encountered, possibly due to overfixation of the tissue. Secondly due to unforeseen circumstances, the experimental tissue was lost, so no more antibody data could be obtained. However, in view of these set backs, some inferences about cell types were made from morphological observations.

4.5.2 Area specific integration of grafted oligodendrocyte precursors into E16 and P2 host brains

Oligodendrocyte progenitor cells integrated primarily into the ventricular zones of the cortex and striatum of both E16 and P2 host brains. The pattern of integration of cells was similar in both ages of host brain, however, cells also integrated into the diencephalon of P2 host brains.

4.5.2.1 Cortical and striatal integration

In the P2 host brains, transplanted cells had integrated into the ventricular zones of cortex and striatum by 48 hours post-transplantation and by 66 hours post transplantation in the E16 host brains. It is possible that cells had integrated into the E16 host brain earlier than 66 hours after transplantation, but only this one time point was investigated in this study. Hence, it is likely that mechanisms allowing cell integration act between 24 and 48 hours after transplantation.

The majority of transplanted cells in the E16 environment remained in the VZ (for the period of study) and retained cell morphologies similar to the morphologies of proliferating cells. In contrast, cells that integrated into VZ of the P2 host brains adopted morphologies that closely resembled the morphologies of migrating cells (bi-polar morphology).

These results are complimentary to the findings reported in the previous chapter in which E15 derived soluble factors were suggested to block/inhibit migration and differentiation of glial precursors, whereas older cortically derived factors either instructed or allowed cell differentiation to occur. For example, the E16 host brain could be releasing signals that inhibit cell differentiation, whereas the P2 host environment may provide a suitable environment for normal cell migration and differentiation. Before such conclusions are made it would is necessary to ascertain if the cells are actually proliferating and migrating as hypothesised above. Experiments designed to address these issues are discussed in the summary chapter at the end of this thesis.

In addition to integration close to the injection site, cells also integrated into the VZ of the cortex and striatum at considerable distances (both rostrally and caudally) from the injection site in both E16 and P2 brains. The widespread integration of the transplanted cells is not surprising due to their ability to migrate through the ventricular system. Their mechanism of entry into the brain is unknown. In each region of the brain in which cells integrated, cells occurred in-groups. This may be due either to the entry of more than one cell in an area or clonal amplification of one cell. This could be tested by using various antibodies to determine if the cells are clonally related.

A small proportion of transplanted precursors cells were seen in the cortical plate in the E16 host tissue. These cells had adopted pyramidal cell morphologies (figure 4.4A). During normal cortical development *in vivo*, neuronal progenitors proliferate in the VZ, migrate into the overlying CP and reside in a specific laminar position, where they undergo their final differentiation. One explanation could be that the pyramidal cells observed in the cortical plate, had migrated there from the VZ, as they would have done in normal development. How these cells were instructed to migrate and differentiate remains unclear. Previous studies have examined factors that are involved in specifying a cells laminar fate. McConnell *et al.* (1991) have shown that cortical neurones are specified to their laminar fate just before a cell undergoes mitosis. Unfortunately very little is known about the mechanisms by which glial cells are specified to specific positional fates.

The observation of transplanted cells with pyramidal morpholgies in the CP is suggestive that some glial precursor cells are able to later their original cell fate in response to cues within the local environment, or they somehow managed to get through the selection process i.e. they were neuronal progenitors. It is interesting that these cells also migrated to regions within the cortical plate as would neuronal progenitors would do in their normal *in vivo* environment. It would be interesting to determine if they were morphologically similar to layer II or layer VI neurones (P2 or E16 born cells).

4.5.2.2 Diencephalic integration

Unlike cells transplanted into the E16 host tissue, oligodendrocyte precursors integrated into the diencephalon (hypothalamus and ventral thalamus) of the P2 host tissues. The morphology of these cells (figure 4.6C) strongly resembled the morphologies of differentiated oligodendrocytes (Chapter 3: figure 3.11 & 3.13). These results are consistent with the hypothesis that the P2 host brain provides a suitable environment which allows / instructs normal glial cell development. As mentioned in chapter 3, it is unclear whether this is a permissive or instructive effect.

4.5.3.3 White matter tracts

Transplanted oligodendrocyte precursors were commonly seen on white matter tracts in both the E16 and P2 host tissues. Gates *et al.* (1998) have previously shown that the developing white matter tracts release a substance that glial cells are highly favourable towards. Similar findings were seen in both P2 and E16 host environments, so if a soluble factor is released that instructs cells to migrate towards it, then this factor must be present in both ages of tissues. Alternatively, other mechanisms may control the integration of cells to the white matter tracts.

4.5.4 Hypothesis

Along with the results from chapter 3, these data suggest that the older cortical environment instructs or allows normal glial cell development to occur, while the younger environment inhibits or blocks the process of normal development. A schematic representation of this is shown in figure 4.8. During corticogenesis, neurogenesis and gliogenesis occur sequentially. Hence, when glial progenitors were transplanted into a P2 environment (a time when gliogenesis predominates) the transplanted cells behaved fairly normally by migrating and differentiating into cells with the morphology of mature oligodendrocytes. Upon transplantation into an E16 brain (a time when neurogenesis predominates), the majority of transplanted cells were unable to differentiate or migrate, and retained proliferative cell morphology of an as yet unidentified phenotype. In addition to these cells, pyramidal cells were also seen in the E16 environment. One explanation could be that the E16 environment is perhaps not only blocking / inhibiting normal glial cell

Figure 4.8

A summary diagram illustrating the behaviour of oligodendrocyte precursor cells upon transplantation into E16 and P2 host brains. The yellow and blue arrows represent the sequential process of neurogenesis and gliogenesis during cortical development. The ages indicated are the times at which these process occur in the developing rat brain. The oligodendrocyte precursors (blue circles) were transplanted into an environment where neurogenesis was predominating (E16: yellow arrow) and into an environment where gliogenesis was predominating (P2: blue arrow). After transplantation, cells that were transplanted into the P2 environment had continued developing down the glial lineage to produce differentiated oligodendrocytes. Upon transplantation into the E16 environment cells either differentiated into neurones (yellow circles), possibly stayed as proliferating glial precursors (blue circles) or adopted an undetermined phenotype (green cells).

Figure 4.8

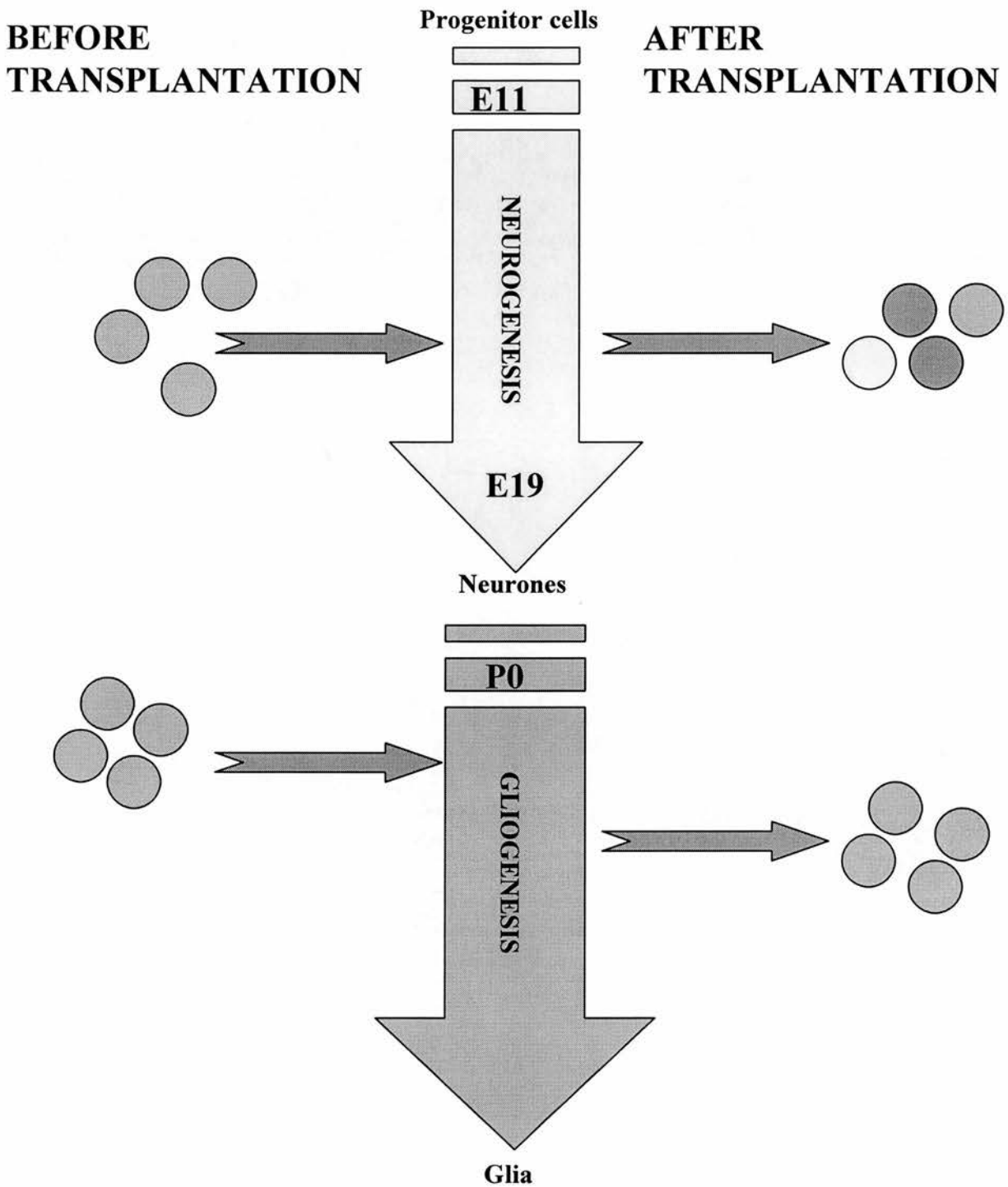
BEFORE TRANSPLANTATION
Progenitor cells
AFTER TRANSPLANTATION
E11
NEUROGENESIS
E19
Neurones
P0
GLIOGENESIS
Glia

differentiation but also actually reversing the normal developmental pathway, which could explain the presence of cells with a neuronal morphology within this environment. A similar type of "reverse development" was observed in chapter 3 with cells of the astrocytic lineage.

4.5.5 Conclusions

The results from this study suggest that oligodendrocyte precursors can integrate into specific regions within E16 and P2 host brains. In E16 host brain, the transplanted cells remained in an apparently proliferative state, whereas in the older host environments the cells appeared to migrate and differentiate, as they would do during normal development. These results along with the results in chapter 3 are consistent with the hypothesis that the E16 environment inhibits / blocks normal glial cell development, whereas the older environment instructs/allows normal glial cell development.

CHAPTER 5: EXPRESSION PATTERN OF A NOVEL RNA BINDING PROTEIN

5.1 ABSTRACT

Throughout this thesis the research has been aimed at studying cells in the transition period between neurogenesis and gliogenesis. As mentioned in earlier chapters, this area of research has been hampered by the lack of early specific glial markers. Screening a subtractive cDNA library is a potentially useful way of identifying novel / rare transcripts that could lead to the isolation of glial specific markers or indeed novel genes of functional importance in the neuronal / glial switch.

Using this approach, a novel cDNA clone (OL391) was isolated and identified from a differentiated glial subtractive library and shown by northern blot analysis to be nervous system specific and developmentally expressed. Clone OL391 was used to screen a brain cDNA library, and a second clone was isolated showing extensive homology to an *ELAV*-like RNA binding protein. This was called ETRR3.

Due to the increasing amount of interest in the role of RNA-binding proteins during neuronal and glial development, ETRR3 was further investigated. To gain an understanding of the role and function of this novel RNA binding protein, its expression pattern was characterised in the developing mouse brain. *In situ* hybridisations were performed on mouse brain sections to determine if ETRR3 was expressed in specific cell types.

The results show that ETRR3 was expressed in postmitotic cells of the developing nervous system. Its expression pattern was stronger in some subsets of cells than others, suggesting that it may have specific roles in discrete sets of developing and adult neurones during development.

5.2 INTRODUCTION

5.2.1 Screening for novel transcripts

Subtractive hybridisation is a powerful tool for isolating and identifying novel genes that are expressed in specific cell types in the mammalian CNS. In the mammalian genome there are approximately 60,000 different genes, of which approximately half are expressed in the brain (Bantle, 1987; Milner, 1983). A systematic investigation of individual brain specific mRNAs has provided an insight into the function and composition of the nervous system at a molecular level.

More than 200 different proteins have been identified that are specific to the brain. These have been biochemically identified, using protein purification, functional assays or through isolation and characterisation of mRNAs from brain cDNA libraries (Sutcliffe, 1988). Many of the early-identified proteins within the brain have been shown to be relatively abundant such as neurofilaments and microtubule associated proteins. However, in addition to these proteins, there are many more rare and unidentified proteins that may have important roles in glial cell development, such as cell-cell interaction, cell fate decisions, or repair of the nervous system. Novel proteins and isoforms are continually being discovered and characterised.

There are several different methods that are used to isolate and characterise rare and novel proteins (Ausubel *et al.,* (1992). These techniques include 1) differential screening of cDNA libraries, 2) differential display, 3) subtractive hybridisation and 4) more recently DNA arrays on microchips. In this study the favoured technique was subtractive hybridisation. Briefly, a cDNA library representing a specific population is used to remove all the same sequences in a second specific DNA library, resulting in a library of cDNA clones which are present exclusively in the second cDNA library.

5.2.2 Generation of subtractive cDNA libraries

For the purpose of this study, two different subtractive libraries were screened. A progenitor cell subtractive library and a differentiated glial cell subtractive library. These subtractive libraries were constructed according to the method of Herfort and

Garber, (1991) by Professor P.J. Brophy and Dr C.S. Gillespie (Edinburgh). The same technique was used for the construction of both the libraries. Below, is a description of the construction of the differentiated glial cell subtractive library.

The subtraction was performed, using two independent, directionally cloned cDNA libraries (progenitor library and a differentiated glial library) in phagemid vectors. Dr C.S. Gillespie constructed these cDNA libraries. Figure 5.1 is a schematic representation of the construction of the library. In brief, single stranded cDNA (ssDNA) from the progenitor cell library was biotinylated. Not1 and Sal1 (used for directional cDNA cloning) digests were performed on the differentiated glial library to release the insert sequences from the pSPORT1 plasmid vector. The 10 fold excess biotinylated ssDNA was mixed with the digested oligodendrocyte cDNA library, heated to allow denaturation and then cooled to facilitate the annealing of complementary sequences. On cooling, complementary sequences hybridised to each other so vector sequences common to both libraries rehybridised, as did common insert sequences. Insert sequences that were unique to differentiated glia rehybridised with one another. Some unpaired vector and insert fragments were also present. The addition of streptavidin results in the removal of all biotin containing cDNAs and therefore those that were common to both libraries, in the organic phase of a phenol chloroform extraction. In the aqueous phase of the extraction there should be double stranded cDNAs encoding sequences specifically expressed by differentiated glia, which are then ligated into the vector pSport1 (Not1/Sal1 digested) and transfected into E.Coli using electroporation. The resultant library of subtracted clones should comprise messages specific to differentiated oligodendrocytes.

5.2.3 RNA binding proteins

RNA binding proteins are expressed in several different species, and have been implicated as ideal candidates for post-transcriptional regulators (Siomi and Dreyfuss, 1997). Such mechanisms include alternative splicing, polyadenylation and capping of pre-mRNA, regulation of mRNA stability, and intracellular localisation of mRNA, all of which affect the availability of the mRNA for translation.

There are two main gene families represented by the neural RNA binding proteins. These are the embryonic lethal abnormal vision (*elav*) gene family and the musashi (*msi*) gene family.

The *elav* family includes the Drosophila *elav* and *sxl* genes (Yao *et al.,* 1993; Beil *et al.,* 1988; Robinow and White, 1991) and their mammalian homologues, the *Hu* genes (Szabo *et al.,* 1991;Wakamatsu and Weston, 1997). The Hu proteins were first identified as neurone-specific antigens in the degenerative autoimmune disorders, paraneoplastic encephalomyelitis, which are particularly associated with patients who have small cell lung cancer (Graus *et al.,* 1985; Sekido *et al.,* 1994; Graus and Ferrer., 1990; Darnell., 1996). In the mouse, four genes (*m-HuA-D*) have been shown to code for as many as 18 different proteins that are expressed differentially from the embryo into the adult in different cell types. It has been speculated that the hierarchical developmental expression of these proteins is critical for both the proper development and function of mature neurones (Okano and Darnell, 1997).

Their Drosophila homologues, the *elav* genes, are expressed during all stages of development and first appear during neurogenesis but persist into adulthood. These proteins are present exclusively in all immature and mature neurones (Robinow and White, 1991). *Elav* loss of function alleles are embryonic lethal, and embryonic mutants have abnormally formed neuropil. The results from the mutant analysis suggest that the elav protein is essential for the development and maintenance of the nervous system (Campos *et al.,* 1985). Both the Drosophila *elav* genes and the human *Hu* proteins appear to be expressed exclusively in post mitotic neurones.

The second family of RNA binding proteins is the *msi* family, which is, composed of the *Drosophila musashi (d-msi)* (Nakamura *et al.,* 1994), *Xenopus laevis nrp-1* (Richter *et al.,* 1990) and the mouse homologue *mouse-musashi-1 (m-msi-1).* In contrast to the *elav* family, the m-msi family are expressed in precursor cells that are capable of generating both neuronal and glial cells during development. Furthermore, in the adult CNS the expression of *m-msi* is restricted to proliferating

cells that reside in the SVZ (an area in which there are populations of adult stem cells) rather than in post-mitotic neurones (Sakakibara *et al.,* 1996).

The role of the RNA binding proteins and their *in vivo* targets are not well understood. However the differential patterns of expression of the *Elav* and *msi* family suggest that they play differing roles in the development and maintenance of the CNS.

5.2.4 Aim

In an attempt to isolate novel transcripts of potential interest to the neuronal glial switch issue, clones from the progenitor cell subtractive library were screened by northern blot analysis. It was decided that if a clone was to be further investigated, two main criteria were to be fulfilled. The clone had to be brain specific and also be developmentally regulated. Several brain specific clones were isolated from the progenitor cell library, although they were not developmentally regulated, and hence unlikely to be of any potential relevance and importance to the neuronal/glial switch issue. These clones were therefore not investigated any further.

However, in a parallel study a novel RNA binding protein was isolated by a colleague (Dr Steven Tait) from the differentiated glial cDNA library. Two recent studies have suggested a role for RNA binding proteins in neuronal and glial cell development. Sakakibara *et al.,* (1997) have suggested a role for *Mouse-Musahi-1* (*m-Msi1*) in neuronal and glial cell development and Hardy (1998) has shown that *QK1* is involved in neuronal/glial cell fate decisions. In light of these studies ETRR3 was further characterised, and its expression in the developing mouse brain was examined.

5.2.5 Summary of results

A novel rat RNA binding protein ETRR3 showing extensive homology to human and Xenopus ETR-3 proteins was isolated from a differentiated glial cDNA library. ETR3 proteins are similar to the Hu proteins in that they belong to the same family of *elav*-like RNA binding proteins. Although the DNA sequence of human ETRR3

is known, no information is available on its location except that it was isolated from a foetal heart library. To address the possible role of ETRR3 in neuronal glial cell fate decisions the expression pattern in both the adult and developing mouse brain was characterised. The results suggest that ETRR3 is present only in postmitotic cells of the developing nervous system, suggesting that ETRR3 does not have a role in neuronal/glial cell fate decisions. Furthermore its expression pattern was stronger in some subsets of cells than others. However, it is possible that ETRR3 may have specific roles in discrete sets of developing and adult neurones during development. These observations suggest also that ETRR3 is a novel marker of post-mitotic neurones.

Figure 5.1. A schematic diagram illustrating the construction of the differentiated glial subtractive library from two cDNA libraries. A cDNA library encoding clones expressed by O-2A progenitor cells was subtracted from a cDNA library encoding clones expressed by differentiated glial cells. The resulting subtractive library encoding cDNAs expressed specifically by differentiated glia. See main text for details.

igure 5.1

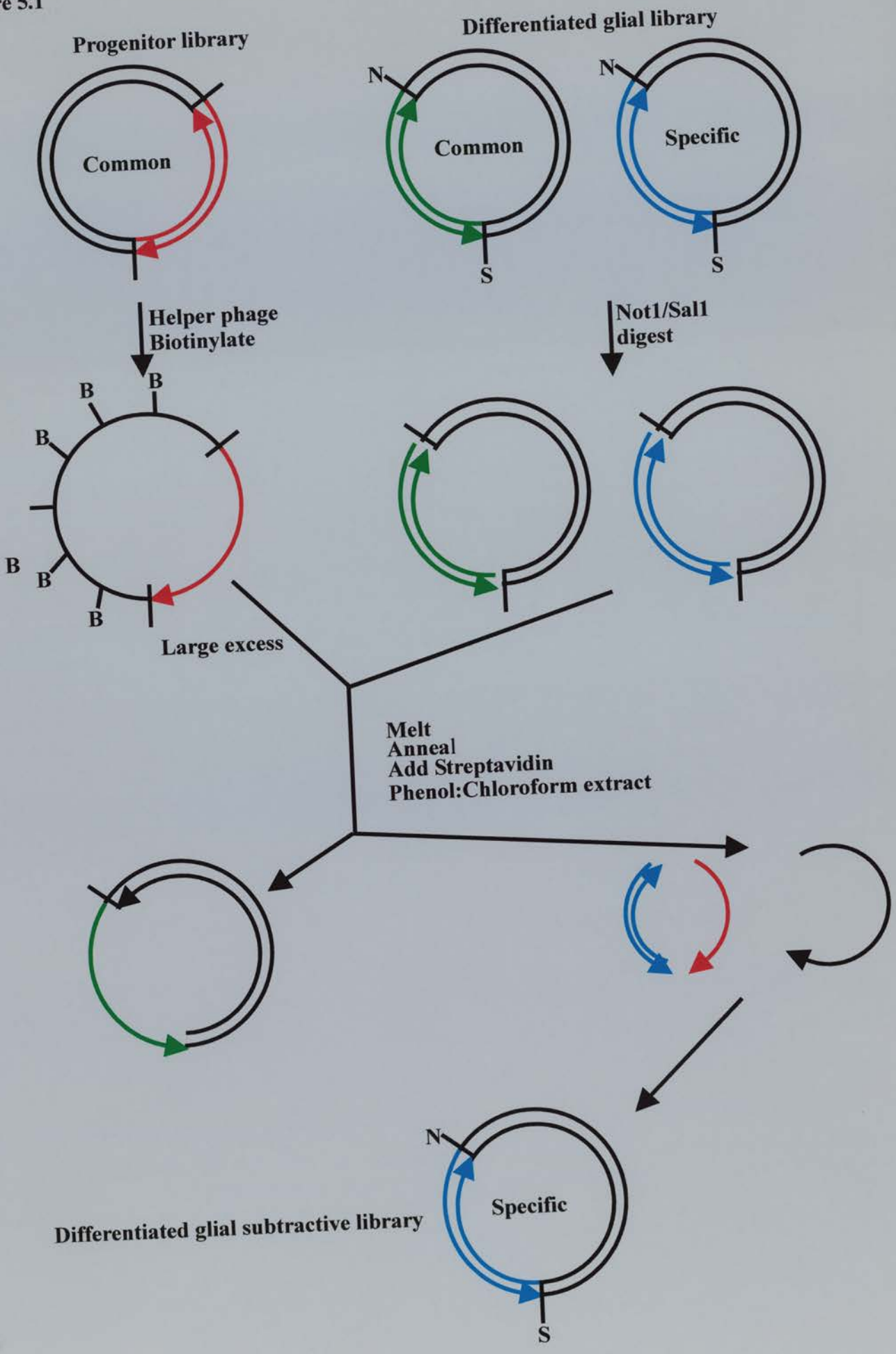
Progenitor library
Common
Differentiated glial library
N
Common
S
N
Specific
S
Helper phage
Biotinylate
Not1/Sal1
digest
B
B
B
B
B
B
Large excess
Melt
Anneal
Add Streptavidin
Phenol:Chloroform extract
N
Specific
S
Differentiated glial subtractive library

5.3 MATERIALS AND METHODS

5.3.1 Northern blotting

5.3.1.1 Extraction of total RNA from rat tissue

Postnatal day 10 (P10) Wistar rats were sacrificed and various tissues (lungs, liver, testes, muscle, heart, brain spleen and thymus) were dissected out using sterile instruments. Tissues were immediately frozen in liquid nitrogen and stored at -70^0C until required. For developmental northern blots, tissues were dissected from rats aged between P1 and P21.

Tissue samples were homogenised with RNAzol B (Biogenesis) in a glass Teflon homogenisor as indicated by the manufacturer instructions (appendix 3). The RNA was isolated by phenol/chloroform extraction and ethanol precipitation (appendix 4).

The purity and concentration of the RNA samples were calculated from spectrophotometric measurements (LKB-Ultrospec III, Pharmacia Biotech). A base line reading was obtained by placing 1ml of MilliQ dH_2O into a quartz cuvette to set as a reference on the spectrophotometer. The RNA (2µl) sample was diluted in 1ml of MilliQ dH_2O and optical density (OD) readings were recorded at 260nm and 280nm to estimate the nucleic acid and protein content respectively. The purity of the sample is determined by the ratio of the protein to nucleic acid content. Standard figures are usually in the range of 1.8 to 2.2.

5.3.1.2 Membrane preparation

To prepare RNA-bound membranes 10µg of total RNA was denatured by incubating in 10µl of freshly made denaturation buffer (appendix 5) at 65°C for 30 minutes. The solution was then plunged onto ice and briefly centrifuged before adding 1µl of loading buffer (appendix 5). The sample was electrophoresed on a 1% agarose gel containing 0.8% formaldehyde (appendix 5). Following electrophoresis the RNA was transferred onto a Hybond-N nylon membrane (Amersham) under vacuum (40mBar) for 90 minutes whilst submerged in 20xSSC (3M NaCl, 0.3M trisodium citrate, pH 7). The gel was discarded and the membrane baked overnight at 80^0C. Membranes were stored at room temperature until required.

5.3.1.3 Probe preparation

Plasmid DNA was radioactively labelled with [α-^{32}P] dCTP (Amersham) using a random primer kit (Gibco) according to the manufacturers instructions. In brief, isolated plasmid DNA (25ng) was placed in boiling water for 5 minutes and then plunged onto ice. 2μl each of GTP, ATP and TTP, 15μl Random primers, 13μl dH_2O, 1μl Klenow fragment and 5μl (50μCi) [α-^{32}P] dCTP was added to the DNA and gently mixed. The reaction mixture was incubated for 1 hour at 25°C. The reaction was stopped with the addition of 5μl of stop solution, and 100μl of sheared salmon sperm (1mg).

5.3.1.4 Hybridisation

Membranes were rinsed with MilliQ dH_2O to remove excess salts and then placed in a 50ml Universal tube with 3 mls of QuikHyb Hybridisation solution (Stratagene). Tubes were placed in a rotary hybridisation oven at 60°C for 30 minutes. Radioactive labelled probes were boiled for 10 minutes before adding to the tube. Membranes were left to hybridise at 65°C for 90 minutes in the rotary oven. Following hybridisation the membranes were washed twice in a low stringency solution (2xSSC/0.1% SDS) for 10 minutes each at room temperature followed by a high stringency wash (0.2xSSC/0.1% SDS) for 40 minutes at 65°C.

Filters were exposed to AGFA RF1 photographic film for 1 week and developed using Kodak LX24 developer and FX40 fixer.

For developmental northern blots, the preparation of the probe and the hybridisation reaction was identical to the method described above. The membrane was prepared by transferring RNA of various ages (P1-P21) of rat brain.

5.3.2 Screening of a cDNA library

The original clone isolated from the differentiated glial cDNA library was only 1.6kb in length, and showed no sequence homology to any sequences in the nucleic acid database. The clone was radiolabelled with ^{32}P and used to screen an adult brain library with the intention of isolating a full-length cDNA clone. The construction of

this library has been previously described in Collinson *et al., (*1998). This was done by Dr Steven Tait.

5.3.3 Isolation of the mouse isoform of ETRR3

5.3.3.1 Reverse transcription (First strand synthesis)

RNA was isolated from P13 mouse brain with RNAzol B (biogenesis), as described in appendix 3. Reverse transcriptions were performed according to the manufacturers instructions. Briefly, a mixture of 1µl random primers (100ng), 3µl total mouse RNA (1µg) and 12µl MilliQ dH_2O was heated to 70^0C, and plunged onto ice. The sample was centrifuged and 4µl of first strand synthesis buffer (0.5mM), 2µl DTT (10mM) and 1µl dNTPs (0.5mM) were added and the sample was incubated at 25^0C for 10 minutes and 42^0C for 2 minutes. 1µl of SuperScript reverse transcriptase (200U) (Life technologies Inc., Paisley, Scotland) was added and the reaction was incubated at 42^0C for 50 minutes. The reaction was inactivated by heating to 70^0C for 15 minutes. After phenol-chloroform extraction and ethanol precipitation the cDNA products were resuspended in water (20µl).

5.3.3.2 PCR amplification

5.3.3.2.1 Primer preparation

Specific primers were designed from the rat sequence of ETRR3. They were designed so that the whole open reading frame (ORF) was amplified. The forward strand was flagged with a NotI site, and the reverse strand was flagged with a SalI site. Detachment of the synthesised primer from the column involved flushing the column with 0.6mls of ammonium hydroxide for 20 minutes. This was repeated twice so a total volume of 1.8mls was collected. The primer/ammonium hydroxide solution was incubated at 56^0C overnight, and then precipitated. Precipitation involved the addition of 200µl of the primer/ammonium hydroxide solution to 1ml of butanol. The solution was vortexed then centrifuged at 13,000g for 2 minutes. The supernatant was discarded and the process repeated until all of the primer solution had been processed. The pellet was resuspended in MilliQ dH_2O.

To calculate the concentration of the primers the optical density (OD) was measured on a spectrophotometer. 5µl of primer solution was diluted in 1ml of MilliQ dH_2O and the OD recorded at 260nm to estimate nucleic acid content. The concentration and molarity of the primers was calculated using the following formulae.

$$\frac{33 \times OD260nm}{5} = \mu g/\mu l$$

$$\frac{\mu g/\mu l}{MW} = \text{Molarity}$$

The molecular weight (MW) of the primer was calculated from its sequence.

5.3.3.2.2 PCR

A 1µl aliquot of the reverse transcription template (cDNA) was taken for PCR using the following primer pairs:

Primer 5' ETR5NOT GCTCATGCGGCCGCCAACAAGATGAACCGGAGCT

Primer 3' ETR3SAL TGAGCTGTCGACGATCAGTAACGTTTGCTGTCG

2.5µl of 10x buffer (conc), 1µl of cDNA template (conc), 2.5µl dNTPs (2mM), 2.5µl of primer F ETR5N (5µM), 2.5µl of primer R ETR3S (5µM) made up to a total volume of 24µl with sterile MilliQ dH_2O was heated to 94^0C before the addition of 1µl PfU DNA polymerase (1U). Positive and negative controls were also prepared. The amplification settings were as follows:- 35 cycles of denaturation at 94^0C for 30 seconds, annealing at 58^0C for 1 minute and extension at 72^0C for 2 minutes followed by a final cycle with extension for 10 minutes at 72^0C. To confirm the presence of the ETRR3 band a 10µl aliquot of the PCR reaction product was run on a 1% agarose gel in TAE. The size of this band was 140 base pairs (figure 5.2).

Figure 5.2

Gel showing the PCR product of reverse-transcription PCR. Primers ETR5N and ETR3S were used to amplify the ORF of the mouse ETRR3. Lane 1 indicates the PCR product. A band of 1.4Kb was observed. Lane 2 indicates a positive control (rat ETRR3).

Figure 5.2

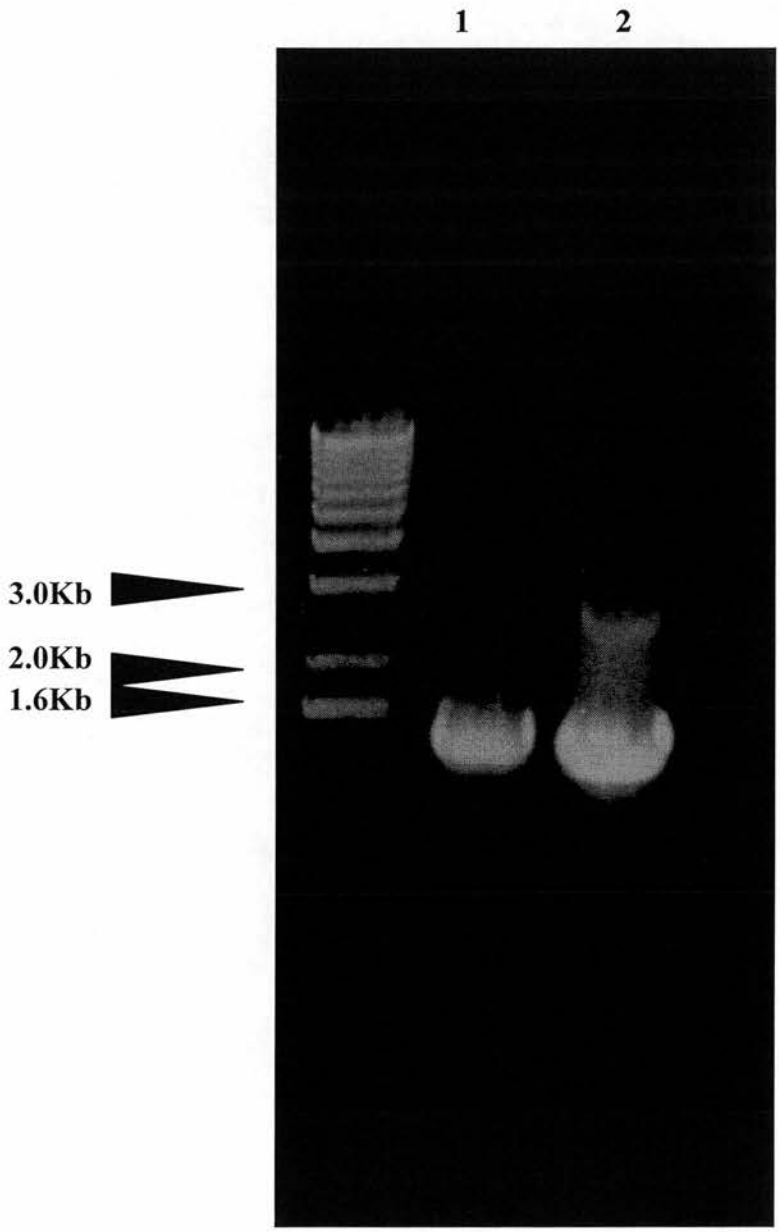

5.3.4 Sub-cloning

5.3.4.1 Digestion of plasmid

The plasmid, pSPORT I (Gibco) (figure 5.3) was digested with NotI and SalI. The reaction was carried out in a final volume of 10µl, consisting of 1µl pSPORT I, 0.5µl NotI (5U), 0.5µl SalI (5U), 7µl MilliQ dH_2O and 1µl 10x H buffer (Boehringer). The reaction was incubated for 2 hours at 37^0C. The plasmid was purified by phenol/chloroform extraction (1:1) and ethanol precipitation (appendix 4).

5.3.4.2 Purification of PCR product

The PCR reaction was electrophoresed on a 1% agarose gel in 1x TAE. The band was excised form the gel using the QUIAX II gel extraction Kit (Quiagen) according to the manufacturers instructions (appendix 6). After purification of the band, the product was digested with NotI and SalI, and purified using phenol/chloroform (1:1) and ethanol precipitation (appendix 4).

5.3.4.3 Ligation

The purified NotI/SalI digested PCR DNA was ligated into the NotI/SalI digested pSPORT I plasmid (Gibco). The following ligation reaction was set up:- 1µl NotI/SalI digested plasmid (10ng), 2µl of 5x T4 ligase buffer, 0.5µl T4 ligase (0.5U), in a total volume of 10µl. The reaction was incubated overnight at 21^0C.

5.3.4.4 Transformation of ligated plasmid into competent XL-1 blue E.Coli

The ligation mixture was added to 100µl of competent cells (appendix 7), and incubated on ice for 30 minutes. Cells were heat shocked at 42^0C for 2.5 minutes before adding to 5mls L-Broth. The cells were incubated for 1 hour in the orbital shaker at 37^0C (220rpm), and centrifuged for 10 minutes at 2000rpm. The majority of the supernatant was discarded, leaving 50µl to resuspend the pellet. This solution was spread onto X-gal agar plates (L-Broth (500ml; Agar (7.5g); ampicillin (50mg); 4% X-Gal (1ml) and 1M IPTG (150µl)), which were incubated at 37^0C overnight. Blue/white selection of clones was performed. All recombinant plasmids will appear white. Ten white colonies were picked, each one being placed into 3mls L-Broth

containing ampicillin (5mg). These were cultured at 37^0C overnight in the orbital shaker (220rpm).

5.3.4.5 Plasmid purification by alkaline lysis

Of the 10 cultures 1.5ml was taken from each and poured into 1.5ml eppendorf tubes. The cultures were centrifuged at 13,000g for 30seconds. The supernatant was discarded and 100µl of P1 solution added. The mixture was vortexed and 200µl of freshly made P2 solution was added. This was mixed by inversion and left at room temperature for 5 minutes. 150µl of P3 solution was added, inversion mixed and left on ice to precipitate for 5 minutes. Following centrifugation at 13,000g for 30 seconds the supernatant was collected in a clean eppendorf tube to which 450µl phenol/chloroform (1:1) was added. The solution was centrifuged at 13,000g for 10 minutes and the aqueous phase collected. 0.1x volume of 3M Na acetate, pH5.5 and 2x volume of 100% ethanol was added to the aqueous phase and placed at -70^0C for 30 minutes. The sample was centrifuged for 40 minutes at 13,000g, the supernatant discarded and the pellet washed in 0.5ml of 70% ethanol. The pellets were air dried and resuspended in 20µl of TE. For solutions see appendix 5.

5.3.4.6 Screening digest

1µl of the above samples were digested with 0.5µl NotI, 0.5µl SalI, 1µl 10x buffer H and 7µl H_2O at 37^0C for 2 hours, and then run on a 1% agarose gel in 1 x TAE to determine if the insert was of the correct size.

5.3.4.7 Plasmid preparation (Midi-prep)

The plasmids with the correct inserts were chosen from the gel, and the remaining 1.5ml of the cultures were added to 20ml of L-Broth containing ampicillin. These were cultured overnight at 37^0C in an orbital shaker (220rpm) and purified with the Quiagen midi prep kit according to the manufacturer instructions.

The samples were sent for automated sequencing, and sequence comparisons between the rat and mouse were made using MacVector.

Figure 5.3

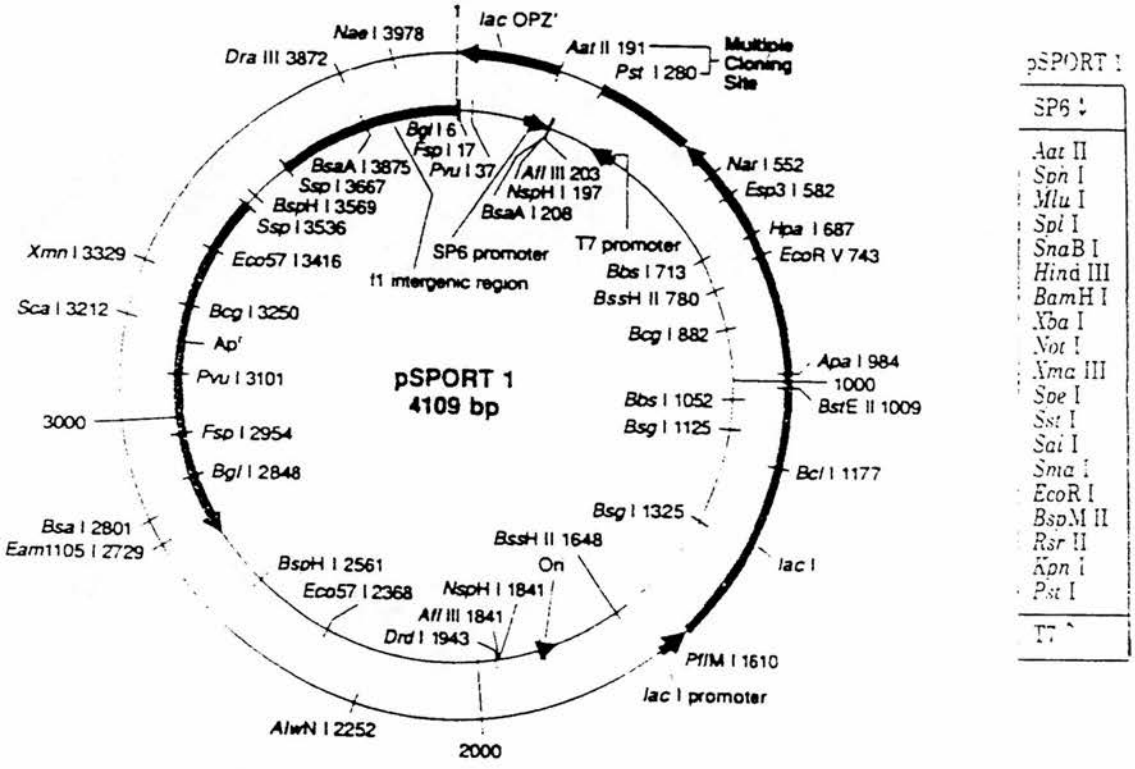

Figure 5.3. Map of DNA plasmid vector pSPORT1 (Gibco) indicating cloning sites.

5.3.5 *In-situ* hybridisations

5.3.5.1 Animals

Swiss mice from an isolated colony were mated overnight and checked for a vaginal plug at 9am the following day. The day of plug was considered to be day 1 (E1). Pregnant dams were deeply anaesthetised with urethane (0.3ml of a 25% solution in normal saline i.p) and embryos were removed between E9 to E19. Embryos were dissected in cold PBS and immersion fixed in 4% paraformaldehyde in PB overnight. Post-natal pups were fixed by cardiac perfusion, the brains dissected in cold PBS and immersed in fixative overnight.

5.3.5.2 Preparation of equipment

All equipment used for the *in situ* hybridisation protocol was washed in MilliQ dH_2O, rinsed in 100% ethanol and baked in an oven at 180^0C for at least 4 hours before use. All solutions were autoclaved and made with DEPC treated MilliQ dH_2O.

5.3.5.3 Coating slides

Glass slides were washed in chromic sulphuric acid, rinsed in MilliQ dH_2O then baked at 180^0C for 4 hours before coating. Slides were immersed in 2% Tespa (3-aminopropyl-triethoxysilane) in acetone for 2 minutes, followed by two further immersions in acetone (2 minutes each) and one immersion in MilliQ dH_2O (2 minutes). After each step the slides were air dried for 1 minute. Slides were baked at 180^0C for 4 hours and stored at room temperature until required (maximum 4 weeks).

5.3.5.4 Tissue processing

Tissue was processed either for whole mount *in situ* hybridisations or for DIG-labelled *in situ* hybridisations on wax sections.

5.3.5.4.1 Whole mount *in situ* hybridisations

Whole embryos (E10-E12) were dissected in PBS + 2mM EGTA, and fixed in 10mls of 4% formaldehyde in PBS + 2mM EGTA overnight at 4^0C. Embryos were washed

twice in PTW, once in 50% Methanol/PTW, and twice in 100% methanol. Embryos could be stored in 100% methanol at -20^0C.

5.3.5.4.2 *in situ* hybridisations (sections)

Fixed tissue was dehydrated and embedded in wax using an automated tissue processor. This has been previously described in the materials and methods section in chapter 2. Tissue was sectioned at 7µm in a coronal plane and mounted onto Tespa (3-aminopropyl-triethoxysilane) coated slides. Slides were dewaxed using a similar method, as described in chapter 2.

5.3.5.5 Probe preparation

5.3.5.5.1 Linearisation of Plasmid

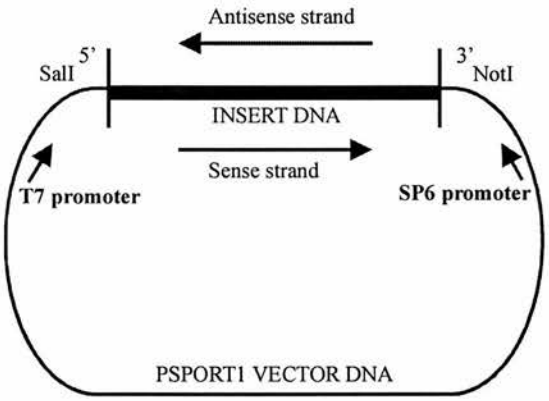

The plasmid DNA has a NotI and SalI restriction site. Linearising the plasmid with Not1 allows a sense strand to be transcribed using the T7 promoter whereas linearising the plasmid with SalI using the SP6 promoter produces the antisense strand. Digests were carried out in a final volume of 50µl, and were set up as below:-

To produce the sense strand:-

5µl (10µg) of plasmid DNA
5µl buffer H
38µl H_20
2µl NOT1

To produce the anti-sense strand:-

5µl (10µg)of plasmid DNA
5µl buffer H
38µl H_20
2µl SAL1

Digest reactions were incubated over night at 37^0C, and purified by phenol/chloroform extraction (1:1) and ethanol precipitation (Appendix 2). Assuming 100% recovery, the final linearised plasmid is at a concentration of 1µg/µl. To confirm the concentration a 1µl aliquot was run on a 1% agarose gel in 1 x TAE against a control of known concentration.

5.3.5.5.2 Transcription

The linearised plasmid was transcribed using the Boehringer Mannheim DIG RNA labelling kit. Transcription reactions were done in a final volume of 20µl. For both the sense and antisense reactions 2µl of 10x NTP labelling mix, 2µl of 10x transcription buffer and 1µl of RNase inhibitor (33 U/µl) were added into a 1.5ml eppendorf. 1µl of linearised plasmid (1µg) (Not1 or SalI digested) was added and the volume made up to 18µl with MilliQ dH_2O. 2µl of the appropriate polymerase were added and the reaction was incubated for 2 hours at 37^0C. The DNA template was removed by the addition of 2µl of DNase 1 at 37^0C for 15 minutes. Transcription was stopped with the addition of 200µl of 200mM EDTA, pH8.0.
RNA was precipitated with 2.2µl of 4M LiCl and 65µl of chilled 100% ethanol. The solution was mixed and incubated at -80^0C for 30 minutes, centrifuged (13,000g) for 15 minutes at 4^0C, the supernatant removed and the pellet washed with 100µl of chilled 70% ethanol. The pellet was left to air dry for 15 minutes at 37^0C, and redissolved in 100µl of DEPC treated water. Probes were stored at -20^0C until required.

5.3.5.5.3 Dot-Blot

DIG riboprobes and control DIG-labelled RNA were diluted to the following ratios $1x10^{-3}$, $1x10^{-4}$, $1x10^{-5}$ and $1x10^{-6}$. 1µl of each dilution was spotted onto a nylon membrane and crosslinked by exposure to UV (Optimal crosslink = 1200mJ). The membrane was rinsed in buffer 1, blocked in buffer 2 for 30 minutes and incubated in a 1:5000 dilution of anti DIG-AP Fab fragments (Boehringer Mannheim) for 30 minutes. Two wash steps each of 15 minutes were made in buffer 1, before equilibrating the membrane in buffer 3 for 3mins. The membrane was placed into a colour reaction solution consisting of 45µl of NBT (Boehringer Mannheim), 35µl of

X-phosphate (Boehringer Mannheim) and 10mls of buffer 3 and left to develop in the dark. The concentration of the DIG-riboprobe was estimated by comparing the intensity of the stain to the control RNA. A successfully labelled riboprobe redissolved in 100µl should have a concentration of approximately 100ng/µl. Solutions are shown in appendix 3.

5.3.5.6 Hybridisation reaction

5.3.5.6.1 Whole mount

Whole mount *in situs* were performed as described by Conlon and Rossant (1992) on E10-E12 embryos.

Pre-hybridisation

Embryos were rehydrated through 75%, 50%, 25% methanol/PTW, finally washing in PTW (4 minutes in each alcohol). The embryos were then immersed in 10µg/ml proteinase K in PTW for 20 minutes, rinsed in PTW and post-fixed for 20 minutes in 4% formaldehyde and 0.1% glutaraldehyde in PTW. Embryos were washed once in PTW and transferred to a round-bottom microtube.

Hybridisation

The embryos were rinsed once in 1:1 PTW/hybridisation mix and left to settle. This solution was replaced with 1ml hybridisation mix and incubated horizontally for 3 hours at 65^{0}C. The appropriate volume of DIG-labelled probe was added to 1ml pre-warmed hybridisation mix to give a final concentration of 1µg/ml, and placed at 65^{0}C for 5 minutes. Embryos were then incubated overnight at 65^{0}C in the above solution.

Post-hybridisation washes

Embryos were rinsed twice in pre-warmed (65^{0}C) hybridisation mix, and then washed (2x30 minutes) in the same solution. Following a 10 minute wash in 1:1 hybridisation mix/MABT at 65^{0}C, the solution was left to cool and replaced with MABT.

Antibody stage

Following two 15 minute incubations in MABT, the embryos were placed into a solution of MABT and 2% blocking reagent (Boehringer) for 1 hour, followed by 1 hour incubation in the above solution + 20% heat-treated serum. Embryos were

incubated overnight in a 1:2000 dilution of AP anti-DIG antibody (Boehringer) in the above solution. This solution was preadsorbed for 1 day prior to use.

Post antibody washes

The antibody solution was removed and embryos were washed three times in MABT (each for 1 hour), before being washed twice in NTMT for 10 minutes each. The embryos were then placed into colour reaction (1.5ml NTMT, 4.5µl/ml NBT, 3.5µl/ml BCIP) for 20 minutes with rocking and then incubated at room temperature for up to 3 days. When the colour reached the desired intensity, embryos were rinsed and washed three times in PTW, and then refixed in 4% formaldehyde/0.1% glutaraldehyde/PTW overnight at 4^0C. The staining pattern was then photographed.

5.3.5.6.2 Wax sections

In situ hybridisations using a digoxygenin–labelled riboprobe transcribed from the ETR-R3 cDNA clone were performed on a series of sections throughout the rostral-caudal axis of the brain.

Pre-hybridisation

Slides were placed in a glass slide dish containing 2 x SSPE for 5 minutes. Slides were incubated at 37^0C in 20µg/ml of proteinase K in P buffer, fixed in 4% paraformaldehyde at room temperature and placed into 0.2M HCl at room temperature. Each of these steps was 15 minutes and were all followed by a 5 minute wash in 2xSSPE. Slides were acetylated by immersing in 0.5% acetic anhydride in 0.1M Tea for 10 minutes. Slides were placed into 2xSSPE until the probe was applied.

Hybridisation

The appropriate volume of probe was added to hybridisation mix to give a concentration of 80ng per slide (60µl of solution per slide). The probe was heated to 80^0C for 5 minutes plunged onto ice for 2 minutes, centrifuged briefly and applied to the slides (60µl per slide). The slides were coverslipped and incubated overnight at 50^0C in a humidity chamber (50% formamide in 1x salts).

Post-hybridisation

Slides were placed into 2xSSC at 50^0C and left until the coverslips fell off. The solution was then replaced with 2xSSC/50% formamide at 65^0C for 45 minutes,

4xSSPE at 50^{0}C for 5 minutes, 4xSSPE containing 20µg/ml RNaseA at 37^{0}C for 30 minutes and 2xSSC/50% formamide at 65^{0}C for 45 minutes. Slides were then placed into prewarmed 2xSSC (50^{0}C) and left to cool to room temperature.

Antibody stage

Before addition of the antibody, slides were permeabilised in PBST for 10 minutes and blocked in 1% blocking buffer (Boehringer Mannheim) in PBST for 30 minutes. Anti Dig-AP FAB fragments were preabsorbed in 1% blocking buffer/2% sheep serum/PBST at a 1:5000 dilution for 4 hours before being applied to the slides. Slides were incubated in antibody solution overnight at 4^{0}C.

Post antibody washes

Three washes (20 minutes each) were made in PBST. Freshly made alkaline phosphatase buffer was applied to the slides for 5 minutes, before being replaced with alkaline phosphatase buffer (75mls) containing 150µl NBT/BCIP stock solution (Boehringer Mannheim). The slides were incubated in the dark until the coloured product was visible to the eye.

Slides were rinsed in MilliQ dH_2O and counterstained in nuclear fast red (Chemicon) for 4 minutes. The sections were then dehydrated through a series of increasing alcohols and mounted in DPX directly from xylene.

All solutions for both *in situ* protocols are shown in appendix 5.

5.3.5.7 Raising a polyclonal antibody

Rabbit polyclonal Antisera was raised against the C-terminal peptide for the ETRR3 isoform. This was coupled via an N-terminal cysteine residue to keyhole limpet hemcyanin by standard techniques. The antibody was affinity purified by immunoabsorption to a column of peptide coupled to aminohexyl-Sepharose 4B (Sigma).

5.3.5.8 Immunocytotochemistry

Immunocytochemistry was performed using Rabbit anti-ETR-R3 antisera. Briefly, embryos were perfused trans-cardially with saline followed by 4% paraformaldehyde in 0.1M phosphate buffer (pH7.4). Brains were removed and post fixed overnight in the same solution and embedded in paraffin wax as described earlier. Serial coronal sections (10μm) were cut and mounted on to poly-L-lysine coated slides. Sections were rehydrated using the following procedure (16mins Xylene, 3mins in 100%, 95%, 70% ethanol and 3 min in distilled water). Sections were incubated in 0.1% trypsin in 0.1% CaCl2 for 25 minutes at 37^0C, rinsed twice in PBS-TX (PBS/0.2% triton). Sections were incubated in 10% swine serum/PBS for 1 hour, and then incubated overnight at 4^0C in primary antibody (1:500) diluted in the above solution. Sections were washed three times in PBS-TX (20 minutes each) and then incubated in either a fluorochrome conjugated secondary antibody or a biotinylated secondary antibody (Dako). In the latter case cells were identified using the peroxidase method, as described in chapter 2.

5.4 RESULTS

A subtraction based cDNA screening protocol to search for novel brain specific genes resulted in the identification of a novel sequence showing extensive homology to members of the ELAV RNA binding protein family. An anti-sense digoxygenein riboprobe was constructed, and the expression of the mRNA was analysed in the developing embryonic and early post-natal mouse brain.

5.4.1 Isolation of a novel rat RNA-binding protein clone

Clone OL0391 was isolated from a differentiated glial cDNA library, radiolabelled and used as a probe in northern blots of RNA from various tissues. It was found to be nervous system specific which fulfilled the first criteria of our search for a protein and also expressed at about the time that gliogenesis was starting. Clone OL0391 was 1.6Kb in length and showed no similarity to any other sequence held within the Gembank database. This 1.6Kb fragment was used to screen a cDNA library with the intention of isolating the full-length clone. Upon doing so a second clone of 4.2Kb was isolated and was found to contain a 1474 base pair open reading frame (ORF) (figure 5.4). This clone displayed 94% homology to a human sequence derived from a foetal heart library and to a Xenopus laevis sequence identified as ETR-3, an ELAV-like RNA binding protein. The high level of sequence identity is typical of other ELAV-like RNA binding proteins.

At the amino acid level (appendix 8) the sequences from rat and human ETRs are almost identical. This putative protein was named ETRR3 (Elav-type RNA-binding protein rat type 3) and comprised 491 amino-acids with a predicted molecular weight of 52,250kDa. The presence of the open reading frame and the molecular weight of the putative protein was confirmed in an experiment in which the cDNA of clone OL0391 was transcribed and translated in the presence of 35S methionine. The resulting protein was shown to have a molecular weight of approximately 54,000kD (figure 5.5).

At a similar time to this study clone OL0424 was isolated from the same library by a colleague (Dr Marie-Christine Birling). This clone showed sequence homology to ETR-R3 and was presumably a product of alternative splicing.

Figure 5.4

The nucleotide sequence of the open reading frame of rat and mouse ETR. The ORF is 1474 base pairs long. The sequence along the top indicates the mouse sequence and the lower sequence indicates the rat sequence.

ORF: Open reading frame.

```
Metr-orf    ATG AAC GGA GCT TTG GAT CAT TCA GAC CAG CCA GAC CCA GAT GCC ATT

1. etr-orf             10          20          30          40
[ 5642 ]    ATG AAC GGA GCT TTG GAT CAT TCC GAC CAG CCA GAC CCA GAT GCC ATT>
            ||| ||| ||| ||| ||| ||| ||| ||  ||| ||| ||| ||| ||| ||| ||| |||
Metr-orf    ATG AAC GGA GCT TTG GAT CAT TCA GAC CAG CCA GAC CCA GAT GCC ATT


           50
Metr-orf    AAG ATG TTT GTC GGA CAG ATC CCT AGG TCC TGG TCG GAA AAG GAG CTG

1. etr-orf 50          60          70          80          90
[ 5642 ]    AAG ATG TTT GTC GGA CAG ATC CCT AGG TCC TGG TCA GAA AAG GAG CTG>
            ||| ||| ||| ||| ||| ||| ||| ||| ||| ||| ||| ||  ||| ||| ||| |||
Metr-orf    AAG ATG TTT GTC GGA CAG ATC CCT AGG TCC TGG TCG GAA AAG GAG CTG


          100
Metr-orf    AAA GAA CTT TTT GAG CCT TAT GGA GCT GTC TAC CAG ATC AAC GTC CTC

1. etr-orf   100         110         120         130         140
[ 5642 ]    AAA GAA CTT TTT GAG CCT TAT GGA GCT GTC TAC CAG ATC AAC GTC CTC>
            ||| ||| ||| ||| ||| ||| ||| ||| ||| ||| ||| ||| ||| ||| ||| |||
Metr-orf    AAA GAA CTT TTT GAG CCT TAT GGA GCT GTC TAC CAG ATC AAC GTC CTC


         150
Metr-orf    CGG GAC CGG AGT CAG AAC CCT CCC CAG AGT AAA GGT TGT TGT TTC GTA

1. etr-orf     150         160         170         180         190
[ 5642 ]    CGG GAC CGG AGT CAG AAC CCT CCC CAG AGC AAA GGT TGT TGT TTC GTA>
            ||| ||| ||| ||| ||| ||| ||| ||| ||| ||  ||| ||| ||| ||| ||| |||
Metr-orf    CGG GAC CGG AGT CAG AAC CCT CCC CAG AGT AAA GGT TGT TGT TTC GTA


             200
Metr-orf    ACA TTT TAT ACA AGA AAA GCT GCA CTT GAG GCC CAG AAT GCA CTG CAC

1. etr-orf        200         210         220         230         240
[ 5642 ]    ACA TTT TAT ACA AGA AAA GCT GCA CTT GAG GCC CAG AAT GCA CTG CAC>
            ||| ||| ||| ||| ||| ||| ||| ||| ||| ||| ||| ||| ||| ||| ||| |||
Metr-orf    ACA TTT TAT ACA AGA AAA GCT GCA CTT GAG GCC CAG AAT GCA CTG CAC


                250
Metr-orf    AAT ATT AAA ACT TTA CCT GGG ATG CAT CAT CCC ATT CAG ATG AAA CCT

1. etr-orf          250         260         270         280
[ 5642 ]    AAT ATT AAA ACT TTA CCT GGG ATG CAT CAT CCC ATT CAG ATG AAA CCT>
            ||| ||| ||| ||| ||| ||| ||| ||| ||| ||| ||| ||| ||| ||| ||| |||
Metr-orf    AAT ATT AAA ACT TTA CCT GGG ATG CAT CAT CCC ATT CAG ATG AAA CCT


                  300
Metr-orf    GCA GAT AGT GAA AAG TCA AAC GCT GTG GAA GAC AGA AAA TTG TTC ATA

1. etr-orf 90         300         310         320         330
[ 5642 ]    GCA GAT AGT GAA AAG TCA AAC GCT GTG GAA GAC CGA AAA TTG TTC ATA>
            ||| ||| ||| ||| ||| ||| ||| ||| ||| ||| |||  || ||| ||| ||| |||
Metr-orf    GCA GAT AGT GAA AAG TCA AAC GCT GTG GAA GAC AGA AAA TTG TTC ATA


                     350
Metr-orf    GGA ATG GTT TCC AAG AAA TGT AAC GAG AAT GAT ATC AGA GTG ATG TTT

1. etr-orf   340         350         360         370         380
[ 5642 ]    GGA ATG GTT TCC AAG AAG TGT AAC GAG AAT GAC ATC AGA GTG ATG TTT>
```

```
                |||  |||  |||  |||  |||  ||   |||  |||  |||  |||  ||   |||  |||  |||  |||  |||
Metr-orf        GGA  ATG  GTT  TCC  AAG  AAA  TGT  AAC  GAG  AAT  GAT  ATC  AGA  GTG  ATG  TTT


                                    400
Metr-orf        TCT  CCA  TTC  GGT  CAG  ATA  GAA  GAA  TGC  CGG  ATT  CTC  CGG  GGA  CCT  GAT

1. etr-orf           390             400             410             420             430
[ 5642 ]        TCT  CCC  TTC  GGT  CAG  ATA  GAA  GAA  TGC  CGG  ATT  CTC  CGG  GGA  CCT  GAC>
                |||  ||   |||  |||  |||  |||  |||  |||  |||  |||  |||  |||  |||  |||  ||
Metr-orf        TCT  CCA  TTC  GGT  CAG  ATA  GAA  GAA  TGC  CGG  ATT  CTC  CGG  GGA  CCT  GAT


                                    450
Metr-orf        GGG  CTG  AGT  CGA  GGC  TGT  GCG  TTT  GTC  ACA  TTT  TCT  ACA  AGG  GCA  ATG

1. etr-orf           440             450             460             470             480
[ 5642 ]        GGG  CTG  AGT  CGA  GGC  TGT  GCG  TTT  GTC  ACA  TTT  TCT  ACC  AGG  GCA  ATG>
                |||  |||  |||  |||  |||  |||  |||  |||  |||  |||  |||  ||   |||  |||  |||
Metr-orf        GGG  CTG  AGT  CGA  GGC  TGT  GCG  TTT  GTC  ACA  TTT  TCT  ACA  AGG  GCA  ATG


                                    500
Metr-orf        GCA  CAG  AAT  GCA  ATC  AAA  GCC  ATG  CAT  CAG  TCT  CAG  ACC  ATG  GAG  GGC

1. etr-orf              490             500             510             520
[ 5642 ]        GCA  CAG  AAT  GCA  ATC  AAA  GCC  ATG  CAT  CAG  TCT  CAG  ACC  ATG  GAG  GGC>
                |||  |||  |||  |||  |||  |||  |||  |||  |||  |||  |||  |||  |||  |||  |||
Metr-orf        GCA  CAG  AAT  GCA  ATC  AAA  GCC  ATG  CAT  CAG  TCT  CAG  ACC  ATG  GAG  GGC


                                    550
Metr-orf        TGC  TCT  TCA  CCA  ATC  GTG  GTG  AAG  TTT  GCT  GAC  ACT  CAG  AAG  GAC  AAA

1. etr-orf  30          540             550             560             570
[ 5642 ]        TGC  TCT  TCA  CCT  ATC  GTG  GTG  AAG  TTC  GCT  GAC  ACT  CAG  AAG  GAC  AAG>
                |||  |||  |||  ||   |||  |||  |||  |||  ||   |||  |||  |||  |||  |||  ||
Metr-orf        TGC  TCT  TCA  CCA  ATC  GTG  GTG  AAG  TTT  GCT  GAC  ACT  CAG  AAG  GAC  AAA


                                    600
Metr-orf        GAG  CAA  AGG  CGC  CTC  CAG  CAG  CAG  CTT  GCA  CAG  CAG  ATG  CAA  CAG  CTC

1. etr-orf    580           590             600             610             620
[ 5642 ]        GAG  CAA  AGG  CGC  CTC  CAG  CAG  CAG  CTT  GCA  CAG  CAG  ATG  CAA  CAG  CTC>
                |||  |||  |||  |||  |||  |||  |||  |||  |||  |||  |||  |||  |||  |||  |||
Metr-orf        GAG  CAA  AGG  CGC  CTC  CAG  CAG  CAG  CTT  GCA  CAG  CAG  ATG  CAA  CAG  CTC


                                    650
Metr-orf        AAC  ACT  GCC  ACT  TGG  GGG  AAC  CTA  ACA  GGA  CTG  GGT  GGA  CTT  ACC  CCG

1. etr-orf           630             640             650             660             670
[ 5642 ]        AAC  ACT  GCC  ACT  TGG  GGG  AAC  CTG  ACA  GGA  CTG  GGT  GGA  CTT  ACC  CCA>
                |||  |||  |||  |||  |||  |||  |||  ||   |||  |||  |||  |||  |||  |||  ||
Metr-orf        AAC  ACT  GCC  ACT  TGG  GGG  AAC  CTA  ACA  GGA  CTG  GGT  GGA  CTT  ACC  CCG


                                    700
Metr-orf        CAG  TAC  CTG  GCG  CTT  CTG  CAG  CAG  GCC  ACC  TCC  TCC  AGC  AAC  CTG  GGT

1. etr-orf           680             690             700             710             720
[ 5642 ]        CAG  TAC  CTG  GCG  CTT  CTG  CAG  CAG  GCC  ACC  TCC  TCC  AGC  AAC  CTG  GGT>
                |||  |||  |||  |||  |||  |||  |||  |||  |||  |||  |||  |||  |||  |||  |||
Metr-orf        CAG  TAC  CTG  GCG  CTT  CTG  CAG  CAG  GCC  ACC  TCC  TCC  AGC  AAC  CTG  GGT
```

```
                                                  750
Metr-orf    GCA TTC AGT GGC ATT CAG CAA ATG GCT GGC ATG AAT GCT TTA CAG TTA

1. etr-orf            730          740          750           760
[ 5642 ]    GCA TTC AGT GGC ATT CAG CAA ATG GCT GGC ATG AAT GCT TTA CAG TTA>
            ||| ||| ||| ||| ||| ||| ||| ||| ||| ||| ||| ||| ||| ||| |||
Metr-orf    GCA TTC AGT GGC ATT CAG CAA ATG GCT GGC ATG AAT GCT TTA CAG TTA


                                                        800
Metr-orf    CAG AAT CTG GCA ACA CTG GCT GCT GCT GCA GCT GCT GCT CAA ACC TCA

1. etr-orf  70          780           790          800           810
[ 5642 ]    CAG AAT CTG GCA ACG CTG GCT GCA GCT GCA GCT GCC GCC CAA ACC TCA>
            ||| ||| ||| ||| ||  ||| ||| ||  ||| ||| ||| ||  ||  ||| ||| |||
Metr-orf    CAG AAT CTG GCA ACA CTG GCT GCT GCT GCA GCT GCT GCT CAA ACC TCA


                                                      850
Metr-orf    GCC ACC AGC ACC AAT GCA AAC CCT CTG TCT AGC ACA AGC AGT GCC CTG

1. etr-orf    820          830          840           850          860
[ 5642 ]    GCC ACC AGC ACC AAT GCA AAC CCT CTC TCC AGC ACA AGC AGT GCC CTG>
            ||| ||| ||| ||| ||| ||| ||| ||| ||  ||  ||| ||| ||| ||| ||| |||
Metr-orf    GCC ACC AGC ACC AAT GCA AAC CCT CTG TCT AGC ACA AGC AGT GCC CTG


                                                    900
Metr-orf    GGA GCC CTC ACA AGC CCT GTG GCT GCT TCA ACC CCC AAT TCC ACG CTT

1. etr-orf      870           880          890           900           910
[ 5642 ]    GGG GCC CTC ACA AGT CCC GTG GCT GCT TCA ACC CCC AAT TCT ACT GCT>
            ||  ||| ||| ||| ||  ||  ||| ||| ||| ||| ||| ||| ||| ||  ||    |
Metr-orf    GGA GCC CTC ACA AGC CCT GTG GCT GCT TCA ACC CCC AAT TCC ACG CTT


                                                        950
Metr-orf    GGT GCG GCC ATG AAT TCC TTG ACC TCT CTT GGG ACT CTA CAA GGA TTG

1. etr-orf        920          930           940          950           960
[ 5642 ]    GGT GCA GCC ATG AAC TCC TTG ACC TCT CTT GGG ACT CTG CAA GGA TTG>
            ||| ||  ||| ||| ||  ||| ||| ||| ||| ||| ||| ||| ||  ||| ||| |||
Metr-orf    GGT GCG GCC ATG AAT TCC TTG ACC TCT CTT GGG ACT CTA CAA GGA TTG


                                                            1000
Metr-orf    GCT GGA GCC ACT GTC GGA TTG AAT AAT ATT AAT GCA CTA GCA GTT GCT

1. etr-orf            970          980           990          1000
[ 5642 ]    GCT GGA GCC ACT GTC GGA TTG AAT AAT ATT AAT GCA CTA GCA GTT GCT>
            ||| ||| ||| ||| ||| ||| ||| ||| ||| ||| ||| ||| ||| ||| ||| |||
Metr-orf    GCT GGA GCC ACT GTC GGA TTG AAT AAT ATT AAT GCA CTA GCA GTT GCT


                                                          1050
Metr-orf    CAA ATG CTC TCA GGT ATG GCG GCT CTG AAT GGA GGA CTT GGC GCC ACA

1. etr-orf  10          1020          1030          1040          1050
[ 5642 ]    CAA ATG CTC TCA GGT ATG GCG GCT CTG AAT GGA GGA CTT GGC GCC ACA>
            ||| ||| ||| ||| ||| ||| ||| ||| ||| ||| ||| ||| ||| ||| ||| |||
Metr-orf    CAA ATG CTC TCA GGT ATG GCG GCT CTG AAT GGA GGA CTT GGC GCC ACA


                                                        1100
Metr-orf    GGC TTG ACG AAT GGT ACG GCT GGC ACC ATG GAC GCC CTG ACC CAG GCC

1. etr-orf   1060          1070          1080          1090          1100
```

```
[ 5642 ]    GGC TTG ACG AAT GGT ACG GCT GGC ACC ATG GAC GCC CTC ACG CAG GCC>
            ||| ||| ||| ||| ||| ||| ||| ||| ||| ||| ||| ||  ||  ||| |||
Metr-orf    GGC TTG ACG AAT GGT ACG GCT GGC ACC ATG GAC GCC CTG ACC CAG GCC


                                                                      1150
Metr-orf    TAC TCA GGA ATT CAG CAG TAT TGT CGC AGC TGC ACT GCC CAC TTT GTA

1. etr-orf     1110          1120          1130          1140          1150
[ 5642 ]    TAC TCA GGA ATT CAG CAG TA- CGC GGC AGC TGC ACT GCC CAC TTT GTA>
            ||| ||| ||| ||| ||| ||| ||   |   || ||| ||| ||| ||| ||| ||| |||
Metr-orf    TAC TCA GGA ATT CAG CAG TAT TGT CGC AGC TGC ACT GCC CAC TTT GTA


                                                                    1200
Metr-orf    CAG CCA GAG CTT GCT GCA ACA GCA GAG TGC TGC AGG CAG CCA GAA GGA

1. etr-orf         1160          1170          1180          1190
[ 5642 ]    CAG CCA GAG CCT GCT GCA GCA GCA GAG CGC TGC AGG CAG CCA GAA GGA>
            ||| ||| ||| | | ||| |||  || ||| |||  || ||| ||| ||| ||| ||| |||
Metr-orf    CAG CCA GAG CTT GCT GCA ACA GCA GAG TGC TGC AGG CAG CCA GAA GGA


Metr-orf    AGG TCC AGA GGG GGC AAA CCT CTT TAT TTA CCA CCT TCC ACA GGA GTT

1. etr-or1  0          1210          1220          1230          1240
[ 5642 ]    AGG TCC AGA GGG GGC AAA CCT CTT TAT TTA CCA CCT TCC ACA GGA GTT>
            ||| ||| ||| ||| ||| ||| ||| ||| ||| ||| ||| ||| ||| ||| ||| |||
Metr-orf    AGG TCC AGA GGG GGC AAA CCT CTT TAT TTA CCA CCT TCC ACA GGA GTT


          1250
Metr-orf    TGG AGA CCA GGA CAT TCT GCA GAT GTT CAT GCC CTT TGG AAA TGT TAT

1. etr-orf  250           1260          1270          1280          1290
[ 5642 ]    TGG AGA CCA GGA CAT TCT GCA GAT GTT CAT GCC CTT TGG AAA TGT TAT>
            ||| ||| ||| ||| ||| ||| ||| ||| ||| ||| ||| ||| ||| ||| ||| |||
Metr-orf    TGG AGA CCA GGA CAT TCT GCA GAT GTT CAT GCC CTT TGG AAA TGT TAT


           1300
Metr-orf    CTC TGC TAA AGT CTT CAT TGA CAA ACA GAC CAA TCT GAG CAA GTG CTT

1. etr-orf    1300          1310          1320          1330          1340
[ 5642 ]    CTC TGC TAA AGT CTT CAT TGA CAA ACA GAC CAA TCT GAG CAA GTG CTT>
            ||| ||| ||| ||| ||| ||| ||| ||| ||| ||| ||| ||| ||| ||| ||| |||
Metr-orf    CTC TGC TAA AGT CTT CAT TGA CAA ACA GAC CAA TCT GAG CAA GTG CTT


             1350
Metr-orf    TGG TTT GTT TAG CTA TGA CAA TCC AGT CTC TGC ACA AGC TGC AAT CCA

1. etr-orf       1350          1360          1370          1380          1390
[ 5642 ]    TGG TTT TGT TAG CTA TGA CAA TCC AGT CTC TGC ACA AGC TGC AAT CCA>
            ||| |||   | ||| ||| ||| ||| ||| ||| ||| ||| ||| ||| ||| ||| |||
Metr-orf    TGG TTT GTT TAG CTA TGA CAA TCC AGT CTC TGC ACA AGC TGC AAT CCA


              1400
Metr-orf    GGC TAT GAA CGG CTT TCA GAT CGG CAT GAA ACG CTT GAA GGT GCA GCT

1. etr-orf         1400          1410          1420          1430
[ 5642 ]    GGC TAT GAA CGG CTT TCA GAT CGG CAT GAA ACG CTT GAA GGT GCA GCT>
            ||| ||| ||| ||| ||| ||| ||| ||| ||| ||| ||| ||| ||| ||| ||| |||
Metr-orf    GGC TAT GAA CGG CTT TCA GAT CGG CAT GAA ACG CTT GAA GGT GCA GCT
```

```
                    1450
Metr-orf    GAA ACG CTC CAA AAA CGA CAG CAA ACC TTA CTG ATC GTC GAC CCG GGA

1. etr-or1  0         1450         1460          1470
[ 5642 ]    GAA GCG CTC CAA AAA CGA CAG CAA ACC TTA CTG A>
            |||  || ||| ||| ||| ||| ||| ||| ||| ||| ||| |
Metr-orf    GAA ACG CTC CAA AAA CGA CAG CAA ACC TTA CTG A


                   1500
Metr-orf    ATT CCG GAC CGG TAC CTG CAG GCG TAC CAG CTT TCC C
```

Figure 5.5

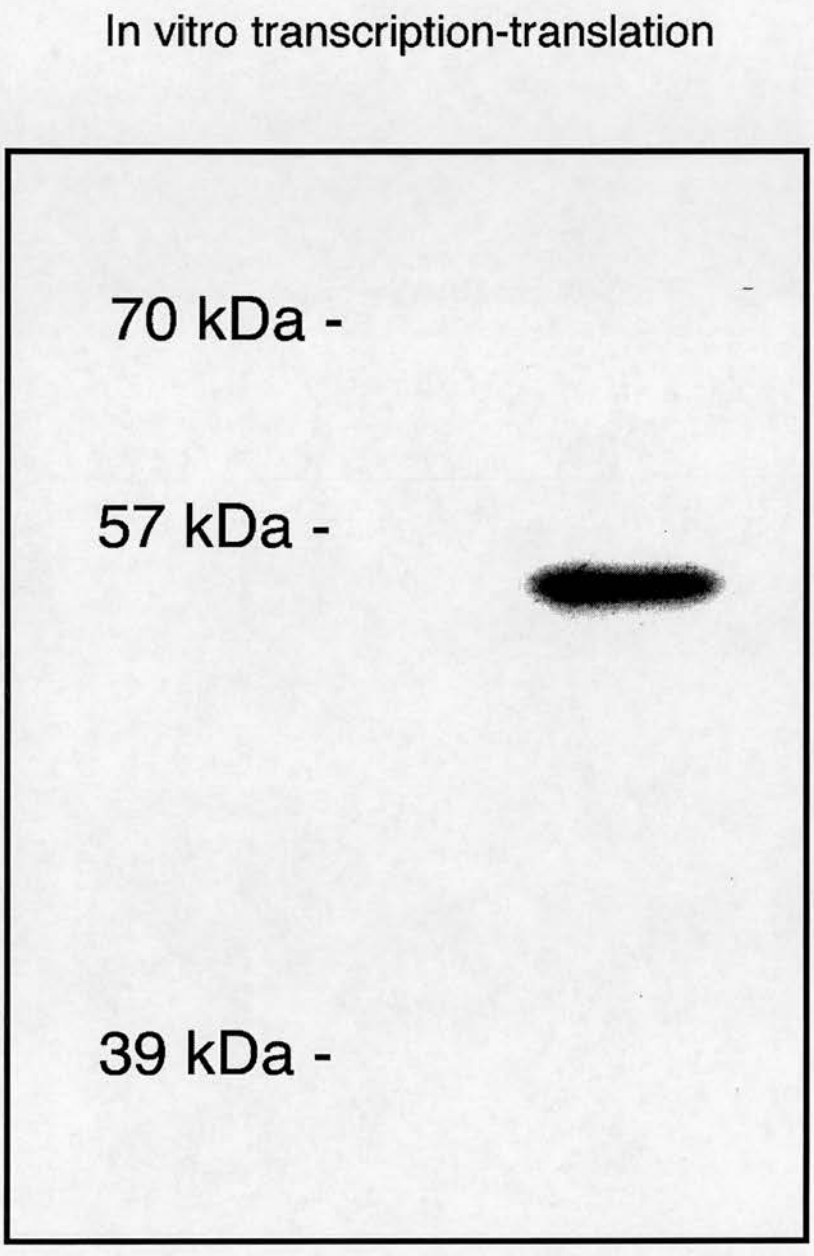

Figure 5.5

SDS-PAGE of the *in vitro* transcription-translation product derived from clone ETRR3. A single product of approximately 54kDA is given.

5.4.2 Northern blot analysis

Northern blot analysis allowed the tissue specificity of the ETRR3 sequence to be determined. Total RNA was extracted from the following tissues:- P10 heart, lung, spleen, testis, kidney, liver, spleen, thymus, and P1 and P10 brain, and transferred to Hybond-N membrane.

Figure 5.6 shows the tissue specificity of ETRR3. The probe was designed so that it comprised a large portion of the ORF sequence of ETRR3. The probe only hybridised to mRNA within the brain, further clarifying that this clone was specific to the nervous system. Three separate mRNAs were recognised by the probe, all of different sizes. The three messages were 9.5kb, 7.5kb and 2.5kb in size. The three mRNAs that the probe recognises are likely to be alternatively spliced isoforms of ETR-R3. It is unclear which of the three messages belongs to clone OL0391. The original 1.6Kb fragment also hybridised to these three messages.

To further investigate the specificity of this clone, a developmental northern was performed to assess the developmental pattern of expression of ETRR3 over postnatal ages. Total RNA from 1, 5, 9, 11, 15, 21 and 42 day old and adult rats was transferred to a nylon membrane. To ensure equal amounts of RNA were transferred to the filter, the samples were run out on a gel as described above for control purposes. The result reveal that the expression pattern of ETRR3 is developmentally regulated (figure 5.7). All three mRNAs are identified at every age. The level of expression of all three transcripts increased up until 9 days post natal. At ages greater than 9 days the level of expression appeared to be increasingly down regulated into adulthood.

Summary

ETRR3 is a novel protein that shows extensive sequence homology to the ELAV family of RNA binding proteins. ETRR3 is expressed specifically in the central nervous system, and is developmentally regulated. After post-natal day 9, the expression is down-regulated although it is still present in very low levels in the adult. ETRR3 identifies three messages 9.5, 7.5 and 2.5kb fragments by northern

Figure 5.6

Northern blot hybridised with a probe of 1.2Kb containing most of the ORF of ETRR3. 10μg of total RNA from each of the tissues was loaded onto each lane. Expression is specific to the brain. All three transcripts were hybridised with this probe. The 18S ribosomal RNA band is shown as a loading standardisation. **M**: Muscle; **H**: Heart; **S**: Spleen; **T**: testis; **Lv**: Liver; **K**: Kidney; **L**: Lung; **B**: Brain.

Figure 5.6

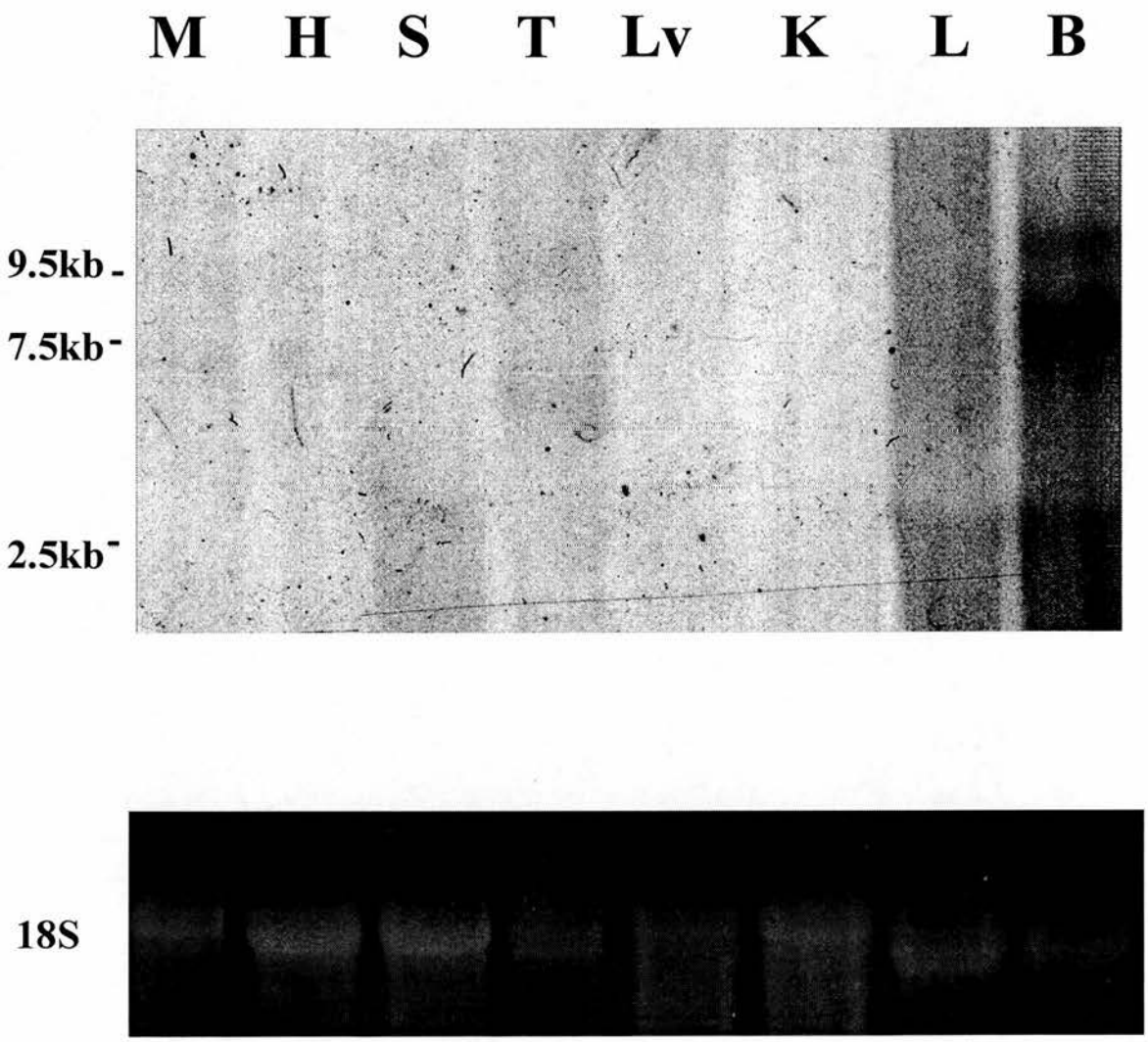

Figure 5.7.

Developmental northern blot hybridised with a probe of 1.2Kb containing most of the ORF of ETRR3. 10μg of total RNA from postnatal day 1-42 was loaded each lane. The 18S ribosomal RNA band is shown for loading standardisation. All three transcripts were down regulated after 9 days.

Figure 5.7

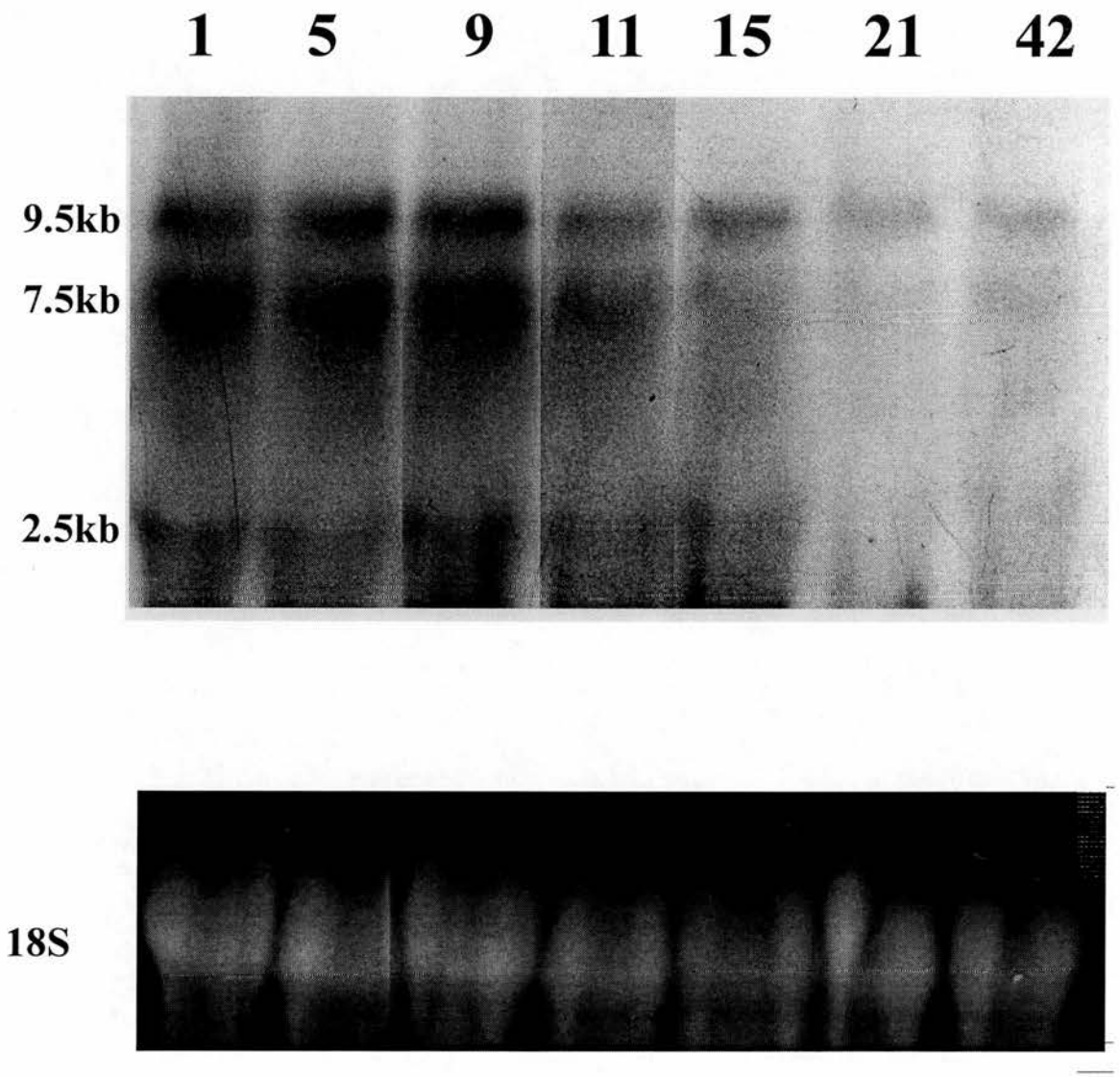

blot analysis, which are also developmentally regulated. *In vitro* transcription-translation of ETRR3 produces a protein of approximately 54kDa.

5.4.3 Isolation of the mouse isoform ETRR3 sequence

The mouse isoform of ETRR3 was isolated by RT-PCR and the sequence was compared to the rat sequence using MacVector. Figure 5.4 shows the nucleotide sequences of mouse and rat ETR-R3. The mouse sequence was 98% homologous to the rat sequence at the DNA level.

5.4.4 Embryonic expression patterns

To determine the expression pattern of ETRR3 mRNA throughout embryonic development a series of *in situs* were performed on mouse brain. A DIG labelled ribo-probe was designed to recognise the ORF of the rat ETRR3 sequence and the expression of the ETRR3 message was examined between E9 and P10 in the developing mouse brain.

5.4.4.1 E10-E12 embryos

Whole mount *in situ* hybridisations confirmed the earliest age of ETRR3 expression at E10 in the developing mouse brain. Expression was observed primarily in the developing forebrain (mainly the telencephalon and diencephalon). Similar expression patterns were seen in E10, E11 and E12 embryos although the intensity of the stain was stronger at the older ages. The greatest intensity of staining was seen in the telencephalic hemispheres, of which the ventral and lateral regions of the cortex showed the strongest expression (figures 5.8A and 5.8B).

Expression of the message was also observed in the diencephalon, although the intensity of staining was much less than was observed in the telencephalic hemispheres. Furthermore, hypothalamic nuclei were shown to be specifically expressing ETRR3 (figures 5.8B&C).

Without dissecting the tissue further it was difficult to categorise the expression of ETRR3 to a specific nuclear location within the hemispheres.

Figure 5.8

Whole mount *in situ* hybridisation of an E11 mouse embryo using a DIG-labelled riboprobe containing most of the ORF of ETRR3. **(A)** Shows the whole brain dorsal side up and **(B)** shows the ventral side up. Staining is present in the telencephalon and the diencephalon. Strongest staining is in the ventral, lateral and caudal region of the telencephalon. **(C)** A higher power view of the staining in the hypothalamus. **M:** Medial telencephalon; **R:** rostral telencephalon; **C:** Caudal; **L:** Lateral; **Tel:** telencephlaon; **Di**: Diecephalon; **H:** Hypothalamus.

Figure 5.8

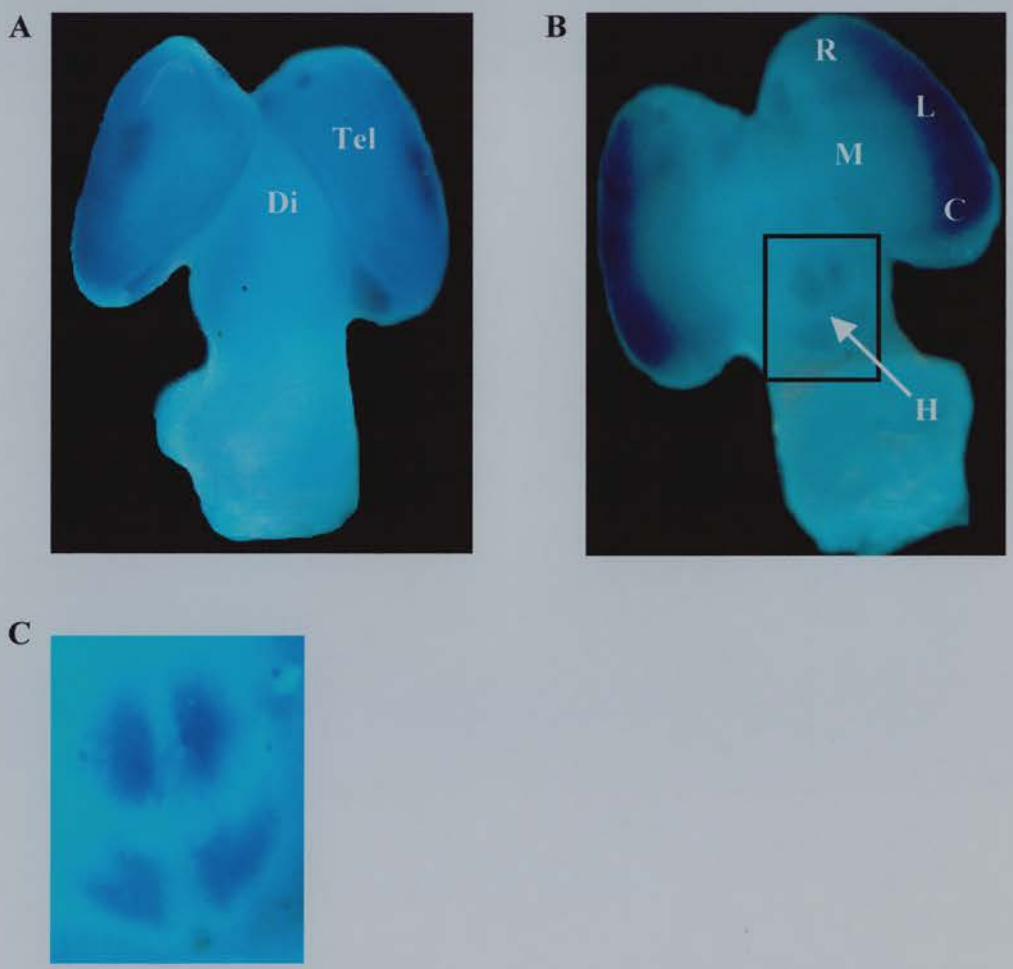

5.4.4.2 Expression of ETRR3 in E13 to E19 embryos

To determine more precisely the location of ETRR3 expression, in situ hybridisations were performed on 10μm brain sections of E13 to E19 embryos. The expression patterns of ETRR3 at E13 are shown in figure 5.9. By E13 the expression of ETRR3 was restricted to specific areas / nuclei of the developing brain. Expression was observed throughout the rostral-caudal axis of the whole brain (figure 5.9A–5.9C). Within the cortex, expression of ETRR3 was restricted to the preplate / cortical plate. Furthermore, the expression was strongest in the lateral / ventral regions of the cortex, which was consistent with the results of the whole mount *in situ* hybridisations.

Staining was also present in the ganglionic eminence (future striatum) (LGE and MGE) (figure 5.9A and 5.9B), and the diencephalon. Higher levels of expression were seen in the diencephalon than at the younger ages. Staining was present in both the ventral and dorsal thalamus, the intensity being stronger in the dorsal thalamus.

By E15, similar staining patterns were observed as there were at E13, although the intensity of staining was greater. In the cortex, expression was maintained in the developing cortical plate (figure 5.10A and 5.10B), with specific expression in the SP and MZ (figure 5.10B). Occasionally, labelled cells were observed in the white matter and the ventricular zone. The intensity of staining in the diencephalon was further increased in comparison with the expression levels at younger ages. A clearly defined expression boundary between the dorsal and ventral thalamus was observed (figure 5.10A), with higher levels of expression in the dorsal thalamus.

Similar patterns of expression were observed for E17 and E19 brain sections (figure 11A and B). Staining was more intense at E17 than at the earlier observed ages, but did not further intensify at older ages. Very little staining was observed in the ventricular zones of the developing cortex, ganglionic eminence (LGE and MGE) or thalamus (dorsal and ventral) at any of the ages studied.

Figure 5.9

In situ hybridisation of E13 mouse embryos using a DIG-labelled riboprobe of 1.2KB containing most of the ORF of ETRR3. **(A)** Rostral section through the brain, showing staining in the preplate and ganglionic eminence. **(B)** Medial section showing staining in the preplate, ganglionic eminence and the dorsal thalamus. Staining is stronger in the lateral / medial regions of the cortex. **(C)** Illustrates staining in a caudal section. No expression of ETRR3 was observed in the ventricular zone of any region of the brain. ETRR3 expression is indicated in blue and counterstain is in red.

PP: Preplate: **GE:**ganglionic eminence; **DT:** dorsal thalamus; **Ctx:** cortex; **VZ:** Ventricular zone; **LV:** Lateral ventricle; **iiiV:** Third ventricle; **LGE**: Lateral ganglionic eminence; **MGE:** Medial ganglionic eminence.

Figure 5.9

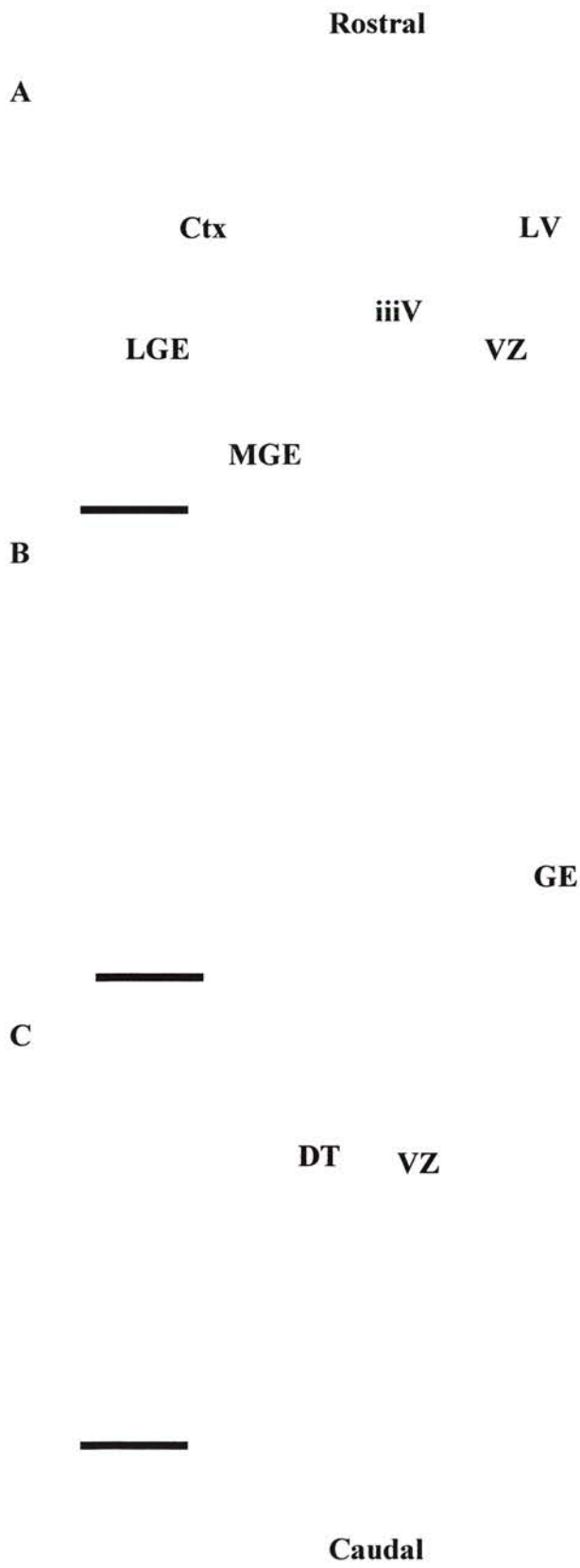

Figure 5.10

In situ hybridisations showing the expression pattern of ETRR3 in E15 mouse embryos. A DIG-labelled riboprobe of 1.2KB in length containing most of the ORF of ETRR3 was used. **(A)** Coronal section through the brain shows the expression of ETRR3 in the developing cortex, dorsal thalamus and ganglionic eminence. **(B)** High power view of the developing cortex. Staining is most prominent in the subplate (black arrow) and the marginal zone. A few cells in the ventricular zone also expressed ETRR3 as indicated by the arrowheads. ETRR3 expression is blue, counterstain is red.

GE: Ganglionic eminence; **DT:** Dorsal thalamus; **Ctx:** Cortex; **VZ:** Ventricular zone; **SP:** Subplate; **MZ:** Marginal zone; **IZ/WM:** Intermediate zone / White matter. Scale bars (A) 500μm and (B) 100μm.

Figure 5.10

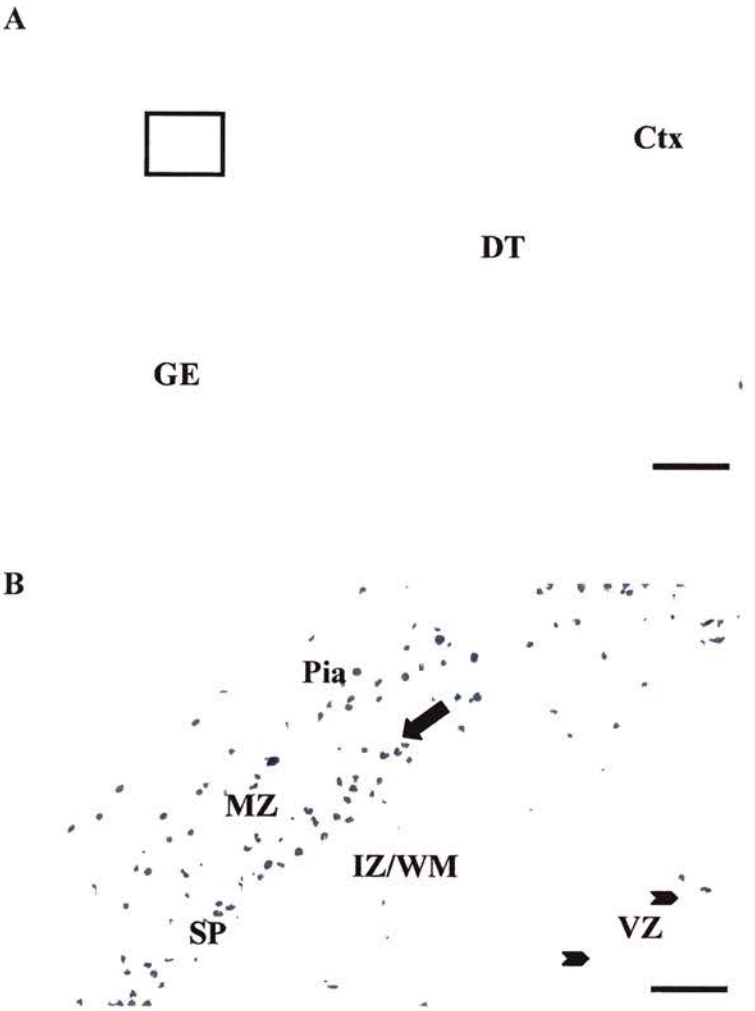

Figure 5.11

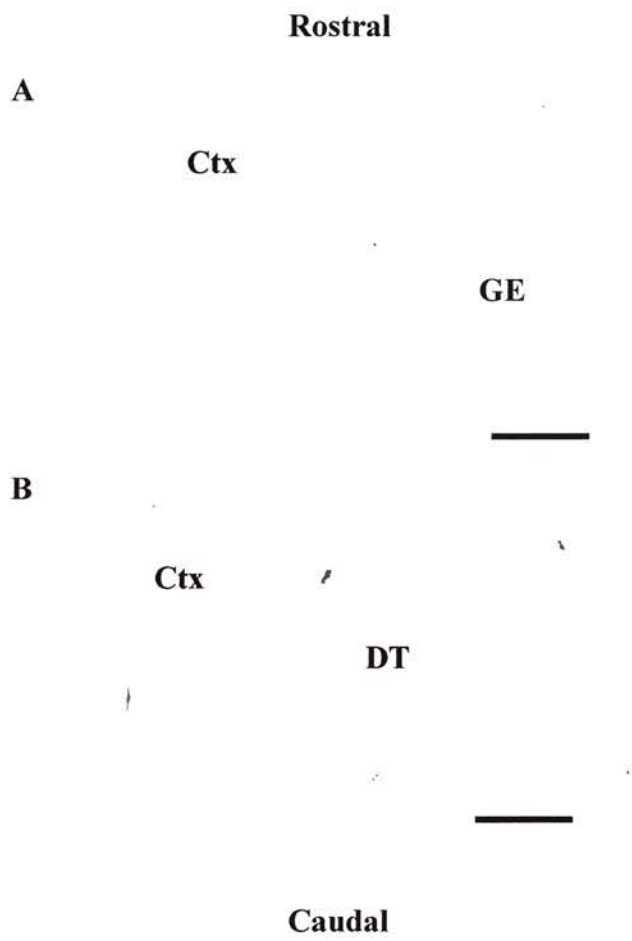

Figure 5.11
In situ hybridisations of E19 mouse embryos using a a DIG-labelled riboprobe of 1.2Kb in length containing most of the ORF of ETRR3. **(A)** Rostral section showing expression of ETRR3. Staining was observed in the cortex and ganglionic eminence.
(B) Caudal section showing expression pattern of ETRR3. The expression was seen in the cortex and dorsal thalamus.
GE: Ganglionic eminence; **DT:** Dorsal thalamus; **Ctx:** Cortex. **ORF:**Open reading frame

5.4.5 Expression of ETRR3 in early postnatal brains

By P4 the whole width of the cortical grey matter was expressing the transcript. Apart for the occasional labelled cell, the white matter and ventricular zones were not expressing the transcript.

At P10 the expression of the transcript was dramatically reduced and only low levels were seen throughout the width of the cortex, although the hippocampus maintained high levels of expression at this age.

5.4.6 Localisation of the ETRR3 protein

To determine the distribution of the ETRR3 protein in the developing mouse brain, an antibody was raised to a specific peptide sequence. The immuno-purified antisera as revealed by immunocytochemistry, paralleled that of the transcript as seen in digoxygenin labelled *in situs* at all ages studied. Staining was observed in the developing cortical plate, ganglionic eminence and thalamic nuclei. Similar to the expression of mRNA, very little staining was observed in the ventricular regions or white matter (not shown). By P10, protein levels had decreased, also in correlation with the mRNA expression.

Summary

Both ETRR3 transcripts and protein were expressed in developing mouse embryos from E10 to P10. Expression was strongest at E17, and decreased in intensity between P4 and P10. These results were consistent with the developmental northern blots. ETRR3 expression was strongest in the developing cortical plate, ganglionic eminence (future striatum) and the dorsal thalamus.

5.5 DISCUSSION

This study reveals the existence of a novel gene, termed ETRR3, isolated from a differentiated oligodendrocyte cDNA subtractive library. ETRR3 is a member of the Elav-like RNA binding protein family, and is expressed in discrete populations of post-mitotic neurones in the developing mouse brain.

5.5.1 Isolation of the mouse isoform

The expression pattern of ETRR3 in the developing mouse brain was examined by *in situ* hybridisation using a probe determined from the rat sequence. This thesis addresses neocortical development in the mouse therefore subsequent *in situ* hybridisations were performed in this species. The rat and mouse sequences were 98% homologous at the DNA level. This high degree of specific homology ensures that the observed staining patterns correspond to the expression of the ETRR3 gene in mouse.

5.5.2 What is known about related members of ETRR3

When the isolated sequence was compared against the Genbank and the EMBL databases, it was found to share significant homology with a human and a *Xenopus laevis* ETR sequence. The human form was isolated from a foetal heart library and nothing is known of its function or location. Similarly, the location and function of the *Xenopus* protein is also unknown.

ETRR3 shares sequence homology with the *elav*-like gene family of RNA binding proteins. Other members of this family include the Drosophila *elav* and *sxl* genes (Yao *et al.,* 1993; Beil *et al.,* 1988; Robinow and White, 1991), the human *Hu* genes (Graus *et al.,* 1985) and their mouse homologues, *mHu* genes (Okano *et al.,* 1997), and the vertebrate *elr* family (Good, 1995). The characteristic factor of RNA binding proteins is that they contain one or more RNA recognition motifs (RRM) of approximately 80 amino acids each (Burd and Deyfuss, 1994; Kenan *et al.,* 1991). ETRR3 was shown to contain several sequences characteristic of RRM, confirming that the product of the ETRR3 gene was indeed an RNA binding protein.

All *elav*-like gene family members are present in post-mitotic neurones throughout different stages of development. Although the role of the *Hu* genes are not well understood they are expressed in immature and mature neurones of the CNS and are believed to play a role in the proper development and function of mature neurones (Okano et al., 1997). The *mHu* genes encode a large number of alternatively spliced transcripts, which produce a series of related neurone-specific RNA binding proteins, expressed in a hierarchical fashion. For example *mHuB* is expressed in very early post-mitotic neurones, *mHuD* is expressed in migrating neurones of the intermediate zone and *mHuC* is expressed in mature cortical plate neurones.

The *elav* gene is better characterised and understood. A genetic analysis of the functions of *elav* suggests a role in the development and maintenance of the nervous system (Campos *et al.,* 1985; Yao *et al.,* 1993). It is neurone specific and plays a role in neurone-specific alternative splicing (Koushika *et al.,* 1996). The vertebrate *elr* family, similar to the above two families is present only in post-mitotic neurones and is suggested to have a role in early development and neural differentiation.

For reasons outlined below, the pattern of expression of ETRR3, and the possible presence of alternatively spliced transcripts (see next section) confirm that this gene is a member of the *elav* family of RNA binding proteins, and may also play a role in neural differentiation.

5.5.3 Alternative splicing

As mentioned above, other members of the *elav*-like gene family are involved in various post-transcriptional mechanisms of gene expression, an example of this being alternative splicing. The Drosophila *elav* gene regulates the splicing of a *neuroglian* gene (*nrg*) to produce a neurone-specific isoform (Koushika *et al.,*1996) whereas the *Hu* genes encode a variety of alternatively spliced isoforms (Okano and Darnell, 1997).

The northern blot analysis for ETRR3 indicates the presence of three separate transcripts of 9.5, 7.5 and 2.5kb in size. It is likely that these transcripts are the

products of alternatively spliced isoforms of ETRR3, similar to the *Hu* genes. It would be interesting to isolate these alternatively spliced isoforms and examine their expression patterns during development. The sequence of ETRR3 is further removed from the drosophila *elav* gene, than from the *Hu* genes. I therefore hypothesise that the alternatively spliced isoforms are expressed in a hierarchical fashion during development, similar to *Hu* genes.

5.5.4 Expression pattern of ETRR3 in the developing mouse cortex

The observed expression pattern of ETRR3 in the developing mouse cortex was similar to expression patterns of other *elav*-like genes. Expression was only seen in post mitotic neurones of the developing brain.

ETRR3 expression was first observed at E11 in the developing mouse brain and was maintained up until P10. At older ages, staining was still present although at much lower levels. At all ages studied ETRR3 expression appeared to be in regions correlating with the position of post-mitotic neurones. Specifically, expression was restricted mainly to the developing cortical plate, striatum, and thalamus.

In the E13 cortex expression was restricted specifically to the pre-plate. Preplate cells are the first post-mitotic cells to emerge from the ventricular zone in the developing cortex (Marin Padilla 1971). Preplate cells first emerge from the ventricular zone by E11. It is highly probable that ETRR3 expression observed at E11 by whole mount *in situ* was due to the probes recognising ETRR3 in the first born preplate cells. By E15, expression in the cortical plate was restricted to the deeper layers of the cortex or possibly the subplate. It is impossible to distinguish between these subplate and deep layer neurones at this age without doing birth dating (Brd-U) studies. However, a few labelled cells were also observed in the marginal zone. During cortical development the preplate splits into the subplate and the marginal zone by insertion of later born cortical neurones, suggesting that these labelled cells could be within the subplate.

At older ages expression was maintained throughout the whole width of the cortical plate in all layers, until between P4 and P10.

The observations from this study suggest that ETRR3 expression is restricted to early post-mitotic neurones in specific populations of the developing brain, suggesting a possible role in neuronal differentiation.

5.5.5 Ectopic expression of ETRR3

Occasionally ETRR3 positive cells were seen in the ventricular zone and intermediate zone of the developing cortex. The results above lead us to believe that ETRR3 is expressed primarily in post-mitotic cells. Therefore it was surprising to observe ETRR3 positive cells in areas of cell proliferation and migration. One possible explanation is that a population of post-mitotic cells reside within the ventricular zone and intermediate zone during development. A recent paper by Lillien *et al.,* (1998) suggests that the ventricular zone is a heterogeneous structure, containing not only proliferating cells, but also some postmitotic cells. The ETRR3 observed in the ventricular zone may be specific to the population of cells as described by Lillien *et al.,* (1998). Alternatively ETRR3 expression may label a very small subset of proliferating cells, although this is unlikely. This could be easily determined using BrdU or PCNA antibody studies.

A recent paper by Schramm et al., (1999) provided the first evidence that *elav*-like gene products are involved in the glial cell lineage. This leads to the possible explanation that ETRR3 positive cells within the IZ could be cells of the glial lineage. Again this is unlikely, but to make any further inferences on this it would be necessary to label the ETRR3 positive cells with various glial markers.

5.5.6 Role of ETRR3 in neuronal differentiation

Expression of ETRR3 is present mainly in post-mitotic neurones of the developing brain throughout a specific developmental time window (E11 to P10). In view of the expression pattern and the timing of expression, it is likely that product of the ETRR3 gene is involved in early neuronal differentiation. The fact that its

expression pattern is not maintained at the older ages suggests that it is not involved in the maintenance of neurones.

Differentiation is a complex process that involves much more than transformation of mitotic precursor cells into postmitotic cells. The morphology and physiology of the cell must be altered in order for the cell to become a functional component of the nervous system. The limitation on considering the possible roles of ETRR3 in neuronal differentiation is only controlled by the imagination of the experimenter. For example, ETRR3 may affect the cellular decisions made by a cell that influence its developmental potential or it may be involved in processes such as synaptogeneis or formation of dendrtitic arborisations. In view of the vast number of possible roles it could play in neuronal differentiation, it is impossible to suggest a specific role for ETRR3 without carrying further detailed experiments. Possible future experiments are described in the final discussion chapter to this thesis.

5.5.7 Possible mode of action of ETRR3

Identification of the RNA processing events that are regulated by the transcripts, requires localisation of the protein within the cell. The production of antisera and the immunohistochemistry analysis determined the presence of the ETRR3 protein in the nucleus of the cell, thus suggesting that the ETRR3 protein may regulate events in the nucleus such as alternative splicing, poly-adenylation and nuclear transport. Previous studies by Abe et al (1996 ;1996), have shown that *elav*-like proteins also have the ability to bind to their own messages, as well as other transcripts, so it is possible that ETRR3 may play a role in the metabolism of its own RNA.

5.5.8 Was subtraction a good method for isolating novel clones?

The isolation of a neuronal specific clone from a differentiated glial subtractive was surprising. However, when you consider the complexity of the library, it is perhaps not too surprising that the low abundance of the ETRR3 clones in the library resulted in it being avoided in the subtraction process. If the subtraction had been repeated twice, the ETRR3 clone would possibly have been removed.

5.6 Conclusions

A novel RNA binding protein of the *elav* family was isolated and cloned from an oligodendrocyte differentiated library. Northern blot analysis revealed three separate messages of 9.5, 7.5 and 2.5kB, which presumably represent products of alternative splicing. Expression of ETRR3 was restricted to post mitotic neurones of the developing mouse brain, primarily in the cortex, hippocampus, striatum and thalamus. The expression was restricted between E11 and P10, which leads to the hypothesis that ETRR3 is not required to generate neurones but is presumably involved in early cell differentiation.

5.7 Acknowledgement

The work in this chapter was performed as part of a collaborative study with Dr Steven Tait, Edinburgh. Dr Tait isolated and cloned ETR R3. I isolated the mouse isoform and performed the expression studies in both embryonic and postnatal mouse brains.

CHAPTER 6 SUMMARY AND FUTURE EXPERIMENTS

In this thesis the processes of neurogenesis and gliogenesis were examined in the developing mouse cerebral cortex. In particular, the study was aimed at addressing extrinsic and intrinsic mechanisms involved in cell fate decisions. Several different techniques were employed to address these issues. Firstly an *in vitro* tissue culture technique was employed to determine if cortically derived soluble factors were able to alter the behaviour of glial progenitors within the developing cortex. Secondly an *in vivo* transplant technique was employed in an attempt to determine if transplanted glial progenitors were able to alter their behaviour in response to factors within different host environments or if their behaviour was predetermined prior to transplantation. Finally a screening approach was used in which a cDNA library was screened in an attempt to isolate novel clones that may be of importance in neuronal/glial cell fate decisions within the developing neocortex.

Chapter 2

As discussed above this thesis was involved primarily at studying the mechanisms involved in cell fate decisions during the time period in which neurogenesis ends and gliogenesis begin. However, before these issues could be investigated it was important to establish exactly when gliogenesis started within the mouse neocortex. This information is not available in the literature, presumably because of the technical problems involved in studying glial cells. Although the literature states clearly that neurogenesis finishes during late embryogenesis and gliogenesis follows on from this sequentially in the postnatal period, there was no indication of the exact timings at which these processes occurred.

Using BrdU incorporation, the behaviour of E18, E19 and P0 labelled cells were followed over a 20-day period, and the cell types into which they differentiated was investigated using various antibodies. Firstly this study suggested that cells labelled with BrdU on E18 in the mouse neocortex gave rise to the last born neurones of the cortex and also to the first born glial cells (apart from the radial glial cells). The conclusions that the E18 labelled cells were neurones was based upon their position that they migrated to within the cortical plate, their size and their lack of expression

of glial markers. Further studies using antibodies specific to neurones need to be performed to further this hypothesis. Although technical problems were encountered when trying to label these cells with MAP2, other antibodies such as NeuN may be a suitable alternative.

Using the recently characterised QK1 antibody, cells were confirmed to be of the glial lineage. This marker unfortunately was not able to distinguish between the different types of glial cells. Interesting future studies would be to determine the phenotype of the QK1 positive glial cells, although this would require specific early markers of both astrocytes and glial cells, which are at present either unavailable or not possible to use in an *in vivo* study. The obvious marker for early oligodendrocytes is O4, but unfortunately it is notoriously difficult to get optimum staining this antibody and it was not useable on paraffin embedded tissue.

In addition to characterising the time point at which neurogenesis ended and gliogenesis began, the density and distributions of these cells were examined overtime. The results showed that the density of E19 and P0 labelled cells decreased more dramatically than could be explained by cortical expansion. How and where these cells disappeared to remains unclear. Future investigations could involve addressing such issues as migration and cell death as possible mechanisms for the reduction in cell density. For example, TUNEL staining could be used in combination with BrdU immunocytochemistry to provide a clearer indication of the proportion of cells that die.

In conclusion, the results from this study suggest that E18 born cells within the developing mouse neocortex give rise to both neurones and glial cells, whereas E19 and P0 born cells give rise purely to glial cells. Furthermore the density of E19 and P0 born cells reduced over time. This reduction is thought to result from either cell death, further proliferation or migration to another brain region, or a combination of any of these three processes.

Chapter 3

Having established that E19 born cortical cells gave rise to a pure glial cell population, this study was aimed at determining whether the E19 born cells were predetermined in their behaviour and phenotype or whether they were susceptible to change due to signals within the environment. A tissue culture paradigm was employed to address these issues.

E19 cortical slices were grown in cortical conditioned medium from E15 cortex, and their behaviour compared with E19 cortical slices grown in E19 cortical conditioned medium and normal serum free culture medium. The results provide further evidence for a general role of extrinsic factors regulating cortical development. More specifically, the results suggest that factors released from E19 cortical conditioned medium have either a permissive or instructive role for normal glial cell development, in terms of migration, proliferation and differentiation, whereas factors released from E15 cortex appear to be inhibiting or lacking in instructive signals. The interesting finding of these experiments was that the E19 derived factor appeared to have a abnormal effects on cells of the astrocytic lineage at higher concentrations. It would be interesting to confirm the inhibitory effects of the E15 factor, by replacing the E19CM with E15CM in an attempt to reverse the radial glial cell like effects that was observed.

The data obtained for the density of the O4 cells did not appear to correlate with the speculations made above about the possible opposing roles of E15 and E19 cortical conditioned medium. These results are curious and before any conclusions can be made about their role, a series of further investigations need to be made. It is unlikely that these results are an artefact of the tissue culture system due to the consistency of the data. It is possible that the cortex releases a cocktail of environmental factors each of which have different actions on different subtypes of cells.

These data do confirm the existence of environmental signalling processes being involved in cortical development, although the nature of these molecules remains

unknown. Futures studies are aimed at isolating and characterising the factor or factors that are released from E15 and E19 cortex. This could result in the isolation of a novel factor involved in the regulation of cortical development.

Chapter 4

This study was performed to compliment the *in vitro* study described in chapter 3. O-2A progenitor cells were isolated from P2 rat cerebral cortices and their cell identity challenged by transplanting them into two different ages of host tissue. Initially, the idea was to use dissociated cells from the cortex of mice at a time when gliogenesis was predominating. However, at the time of this study chapter 2 was incomplete and the age of cortex that should be used remained unclear. Furthermore, it would be difficult to isolate just a pure population of progenitor cells, and transplantation would probably result in glial progenitors, post-mitotic neurones and possibly mature glial cells all being transplanted into the host brains. Hence it would be difficult to assess the role of the environment upon the behaviour of these cells as to the phenotype of the cells as it was unclear at the time of transplantation. Therefore by using O-2a cells, the population of cells for transplantation were known to be a pure glial population.

These experiments provide a basic groundwork for future transplantation experiments, although the data remain incomplete. The results obtained lead to the suggestion that some oligodendrocytes are not restricted to the glial lineage, but have the ability to differentiate into neurones. However, these conclusions were based only on cell morphology and further confirmation would require labelling the transplanted cells with neuronal or glial specific antibodies. Unfortunately, for technical reasons the antibody reactions were not working to their maximum efficiency. This presumably resulted from the long periods for which the tissue was stored in fixative and the processing technique employed.

Future studies are planned in which the processing technique will be varied to enable a variety of antibodies to be used to label the transplanted cells. These would include

neuronal markers such as MAP2 and ß-tubulin, astrocyte markers such as GFAP and vimentin and oligodendrocyte markers such as O4 and CNPase.

One hypothesis that emerged from this study was that the E16 environment may release soluble signals that instruct oligodendrocyte precursor cells to remain in a proliferative state or differentiate into neuronal cells. In an attempt further clarify this hypothesis it would be interesting to transplant these oligodendrocyte precursor cells into younger and older ages of host tissue and follow their fate and identity.

An alternative and simpler way in which to address the role of extrinsic factors upon cell behaviour would be to use a similar approach to the tissue culture technique described in chapter 3. Culturing pure populations of O-2A cells in conditioned medium from various ages of hosts (E14-adult) cortex would give some further insight into the role of environmental signals on cell fate determination. Subsequent studies from this may involve trying to isolate the specific factors.

Bohner *et al.* (1997) used several different culture techniques to investigate the nature of various environmental signals involved in laminar specification. Their system allowed the issues of cell-cell contact, and short and long distance cues to be addressed. By using similar methods to Bohner *et al.*, (1997) it would be interesting to establish if cell contact or short and long-range cues are involved in migration and differentiation of oligodendrocyte precursor cells cells.

When using tissue culture techniques as described above and in chapter 3 it is important to realise the limitations of these techniques and how they agree with the *in vivo* situation. For example, O-2A cells have been shown *in vitro* to differentiate into type 2 astrocytes and oligodendrocytes, whereas *in vivo* they are known to only differentiate into cells of the oligodendrocyte lineage. Therefore to get a full understanding of the developmental mechanism it is important to couple *in vivo* and *in vitro* experiments together where possible.

Chapter 5

During this study a completely different approach was used to that described in the previous two chapters, although it was still aimed at addressing the neuronal / glial switch issue in the developing cortex. A screening approach was employed in an attempt to isolate novel clones that may be involved in neuronal/glial cell fate mechanisms.

Subtractive cDNA libraries are a valuable source for isolating potential novel and rare clones. In this chapter an RNA binding protein was isolated from an oligodendrocyte subtractive library and further characterised to examine any possible role in cell fate mechanisms. Although this protein was not found to have any obvious roles in cell fate decisions it was shown to be expressed only in post-mitotic neurones. Interestingly its expression was first noticed in cells that had only just become postmitotic, and its expression was down regulated into adulthood. Therefore this RNA binding proteins is potentially useful as an early marker of post-mitotic cells

Possible future experiments could be aimed at identify the role of the RNA binding protein. Experiments could be designed to determine the target action of the protein in an attempt to suggest a possible role of the RNA binding protein. In addition to further characterising this protein, additional screening of the cDNA subtractive library could lead to isolation of other clones that may be involved in the neuronal glial switch process.

REFERENCES

Abe, R., Yamamoto, K., Sakamoto, H. (1996). Target specificity of neuronal RNA-binding protein, Mel-N1:direct binding to the 3'untranslated region of it's own mRNA. *Nuc.Acids.Res.* 24(11), 2011-2016.

Abe, R., Sakashita, E., Yamamoto, K., Sakamoto, H. (1996). Two different RNA binding activities for the AU-rich element and the poly(A) sequence of the mouse neuronal protein mHuC. *Nuc. Acid Res.* **24(11),** 4895-4901.

Akers, R.M. (1977). Radial fibres and astrocyte development in the rat cerebral cortex. *Anat.Rec.* **187,** 520-521.

Allendoerfer, K.L. and Shatz, C.J. (1994). The subplate, a transient neocortical structure: its role in the development of connections between the thalamus and the cortex. *Ann. Rev. Neurosci.* **17,** 185-218.

Altman, J. (1966). Proliferation and migration of undifferentiated precursor cells in the rat during postnatal gliogenesis. *Exper. Neurol.* **16,** 263-278.

Altman, J. and Bayer, S.A. (1990). Vertical compartmentation and cellular transformations in the germinal matrices of the embryonic rat cerebral cortex. *Exp. Neurol.* **107,** 23-35.

Altshuller, Y., Copeland, N.G., Gilbert, D.J., Jenkins, N.A., and Frohman., M.A. (1996). *Gcm1,* a mammalian homolog of *Drosophila glial cells missing. F.E.B.S.,***393,** 201-204.

Anderson, D.J. (1995). A molecular-switch for the neurone-glia developmental decision. *Neuron,* **15,** 1219-1222.

Andersson, C., Tytell, M., and Brunso-Betchold, J. (1993). Transplantation of cultured type 1 astrocyte cell suspensions into young, adult and aged rat cortex: Cell migration and survival. *Int. J. Dev. Neurosci.* **11(5),** 555-568.

Angevine, J.B. and Sidman, R.L. (1961). Autoradiographic study of cell migration during histogenesis of cerebral cortex in the mouse. *Nature* **192,** 766-768.

Ausubel, F.M., Brent, R., Kingston, R.E., Moore, D.D., Seidman, J.G., Smith, J.A., and Struhl, K. (1992). Current protocols in molecular biology. *Published by Wiley.*

Baillarger, J.G.F. (1840). Recherches sur la structure de la couche corticale des circonvolutions du cerveau. *Mem. Acad. R. Med.* **8**, 149.

Bantle, J.A., Hahn, W.E. (1987). Complexity and characterisation of polyadenylated RNA in the mouse brain. *Cell,* **8**, 139-150.

Barbe, M.F. (1996). Tempting fate and commitment in the developing forebrain. *Neuron* **16,** 1-4.

Barbe, M.F., and Levitt, P. (1991). The early commitment of fetal neurons to the limbic cortex. *J. Neurosci.* **11,** 519-533.

Barbe, M.F., and Levitt, P. (1995). Age-dependent specification of the corticocortical connections of cerebral grafts. *J. Neurosci.* **15,** 1819-1834.

Barres, B.A., and Raff, M.C (1994). Control of oligodendrocyte number in the developing rat optic nerve. *Neurone* **12,** 935-942.

Bayer, S.A., and Altman, J. (1991). Neocortical development. *New York: Raven.*

Beil, L.R., Maine, E.M., Schedl, P., and Cline, T.W. (1988). Sex-lethal, a drosophila sex determination switch gene, exhibits sex-specifc RNA splicing and sequence similarity to RNA binding proteins. *Cell,* **55,** 1037-1046.

Bellen, H.J., Kooyer, S., D'Evelyn, D., and Pearlman, J. (1992). The Drosophila couch potato protein is expressed in nuclei of peripheral neuronal precursors and shows homology to RNA-binding proteins. *Genes Dev.* **6,**2125-2136.

Berman, N.E.J., Johnson, J.K, and Klein, R.M. (1997). Early generation of glia in the developing cerebral cortex. *Dev. Brain. Res.* **101,** 149-164.

Bernhardt, R., and Matus, A. (1984). Light and electron microscopic studies of the distribution of microtubule-associated protein 2 in rat brain: a difference between dendritic and axonal cytoskeletons. J. Comp. Neurol., **226(2),** 203-21.

Berry, D.M., Rogers, A.W and Eayrs, J.T. (1964). Pattern of cell migration during cortical histogenesis. *Nature,* **208,** 591-593.

Berry, M. and Rogers, A.W. (1965). The migration of neuroblasts in the developing cerebral cortex. *J.Anat.*, **99,** 691-709.

Blaschke, A., Staley, K. and Chun, J. (1996). Widespread programmed cell death in proliferative and post-mitotic regions of the fetal cerebral cortex. *Development,* **122,** 1165-1174.

Blaschke, A., Weiner, J. and Chun, J. (1998). Programmed cell death is a universal feature of embryonic and postnatal neuroproliferative regions throughout the central nervous system. *J.Comp. Neurol.,* **396,** 39-50.

Bohner, A.P., Akers, R.M., and McConnell, S.K. (1997). Induction of deep layer cortical neurons in vitro. *Development* **124,** 915.923.

Bonni, A., Sun., Nadal-Vicens, M., Bhatt., A., Frank, D.A., Rozovsky, I., Stahl, N., Yancopoulos, G.D., Greenberg, M.E. (1997). Regulation of gliogenesis in the central nervous system by the JAK-STAT signalling pathway. *Science,* **278,** 477-483.

Boulder Committee (1970). Embryonic vertebrate nervous system: revised terminology. *Anat Rec.* **166,** 257-262.

Brodmann, K. (1903). Beitrage zur histologischen lokalisation der grosshirnrinde: die regio Rolandica. *J. Psychol. Neurol.* **2,** 133.

Bronner-Fraser, M., and Fraser, S.E. (1988). Cell lineage analysis shows multipotentiality of some avian neural crest cells. *Nature,* **335,** 161-164.

Brustle, O., Maskos, U., and McKay, R.D.G. (1995). Host-guided migration allows targeted introduction of neurones into the embryonic brain. *Neuron* **15,** 1275-1285.

Brustle, O., Spiro, C.A., Karram, K., Choudhary, K., Okabe, S., McKay, R.D.G. (1997). In vitro-generated neural precursors participate in mammalian brain development. *Proc. Natl. Acad. Sci. USA* **94,** 14809-14814.

Burd, C.G., and Dreyfuss, G., (1994). Conserved structures and diversity of functions of RNA-binding proteins. *Science.* **265**,615-620.

Caceres, A., Banker, G., Steward, O., Binder, L,. Payne, M. (1984). MAP2 is localized to the dendrites of hippocampal neurons which develop in culture. *Brain. Res.* **315(2),**314-8.

Cajal, S.R. (1899). Apuntes para el estudio estructural de la corteza visual del cerebro humano. *Rev. Ibero-Am. Cie. Med.* **March,** 1-14.

Cajal, S.R. (1911). Histologie du Systeme Nerveux de l'homme et des vertebres. *Paris, Maloine.*

Cameron, H.A., Hazel., T.G., and McKay. (1998). Regulation of neurogenesis by growth factors and neurotransmitters. *J. Neurobiol.,* **36,** 287-306.

Cameron, R.S. and Rakic, P. (1991). Glial cell lineage in the cerebral cortex: A review and synthesis. *Glia,* **4,** 124-137.

Campbell, K., Olsson, M., and Bjorklund, A. (1995). Regional incorporation and sire-specific differentiation of striatal precursors transplanted to the embryonic forebrain ventricle. *Neuron* **15,** 1259-1273.

Campos, A.R., Grossman, D., and White K. (1985). Mutant alleles at the locus elav in drosphila melanogaster lead to nervous system defects. A developmental genetic analysis. *J. Neurogenetics,* **2**,197-218.

Canoll, P.D., Musacchio, J.M., Hardy, R.J., Reynolds, R., Marchionni, M.A. and Salzer, J.L. (1996). GGF/Neuroregulin is a neuronal signal that promotes the proliferation and survival and inhibits the differentiation of oligodendrocyte progenitors. *Neurone,* **17,** 229-243.

Cattaneo, E., and McKay. (1990). Proliferation and differentiation of neuronal stem cells regulated by nerve growth factor. *Nature.,* **347(6295),** 762-5.

Catteneo, E., Magrassi, L., Butti, G., Santi, L., Giavazzi, A., and Pezzotta, S. (1994). A short term analysis of the behaviour of conditionally immortalised neuronal progenitors and primary neuroepithelial cells implanted in the fetal rat brain. *Dev. Brain Res.* **83,** 197-208.

Caviness, V. S. Jr. (1982). Neocortical histogenesis in normal and reeler mice: a developmental study based upon [^{3}H] thymidine autoradiography. *Develop. Brain. Res.* **4** 293-302.

Caviness. V.S.Jr. and Sidman, R.L. (1973). Time and origin of corresponding cell classes in the cerebral cortex of normal and reeler mutant mice: an autoradiographic analysis. *J. Comp. Neurol.* **148,** 141-152.

Caviness, V.S.Jr., Takahashi, T. and Nowakowski, R.S. (1995). Numbers, time and neocortical neurogenesis: a general developmental and evolutionary model. *T.I.N.S.* **18(9),** 379-383.

Chenn, A. and McConnell, S.K. (1995). Cleavage orientation and the assymmetric inheritance of Notch 1 immunoreactivity in mammalian neurogenesis. *Cell.* **82,** 631-641.

Choi, B.H. (1988). Prenatal gliogenesis in the developing cerebrum of the mouse. *Glia,* **1,** 308-316.

Collinson, J.M., Marshall, D., Gillespie, S., Brophy, P. (1998). Transient expression of Neurofascin by oligodendrocytes at the onset of Myelinogenesis: Implications for mechanisms of Axon-glial interaction. *Glia,* **23**,11-23.

Couly, G.F., and Le Douarin, N.M. (1985). Mapping of the early neural primordium in quail-chick chimeras. I. Developmental relationships between placodes, facial ectoderm, and prosencephalon. *Dev. Biol.* **110,** 422-439.

Couly, G.F., and Le Douarin, N.M. (1987). Mapping of the early neural primordium in quail-chick chimeras. II. The prosencephalic neural plate and neural folds: Implications for the genesis of cephalic human congenital abnormalities. *Dev. Biol.* **120,** 198-214.

Cullican, S., Baumrind, N., Yammamoto, M. and Pearlman, A. (1990). Cortical radial glia: Identification in tissue culture and evidence for their transformation to astrocytes. *J. Neurosci.* **10,** 684-692.

Darnell, R.B., (1996). Onconeural antigens and the paraneoplastic neurologic disorders: at the intersection of cancer, immunity and the brain. *Proc. Natl. Sci. (USA).* **93**,4529-4536.

Davis, A.A., and Temple, S. (1994). A self-renewing multipotential stem cell in embryonic rat cerebral cortex. *Nature* **372,** 263-266.

Del Rio, J.A. and Soriano, E. (1989). Immunocytochemical detection of 5' Bromodeoxyuridine incorporation in the central nervous system of the mouse. *Dev. Brain. Res.* **49 (2),** 311-317.

Doetsch, F., Caille, I., Lim, D.A., Garcia-Verdugo, J.M., and Alvarez-Buylla, A. (1999). Subventricular zone astrocytes are neural stem cells in the adult mammalian brain. *Cell,* **97,** 703-716.

Dunnett, S.B., Everitt, B.J., and Robbins, T.W. (1991). The basal forebrain-cortical cholinergic system: interpreting the functional consequences of excitotoxic lesions. *Trends Neurosci.* **14,** 494-501.

Edwards, M.A., Yamamoto, M., and Caviness, V.S. Jr. (1990). Organisation of radial glial and related cells in the developing murine CNS. An analysis based upon a new monoclonal antibody marker. *Neurosci.* **36,** 121-144.

Espinosa de Los Monteros, A., Zhang, M., and DeVellis, J. (1993). O2a progenitor cells transplanted into the neonatal rat brain develop into oligodendrocytes but not astrocytes. *Proc. Natl. Acad. Sci. USA* **90,** 50-54.

Finlay, B.L. and Slattery, M. (1983). Local differences in the amount of early cell death in neocortex predict adult local speacialisations. *Science,* **219,** 1349-1351.

Fishell, G. (1995). Striatal precursors adopt cortical identities in response to local cues. *Development* **121,** 803-812.

Fishell, G. (1997). Regionalisation in the mammalian telencephalon. *Curr. Opn. Neurobiol.* **7,** 62-69.

Frantz, G.D., and McConnell. (1996). Restriction of late cerebral cortical progenitors to an upper layer fate. *Neuron* **17(1),** 55-61.

Fujita, S. (1960). Mitotic pattern and histogenesis of the central nervous system. *Nature,* **187,** 702-703.

Fujita S. (1963). The matrix cell and cytogenesis in the developing central nervous system. *J. Comp. Neurol.* **120,** 37-42.

Gard, A.L., Williams, W.C., and Burrell, M.R. (1995). Oligodendroblasts distinguished from O-2A glial progenitors by surface phenotype (04+GalC-) and response to cytokines using signal transducer LIFRß. *Dev. Biol.,* **167,** 596-608.

Gates, M.A., Olsson, M., Bjerregaard, K., and Bjorkland, A. (1998). Region-specific migration of embryonic glia grafted to the neonatal brain. *Neurosci.* **84 (4),** 1013-1023.

Gaiano, N., and Fishell, G. (1998). Transplantation as a tool to study progenitors within the vertebrate nervous system. *J. Neurobiol.* **36,** 152-161.

Gard, A.L., and Pfeiffer, S.E. (1990). Two proliferative stages of oligodendrocyte lineage ($A2B5^{+}O4^{-}$ and $O4^{+}GalC^{-}$) under different mitogenic control. *Neurone,* **5,** 615-625.

Gennari, F. (1782). De peculiari structura cerebri nonnullisque eius morbus, parma.

Ghosh, A, and Greenberg, M.E. (1995). Distinct roles of bFGF amd NT-3 in the regulation of cortical neurogenesis. *Neurone* **15,** 89-103.

Gillies, K. and Price, D.J. (1993). The fates of cells in the developing cerebral cortex of normal and methyazoxymethanol acetate-lesioned mice. *Europ. J. Neurosci.* **5(1),** 73-84.

Goldman, J.E. and Vayesse, P.J.J. (1991). Tracing glial cell lineages in the mammalian forebrain. *Glia,* **4,** 149-156.

Gonye, G.E., Warrington, A.E., DeVito, J.A. and Pfeiffer, S.E. (1994). Oligodendrocyte precursor quantitation and localisation in perinatal brain using a retrospective bioassay. *J. Neurosci.* **14 (9),** 5365-5372.

Good, P.J. (1995). A conserved family of *Elav*-like genes in vertebrates. *Proc. Natl. Acad. Sci. USA.* **92,** 4557-4561.

Gotz, M and Bolz, J. (1992). Formation and preservation of cortical layers in slice cultures. *Neurobiology* **23(7),** 83-802.

Gotz, M., Wizenmann, A., Reinhardt, S., Lumsden, A., and Price, J. (1996). Selective adhesion of cells from different telencephalic regions. *Neurone,* **16,** 551-564.

Grapin-Botton, A., Bonnin, M.A., McNaughton, L.A., Krumlauf, R., and Le Dourain, N.M. (1995). Plasticity of transposed rhombomeres: Hox gene induction is correlated with Phenotypic modifications. *Development* **121,** 2707-2721.

Graus, F., and Ferrer, I. (1990). Analysis of neuronal antigen (Hu) expression in the developing rat brain detected by autoantibodies from patients with paraneoplastic encephalomyelitis. *Neusrosci. Lett.* **112,** 14-18.

Graus, F., and Cordon-Cardo, C., and Posner, J. (1985). Neuronal antinuclear antibody in sensory neuronopathy from lung cancer. *Neurology,* **35,**538-543.

Gressons, P., Richelme, C., Kadhim, H.J., Gadisseux, J. and Evrard, P. (1992). The germinative zone produces the most cortical astrocytes after neuronal migration in the developing brain. *Biol. Neonate.* **61,** 4-24.

Gritti, A., Parati, E.A., Cova, L., Frolichssthal, P., Galli, R., Wanke, E., Faravelli, L., Morassutti, D.J., Roisen, F., Nickel, D.D., Vescovi, A. (1996). Multipotential cells from the adult mouse brain proliferate and differentiate in response to basic fibroblast growth factor. *J. Neurosci.,* **16**, 1091-1100.

Gross, R.E., Mehler, M.F., Mabie., P.C., Zhang, Z., Santschi, L., and Kessler., J. (1996). Bone morphogenetic proteins promote astroglial lineage commitment by mammalian subventricular zone progenitor cells. *Neurone,* **17**, 595-606.

Grove, E.A., Williams, B.P., Li, D.Q., Hajihosseini, M., Friedrich, A., and Price, J. (1993). Multiple restricted lineages in the embryonic rat cerebral cortex. *Development.* **117,** 553-561.

Halliday, A.L., and Cepko, C.L. (1992). Generation and migration of cells in the developing striatum. *Neuron* **9,** 15-26.

Hardy, R.J. (1997). Dorso-ventral patterning and oligodendrocyte specification in the developing nervous system. *J. Neurosci. Res.,* **50,** 139-145.

Hardy, R.J. (1998). QK1 expression is regulated during neurone-glial cell fate decisions. *J. Neurosci. Res.* **54(1),** 46-57.

Hardy, R., and Reynolds, R. (1993). Neurone-oligodendroglial interactions during central nervous system development. *J. Neurosci. Res.* **36,** 121-126.

Hardy, R., and Reynolds, R. (1993). Rat cerebral cortical neurones in primary culture release a mitogen specific for early (G_{D3}^{+}/O4^{-}) oligodendroglial progenitors. *J. Neurosci. Res.* **34,** 589-600.

Hardy, R.J., and Friedrich, V.L. (1996). Oligodendrocyte progenitors are generated throughout the embryonic mouse brain, but differentiate in restricted foci. *Development.,* **122,** 2059-2069.

Hardy, R.J., Loushin, C.L., Friedrich, V.L., Chen, Q., Ebersole, T.A., Lazzarini, R.A., and Artz, K. (1996). Neural cell-type specific expression of QK1 proteins is altered in *quakingviable* mutant mice. **16(24),** 7941-7949.

Hatten, M. (1990). Riding the glial monorail: a common mechanism for glial guided neuronal migration in different regions of the developing mammalian brain. *T.I.N.S.* **13(5),** 179-84.

Hatten, M. (1993). The role of migration in central nervous system neuronal development. *Curr. Opin. Neurobiol.,* **3,** 38-44.

Herfort, M.R., and Gaber, A.T. (1991). Simple and efficient subtractive hybridisation screening. *Biotechniques,* **11,**598-605.

Hinds, J.W., and Ruffett, T.L. (1971). Cell proliferation in the neural tube: an electron microscopic and Golgi analysis in the mouse cerebral vesicle. *Z. Zellforsch.* **115,** 226-264.

Hosoya, T., Takizawa, K., Nitta, K., and Hotta, Y. (1995). *Glial cells missing:* a binary switch between neuronal and glial determination in *Drosophila. Cell,* **82,** 1025-1036.

Hughes, S., Lilien, L.E., Raff, M.C., Rohrer, H, Sendtner, M. (1988). Ciliary neurotrophic factor induces type 2 astrocyte differentiation in culture. *Nature.,* **335,** 70-73.

Humphreys, P., Jones, S. and Hendelman, W. (1996). Three dimensional cultures of fetal mouse cerebral cortex in a collagen matrix. *J. Neurosci.Met.* **66,** 23-33.

Hunter, K.E., and Hatten, M.E. (1995). Radial glial transformation to astrocytes is bideirectional:Regulation by a diffusible factor in the embryonic forebrain. *Proc. Natl. Acad. Sci.,* **92,** 2061-2065.

Huttner, W.B., and Brand, M. (1997). Asymmetric division and polarity of neuroepithelial cells. *Curr. Opin. Neurobiol.* **7,** 29-39.

Jackson, C.A., Peduzzi, J.D. and Hickey, T.L. (1989). Visual cortex development in the ferret: genesis and migration of visual cortical neurones. *J. Neurosci.* **9,** 1242-1253.

Jan, Y.N., and Jan, L.Y. (1995). Maggots hair and bugs eye: role of cell interaction and intrinsic factors in cell fate specifiication. *Neurone,* **14,** 1-5.

Johe, K.K., Hazel, T.G., Muller, T., Dugich-Djord-Jevic, M.M., and McKay, R.D. (1996). Single factors direct the differentiation of stem cells from the foetal and adult central nervous system. *Genes Dev., 10, 3129-3140.*

Jones, A.R., Fetter, R.D., Tear, G, and Goodman, C.S. (1995). *Glial cells missing:* a genetic switch that controls glial versus neuronal fate. *Cell,* **82,** 1013-1023.

Kandel, E.R., Schwartz, J.H., and Jessel, T.M. (1991). Principles of neural science. *Elsevier,* third edition.

Kenan, D.J., Query C.C., and Keene J.D. (1991). RNA recognition: towards identifying the determinants of specificity. *T.I.N.S.* **16,**214-220.

Kilpatrick, T.J., and Bartlett, P.F. (1993). Cloning and growth of multipotential neural precursors: requirements for proliferation and differentiation. *Neuron* **10,** 3255-3265.

Kilpatrick, T.J. (1995). The regulation of neural precursor cells within the mammalian brain. *Mol. Cell. Neurosci.,* **6(1),** 2-15.

Kim, J., Jones, B.W., Zock, C., Chen, Z., Wang, H., Goodman, C.S., and Anderson, D.J. (1998). Isolation and characterisation of mammalian homologs of the *Drosophil*a gene *glial cells missing. Proc. Natl. Acad. Sci.* USA. **95,** 12364-12369.

King, P.H., Levine, T.D., Fremeau R.T., Keene, J.D. (1994). Mammalian homologs of Drosophila ELAV localised to a neuronal subset can bind in vitro to the 3'UTR of mRNA encoding the id transcriptional repressor. *J. Neurosci.***14(4),** 1943-1952.

Kostovic. I. and Molliver, M.E. (1974). A new interpretation of the laminar development of cerebral cortex: synaptogenesis in different layers of neopallium in the human foetus. *Anat. Rec.* **178,** 395.

Koushika, S.P., Lisbin, M.J., and White, K. (1996). *ELAV,* a Drosophila neurone-specific protein, mediates the generation of an alternatively spliced neural protein isoform. *Curr. Biol.,* **6(12).,** 1634-1641.

LaMantia, A.S (1995). The usual suspects: GABA and Glutamate may regulate proliferation in the neocortex. *Neuron,* **15,**1223-1225.

Levine, S.M., and Goldman, J.E. (1988). Embryonic divergence of oligodendrocyte and astrocyte lineages indeveloping rat cerebrum. *J. Neurosci.* **8,** 3992-4006.

Levine, S.M., and Goldman, J.E. (1988). Spatial and temporal patterns of oligodendrocyte differentiation in rat cerebrum and cerebellum. *J. Comp. Neurol.* **277,** 441-455.

Levison, S.W., Chuang, C., Abramson, B.J. and Goldman, J.E. (1993). The migrational patterns and developmental fates of glial precursors in the rat subventricular zone are temporally regulated. *Development* **119,** 611-622.

Levison, S.W. and Goldman, J.E. (1993). Both oligodendrocytes and astrocytes develop from progenitors in the subventricular zone of the postnatal rat forebrain. *Neuron* **10,** 201-212.

Levitt, P., and Rakic, P. (1980). Immunoperoxidase localisation of glial fibrillary acidic protein in radial glial cells and astrocytes of the developing rhesus monkey brain. *J. Comp. Neurol.,* **193,** 815-840.

Levitt, P, Cooper, M.L., and Rakic, P. (1981). Coexistence of neuronal and glial precursor cells in the cerebral ventricular zone of the foetal monkey: an ultrastructural immunoperoxidase analysis. *J. Neurosci.* **1,** 27-39.

Levitt, P., Ferri, R.T., and Barbe, M.F. (1993) Progressive acquisition of cortical phenotypes as a mechanism for specifying the developing cerebral cortex. *Persp. Dev. Neurol.* **1,** 65-74.

Lewis, P.D. (1968). The fate of subependymal cells in the adult rat brain, with a note on the origin of microglia. *Brain,* **91,** 721-738.

Lillien, L. (1998). Neural progenitors and stem cells: mechanisms of progenitor heterogeneity. *Curr. Opin. Neurobiol.,* **8,** 37-44.

Lillien, L.E., and Raff, M. (1990). Differentiation signals in the CNS: type 2 astrocyte development *in vitro* as a model system. *Neuron.,* **5, 110-119.**

Lillien, L.E., Sendtner, M., and Raff, M. (1990). Extracellular matrix-associated molecules collaborate with ciliary neurotrophic factor to induce type-2 astrocyte development. *J. Cell. Biol.,* **111,** 635-644.

Lim, D.A., Fishell, G.J., and Alvarez-Buylla, A. (1997). Post-natal mouse subventricular zone neuronal precursors can migrate and differentiate within multiple levels of the developing neuroaxis. *Proc. Natl. Acad. Sci. USA* **94,** 14832-14836.

Louis, C., and Alvarez-Buylla, A. (1994). Long-distance neuronal migration in the adult mammalian brain. *Science* **264,** 1145-1147.

Louis, J.C., Magal, E., Muir, D., Manthorpe, M., and Varon S. (1992). CG-4, a new bipotential glial cell line from rat brain, is capable of differentiating in vitro into either mature oligodendrocytes or type-2 astrocytes. *J. Neurosci. Res.* **31,** 193-204.

Lumsden, A., Clarke, J.D., Keynes, R., and Fraser, S. (1994). Early phenotypic choices by neuronal precursors, revealed by clonal analysis of the chick embryo hindbrain. *Development,* **120,** 1581-1589.

Lund, R.D. and Mustari, M.J. (1977). Development of the geniculocortical pathway in rats. *J. Comp. Neurol.* **173,** 289-306.

Luskin, M.B. (1998). Neuroblasts of the postnatal mammalian forebrain; their phenotype and fate. *J. Neurobiol.* **36(2),** 221-233.

Luskin, M.B. and Shatz, C.J. (1985a). Studies of the earliest generated cells of the cat's visual cortex: cogeneration of subplate and marginal zones. *J. Neurosci.* **5,** 1062-1075.

Luskin, M.B. and Shatz, C.J. (1985b). Neurogenesis of the cat's primary visual cortex. *J. Comp. Neurol.* **242,** 611-631.

Luskin, M.B., Pearlman, A.L. and Sanes, J.R. (1988). Cell lineage in the cerebral cortex of the mouse studied *in vivo* and *in vitro* with a recombinant retrovirus. *Neurone,* **1,**635-647.

Luskin, M.B. Parnavelas, J.G. and Barfield, J.A. (1993). Neurones, astrocytes and oligodendrocytes of the rat cerebral cortex originate from separate progenitor cells: an ultrastructural analysis of clonally related cells. *J. Neurosci,* **23(4),** 1730-1750.

Mabie, P.C., Mehler, M.F., Marmur, R., Papavasiliou, A., Song, Q., and Kessler, J.A. (1997). Bone morphogenetic proteins induce astroglial differentiation of oligodendroglial-astroglial progenitor cells. *J. Neurosci.,* **17(11),** 4112-4128.

Marin-Padilla, M. (1971). Early prenatal ontogenesis of the cerebral cortex (neocortex) of the cat (felis domestica): a golgi study of primordial neocortical organisation. *Z. Anat. Entickl.-Gesch.* **134,** 117-145.

Marin-Padilla, M. (1978). Dual origin of the mammalian neocortex and evolution of the cortical plate. *Anat. Embryol.* **152,** 109-126.

Marres, V., and Bruckner, G. (1978). Postnatal formation of non-neuronal cells in the rat occipital cerebrum: an autoradiographic study of the time and space pattern of cell division. *J. Comp. Neurol.* **177,** 519-528.

Martinez-Serrano, A., and Bjorkland, A. (1997). Immortalised neural progenitor cells for the CNS gene transfer and repair. *T.I.N.S.* **20,** 530-538.

McKay, R.D. (1989). The origins and cellular diversity in the mammalian central nervous system. *Cell,* **58(5),** 815-21.

McConnell, S.K. (1985). Migration and differentiation of cerebral cortical neurones after transplantation into the brains of ferrets. *Science* **229,** 1268-1271.

McConnell, S.K. (1988). Fates of visual cortical neurones in the ferret after isochronic and heterochronic transplantation. *J. Neurosci.* **8,** 945-974.

McConnell, S.K. (1988). Development and decision-making in the mammalian cerebral cortex. *Brain. Res.* **13,** 1-23.

McConnell, S.K., and Kaznowski, C.E. (1991). Cell-cycle dependence of laminar determination in developing cerebral cortex. *Science* **254,** 282-285.

McConnell, S.K. (1995). Constructing the cerebral cortex: neurogenesis and fate determination. *Neuron,* **15(4),** 761-768.

McEwan, N.R. (1996). 2'3'-CNPase and actin distribution in oligodendrocytes, relative to their mRNAs. *Biochem. Mol. Biol. Int.,* **40(5),** 975-9.

Mione, M.C., Danevic, C., Boardman, P., Harris, B. and Parnavelas, J.G. (1994). Lineage analysis reveals neurotransmitter (GABA or glutamate) but not calcium-binding protein homogeneity in clonally relates cortical neurones. *J. Neurosci.,* **14,** 107-123.

Mione, M.C., Cavangh, J.F.R., Harris, B. and Parnavelas, J.G. (1997). Cell fate specification and symmetrical/asymmetrical divisions in the developing cerebral cortex. *J.Neurosci.* **17(6),** 2018-2029.

Milner, R.J., Sutcliffe, J.G. (1983). Gene expression in rat brain. *Nucleic acids. Res.,* **11,** *5497-5520.*

Misson, J.P., Edwards, M.A., Yamanoto, M, and Caviness, V.S. Jr. (1988a). Mitotic cycling of radial glial cells of the foetal murine cerebral wall: a combined autoradiographic and immunohistochemical study. *Dev. Brain. Res,* **38,** 183-190.

Misson, J.P., Edwards, M.A., Yamanoto, M, and Caviness, V.S. Jr. (1988b). Identification of radial glial cells within the developing murine central nervous system: Studies based on a new immunohistochemical marker. *Dev. Brain. Res.,* **44,** 95-108.

Misson, J.P., Takahashi, T., and Caviness, V.S. (1991). Ontogeny of radial and other astroglial cells in the murine cerebral cortex. *Glia,* **4,** 138-148.

Morshead, C.M., and Van der Kooy, D. (1992). Post-mitotic death is the fate of constitutively proliferating cells in the subependymal layer of the adult mouse brain. *J. Neurosci.,* **12(1),** 249-256.

Nakamura, M., Okano, H., Blendy, J., and Montell, C. (1994). Musashi, a neural RNA-binding protein required for Drosophila adult external sensory organ development. *Neuron.* **13**,67-81.

Okano, H.J,. and Darnell, R.B,. (1997). A Hierarchy of Hu RNA binding proteins in developing and adult neurons. *J. Neurosci.* **17(9),**3024-3037.

O'Leary, D.D., and Stanfield, B.B. (1989). Selective elimination of axons extended by developing cortical neurones is dependant on regional locale: experiments using fetal cortical transplants. *J. Neurosci.* **9,** 2230-2246.

O'Leary, M.T., and Blakemore, W.F. (1997). Oligodendrocyte precursors survive poorly and do not migrate following transplantation into the normal adult central nervous system. *J. Neurosci. Res* **48(2),** 159-67.

Olsson, M., Bjerregaard, K., Winkler, C., Gates, M., Bjorkland, A., and Campbell, K. (1998). Incorporation of mouse neural progenitors transplanted into rat embryonic forebrain is developmentally regulated and dependent on regional and adhesive properties. ***Eur. J. Neurosci.*** 10,**71-85.**

Onifer, S.M., Whittemore, S.R., and Holets, V.R. (1993). Variable morphological differentiation of a raphe-derived neuronal cell line following transplantation into the adult rat CNS. *Exp. Neurol.* **122,** 130-142.

O'Rourke, N.A., Dailey, M.E., Smith, S.J. and McConnell, S.K. (1992). Diverse migratory pathways in the developing cerebral cortex. *Science* **258,** 299-302.

O'Rourke, N.A., Sullivan, D.P., Kaznowski, C.E., Jacobs, A.A. and McConnell, S.K. (1995). Tangential migration of neurones in the developing cerebral cortex. *Development,* **121,** 2165-2176.

O'Rourke, N.A., Chenn, A., and McConnell, S.K. (1997). Postmitotic neurons migrate tangentially in the cortical ventricular zone. *Development* **124,** 997-1005.

Parnavelas, J.G. (1999). Glial cell lineages in the rat cerebral cortex. ***Experimental Neurology,*** 156, **418-429.**

Parnavelas, J.G and Edmunds, S.M. (1983). Further evidence that Retzius-Cajal cells transform to non-pyramidal neurones in the developing rat visual cortex. *J. Neurocytol.* **12(5),** 863-71.

Parnavelas, J.G., Barfield, J.A., Franke, E. and Luskin, M.B. (1991). Separate progenitor cells give rise to pyramidal and non-pyramidal neurones in the rat telencephalon. *Cerebral Cortex* **1(6),** 463-468.

Patterson, J.A., Privat, A., Ling, E.A., and Leblond, C.P. (1973). Investigations of glial cells in semithin sections. III. Transformation of subependymal cells into glial cells, as shown by autoradiography after 3H-thymidine injection into the lateral ventricle of the brain of young rats. *J. Comp. Neurol.* **149,** 83-102.

Pixley, S.R., and J.de Vellis (1984). Transition between immature and radial glia and mature astrocytes studied with a monoclonal antibody to vimentin. *Dev. Brain. Res.* **15,** 201-209.

Polleux, F., Dehay, C., Moraillon, B. and Kennedy, H. (1997). Regulation of neuroblast cell-cycle kinetics plays a crucial role in the generation of unique features of neocortical areas. *J. Neurosci.* **17(20),** 7763-7783.

Price, D.J., and Lotto, B. (1996). Influences of the thalamus on the survival of subplate and cortical plate cells in cultured embryonic mouse brain. *Neuorsci.* **16,(10),** 3247-55.

Price, D.J., Aslam, S., Tasker, L. and Gillies, K. (1997). Fates of the earliest generated cells in the developing mouse neocortex. *J.Comp. Neurol.* **377,** 414-422.

Price, J. and Thurlow, L. (1988). Cell lineage in the rat cerebral cortex: a study using retroviral-mediated gene transfer. *Development,* **104,** 473-482.

Pringle, N., and Richardson, W.D. (1993). A singularity of PDGF alpha-receptor expression in the dorsoventral axis of the neural tube may define the origin of the oligodendrocyte lineage. *Devlopment.* **117,** 525-533.

Privat, A. and Leblond, C.P. (1972). The subependymal layer and neighbouring region in the brain of the young rat. *J. Comp. Neurol.* **146,** 277-302.

Privat, A. (1975). Postnatal gliogenesis in the mammalian brain. *Int. Rev. Cytol.* **40,** 281-323.

Qian, X., Davis, A.A., Goderie, S.K., and Temple, S. (1997). FGF2 concentration regulates the generation of neurones and glia from mulit-potential cortical stem cells. *Neurone,* **18,**81-93.

Rakic, P. (1972). Mode of cell migration to the superficial layers of fetal monkey neocortex. *J. Comp. Neurol.* **145,** 61-84.

Rakic, P. (1974). Neurones in the rhesus monkey visual cortex: systematic relationship between time of origin and eventual deposition. *Science* **183,** 425-427.

Rakic, P. (1977). Prenatal development of the visual system in the rhesus monkey. *Phil.Trans.Royal Soc. Lond.* **B278,** 232-237.

Rakic, P. (1988). Specification of cerebral cortical areas. *Science* **241,** 170-176.

Rakic, P. (1990). Principles of neural cell migration. *Experientia* **46(9),** 882-91.

Rakic, P. (1995). Radial versus tangential migration of neuronal clones in the developing cerebral cortex. *Proc. Natl. Sci. USA,* **92,** 11323-11327.

Raff, M., Miller, R.H., Noble, M. (1983). A glial progenitor cell that develops in vitro into an astrocyte or an oligodendrocyte depending upon culture medium. *Nature* **303,** 390-396.

Rao, M.S., and Mayer-Proschel., M. (1997). Glial-retricted presursors are derived from multipotent neuroepithelial stem cells. ***Dev. Biol.*** 188, **48-63.**

Reh, T.A., and Cagan, R.L. (1994). Intrinsic and extrinsic signals in the developing vertebrate and fly eyes: viewing vertebrate and invertebrate eyes in the same light. *Persp. Dev. Neurobiol.*, **2,** 183-190.

Reid, C.B., Liang, I., and Walsh, C. (1995). Systemic widespread clonal organisation in cerebral cortex. *Neurone,* **15,** 299-310.

Renfranz, P.J., Cunninghamm, M.G. and McKay, R.D.G. (1991). Region-specific differentiation of the hippocampal stem cell line HiB5 upon implantation into the developing mammalian brain cell. *Cell* **66,** 713-729.

Richardson, W.D., Pringle, N., Mosley, M.J., Westermark, B., and Dubois-Dalcq, M. (1988). A role for platelet-derived growth factor in normal gliogenesis in the central nervous system. *Cell* **53,** 309-319.

Richter, K., Good, P.J., David, I.B.(1990). A developmentally regulated, nervous system-specific gene in Xenopus encodes a putative RNA-binding protein. *New biologist.* **2**,556-565.

Roberts, J.S., O'Rourke, N.A and McConnell, S.K. (1993). Cell migration in cultured cerebral cortical slices. *Dev. Biol.* **155,** 396-408.

Robinow, S., and White, K. (1991). Characterisation and spatial distribution of the ELAV protein during Drosphila melanogaster development. *J. Neurobiol.* **22**,443-461.

Sakakibara, S., Imai, T., Hamaguchi, K., Okabe, M., Aruga, J., Nakajima, K., Yasutomi, Y., Nagata, T., Kurihara, Y., Uesugi S., Miyata, T., Ogawa, M.,

Mikoshiba, K., and Okano, H (1996). Mouse-Musashi-1, a neural RNA-binding protein highly enriched in the mammalian CNS stem cell. *Dev Biol.* **176**, 230-242.

Sakakibara, S., Okano, H. (1997). Expression of neural RNA-binding proteins in the postnatal CNS: Implications of their roles in neuronal and glial cell development. J. *Neurosci.,* **17(21)**, 8300-8312.

Sauer, F.C. (1935). Mitosis in the neural tube. *J. Comp. Neurol.* **62,** 377-405.

Sauer, F.C., and Walker, B.E. (1959). Radioautographic study of interkinetic nuclear migration in the neural tube. *Proc. Soc. Ext. Biol.* **101,** 557-560.

Schambra, U.B., Lauder, J.M. and Silver, J. (1992). Atlas of the prenatal mouse brain. *Academic press, Inc.* Harcourt Brace Jovanovich, Publishers.

Schlaggar, B.L., and O'Leary, D.D. (1991). Potential of visual cortex to develop an array of functional units unique to somatosensory cortex. *Science* **252,** 1556-1560.

Schmechel, D.E and Rakic, P. (1979). Arrested proliferation of radial glial cells during midgestation in rhesus monkey. *Nature* **277,** 303-305.

Schmechel, D.E and Rakic, P. (1979). A golgi study of radial glial cells in developing monkey telencephalon: Morphogenesis and transformation into astrocytes. *Anatomical Embryology* **156,** 115-152.

Schoenherr, C.J, Anderson, D.J. (1995). The neurone-restrictive silencer factor (NRSF): a coordinate repressor of multiple neurone-specific genes. *Science,* **267,** 1360-1363.

Schramm, M., Falkai, P., Pietsch, T., Neidt, I., and Egensperger, R. (1999). Neural expression profile of Elav-like genes in human brain. *Clin. Neuropathol* **18(1),** 17-22.

Sekido, Y., Bader, S.A., Carbone, D.P., Johnson, B.E., and Minna, J.D. (1994). Molecular analysis of the HuD gene encoding a parneoplastic encephalomyelitis antigen in human lung cancer cell lines. *Cancer. Res.* **54,** 4988-4992.

Shihabuddin, L.S., Hertz, J.A., Holets, V.R., and Whittemore, S.R. (1995). The adult CNS retains the potential to direct region-specific differentiation of a transplanted neuronal precursor cell line. *J. Neurosci.* **15 (10),** 6666-6678.

Sidman, R.L., Miale, I.L. and Feder, N. (1959). Cell proliferation and migration in the primitive ependymal zone: an autoradiographic study of histogenesis in the nervous system. *Exper. Neurol.* **1,** 322-333.

Sidman, R.L., and Rakic, P. (1982). Development of the human central nervous system. *Histology and histopathology of the nervous system (Haymaker, W., Adams, R.D. eds),* pp3-145.

Simon, H., Hornbruch, A., and Lumsden, A. (1995). Independent assignment of antero-posterior and dorso-ventral positional values in the developing chick hind brain. *Curr. Biol.,* **5,** 205-214.

Siomi, H., and Dreyfuss, G. (1997). RNA-binding proteins as regulators of gene expression. *Curr. Ops. Gen. Develop.* **7**,345-353.

Smart, I.H.M. (1961). The subependymal layer of the mouse brain and its cell production as shown by autoradiography after thymidine-H3 injection. *J. Comp. Neurol.* **116,** 325-347.

Smart, I.H.M. (1972). Proliferative characteristics of the ependymal layer during the early development of the mouse diencephalon, as revealed by recording the number, location, and plane of cleavage of mitotic cells. *J. Anat.* **113,** 109-129.

Smart, I.H.M. and Leblond, C.P. (1961). Evidence for division and transformation of neuroglia cells in the mouse brain, as derived from radioautography after injection of thymidine-H3. *J. Comp. Neurol.* **116,** 349-367.

Smart, I.H.M. and Smart, M. (1982). Growth patterns in the lateral wall of the mouse telencephalon: Autoradiographic studies of the histogenesis of the isocortex and adjacent areas. *J. Anat.* **134,** 273-298.

Snyder, E.Y., Deitcher, D.L., Walsh, C., Arnold-Aldea, S., Hartwieg, E.A., and Cepko, C.L. (1992). Multipotential neural cell lines can engraft and participate in development of mouse cerebellum. *Cell* **68.** 33-51.

Sommer, I., and Schachner, M. (1981). Monoclonal antibodies (O1 to O4) to oligodendrocyte cell surfaces: An immunocytological study in the central nervous system. *Dev. Biol.* **83,** 311-327.

Sotelo, C., and Alvarado-Mallart, R.M. (1986). Growth and differntiation of cerebellar suspensions transplanted into the adult cerebellum of mice with heredodegenerative ataxia. *Proc. Natl. Acad. Sci. USA* **83,** 1135-1139.

Stemple, D.L., and Mahanthappa, N.K. (1997). Neural stem cells are blasting off. *Neurone.,* **18(1),** 1-4.

Stensaas, L.J., and Stensaas, S. (1968). An electron microscope study of cells in the matrix and intermediate laminae of the cerebral hemisphere of the 45mm rabbit embryo. *Z. Zellforsch.* **91,** 341-365.

Stoppini, L., Buchs, P.A. and Muller, D. (1991). A simple method for organotypic cultures of nervous tissue. *J. Neurosci. Met.* **37(2),** 173-82.

Stuart, D.K., Torrence, S.A., and Law, M.I. (1989). Leech neurogenesis. I. Positional commitment of neural precursor cells. *Develop. Biol.,* **136 (1),** 17-39.

Sturrock, R.R. and Smart, I.H.M. (1980). A morphological study of the mouse subependymal layer from embryonic life to old age. *J. Anat.* **130,** 391-415.

Sutcliffe, J.G. (1988). mRNA in the mammalian central nervous system. *Ann. Revs. Neusosci.* **11,** 157-198.

Szabo, A., Daimau, J., Manley, G., Rosenfeld, M., Wong, E., Henson, J., Posner, J.B., Furneaux, H.M. (1991). HuD, a parneoplastic encephalomyelitis antigen, contains RNA-binding domains and is homologous to *Elav* and *sex-lethal*. *Cell,* **57**,325-333.

Takahashi, T., Misson, J.P., and Caviness V.S. Jr. (1990). Glial process elongation and branching in the developing murine neocortex: A quantative immunohistochemical analysis. *J. Comp. Neurol.* **302,** 15-28.

Takahashi, T., Nowakowski, R.S., and Caviness V.S. Jr. (1992). BudR as an S-phase marker for quantitative studies of cytokinetic behavior in the murine cerebral ventricular zone. *J. Neurocytol.* **21,** 185-197.

Takahashi, T., Nowakowski, R.S., and Caviness V.S. Jr. (1993). Cell cycle parameters and patterns of nuclear movement in the neocortical proliferative zone of the fetal mouse. *J. Neurosci.* **13,** 820-833.

Takahashi, T., Nowakowski, R.S., and Caviness V.S. Jr. (1994). Mode of cell proliferation in the developing mouse neocortex. *Proc. Natl. Acad. Sci. USA.* **91,** 375-379.

Takahashi, T., Nowakowski, R.S., and Caviness V.S. Jr. (1995). The cell cycle of the pseudostratified ventricular epithelium of the embryonic murine cerebral wall. *J. Neurosci.* **15,** 6046-6057.

Tan, S.S., Kalloniatis, M., Sturm, K., Tam, P.P., Reese, B.E., Faulkner-Jones, B. (1998). Separate progenitors for radial and tangential cell dispersion during development of the cerebral neocortex. *Neurone,* **21(2),** 295-304.

Tan, S. and Breen, S. (1998). Radial mosaicism and tangential cell dispersion both contribute to mouse neocortical development. *Nature,* **362,** 638-640.

Tanabe, Y., Jessel, T.M. (1996). Diversity and pattern in the developing spinal cord. *Science,* **267,** 1360-1363.

Tamamaki, N., Fujimori, K.E. and Takauji, R. (1997). Origin and route of tangentially migrating neurones in the developing neocortical intermediate zone. *J. Neurosci.* **17(21),** 8313-23.

Temple, S., and Quian, X. (1996). Vertebrate neural progenitor cells: subtypes and regulation. *Curr. Opin. Neurobiol.* **6,**11-17.

Todd, P.H., and Smart, I.H.M. (1982). Growth patterns in the lateral wall of the mouse telencephalon. III. Studies of the chronologically ordered column hypothesis of isocortical histogenesis. *J. Anat. (Lon.)* **134,** 633-642.

Torrence, S.A., Law, M.I., Staurt, D.K. (1989). Leech neurogenesis. II. Mesodermal control of neuronal patterns. *Develop. Biol.,* **136(1),** 40-60.

Uylings, H.B.M., Van Eden, C.G., Parnavelas, J.G., and Kalsbeek, A. (1990). The prenatal and postnatal development of rat cerebral cortex. In B. Kolb and R. C. Tees, editors, *The Cerebral Cortex of the Rat.* MIT Press, Cambridge, MA

Vaccarino, F.M., Schwartz, M.L., Raballo, R., Nilsen, J., Rhee, J., Zhou, M., Doetschman, T., Coffin, JD., Wyland, J,J., and Hung, Y.T. (1999). Changes in cerebral cortex size are governed by fibroblast growth factor during embryogenesis. *Nat Neurosci.,* **2(9),**848.

Vaccarino, F.M., Schwartz, M.L., Raballo, R., Rhee, J., and Lyn-Cook R (1999). Fibroblast growth factor signaling regulates growth and morphogenesis at multiple steps during brain development. *Curr. Top. Dev. Biol.,* **46**,179-200.

Varmus, H. (1988). Retroviruses. *Science,* **240,** 1427-1435.

Vicario-Abejon C., Cunningham, M.G., and McKay, R.D.G. (1995). Cerebellar precursors transplanted to the neonatal dentate gyrus express features characteristic of hippocampal neurons. *J. Neurosci.* **15,** 6351-6363.

Vincent, S., Voneesch, J.L., and Giangrande, A. (1996). *Glide* directs glial fate commitment and cell fate switch between neurones and glia. *Develop.* **122,** 131-139.

Voight, T. (1989). Development of glial cells in the cerebral wall of ferrets: Direct tracing of their transformation from radial glial into astrocytes. *J. Comp. Neurol.* **289,** 74-88.

Wakamatsu, Y., and Weston, J. (1997). Sequential expression and role of Hu RNA binding proteins during neurogenesis. *Development., **124,*** 3449-3460.

Walsh, C. and Cepko, C.L. (1988). Clonally related cortical cells show several migration patterns. *Science,* **241,** 1342-1345.

Walsh, C. and Cepko, C.L. (1992). Widespread dispersion of neuronal clones across functional regions of the cerebral cortex. *Science,* **255,** 434-440.

Walsh, C. and Cepko, C.L. (1993). Clonal dispersion in proliferative layers of developing cerebral cortex. *Nature,* **362,** 632-635.

Weisblat, D., Sawyer, R., and Stent, G. (1978). Cell lineage analysis by intracellular injection of a tracer enzyme. *Science,* **202,** 1295-1298.

Whittemore, S.R., and White, L. (1993). Target regulation of neuronal differentiation in a temperature-sensitive cell line derived from medullary raphe. ***Brain Res.*** 615, **27-40.**

Wilkinson, D.G. (1992). *In situ* hybridisations. A practical approach. *The practical approach series. Senior Editors: D.Rickwood and B.D.Hames.*

Williams, B.P., and Price, J. (1995). Evidence for multiple precursor cell types in the embryonic rat cerebral cortex. *Neuron* **14,** 1181-1188.

Wolburg, H., and Bolz, J. (1991). Ultrastructural organisation of slice cultures from rat visual cortex. *J. Neurocytol.,* **20,** 552-563.

Wood, J.G., Martin, S., and Price,D.J. (1992). Evidence that the earliest generated cells of the murine cerebral cortex form a transient population in the subplate and marginal zone. *Dev. Brain. Res.,* **66,** 137-140.

Yao, K-M., Samson, M-L., Reeves, R., White, K. (1993). Gene elav of Drosophila melangastor: a prototype for neuron-specific RNA binding protein gene family that is conserved in flies and humans. *J. Neurobiol.* **24,**723-739.

Zerlin, M., Levison, S.W. and Goldman, J.E. (1995). Early patterns of migration, morphogenesis and intermediate filament expression of subventricular zone cells in the postnatal rat forebrain. *J. Neurosci.* **15(11)** 7238-7249.

Zhong, W., Feder, J.N., Jiang, M.M., Jan, L.Y. and Jan, Y.N. (1996). Asymmetric localisation of a mammalian numb homolog during mouse cortical neurogenesis. *Neuron,* **17(1)** 43-53.

Zhong, W., Jiang, M.M., Weinmaster, G., Jan, L.Y. and Jan, Y.N. (1997). Differential expression of mammalian numb, numblike and notch 1 suggests distinct roles during mouse cortical neurogenesis. *Development,* **124(10)** 1887-97.

Zhou, H.F., Lee, L.H., and Lund, R.D. (1990). Timing and patterns of astrocyte migration from xenographic transplants of the corpus callosum. *J. Comp. Neurol.* **292,** 320-330.

Zhou, H.F., and Lund, R.D. (1992). Migration of astrocytes transplanted to the midbrain of neonatal rats. *J. Comp. Neurol.* **317,** 145-155.

APPENDIX 1

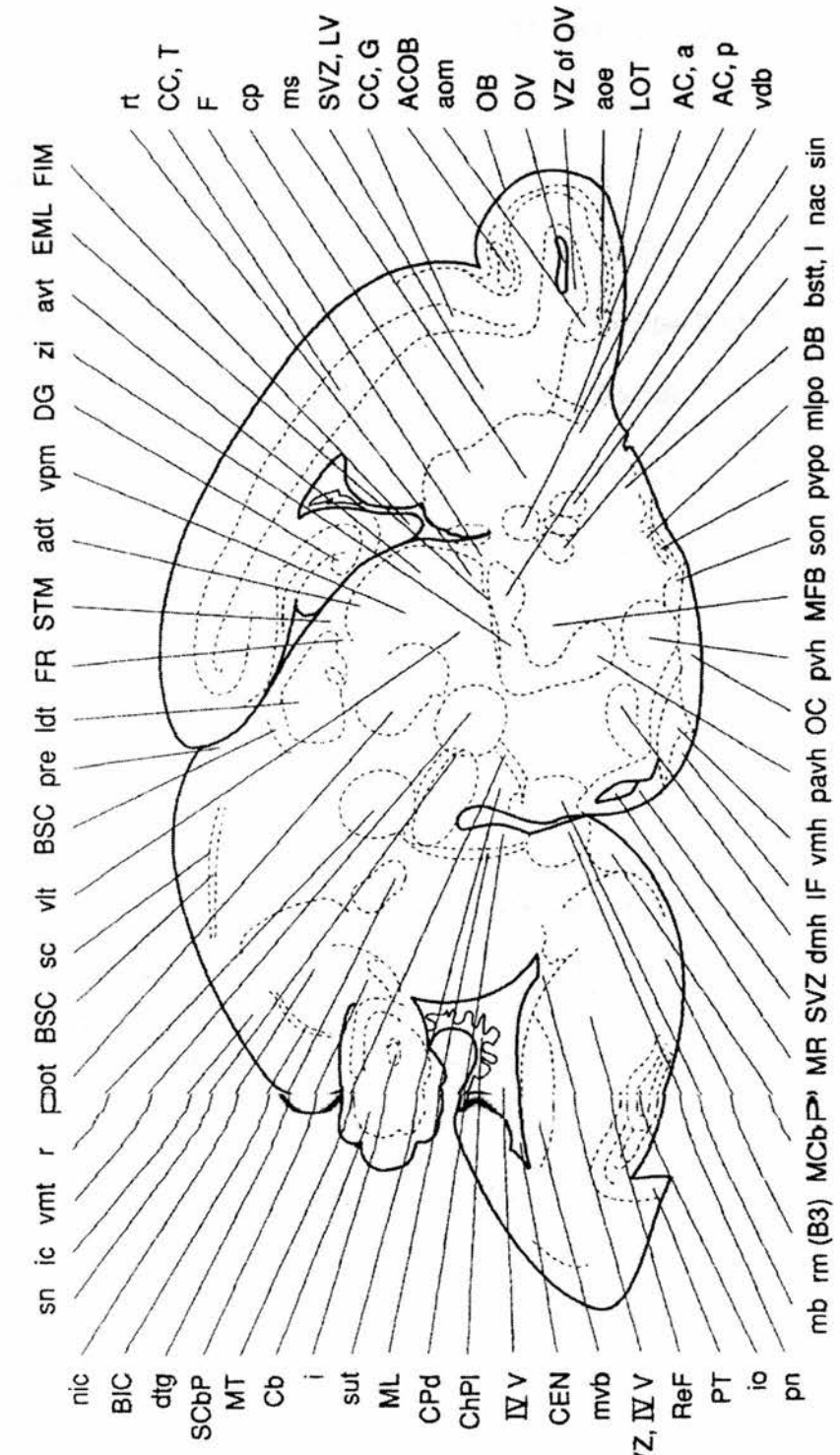

Figure GD18 SAG.7 from Shambra et al ,1992

APPENDIX 2

Normal culture medium

	Sigma Cat. No.	Final conc.
Mix together in a sterile beaker 100 mls F12 (Hams) and 100mls Dulbeco's modified Eagle's medium	N4888 D5761	
Add:		
1mg Insulin	I6634	
5µg/ml		
2mg apo-transferrin	T1147	
10µg/ml		
3ml HEPES buffer	H0887	
2ml antibiotics (gentamycin and kanamycin)	G1264/K1377	
2ml Putrescene	P5780	
16.11µg/ml		
20µl Progesterone	P8783	
0.00629µg/ml		
20µl Na_2SeO_3	S5261	
0.0052µg/ml		
2ml L-glutamine	G2128	
25µg/ml		

Antibiotics

Gentamycin sulphate (100mg)

Kanamycin sulphate (200mg)

Make up to 20ml with double distilled water (sterile), then filter sterilise. Store in 1ml aliquots at -70^0C.

Supplements

100µm **putrescene** (add 161.1mg to 100ml sterile double distilled water and filter sterilise). Store in 2ml aliquots at -70^0C.

20μm **progesterone** (add 6.29mg to 100ml ethanol). Store in 1ml and 50μl aliquots at 70^0C.

30μm **Na_2SeO_3** (add 5.2mg to 100ml sterile double distilled water and filter sterilise). Store in 1ml and 50μl aliquots at 70^0C.

0.2M **L-glutamine** (add 2.5g to 100ml sterile double distilled water and filter sterilise). Store in 2ml aliquots at 70^0C.

NOTES

Transferrin is a beta glycoprotein (iron transport protein in the blood). It transports iron to and possibly within the cell in culture. It may also have a detoxifying role.

Putrescene is the decarboxylated product of the amino acid ornithine. It is needed as a precursor for the synthesis of polyamines which are involved in cell growth and proliferation.

Selenium is a co-factor of glutathione peroxidase, which is, located in the cytosol and catalyses the reduction of radicals by the antioxidant glutathione.

L-glutamine is a non-essential amino acid, which is an important precursor for nucleotide and structural protein synthesis. It is required for L-glutamine and GABA synthesis. At high concentrations it may have neurotoxic side effects.

APPENDIX 3

Extraction of RNA from Rat brains

1) Add 2mls of RNAzol B (Biogenesis, Bournemouth, UK) to 100mg of tissue and homogenize in a glass-teflon homogenisor.

2) Divide samples into 1ml aliquots and place in eppendorfs (1.5ml) on ice.

3) Add 100µl chloroform to each tube and vortex. Leave on ice for 5 minutes.

4) Centrifuge at 13,000g for 15mins at 4^{o} C, and remove the top aqueous layer into a clean eppendorf tube.

5) Add an equal volume of phenol/chloroform (1:1), vortex and centrifuge at 13,000g for 5minutes.

6) Remove the top layer to a clean eppendorf and repeat step 5. Repeat this step until no precipitate of DNA/protein is visible at the interphase of the aqueous and organic phase.

7) Add an equal volume of isopropanol to the isolated aqueous phase, vortex and leave for 15 minutes to precipitate the RNA.

8) Centrifuge at 13,000g at 4^{o} C for 45 minutes to pellet the RNA.

9) Carefully remove the supernatant and wash the pellet in 500µl of 70% ethanol.

10) Centrifuge at 13,000g for 5 minutes at room temperature and remove the supernatant.

11) Air dry the pellet and resuspend in DEPC treated MilliQ dH_2O.

APPENDIX 4

Phenol/chloroform and ethanol precipitation

1) Add same vol. of phenol/Chloroform (1:1) vortex and centrifuge at 13000g for 5 minutes at 4^0C. Remove the upper layer (aqueous phase) to a new eppendorf. Repeat the phenol/chloroform step to the bottom layer. Combine the two aqueous layers.

2) Add 0.1x vol. of 3M NaAc, pH5.5 and 2x vol of 100% ethanol. Vortex and put at -80^0C degrees for at least 30 minutes. Centrifuge at 13,000g for 45 minutes at 4^0C and discard the supernatant.

3) Wash the pellets by resuspending in 100µl of 70% ethanol. Centrifuge at 13,000g for 5 minutes at room temperature. Discard the supernatant.

4) Air-dry the pellets at room temperature for 15 minutes. Resuspend in an appropriate volume of TE or DEPC treated dH^20.

APPENDIX 5

Denaturation buffer (200µls):

20µl 10x Mops (0.2M Mops, 50mM sodium acetate, 10mM EDTA; pH 7), 100µl formamide, 40µl formaldehyde, 20µl ethidium bromide (0.5mg/ml) and 20µl DEPC dH_2O.

0.8% formaldeyde/agaorose gel:

4ml 10x MOPS buffer, 1.2ml formaldehyde and 34.8 ml 1% agarose in MilliQ H_20

Loading buffer

30% Ficol Type 400 (Pharmacia), 0.25% bromophenol blue

Plasmid purification (alkaline lysis)

Buffer P1 50mM glucose; 10mM EDTA, pH8; 25mM Tris-HCL pH8.

Buffer P2 1% SDS; 0.2M NaOH

Buffer P3 29.4g potassium acetate; 11.5ml glacial acetic acid; dH^2O to 100ml; 3M with respect to potassium and 5M with respect to acetate.

Dot-blot solutions

Buffer 1 100mM Maleic acid; 150mM NaCl; 35g NaOH pellets; 13mls 10MnaOH. Make up to 1 litre with MilliQ dH^2O.

Buffer 2 1ml 10% blocking reagent (boehringer); 9ml buffer 1

Buffer 3 100mM Tris/HCL pH9.5; 100mM NaCl; 50mM $MgCl_2$

***In situ* Solutions**

20x SSPE (pH 7.4) 3.0M NaCl; 0.2M NaH_2PO4; 0.02M EDTA

20 x SSC (pH 7.0) 3M NaCl; 0.3M $Na_3Citrate$

10 x PBS (pH 7.4) 1.37M NaCl; 27.6mM KCL; 81mM Na_2HPO_4; 14.7mM KH_2PO_4

PBST 0.1% Tween20 in 1 x PBS

4% paraformaldehyde 4g PFA in 100ml 1x PBS

20 x P buffer 1M Tris/HCL pH 7.5; 0.1M EDTA

10 x salts 3M NaCl; 7.8g NaH_2PO_4; 0.1M Tris pH 6.8; 7.1g Na_2HPO_4; 50mM EDTA. Make up to 1 liter

APPENDIX 6

Purification of DNA using QIAEX II gel extraction kit

Insert DNA was cut from a 1% agarose gel, and the weight of the gel was determined. Buffer QX1 was added to the gel fragment at 3 x volume of the gel (this applies for DNA fragments of 100bp to 4kb) e.g. for 50mg of gel, 150µl of buffer QX1 was added. Qiaex II (10µl) was then added, the tube was vortexed and incubated at 55^0C for 10 minutes. The sample was mixed every 2 minutes. The sample was centrifuged at 13,000g for 30 minutes at room temperature, and the supernatant discarded. The pellet was washed twice with buffer QX1 (0.5mls), centrifuging for 30 seconds and removing the supernatant each time. This was done to remove any salt residues that were present. The pellet was left to air dry for 15 minutes, and then resuspended in TE buffer (15µl). The sample was left at room temperature for 5 minutes to elute the DNA. The solution was then centrifuged at 13,000g for 30 seconds, and the supernatant (containing the DNA) was removed to a clean eppendorf tube. This elution step can be repeated to increase they yields of DNA.

APPENDIX 7

Preparation of XL-1 Blue competent cells

Sterile L-Broth (5ml) containing tetracycline (5µg) was inoculated with XL-1 Blue E.Coli bacteria and incubated overnight at 37^0C in an orbital incubator (220 rpm).

The culture was diluted 1:50 with L-Broth (5ml) and then incubated at 37^0C in the orbital incubator for 3h until the optical density (O.D.) reached 0.4-0.7. The culture was then centrifuged at 2000rpm for 10 minutes at room temperature. The supernatant was discarded and the pellet gently resuspended in cold, sterile 0.1M $CaCl_2$ (2.5ml). This was left on ice for 20 minutes with occasional shaking. The cells were then centrifuged at 2000rpm for 10 minutes at room temperature, supernatant discarded and the pellet resuspended in cold 0.1M $CaCl_2$ (0.5ml).

APPENDIX 8

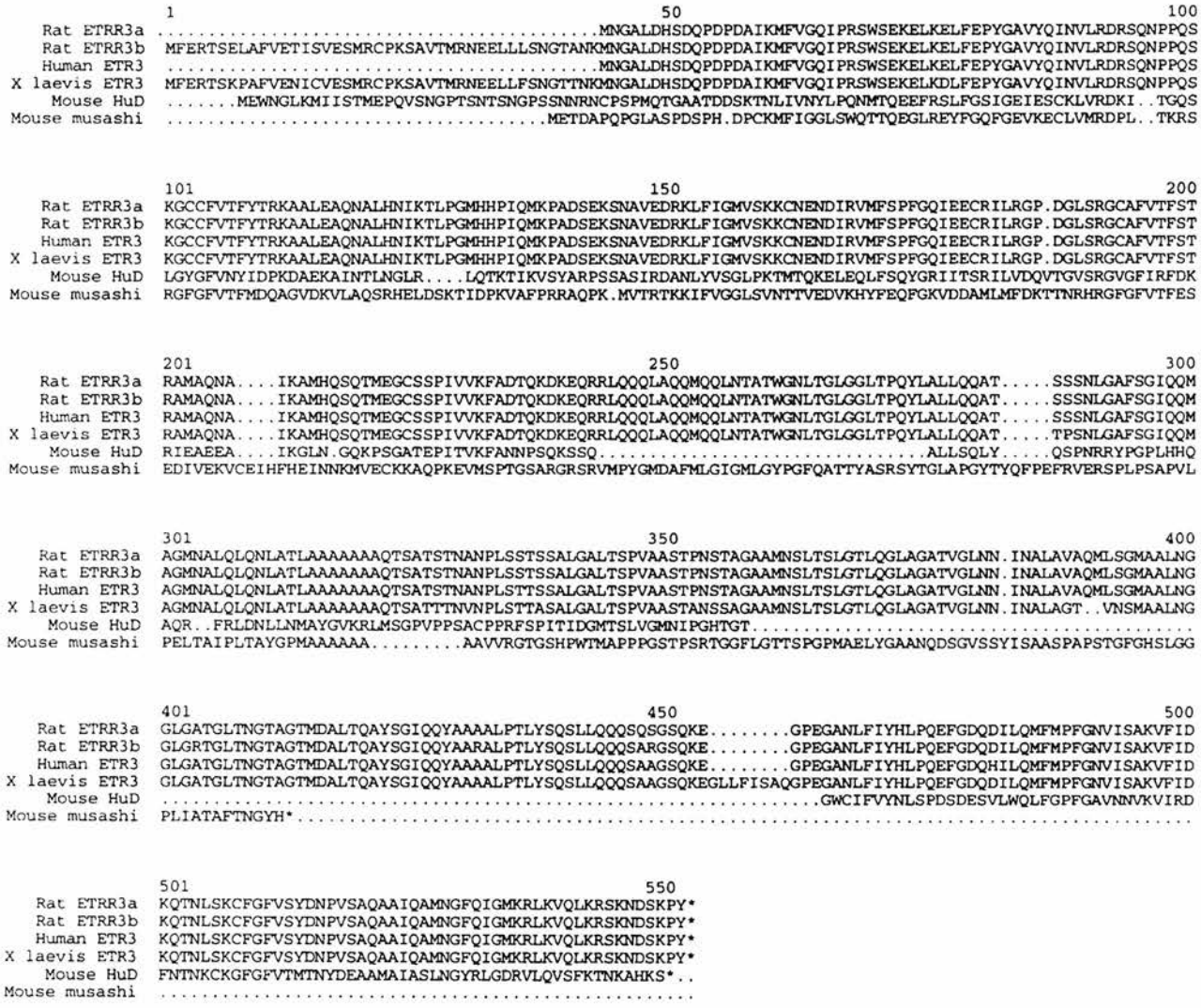

Amino acid sequence of ETRR3 compared to the human and Xenopus laevis, ETR sequences. ETRR3 showed 94% homolgy to both these sequences. Sequences from *m-msi* and mouse *HuD* genes are also included on the figure for comparison purposes.